

**p38(MAPK) NEGATIVELY REGULATES
MONOAMINE OXIDASE-A ACTIVITY
AS WELL AS ITS SENSITIVITY TO Ca²⁺**

A Thesis Submitted to the College of

Graduate Studies and Research

In Partial Fulfillment of the Requirements

For the Degree of Doctor of Philosophy

In the Department of Psychiatry

University of Saskatchewan

Saskatoon

By

Xia Cao

Keywords: mitochondria, monoamine oxidase, calcium, p38 MAP kinase,
phosphorylation, hydrogen peroxide, apoptosis, mutagenesis, activity

© Copyright Xia Cao, December 2007. All rights reserved.

PERMISSION TO USE

In presenting this thesis in partial fulfillment of the requirements for a Doctor's degree from the University of Saskatchewan, I agree that the Libraries of this University may make it freely available for inspection. I further agree that permission for copying of this thesis in any manner, in whole or in part, for scholarly purposes may be granted by the professors who supervised my thesis work, Drs. Darrell D. Mousseau and Xin-Min Li, or in their absence, by the Head of the Department of Psychiatry. It is understood that any copying or publication or use of this thesis or parts thereof for financial gain shall not be allowed without my written permission. It is also understood that due recognition shall be given to me and to the University of Saskatchewan in any scholarly use which may be made of any material in my thesis.

Requests for permission to copy or to make other use of material in this thesis in whole or part should be addressed to:

Director of the Neuropsychiatry Research Unit

and/or

Head of the Department of Psychiatry

University of Saskatchewan

Saskatoon, Saskatchewan S7N 5E4.

Dedication

I would like to extend heartfelt thanks to my dear parents, Dr. Fengtong Cao and Dr. Shufang Zhao, whose unconditional emotional support was critical to my success. They were always ready to lend a hand and allowed me to concentrate on my studies abroad, by taking care of my little son.

On a more personal note, the completion of this thesis would not have been possible without the infinite support, encouragement, and understanding of my husband, Dr. Jingbo Zhang, and my son, Conghao Zhang.

ABSTRACT

Monoamine oxidase (MAO) is a mitochondrial deaminating enzyme that exists as two isoforms, MAO-A and -B. The MAO-mediated reaction generates hydrogen peroxide (H_2O_2) as a normal by-product. Dysregulation of MAO has been implicated in a variety of neuropsychiatric and neurodegenerative disorders, as well as in the aging process. Endogenous regulators of MAO-A function include calcium (Ca^{2+}) and the p38 mitogen-activated protein kinase (MAPK). Although the effect of p38(MAPK) is thought to rely on induction of *mao-A* gene expression, post-translational modification of the MAO-A protein is also possible.

Using standard biochemical approaches in combination with pharmacological interventions and recombinant DNA strategies, specific aspartic acid residues (within putative Ca^{2+} -binding motifs) were demonstrated to contribute to MAO-A activity. Furthermore, MAO-A activity and its sensitivity to Ca^{2+} was negatively regulated by the p38(MAPK), which is usually activated during cell stress. The effect of p38(MAPK) on MAO-A function relies specifically on Serine209 in MAO-A, which resides in a p38(MAPK) consensus motif. The serine phosphorylation status of MAO-A determines its capacity for generating peroxy radicals and its toxicity in established cell lines (*e.g.* C6, N2a, HEK293A, HT-22) and in primary cortical neurons. p38(MAPK)-regulated MAO-A

activity is also linked to neurotoxicity associated with the Alzheimer disease-related peptide, β -amyloid ($A\beta$). These data suggest a unique neuroprotective role for p38(MAPK) centered on a negative feedback regulation of the Ca^{2+} -sensitive, H_2O_2 -generating enzyme MAO-A.

ACKNOWLEDGMENTS

I extend sincere thanks to the people responsible for seeing me through my time as a graduate student. First, my research supervisor, Dr. Darrell D. Mousseau, and co-supervisor, Dr. Xin-Min Li, for their patience, encouragement, support, guidance, and suggestions toward pursuing a Doctorate, fulfilling one of my life goals. I have gained valuable insight from them, not only into the world of research science, but also on gaining better attitudes to life, which has allowed me to improve as a person and to create new prospects for my future.

I also thank my Advisory Committee: Dr. Adil Nazarali and Dr. Peter Yu for their constructive suggestions during my research and advice about this thesis. Thank you also to Dr. Glen Baker for serving as the external examiner for my thesis defense.

I sincerely thank the joyful and energetic group of the Cell Signalling Laboratory who never failed to lend a helping hand and to provide ideas when needed. Thanks are also extended to the staff, post-doctoral fellows, and other students of the Neuropsychiatric Research Unit (NRU), all of whom supplied both moral support and assistance in matters big and small. They were an integral part of my experience and contributed to make the NRU a pleasant and helpful place to work.

TABLE OF CONTENTS	Page
PERMISSION TO USE	i
DEDICATION	ii
ABSTRACT	iii
ACKNOWLEDGMENTS	v
TABLE OF CONTENTS	vi
LIST OF TABLES	xiii
LIST OF FIGURES	xiv
LIST OF ABBREVIATIONS	xix
1 LITERATURE REVIEW	1
1.1 Monoamine oxidase	1
1.1.1 Discovery and nomenclature	2
1.1.2 Amine oxidase classification	2
1.1.3 Specificities of inhibitors and substrates, and tissue distribution of MAOs	4
1.1.4 MAOs change during development and aging	6
1.1.5 Cloning of human MAO	7
1.1.5.1 The MAO promoter	8
1.1.5.2 Three dimensional structure of MAO-A and MAO-B and their important domains	9
1.1.5.2.1 Important amino acid residues in MAO	9
1.1.5.2.2 FAD binding site in MAO	11
1.1.5.2.3 Crystal structure of MAO	12
1.1.5.2.4 Membrane insertion region of MAO	12

1.1.5.2.5	Imidazoline binding site on MAO	13
1.1.5.2.6	Substrate and inhibitor recognition and binding domain (active site) in MAO	13
1.1.6	Neurotransmitter and behavioral changes in MAO-A or MAO-B knock-out models	15
1.1.7	MAO and related neurological disorders	16
1.1.7.1	MAO-A inhibition and neuropsychiatric disorders	16
1.1.7.1.1	Depression	17
1.1.7.1.2	MAO-A inhibition and depression	18
1.1.7.1.2.1	The development of MAO-A inhibitors	18
1.1.7.1.2.2	Types of MAO inhibitors	18
1.1.7.1.2.3	MAO-A inhibition in depression	20
1.1.7.2	MAO inhibition and neurodegenerative diseases	20
1.1.7.2.1	Overview of neurodegenerative diseases	20
1.1.7.2.2	Molecular mechanisms well-known for neurodegeneration	21
1.1.7.2.3	Parkinson's disease	22
1.1.7.2.3.1	Brief overview	22
1.1.7.2.3.2	MAO inhibition and Parkinson's disease	23
1.1.7.2.4	Alzheimer's disease	25
1.1.7.2.4.1	Brief overview	25
1.1.7.2.4.2	Oxidative stress in Alzheimer's disease	27
1.1.7.2.4.3	MAO inhibition in Alzheimer's disease	28
1.2	Intracellular Ca ²⁺ signaling	31
1.2.1	Intracellular Ca ²⁺ concentration and adjustment	31
1.2.2	Ca ²⁺ homeostasis and neuronal fate	35
1.2.3	Intracellular Ca ²⁺ is elevated in neurodegenerative disorders.	39
1.3	p38(MAPK) and its signaling pathway	40

1.3.1	Brief overview of the MAPK signaling pathway	40
1.3.1.1	Cell signaling	40
1.3.1.2	MAPK signalling pathway	41
1.3.2	p38(MAPK) as a regulator in neuronal cell fate and cell functions	43
1.3.2.1	Isoforms and inhibitor of p38(MAPK)	43
1.3.2.2	Intracellular location of p38(MAPK)	44
1.3.2.3	Substrates of p38(MAPK)	44
1.3.2.4	Cellular functions of neuronal p38(MAPK)	45
1.3.2.4.1	p38(MAPK) and neuronal differentiation	46
1.3.2.4.2	p38(MAPK) and neuronal viability	47
1.3.2.4.3	p38(MAPK) and other cellular functions	49
1.4	Linking Ca ²⁺ , MAO-A, and p38(MAPK) in a unique mechanism that contributes to cell fate	49
1.4.1	Background	49
1.4.1.1	Ca ²⁺ signaling and the increase in MAO-A activity occur coincidentally in many neurological disorders.	49
1.4.1.2	Evidence of the direct effect of Ca ²⁺ on MAO-A activity	49
1.4.1.3	p38(MAPK) may regulate <i>mao-A</i> transcription, translation, and activity.	50
1.4.2	Hypothesis	51
1.4.3	Objectives of this project	51
2	MATERIALS AND METHODS	53
2.1	Materials	53
2.1.1	Vectors	53
2.1.2	Competent cells	58
2.1.3	Cell cultures	59

2.1.4	Rat neuronal cortical culture	60
2.1.5	Animals	61
2.2	Methods	61
2.2.1	Dissection of rat and mouse brains	61
2.2.2	Detection of MAO activity in the absence or presence of Ca ²⁺	62
2.2.3	Kinetic study of MAO activity in the absence or presence of Ca ²⁺	63
2.2.4	Plasmid construction and confirmation	64
2.2.4.1	MAO-A and MAO -B full-length fragment	64
2.2.4.2	p38(MAPK) full-length fragment	64
2.2.4.3	Subcloning gene fragment into specific vectors	65
2.2.5	Polymerase chain reaction (PCR)	65
2.2.6	Transformation	67
2.2.7	Plasmid DNA preparation	67
2.2.8	Plasmid Transfection	71
2.2.8.1	Homemade preparation of ExGen500	71
2.2.8.2	Transfection using ExGen500	72
2.2.9	Protein concentration determination	73
2.2.10	Immunoblot and immunoprecipitation	73
2.2.10.1	Western blot or immunoblot (IB)	73
2.2.10.2	Immunoprecipitation (IP)	75
2.2.11	Reverse transcriptase polymerase chain reaction (RT-PCR)	77
2.2.11.1	RNA extraction	77
2.2.11.2	First-strand cDNA synthesis	79
2.2.12	Subcellular fractionation	80
2.2.13	Site-directed mutagenesis	81
2.2.14	DSS cross-linking reaction	85
2.2.15	Intracellular Ca ²⁺ concentration detection	86

2.2.16	Reactive oxygen species (ROS) production detection	87
2.2.17	Nuclear condensation detection by Hoechst staining 33258	88
2.2.18	JC-1 and the mitochondrial membrane potential	89
2.3	Statistical analysis	90
3	RESULTS	92
3.1	Endogenous MAO activity in selected cells and the response	
	of MAO to addition of Ca^{2+} to the reaction solution	92
3.1.1	MAO gene expression and activity levels differ across cell lines	92
3.1.2	MAO activity is dependent on protein concentration	94
3.1.3	The effect of Ca^{2+} and incubation time on MAO-A activity	94
3.1.4	Ca^{2+} selectively enhances MAO-A activity in animal brain tissues	94
3.1.5	The effect of Ca^{2+} on MAO activity in glial C6 cells is sensitive to Mg^{2+}	97
3.1.6	MAO-A activity in hippocampal HT-22 cells is also selectively enhanced by Ca^{2+} and is sensitive to Mg^{2+}	97
3.1.7	Ca^{2+} affects MAO-A kinetics in HT-22 cells	101
3.2	Overexpressed MAO-A, but not MAO-B, responds to incubation with Ca^{2+}	101
3.3	The effect of mutations of putative Ca^{2+}-binding sites on MAO-A function	107
3.4	The three MAO-A Ca^{2+}-binding site mutants associate differently with a high molecular weight complex	115
3.5	Overexpressed MAO-A proteins do not respond to Ca^{2+} in HEK293A cells	117
3.6	Overexpressed MAO-A proteins do not respond to Ca^{2+} in N2a cells	117
3.7	Cell confluence diminishes MAO-A activity and its response to	

Ca ²⁺ in C6 cells	117
3.8 p38(MAPK) regulates MAO-A activity and its response to Ca ²⁺	121
3.8.1 p38(MAPK) phosphorylation was inversely correlated with MAO-A activity level in 4 cell lines.	121
3.8.2 p38(MAPK) associates with MAO-A protein, but not with MAO-B protein.	124
3.8.3 Chemical p38(MAPK) inhibition increases MAO-A activity and its response to Ca ²⁺ .	124
3.8.4 Genetic modulation of p38(MAPK) affects MAO-A activity and its response to Ca ²⁺ .	127
3.8.4.1 Overexpression of p38(MAPK) mutants affects MAO-A activity, but not gene expression, in HT-22 cells.	131
3.8.4.2 The effect of activated p38(MAPK) is cell line-dependent.	135
3.8.5 The mutation of a putative p38(MAPK) phosphorylation site in MAO-A influences its activity and sensitivity to Ca ²⁺ .	138
3.8.6 p38(MAPK) associates with, and phosphorylates, MAO-A.	142
3.8.7 Chemical inhibition of p38(MAPK) results in ROS production that is mediated, in part, by MAO-A.	148
3.8.8 Chemical inhibition of p38(MAPK) increases MTT conversion.	148
3.8.9 Chemical inhibition of p38(MAPK) diminishes mitochondrial membrane potential in an MAO-A-sensitive manner.	151
3.8.10 The sensitivity of MAO-A to Ca ²⁺ is revealed by chemical inhibition of p38(MAPK).	151
3.9 Manipulation of Ca ²⁺ levels <i>in vivo</i> affects MAO-A.	151
3.9.1 The Ca ²⁺ ionophore A23187 increases MAO-A activity Independent of a change in <i>mao-A</i> expression.	151

3.9.2	Overexpression of the Ca ²⁺ -binding protein CB28K decreases MAO-A activity independent of a change in <i>mao-A</i> expression.	155
3.10	The AD-related peptide β -amyloid (A β) induces chromatin condensation in primary neuronal cultures; potentiation by inhibition of p38(MAPK) and protection by inhibition of MAO-A.	160
3.11	Additional means of post-translational modification of MAO-A activity.	160
4	DISCUSSION	167
5	FUTURE DIRECTIONS	186
6	REFERENCES	187
7	APPENDIX I: Permission to reproduce published works	209
8	APPENDIX II: ETHICS APPROVAL	213

LIST OF TABLES

Page

Table 1: List of Reagents, and Kits and Suppliers 54

Table 2: List of Antibodies and the Dilutions used for the Western Blotting. 56

Table 3: Names and Addresses of Suppliers 56

LIST OF FIGURES

Page

Fig. 1:	Reaction pathway of monoamine metabolism by oxidative deamination by mitochondrial MAO.	3
Fig. 2:	3-D structure of hMAO A (similar to that of MAO-B).	10
Fig. 3:	The mechanism of neurotoxicity induced by iron and hydrogen peroxide <i>via</i> the Fenton reaction.	29
Fig. 4:	Ca ²⁺ signalling depends on Ca ²⁺ from several sources.	34
Fig. 5:	Mitochondria-mediated generation of reactive oxygen species relies on Ca ²⁺ .	37
Fig. 6:	Schematic of three signaling cascades and the putative motifs targeted by successive kinases in the cascade.	42
Fig. 7:	Gene expression and activity levels of MAO-A and MAO-B in selected cell lines.	93
Fig. 8:	MAO enzyme activity is dependent on protein concentration.	95
Fig. 9:	MAO-A activity in C6 cell homogenates is increased by Ca ²⁺ in a time-dependent manner.	96
Fig. 10:	Ca ²⁺ selectively enhances MAO-A activity in different regions of rat and mouse brain.	98
Fig. 11:	The effect of Ca ²⁺ on MAO-A activity in C6 cell homogenates is not consistent.	99
Fig. 12:	Ca ²⁺ selectively enhances MAO-A activity in HT-22 cell homogenates.	100
Fig. 13:	The response of MAO-A to Ca ²⁺ in HT-22 cells is sensitive to Mg ²⁺ .	102
Fig. 14:	Ca ²⁺ affects MAO-A enzyme kinetics in HT-22 cells.	103
Fig. 15:	MAO-A and MAO-B cDNA were fused to a myc-epitope tag to allow monitoring of the overexpressed protein.	104

Fig. 16:	Representative chromatograms of the cDNA sequence of <i>mao-A</i> in the pCMV/Myc/Mito expression vector.	105
Fig. 17:	Representative chromatograms of the cDNA sequence of <i>mao-B</i> in the pCMV/Myc/Mito expression vector.	106
Fig. 18:	The expression, subcellular distribution and activity of Myc-epitope tagged MAO-A.	108
Fig. 19:	Ca ²⁺ promotes the formation of a high molecular weight complex with overexpressed MAO-A-myc, but not MAO-B-myc.	109
Fig. 20:	Alignment of the MAO-A deduced amino acid sequences from four mammalian species.	111
Fig. 21:	Alignment of the human MAO-A and MAO-B deduced amino acid sequences.	112
Fig. 22:	Ca ²⁺ -binding site mutations affect MAO-A activity.	113
Fig. 23:	Ca ²⁺ -binding site mutations affect the ability of MAO-A to generate peroxy radicals.	114
Fig. 24:	Ca ²⁺ -binding site mutations in MAO-A affect the mitochondrial membrane potential ($\Delta\psi_m$) in N2a cells.	116
Fig. 25:	Mutagenesis of the MAO-A-D328 Ca ²⁺ -binding site diminishes its association with a high molecular weight complex.	118
Fig. 26:	The activities of overexpressed MAO-A(WT) and Ca ²⁺ -binding site mutants in HEK293A cell homogenates do not respond to Ca ²⁺ .	119
Fig. 27:	The activity of overexpressed MAO-A(WT) in N2a cell homogenates does not respond to Ca ²⁺ .	120
Fig. 28:	C6 cell confluence diminishes MAO-A activity and its response to Ca ²⁺ ; correlation with increased phosphorylation of p38(MAPK).	122
Fig. 29:	MAO protein expression and activity, and phosphorylation of p38(MAPK) in four cell lines.	123

Fig. 30:	p38(MAPK) associates selectively with MAO-A protein.	125
Fig. 31:	The specific p38(MAPK) inhibitor SB203580 increases MAO-A activity in HEK293A cells and HT-22 cells.	126
Fig. 32:	SB203580 added directly to HT-22 homogenates does not affect MAO-A activity.	128
Fig. 33:	p38(MAPK) cDNA was subcloned into the pcDNA3.1/Hygro(+) expression vector.	129
Fig. 34:	The sequence of p38(MAPK) cDNA in the pcDNA3.1/Hygro(+) vector was confirmed by sequence analysis.	130
Fig. 35:	Mutagenesis of the “TGY” motif in p38(MAPK).	132
Fig. 36:	Activated and dominant negative forms of p38(MAPK) do not affect <i>mao-A</i> or <i>mao-B</i> gene expression in HT-22 cells.	133
Fig. 37:	The overexpression of p38(MAPK) mutant proteins affects MAO-A activity and its response to Ca ²⁺ in HT-22 cells.	134
Fig. 38:	The overexpression of p38(MAPK) mutant proteins affects <i>mao-A</i> gene expression, but not MAO-A activity, in PC12 cells.	136
Fig. 39:	The effects of overexpression of p38(MAPK) and its upstream kinase MEK3 on <i>mao-A</i> gene expression and MAO-A activity in SH-SY5Y cells.	137
Fig. 40:	MAO contains a putative p38(MAPK) phosphorylation motif, RXXS.	139
Fig. 41:	Confirmation of the mutagenesis of Ser209 in MAO-A cDNA.	140
Fig. 42:	The overexpression of MAO wild type and Serine substitution mutants in HEK293A cells.	141
Fig. 43:	The MAO-A Serine209 substitution mutants have different activities and sensitivities to Ca ²⁺ in HEK293A cells.	143
Fig. 44:	The MAO-B Serine200 substitution mutants do not affect the activity of the overexpressed protein in HEK293A.	144

Fig. 45:	The MAO-A(S/E) protein is less associated with a high molecular complex.	145
Fig. 46:	p38(MAPK) associates with, and phosphorylates, MAO-A.	146
Fig. 47:	The MAO-A Serine209 substitution mutants exert different effects on mitochondrial membrane potential ($\Delta\psi_m$) and reactive oxygen species (ROS) production in N2a cells.	147
Fig. 48:	The p38(MAPK) inhibitor SB203580 induces reactive oxygen species production <i>via</i> a MAO-A sensitive mechanism in HT-22 cells.	149
Fig. 49:	The p38(MAPK) inhibitor SB203580 increases MTT conversion in HT-22 cells.	150
Fig. 50:	The p38(MAPK) inhibitor SB203580 decreases mitochondrial membrane potential ($\Delta\psi_m$) <i>via</i> a MAO-A sensitive mechanism in HT-22 cells.	152
Fig. 51:	MAO-A Ca^{2+} -binding site mutants respond in distinct manners to Ca^{2+} , as revealed by inhibition of p38(MAPK) with SB203580 in HEK293A cells.	153
Fig. 52:	The Ca^{2+} ionophore A23187 increases MAO-A activity and function in HT-22 cells.	154
Fig. 53:	The Ca^{2+} ionophore A23187 induces reactive oxygen species production <i>via</i> a MAO-A sensitive mechanism in HT-22 cells.	156
Fig. 54:	Overexpression of the Ca^{2+} -binding protein CB28K decreases MAO-A activity as well as its sensitivity to Ca^{2+} in HT-22 cells.	157
Fig. 55:	Overexpression of the Ca^{2+} -binding protein calbindinD-28K (CB28K) diminishes reactive species production in HT-22 cells.	158
Fig. 56:	Overexpression of the Ca^{2+} -binding protein calbindinD-28K (CB28K) results in the activation of p38(MAPK) in HT-22 cells.	159
Fig. 57:	Specific p38(MAPK) inhibition is toxic to primary cortical	

	cultures <i>via</i> MAO-A sensitive mechanism: contribution to the toxicity of the AD-related peptide, β -amyloid ($A\beta$).	161
Fig. 58:	The ROS production induced by AD-related peptide $A\beta$ was attenuated by specific MAO-A inhibition in HT-22 cells.	162
Fig. 59:	Inhibition of the ERK and PI3K pathways also enhance MAO-A activity, but not the response to Ca^{2+} .	163
Fig. 60:	Comparison of MAO-A and MAO-B amino acid sequences reveals a TXY motif that is specific to MAO-A.	165
Fig. 61:	Mutagenesis of tyrosine(Y35) in MAO-A affects MAO-A activity.	166
Fig. 62:	Schematic depicting how p38(MAPK) might protect the cell during a transient stress that involves an increase in Ca^{2+} and a corresponding increase in MAO-A activity.	168
Fig. 63:	Continued from Fig.62.	169

LIST OF ABBREVIATIONS

AADC	-	aromatic amino acid decarboxylase
AD	-	Alzheimer's disease
ADP	-	Adenosine diphosphate
AF	-	activated form
ALS	-	amyotrophic lateral sclerosis
amp ^R	-	Ampicillin-resistant gene
AMP	-	Adenosine monophosphate
APP	-	amyloid precursor protein
ASK	-	Apoptosis signal-regulating kinase
ATCC	-	American Type Culture Collection
A β	-	Beta amyloid
BCA	-	bicinchoninic acid
BCP	-	phase separation reagent
BMP	-	Bone morphogenetic protein
bp	-	base pair
BSA	-	Bovine serum albumin
cAMP	-	cyclic AMP
cDNA	-	complementary DNA
CLG	-	Clorgyline
CNS	-	Central nervous system
COMT	-	catechol-O-methyltransferase
CREB	-	cAMP response element-binding
CTL	-	Control
d.p.m.	-	disintegrations per minute
DAO	-	diamine oxidase
DCFH-DA	-	2,7-dichlorofluorescein diacetate
DEPC	-	diethylpyrocarbonate
DIV	-	days in vitro
DMEM	-	Dulbecco's Modified Eagle's Medium
DMSO	-	dimethyl sulfoxide
DN	-	dominant negative
DNA	-	deoxyribonucleic acid
dNTP	-	deoxyribonucleotide triphosphate
DOPEGAL	-	dihydroxy-phenylglycolaldehyde
dsDNA	-	double-stranded DNA
DSS	-	disuccinimidyl suberate
DTT	-	dithiothreitol

DYT	-	double-strength yeast extract/tryptone medium
EDTA	-	ethylenediaminetetraacetic acid
ER	-	endoplasmic reticulum
ERK	-	extracellular signal-regulated kinase
EtBr	-	ethidium bromide
ETOH	-	ethanol
FAD	-	flavin adenine dinucleotide
FBS	-	fetal bovine serum
GDNF	-	glial cell line-derived neurotrophic factor
GFAP	-	glial fibrillary acidic protein
GSH	-	glutathione
HBSS	-	Hank's balanced salt solution
HD	-	Huntington's disease
HEPES	-	4-(2-hydroxyethyl)-1-piperazineethanesulfonic acid
HMWC	-	high molecular weight complex
Hr	-	hour
HRP	-	horseradish peroxidase
IB	-	immunoblot
IP	-	immunoprecipitation
PFA	-	paraformaldehyde
JNK	-	Jun N-terminal kinase
Kb / kb	-	kilo-base pair
kDa	-	kilo-dalton
KGDHC	-	α -ketoglutarate dehydrogenase
LB	-	lysogeny broth
L-DOPA	-	L-3,4-dihydroxyphenylalanine
LPS	-	lipopolysaccharide
MAO	-	monoamine oxidase
MAO-A / -B	-	monoamine oxidase-A/-B isoform
<i>mao-A / -B</i>	-	monoamine oxidase-A/-B gene
MAPK	-	mitogen-activated protein kinase
min	-	minute
MK	-	MAPK-activated protein kinases
MNK	-	MAPK-interacting kinases
MPTP	-	1-methyl-4-phenyl-1,2,3,6-tetrahydropyridine
mPTP	-	mitochondrial permeability transition pore
mRNA	-	Messenger ribonucleic acid
MSK	-	mitogen- and stress-activated kinase
NA	-	noradrenaline
NE	-	norepinephrine
NGF	-	nerve growth factor

NHS	-	amine-reactive <i>N</i> -hydroxysuccinimide ester
nm	-	nanometer
NMDA	-	<i>N</i> -methyl- <i>D</i> -aspartic acid
NMR	-	Nuclear magnetic resonance
NRU	-	Neuropsychiatry Research Unit
PCIA	-	phenol/chloroform/isoamyl alcohol
PCR	-	polymerase chain reaction
PD	-	Parkinson's disease
PEA	-	phenylethylamine
PEG8000	-	polyethylene Glycol 8000
PEI	-	polyethylenimine
PKC	-	protein kinase C
PMA	-	phorbol 12-myristate 13-acetate
PAO	-	polyamine oxidase
PS	-	presenilin
PVDF	-	polyvinylidene difluoride
RCHO	-	Aldehyde
RIMA	-	reversible inhibitor of MAO-A
RNA	-	ribonucleic acid
RNAse	-	Ribonuclease
ROS	-	reactive oxygen species
RPM	-	revolution per minute
RT	-	reverse transcriptase
RT-PCR	-	reverse transcriptase polymerase chain reaction
RyR	-	ryanodine receptor
S	-	Serine
SAPK	-	stress-activated protein kinase
SB	-	SB203580
SDS-PAGE	-	sodium dodecyl sulfate polyacrylamide gel electrophoresis
sec	-	Second
SOC	-	transformation medium
SOD	-	superoxide dismutase
SSAO	-	semicarbazide-sensitive amine oxidase
STE	-	sodium/Tris-HCl/EDTA
TB	-	terrific broth
TBS	-	tris buffered saline
TBST	-	tris buffered saline with tween
TE	-	Tris-Cl/EDTA
TEMED	-	<i>N,N,N',N'</i> -Tetramethylethylenediamine
TH	-	tyrosine hydroxylase
<i>T_m</i>	-	melting temperature

TNF	-	tumor necrosis factor
TTP	-	Tritetraprolin
TUNEL	-	terminal deoxynucleotidyl transferase biotin-dUTP nick end labeling
UV	-	Ultra-violet
V	-	Volts
V _{max}	-	Maximal reaction speed
X _p	-	X chromosome of paternal origin
$\Delta\psi_m$	-	mitochondrial membrane potential

1 LITERATURE REVIEW

Monoamine amine oxidase, intracellular Ca^{2+} levels, and certain cellular signal transduction cascades, such as the p38(MAPK) pathway, are known to play important roles in the process of aging, in neuropsychiatric disturbances, and in neurodegeneration. In the present study, a new mechanism based on monoamine oxidase, p38(MAPK) and Ca^{2+} was characterized and shown to contribute to pathological cell function. This review of the literature will include a review of the MAO literature, a brief review of the relevant literature on the cellular effects and regulation of Ca^{2+} , and a brief review of the p38(MAPK) literature as it pertains to toxicity.

1.1 Monoamine oxidase

Monoamine oxidase (MAO) [amine: oxygen oxidoreductase (deaminating) (flavin-containing); MAO; E.C. 1.4.3.4] is an enzyme located on the outer membrane of the mitochondria in most cell types [1]. Its physiological function is the oxidative deamination of biogenic and xenobiotic monoamines in the central nervous system (CNS) and peripheral tissues. The general reaction is $\text{RCH}_2\text{NH}_2 + \text{H}_2\text{O} + \text{O}_2 \rightarrow \text{RCHO} + \text{NH}_3 + \text{H}_2\text{O}_2$, wherein oxygen is used to remove an amine group from a substrate molecule,

resulting in the generation of the corresponding aldehyde (RCHO), as well as ammonia (NH₃) and hydrogen peroxide (H₂O₂) (Fig. 1).

1.1.1 Discovery and nomenclature

The enzyme was first discovered in human liver tissue and due to the simultaneous oxidation and deamination of tyramine, was named tyramine oxidase [2]. Almost ten years later, it was established that epinephrine, norepinephrine, and dopamine were also substrates for this enzyme and it was renamed monoamine oxidase (MAO) [3]. MAO has two isoforms, MAO-A and MAO-B [4] that, although having evolved from the same ancestral gene [5], are encoded by two different genes [6] located tail-to-tail on the Xp 11.23-Xp 22.1 short arm [7, 8]. Both gene sequences are comprised of 15 exons and 14 introns that span at least 60 kb [5], resulting in a 70% sequence similarity in both genes [6].

1.1.2 Amine oxidase classification

Amine oxidases are classified on the basis of their chemical structures [9] and many can be categorized according to their co-factors. One group contains flavin adenine dinucleotide (FAD) and the other contains copper (Cu²⁺) and topaquinone as second cofactors. FAD-containing amine oxidases can be subdivided into mitochondrial monoamine oxidases (MAOs) and cytoplasmic polyamine oxidases. Copper-containing amine oxidases are often named according to their specific substrates, such as

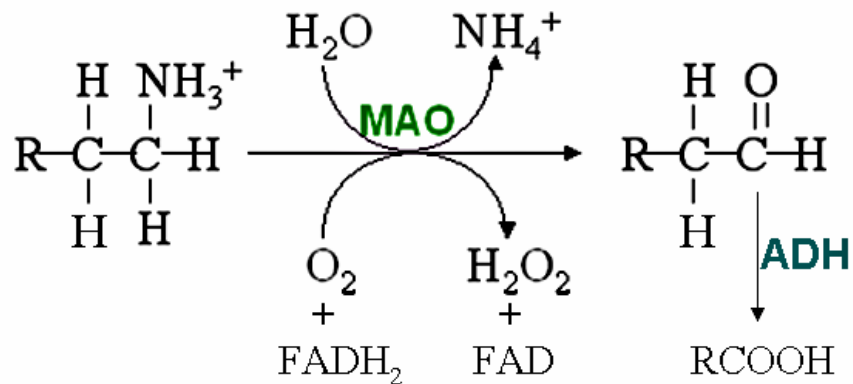


Fig. 1: Reaction pathway of monoamine metabolism by oxidative deamination by mitochondrial MAO. The primary product of MAO acting on a monoamine is the corresponding aldehyde. The aldehyde is rapidly further oxidized by aldehyde dehydrogenase (ADH) to a carboxylic acid, which is the final excreted metabolite. Note that the FAD-FADH₂ cycle generates hydrogen peroxide which itself requires inactivation by catalase or, in the brain, glutathione peroxidase.

semicarbazide-sensitive amine oxidase (SSAO) [10], which can be inhibited by cyanide and semicarbazide [11]. These amine oxidases have their own specific substrates and inhibitors. For example, SSAO is not inhibited by clorgyline and deprenyl, which are specific MAO inhibitors [12].

1.1.3 Specificities of inhibitors and substrates, and tissue distribution of MAOs

The two MAO isoforms differ in their specificities for inhibitors [13-15] and substrates [4, 12, 15, 16], as well as in their cellular and tissue distributions [17-20]. MAO-A is inhibited by clorgyline at low concentrations, with recovery of MAO-A activity and protein levels within 14 days [21], and metabolizes serotonin, noradrenaline, and adrenaline. MAO-B is inhibited by l-deprenyl at low concentrations, and metabolizes benzylamine and beta (β)-phenylethylamine. Clorgyline and deprenyl do not exert any significant influence on other amine oxidases, such as diamine oxidase and SSAO [12]. In humans, dopamine is metabolized by MAO-B [22] or by both isoforms [23] and in rats by MAO-A [4, 24]. In most species, dopamine, tyramine, and tryptamine are common substrates for both MAO isoforms [15, 25, 26]. However, this is not an absolute rule, as under different conditions and in different species various biogenic amines can be metabolized by both forms of MAO [16]. For example, both enzymes show broader substrate preference at a high substrate concentration [12]. Furthermore, the xenobiotic and dopaminergic toxin 1-methyl-4-phenyl-1,2,3,6-tetrahydropyridine (MPTP) can be

oxidized by MAO-B to form a neurotoxic substance, MPP⁺, that can cause permanent Parkinson-like symptoms in human, although not in rodents [27-29].

The distribution of MAO-A and MAO-B in various tissues of different species has been investigated using specific inhibitors in combination with immunohistochemical, enzyme autoradiographic, and *in situ* hybridization techniques. MAO has been detected in rodent, cat, rabbit, cow, dog, gerbil, monkey, and human brain tissues [17-20, 30-42]. In the human brain, MAO-A exists predominantly in catecholaminergic neurons, while MAO-B is found in serotonergic neurons and glial cells [18, 30, 43-45]. The role of MAO in these mismatching regions may protect neurons from stimulation by oxidizing extraneous amines that can act as false neurotransmitters [30, 43]. In the brain, the highest expression of MAO-A is found in the locus coeruleus, whereas the highest expression of MAO-B is found in the raphé nuclei [18, 46]. Studies on MAO activity in the human brain reveal region-specific levels. For example, MAO-A activity occurs in the locus coeruleus, the nucleus subcoeruleus, and the medullary reticular formation > hypothalamus > amygdala > hippocampus > accumbens > substantia nigra > frontal cortex > cerebellum, whereas MAO-B activity occurs in the raphé nuclei > nucleus centralis superior > hypothalamus, accumbens > caudate, hippocampus > amygdala > substantia nigra > frontal cortex > cerebellum [30, 38]. In peripheral tissues, the two MAO isoforms often co-localize. Indeed, the regional distribution patterns of MAO-A and MAO-B do not differ markedly, except in the kidney and in the duodenum. The highest level of MAOs is found in the liver and the lowest in the spleen. In lung and

duodenal mucosa, MAO-A is more abundant than MAO-B, and in myocardium more MAO-B is found than MAO-A [32, 47]. Finally, the human placenta predominantly expresses MAO-A [21], whereas human platelets and lymphocytes express only MAO-B [48].

The distribution of mRNA transcripts of MAO-A and MAO-B in human fetal tissues also varies, with relative concentrations for MAO-A being: small intestine \geq placenta \geq lung \geq muscle \geq kidney \geq brain \geq spinal cord \geq meninges \geq liver $>$ spleen $>$ adrenal gland; and for MAO-B, small intestine $>$ kidney \geq liver $>$ adrenal gland $>$ heart $>$ spinal cord $>$ lung [17, 47].

The widespread tissue distributions of MAO mRNAs, proteins and respective activities do not always directly correlate.

1.1.4 MAOs change during development and aging

The study of MAOs during development and aging is very important as it is believed that monoamine neurotransmitters play an important role during morphogenesis [49-52]. At very early stages of neural tube formation, neurotransmitter monoamines act as multifunctional regulators by acting on second messenger systems. After neurulation, these neurotransmitters play an important role, not only in normal neural transmission, but also in neural differentiation and morphogenesis. As such, any change in MAO responsible for metabolizing these important monoamine neurotransmitters would have vital influences on brain structural and functional development [53]. Northern blot

analysis on the human fetal brain (19 weeks) reveals that MAO-A and MAO-B mRNA are expressed in similar brain regions [17], although the level of MAO-A transcript is generally higher than that of MAO-B. In the human fetal brain, activity of MAO-A presents well before that of MAO-B, and MAO-A activity is almost at adult levels at the time of birth, with little or no increase with aging. In contrast, MAO-B activity is low at birth, but increases steadily with aging [54-57]. MAO activity in rodents shares the same pattern as that in humans. In the brains of rats and mice, MAO-A activity shows a clear decrease between 4 and 9 weeks, a stable level between 9 weeks and 19 months, and a slight increase between 19 and 25 months, whereas MAO-B activity shows an age-related increase [34, 46]. This increase in MAO-B activity with aging may be attributed to the proliferation of glial cells, which is the cell type where MAO-B is predominantly expressed [58]. MAO-A is predominantly expressed in neuronal cells, whose overall number decreases with aging and even more so during neurodegeneration [59]. If this is the case, then little or no increase in total MAO-A activity within the aging brain suggests that MAO-A activity must increase in each remaining neuron.

1.1.5 Cloning of human MAO

The MAO isoforms were sequenced from human liver [6]. Both proteins, when overexpressed in mammalian cells, displayed similar specificities for substrates and inhibitors as their endogenous counterparts [60]. The deduced amino acid sequences of MAO-A and MAO-B consist of 527 and 520 amino acids with molecular weights of 59.7

kDa and 58.8 kDa, respectively, and a 70% sequence similarity. Examination of the primary structure of cloned MAO-A and MAO-B revealed that they are products of two separate genes. Northern blot analysis with MAO-A or -B cDNA probe reveals that the size of *mao* mRNA transcripts in human tissues corresponds with the cloned cDNAs [6]. Moreover, it has been demonstrated the cloned *mao-B* from human platelet is identical to that in the frontal cortex, thus providing a valid [peripheral] biological marker for determining the function of neuronal MAO-B in the human population [61].

1.1.5.1 The MAO promoter

To understand the mechanism for regulation of transcription and cell and tissue distribution specificities of MAO-A and MAO-B, the promoter regions of their respective genes, *mao-A* and *mao-B*, have been extensively investigated. The maximal promoter activity is found in a 0.14 kb fragment for *mao-A* and a 0.15 kb fragment for *mao-B*. Both are GC-rich, containing Sp1 binding sites. The *mao-A* promoter fragment contains three Sp1 sites in reverse orientations and lacks a TATA box, which is often associated with down-regulation of promoter activity. Two of the Sp1 sites are located within the downstream 90 base pair (bp) direct repeat and the third one is at the 3'-end of the upstream 90 bp direct repeat. In contrast, the *mao-B* fragment contains a Sp1-CACCC-Sp1-TATA structure and deletion of any of these elements reduces promoter activity. Additional Sp1 sites, CACCC elements, CCAAT boxes, and direct repeats (four 30 bp direct repeats in *mao-A* and two 29 bp direct repeats in *mao-B*) are

found in both gene sequences farther upstream of the promoter [62]. Using the Sp1 motif of *mao-A* as a bait, a novel controlling factor of *mao-A* promoter activity (R1) has been cloned and shown to repress *mao-A* promoter activity resulting in down-regulation of enzyme activity [63]. Moreover, the different organization of promoters may explain the varying responses of MAO-A and MAO-B to stimulation. For example, phorbol 12-myristate 13-acetate (PMA, a known activator of PKCs) treatment elevates *mao-B* gene and protein levels, while *mao-A*/MAO-A remains constant [64].

1.1.5.2 Three dimensional structure of MAO-A and MAO-B and their important domains

MAO-A and -B cDNAs have been cloned from human, rat, mouse, rabbit, and bovine species. Comparison of the gene sequences of *mao-A* and *mao-B* across species reveals an 87% sequence similarity [65] as well as several functional motifs that contain highly conserved amino acid residues critical for substrate binding, an active site, co-factor flavin adenine dinucleotide (FAD) binding sites, and other binding sites for other factors, such as imidazoline binding sites (Fig. 2).

1.1.5.2.1 Important amino acid residues in MAO

In 2001, a study demonstrated that a single amino acid residue, MAO-A (Ile-335) and MAO-B (Tyr-326), can switch substrate specificities and sensitivity to selective inhibitors between the corresponding enzymes [66, 67]. Phe-208 in rat MAO-A and

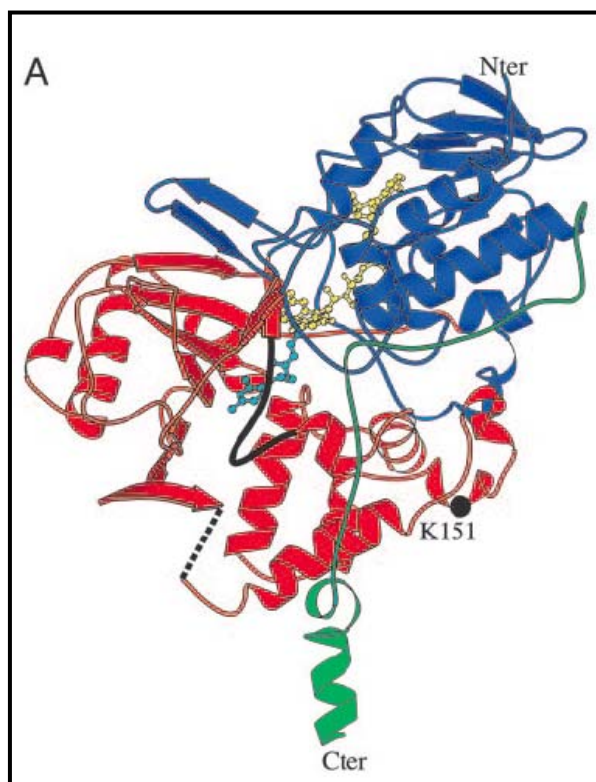


Fig. 2: 3-D structure of hMAO-A (similar to that of MAO-B). Ribbon representation of the MAO-A monomer. The FAD-binding domain (residues 13 – 88, 220 – 294, and 400 – 462) is shown in blue; the substrate-binding domain (89 – 219 and 295 – 399) is shown in red; and the C-terminal membrane region (463 – 506) is shown in green. Residues 1 – 12, 111 – 115, and 507 – 527 are not visible in the electron density map. A dashed line connects residues 110 – 116. FAD and clorgyline are represented by the yellow and light-blue “ball-and-stick” format, respectively. The active site cavity-shaping loop 210 – 216 is depicted as the thick black line [*Used with permission: De Colibus et al. (2005) Three-dimensional structure of human monoamine oxidase A (MAO A): Relation to the structures of rat MAO A and human MAO B. PNAS 102: p12684-9*].

Ile-199 in rat MAO-B are also reported to contribute to substrate and inhibitor specificities [68], although mutations of these two corresponding residues in human MAOs do not cause this switch [69]. It is also reported that in human MAO-A, Lys-305, Trp-397, Tyr-407, and Tyr-444 and their corresponding amino acids in human MAO-B, *e.g.*, Lys-296, Trp-388, Tyr-398, and Tyr-435, play important roles in MAO catalytic activity. The crystal structure further revealed that Lys-305, Trp-397, and Tyr-407 in MAO-A and Lys-296, Trp-388, and Tyr-398 in MAO-B may contribute to FAD binding. Tyr-407 and Tyr-444 in MAO-A (Tyr-398 and Tyr-435 in MAO-B) may be involved in stabilizing the substrate binding, while Asp-132 in MAO-A (Asp-123 in MAO-B) located at the loop of the substrate-binding site has no effect on MAO-A or MAO-B catalytic activity [70].

1.1.5.2.2 FAD binding sites in MAO

Oxidation of amines by MAO is coupled to the reduction of FAD, an essential cofactor. Comparison of MAO-A and MAO-B sequences from many species reveal several regions in MAO-A and MAO-B that are highly conserved (78~86%) [71]. These regions include a nucleotide-binding site near the amino terminal end that is found in the majority of enzymes that require FAD, and an FAD-binding site near the carboxy-terminal region. The location of an ADP-binding fold in the amino terminal region suggests this region is also involved in FAD binding [72]. FAD initially binds to the non-covalent flavin-binding regions near the amino-terminal region and, subsequently,

is covalently bound to Cys-406 in MAO-A and Cys-397 in MAO-B [73]. Another FAD-binding site around residues 222-227 of MAO-B in many species is highly conserved, and residues Gly-226 and Asp-227 are required for covalent flavinylation and catalytic activity of MAO-B, but not for non-covalent binding of FAD [74]. A functional study of all nine cysteines in human MAO-A and MAO-B reports that the MAO-A (Cys374Ser) and MAO-B (Cys397Ser) substitution mutants abolish the full catalytic activity, possibly due to the prevention of covalent binding of FAD [75].

1.1.5.2.3 Crystal structure of MAO

The study of the three-dimensional structure of MAO has advanced due, in large part, to investigations using selective irreversible inhibitors [76]. There is much similarity between human MAO-A and MAO-B; one difference is that human MAO-B is dimeric, whereas human MAO-A crystallizes as a monomer [77]. Another difference is that the cavity-shaping loop is larger in human MAO-A than in human MAO-B or rat MAO-A (*note*: rat MAO-A crystallizes as a homodimer), suggesting that this cavity-shaping loop is involved in the process of dimerization [78].

1.1.5.2.4 Membrane insertion region of MAO

Studies on the membrane insertion region in rat liver MAO-B reveal that deletion of the 28 carboxy-terminal amino acids blocks the localization of MAO-B to mitochondria. The fused protein of cytochrome b5 with this carboxy-terminal 28 amino acids is found

expressed in mitochondria instead of remaining in cytoplasm [79], suggesting that the mitochondrial targeting signal of rat MAO-B is located within this region [79]. Similar studies on human MAO-B show that 30 amino acids within this region determine mitochondrial localization [80, 81]. Recently, crystallography has revealed that the carboxy-terminal amino acids 463-506 in human MAO-A are responsible for membrane anchoring [78].

1.1.5.2.5 Imidazoline binding site on MAO

Imidazoline is an active pharmacological compound known to interact with its own receptor and signaling pathways by interacting with a family of imidazoline-binding proteins. Evidence indicates that MAO-A and MAO-B contain a binding motif that makes both proteins imidazoline binding proteins [82, 83]. The imidazoline binding domain in human MAO-B is contained within residues K149-M222 [84], distinct from the active site which determines substrate and inhibitor binding [85]. Binding of imidazoline inhibits MAO activity independently of the interaction with the catalytic region [83, 86, 87].

1.1.5.2.6 Substrate and inhibitor recognition and binding domain (active site) in MAO

Inhibitor binding studies reveal that the MAO-A inhibitor clorgyline and the MAO-B inhibitor 1-deprenyl identically bind to N(5) of the FAD moiety (*recall*, FAD is the

enzyme co-factor). The binding site is the same in MAO-A and MAO-B, suggesting that differing specificity on both substrate and inhibitor is dependent on the presence of additional recognition sites, presumably near the active site, in each isoform. Studies of MAO structure-inhibitory relationships reveal that the MAO-B recognition site is smaller than that of MAO-A [13]. The size of the recognition site allows MAO-A and MAO-B to differentiate substrates, whereas additional differences in their amino acids explain the selective interaction with different inhibitors. The region between residues 120-220 and residues 50-400 is responsible for determination of the substrate preference of rat liver MAO-A and MAO-B, respectively, while the middle portion of residues 220-400 may contribute to the relative catalytic activity towards their respective substrates [88]. Furthermore, crystal structures of the cavity-shaping loop at residues 210-216 in human MAO-A and 201-206 in human MAO-B [78] indicate that these may also contribute to substrate recognition, while residues 89-219 and 295-399 of human MAO-A may contribute to substrate/inhibitor-binding domains [78]. This supports the observation that the deletion of carboxy-terminal amino acids in human MAO-A loses the enzyme activity [80, 89] and explains why replacement of the carboxy-terminal amino acids of MAO-B with those of MAO-A imparts MAO-A activity and inhibitor specificity to the MAO-B protein [90].

1.1.6 Neurotransmitter and behavioral changes in MAO-A or MAO-B knock-out models

Examinations of MAO-A and/or MAO-B knock-out mice have clearly linked alterations in neurotransmitter metabolism to behavioral changes [91, 92]. Compared to their wild-type litter mates, MAO-A knock-out mice have increased levels of serotonin (5-HT), norepinephrine, and dopamine in the frontal cortex, hippocampus, and cerebellum [93]. Similar changes are observed in mice treated prenatally with MAO-A inhibitors [94], as well as in MAO-A-deficient men (this syndrome is called Brunner syndrome) in a large Dutch kindred [95, 96], all of which manifest aggressive behavior [92, 95]. Males with Brunner syndrome are deficient in MAO-A due to a mutation at C936T in exon 8, resulting in a premature termination, *i.e.*, “stop”, codon [8, 96, 97]. MAO gene deletion is also associated with Norrie disease, which manifests as eye problems, mental retardation, and regression. The proximity of the two *mao* genes on the X chromosome can facilitate conditions where both genes are affected, predisposing to the disease [8, 98].

Recently, overexpression of MAO-A, specifically in the forebrain of MAO-A knock-out mice, has been shown to restore somatosensory cortex organization similar to that seen in wild-type mice and to abrogate aggressive symptoms associated with the MAO-A knock-out genotype, apparently by replenishing levels of 5-HT, noradrenaline and possibly dopamine [99]. This study confirms that the neurotransmitters play important roles in the early stage of neuronal development [51].

MAO-B knock-out mice do not manifest any change in behavior, but do present elevated levels of the MAO-B preferred substrate, phenylethylamine (PEA). Moreover, MAO-B knock-out mice are resistant to MPTP/MPP⁺-induced Parkinson-like pathology [91, 100]. MAO-A knock-out mice present some disruption of emotional learning, such as the classical fear conditional and step-down inhibitory avoidance, resulting from the chronically elevated noradrenaline and 5-HT levels [93]. Thus, both MAO-A knock-out or MAO-B knock-out mice provide a valuable tool with which to study of the role of MAO in neuropsychiatric and neurodegenerative disorders.

1.1.7 MAO and related neurological disorders

The ability of the MAO isoforms to produce the free radical substrate H₂O₂ as a by-product of neurotransmitter catabolism has drawn much attention to these enzymes during the study of aging, neurodegenerative diseases, and psychiatric and behavioral traits.

1.1.7.1 MAO-A inhibition and neuropsychiatric disorders

The altered levels and imbalance of neurotransmitters in the CNS, especially 5-HT, noradrenaline, and other MAO-A preferred monoamines, induce evident psychiatric and behavioral changes: MAO-A inhibition is effective in many neuropsychiatric disorders,

such as depression/aggression [91], smoking [101, 102], alcoholism [103], and schizophrenia [104].

1.1.7.1.1 Depression

Depression is a state of intense sadness, melancholia, or despair that develops to the point of being disruptive to an individual's social functioning and/or activities of daily living. It is a chronic, recurring, and potentially life-threatening illness that affects about 7-18% of the worldwide population [105]. Clinically diagnosed depression is currently one of the leading causes of disability in many countries. In patients with depression, as well as in animal models of depression, levels of 5-HT and noradrenaline (both MAO-A substrates) are lower than normal [106]. MAO inhibitors were the first class of antidepressant agents to be developed and were commonly used from the 1960s until the mid-1980s [107]. However, these drugs presented serious side effects and food-/drug-drug interactions. This, in addition to a better understanding of the neurobiology of depression, led to the development of alternative therapeutic approaches, including novel MAO inhibitors, selective serotonin (or noradrenaline) re-uptake inhibitors, tricyclic antidepressants, triple monoamine re-uptake inhibitors, omega-3 fatty acids, melatonergic agonists, and receptor antagonists for corticotrophin-releasing factor, glucocorticoid, substance-P, and NMDA receptors [108]. Developments in therapeutic focal brain stimulation, including vagus nerve stimulation, transcranial magnetic stimulation, magnetic seizure therapy, and deep brain stimulation are also being

considered [109]. The role of psychotherapy, both as monotherapy and as adjunct therapy, is also an active avenue of investigation [110].

1.1.7.1.2 MAO-A inhibition and depression

1.1.7.1.2.1 The development of MAO-A inhibitors

Many of the original antidepressants were developed based on the structures and the functions of the monoamine oxidase inhibitor iproniazid and the tricyclic agent imipramine [111]. The antidepressant profiles of monoamine oxidase inhibitors were determined serendipitously [112].

As a means of mood elevation, MAO inhibition was revealed during the late 1940s with compounds including isoniazid that were being used to treat tuberculosis patients. Many of the treated patients experienced an episode of mood-elevation while taking these drugs. In the 1950s during clinical trials, it was ultimately determined that these drugs could inhibit MAO activity [113]. Treatment of depression quickly began to rely on MAO inhibitors (MAOIs).

1.1.7.1.2.2 Types of MAO inhibitors

The first generation of MAOIs was non-selective, irreversible, caused severe side effects, including dizziness, sedation, insomnia, weight gain, dry mouth and sexual dysfunction, and included a risk of food/drug-drug interactions, such as severe hypertension after intake of tyramine-rich foods. This latter phenomenon, termed the

“cheese effect” was associated with aged and fermented foods, such as cheese and wine, which contain large amounts of tyramine. Tyramine is normally degraded by MAO-A and MAO-B in the gut and liver, but with irreversible MAO inhibition tyramine cannot be properly metabolized and, subsequently, enters the CNS where it affects noradrenergic neurons and increases the release of noradrenaline, resulting in potentially fatal increases in heart rate and blood pressure. These side effects severely hampered the use of the first generation of MAOIs in the clinic.

The second generation of MAOIs was selective, but still irreversible, with clorgyline being the representative MAO-A inhibitor and l-deprenyl (also called selegiline) being the representative MAO-B inhibitor. Chronic treatment with clorgyline, but not l-deprenyl, results in the reduction of dihydroalprenolol binding (to β -adrenergic receptors) and cyclic AMP response to noradrenaline in the rat cortex, and the elevation of cytoplasmic and synaptic noradrenaline and 5-HT, which mediates pre- and post-synaptic receptor changes [13]. However, its use in the clinic was still hampered by the “cheese effect”.

The third generation of MAOIs is selective and reversible. Moclobemide is a reversible inhibitor of MAO-A (RIMA). The great advantage of RIMAs is that they are safe to use, as their reversibility avoids the “cheese effect”. Tyramine ingested in food can easily replace the RIMA from MAO-A and get metabolized by both the “liberated” MAO-A and by the intact MAO-B (RIMAs do not target MAO-B in the gut or liver).

Another type of MAO inhibitor with cholinesterase inhibition is N-propargyl-3R-aminoindan-5yl-ethyl methylcarbamate (TV-3326). The chronic oral administration of this compound inhibits cholinesterase as well as neuronal MAO-A and MAO-B activity, but has no effect on the small intestine in rats and rabbits. This new inhibitor is the most promising medication in the treatment of depression and dementia in both Alzheimer's disease (AD) and Parkinson's disease (PD) [114].

1.1.7.1.2.3 MAO-A inhibition in depression

MAO-A inhibitors are effective in the clinical treatment of depression, but their association with side-effects and the interactions with food and other drugs made them less appealing for use in the clinic, gradually being replaced by tricyclic antidepressants and selective serotonin reuptake inhibitors [110, 115].

1.1.7.2 MAO inhibition and neurodegenerative diseases

1.1.7.2.1 Overview of neurodegenerative diseases

Neurodegenerative diseases consist of a group of CNS disorders characterized by the gradual and progressive loss of structure and/or function of neurons, mostly resulting from death of neurons [116]. Neuronal death often begins long before the patient experiences any symptoms, which become more noticeable when many cells have died and certain parts of the brain can no longer function properly. Several etiologies can be cause for the initiation of neurodegeneration, including stroke, heat stress, trauma,

bleeding, and inflammation, among others. Depending on the part of the brain affected by neurodegeneration, a different diagnosis and disease will prevail. For example, the death of hippocampal and cortical neurons is responsible for the symptoms of AD; the death of midbrain dopaminergic neurons is responsible for the symptoms of PD; the death of striatal neurons which control body movement results in Huntington's disease (HD); and the loss of motor neurons in the spinal cord results in amyotrophic lateral sclerosis (ALS).

1.1.7.2.2 Molecular mechanisms well-known for neurodegeneration

Over the past several decades, there have been many studies on the molecular mechanisms of neurodegeneration, with the following corresponding hypotheses:

- 1) Oxidative stress: cytotoxic free radicals generated from oxidative reactions lead to cell damage and cell death.
- 2) Calcium homeostasis: disruption of calcium (Ca^{2+}) homeostasis and sustained increases in cytosolic-free Ca^{2+} can lead to cell death.
- 3) Mitochondrial abnormalities: the function of the mitochondrial respiratory enzyme chain is directly impaired.
- 4) Excitotoxicity: excessive excitation is harmful to cells and results in death.
- 5) Immunologic mechanism: autoimmune mechanisms are responsible for a variety of neurological diseases.
- 6) Infectious agents: different infectious agents can cause degeneration.

- 7) Toxins: MPTP/MPP⁺, carbon monoxide, cyanide, manganese, carbon disulfide, and organophosphates directly cause neuronal death.
- 8) Protein misfolding: improper post-translational modifications cause protein misfolding, which precludes recognition or degradation by ubiquitination, resulting in the deposition in the extracellular or intracellular environment which might be toxic to neurons.
- 9) Trace metal level alteration: accumulation of iron or aluminum and other trace metals or the reduction of selenium or magnesium can directly influence the functions of neurons.

1.1.7.2.3 Parkinson's disease

1.1.7.2.3.1 Brief overview

Parkinson's disease (PD) was first described by James Parkinson in 1817 and is the second most-prevalent neurodegenerative disorder in the western world, with a prevalence of 1% at 65 years and 5% at 85 years [117]. Although the etiology of PD is still unknown, it is characterized by the selective and progressive loss of dopaminergic neurons resulting in the depigmentation of the substantia nigra [118, 119]. The depletion of dopamine within the striatum results in the dysregulation of motor functions, thus inducing the clinical symptoms classically associated with PD, including slowness of movement, muscular rigidity, resting tremor, and postural instability [120]. Controlling symptoms by the manipulation of an exogenous dopamine precursor

L-3,4-dihydroxyphenylalanine (L-DOPA) is the basis of therapy for this disease [121]. Subsequent advances in therapy included combining L-DOPA with a peripheral decarboxylase inhibitor to allow more L-DOPA to enter the brain and, similarly, catechol-O-methyltransferase (COMT) inhibition to prolong the half-life of L-DOPA and dopamine. However, these cannot prevent progression of the disease. A better understanding of the neuropathology of PD and the need for new treatment strategies has led research into MAO inhibition, dopamine receptor agonism, glutamate antagonist therapy, antiapoptotic approaches, mitochondrial protection therapy, free radical scavenger therapy, gene therapy, neurotrophic factor therapy, stem cells, neurotransplantation, and neurosurgery as possible courses of action [120, 122].

1.1.7.2.3.2 MAO inhibition and Parkinson's disease

MAO-B inhibition is routinely used in the clinical treatment of PD. Dopamine is a common substrate for MAO-A and MAO-B, but in human basal ganglia, MAO-B is much more abundant. A strong basis for the eventual clinical use of l-deprenyl in PD patients began with experimentation in the 1970s [123] and was championed by the observation that l-deprenyl in combination with L-DOPA slowed down the progress of degeneration of dopaminergic neurons better than L-DOPA alone, without adverse effects such as the “cheese effect” [124-126]. Involvement of MAO-B was confirmed with the pro-neurotoxin N-methy-4-phenyl-1, 2, 3, 6-tetrahydropyridine (MPTP) that can be transformed to MPP⁺ by MAO-B and is toxic to dopaminergic neurons in the

substantia nigra in animal models, resulting in PD-like neurodegeneration. Pretreatment with l-deprenyl protects these neurons [27, 28] and MAO-B knock-out mice are resistant to MPTP-induced neurotoxicity [58]. MAO-B inhibition remains a valid treatment in PD.

Recent research evidence demonstrates that the effect of l-deprenyl on protecting the cells confronted with apoptotic stimulations may be independent of inhibition of MAO-B activity since neuroprotection is associated with concentrations of the drug that are too low to inhibit the enzyme [127, 128]. These so-called neuroprotective effects of l-deprenyl and related compounds, such as rasagiline, include activation of Bcl-2 family members, elevation of SOD and GSH levels, up-regulation of tyrosine hydroxylase (TH) and aromatic amino acid decarboxylase (AADC) [129-132], interactions with the mitochondrial pore complex, and modulation of amyloid precursor protein cleavage [133-135].

Recently, RIMAs such as moclobemide have been used to treat PD patients because of the limited side effects associated with them, particularly the diminished tyramine-associated “cheese effect” [136]. An additional factor is that MAO-A is also responsible for dopamine metabolism *in vivo*. In autopsied brains of patients who received clorgyline or l-deprenyl prior to death, dopamine levels are not as elevated as much as those of 5-HT, noradrenaline, and PEA, suggesting that the two isoforms of MAO are redundant in terms of dopamine metabolism [124, 137, 138]. Additionally, treatment with moclobemide increases dopamine release in rodent brains [136] and improves motor functions in PD patients [139]. Another advantage of RIMAs, such as

moclobemide [140], brofaromine [141], and befloxtone [142], is that dopamine in excess of that required for the binding to its receptors can displace moclobemide and get degraded [107].

Moclobemide is also used to treat PD patients, due to its anti-depressant properties. 20-40% of PD patients also suffer from depression as a result of significant reductions of noradrenaline in the locus coeruleus and of 5-HT in the raphé nucleus, levels of which are enhanced following treatment with moclobemide [143].

1.1.7.2.4 Alzheimer's disease

1.1.7.2.4.1 Brief overview

Alzheimer's disease is the most prevalent of the neurodegenerative disorders, perhaps as a consequence of an ever-increasing aged population. AD affects 2-3% of people aged 65 years, with a prevalence that doubles every five years after the age of 65 and increases drastically to 25-50% in people aged 85 years. It is reported to affect more than 24.3 million people worldwide, with 4.6 million new patients every year. The number of people afflicted with AD doubles every 20 years, with the total expected to reach 81.1 million by 2040 [144, 145].

This neurodegenerative disorder is named after the German psychiatrist, Dr. Alois Alzheimer. In 1901, one of his patients, Mrs. Auguste D., was the first person to be diagnosed with AD. This disease is characterized by the onset of a progressive impairment of memory, associated with cognitive impairment, declining ability to

perform daily activities, and neuropsychiatric symptoms, or behavioral changes. The earliest symptom is loss of memory, *i.e.*, forgetfulness, which deteriorates as the disease progresses. Gradually, cognitive impairment, such as loss of attention, recognition and decision-making, combines with dysfunction of language, movement control, and dementia. Three pathological changes are observed in AD patient brains: (1) prominent neuronal loss in temporoparietal and frontal cortex; (2) extracellular amyloid plaques composed of beta-amyloid ($A\beta$); and (3) intracellular neurofibrillary tangles composed of hyperphosphorylated tau. The exact etiology is still unknown, but according to epidemiological and genetic studies, 5-10% of cases are identified as an autosomal dominant disorder leading to familial [early onset] AD that presents before the age of 65 [146]. These cases are linked to mutations in the amyloid precursor protein (APP) and presenilin (PS) genes, and these mutations have all been linked to increased $A\beta$ production. However, the majority of cases are sporadic [late onset] AD and thought to result from an interaction between genetic and environmental risk factors during the process of aging [145]. A large study based on 11884 pairs of twins revealed that the influence of heritability for sporadic AD is up to 80% in both females and males [147].

The actual molecular mechanisms of AD could include $A\beta$ production and its aggregation and deposition within plaques, tau hyperphosphorylation with tangle formation, oxidative stress, neurotransmitter disturbances, excitotoxicity, mitochondrial dysfunction, inflammatory processes, and neurovascular dysfunction [145, 148-150]. Based on these hypotheses, a variety of treatments have been used in the clinic, including:

acetylcholinesterase inhibitors to maintain the level of acetylcholine in both hippocampus and neocortex where it is important for memory formation [151]; NMDA receptor antagonists to prevent neuronal excitotoxicity induced by glutamate/NMDA receptor activation [152]; secretase modulators, for example, β -secretase inhibitors [153], γ -secretase inhibitors [154], and/or α -secretase activators [155] to “force” APP processing down the non-amyloidogenic pathway (thereby reducing A β production) [156]; A β fibrillization inhibitors, such as small peptides (these would prevent the toxic β -sheet conformation of A β , by inhibiting the interaction of A β with various modulators) [157]; copper and zinc chelators (prevent the effect of metal ions on A β deposition) [158]; anti-tau drugs (decreasing phosphorylation of tau proteins) [159, 160]; anti-oxidants [149]; estrogen supplements [161]; anti-cholesterol drugs [162]; anti-inflammatory drugs [163]; A β immunotherapy [164]; and MAO inhibitors [165, 166].

1.1.7.2.4.2 Oxidative stress in Alzheimer’s disease

Besides A β toxicity and tau hyperphosphorylation, oxidative stress is another well-accepted causal factor in AD pathology. Oxidative stress results from an imbalance between the production of reactive oxygen species (ROS) and the system’s ability to detoxify the ROS or to repair ROS-induced damage (*i.e.*, lipid peroxidation and DNA damage). This often occurs when the body’s antioxidant defenses are unable to cope with a large free radical load. An important source of ROS is the mitochondrion, which

produces these radicals during normal oxidative respiration. Another important source is H₂O₂-generating enzymes, such as MAOs (Fig. 3). There is a great deal of evidence suggesting that oxidative stress plays a crucial role in the initiation and progression of AD [148, 149]. This is supported by the observation that ROS, such as H₂O₂, can mediate A β neurotoxicity [167] and by the elevated oxidative damage in transgenic mouse models of AD [168, 169].

1.1.7.2.4.3 MAO inhibition in Alzheimer's disease

Both neuronal MAO-A and MAO-B have been implicated in AD. MAO-B activity and mRNA have been reported to be increased in platelets of AD patients [170, 171], as well as in the hippocampus, thalamus, and cerebral cortex, which are regions that undergo much neuronal cell death during AD [172, 173]. The MAO-B increase is presumably due to the increase in glial cells in these areas, as MAO-B is mainly expressed in glial cells. These glial cells have been found in the proximity of A β plaques [43, 174, 175].

The contribution of MAO-A to AD is not as clear. Reports indicate that MAO-A activity and mRNA are elevated in several AD brain areas including the occipital cortex, frontal lobe of neocortex, parietal cortex, and locus ceruleus [173, 176, 177], as well as caudate nucleus, thalamus and white matter [178]. Other reports indicate that total MAO-A activity decreases in AD brains [59, 176]. However, the 31% decreased MAO-A activity in locus ceruleus is demonstrated to be concomitant with a nearly 70~80%

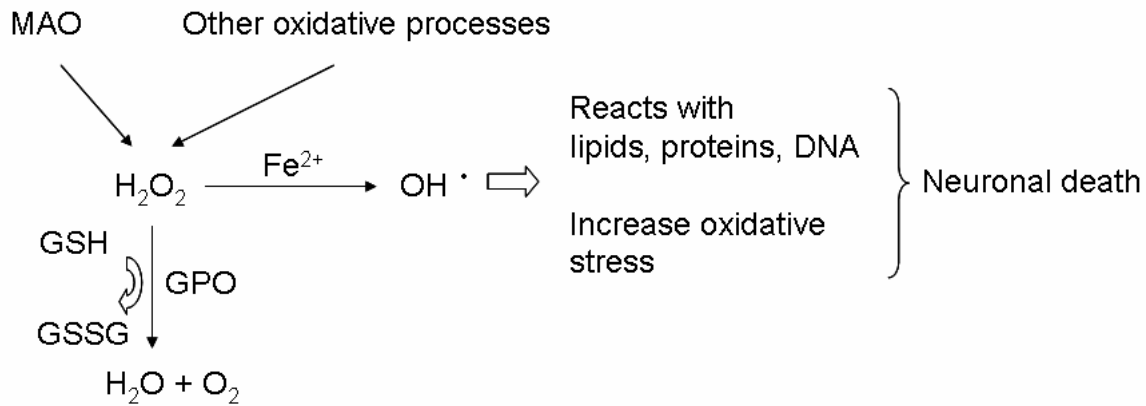


Fig. 3: The mechanism of neurotoxicity induced by iron and hydrogen peroxide via the Fenton reaction. Metabolism of monoamines by MAO is a source of hydrogen peroxide (H_2O_2) in the brain. Normally the H_2O_2 is then inactivated by glutathione peroxidase (GPO), but it can be converted, chemically, by Fe^{2+} ions (Fenton reaction) into the highly reactive hydroxyl radical. This radical has widespread deleterious effects which can cause neuronal damage and death. When GSH levels are low and MAO and Fe^{2+} are increased, the possibility of shuttling H_2O_2 via the Fenton reaction is correspondingly increased. Oxidative damage to neurons is a direct consequence of this reaction.

neuronal cell loss [59, 176, 179], which suggests that the average MAO-A activity per surviving neuron actually increases [176]. In AD patients, total MAO-A activity or the number of MAO-A immunoreactive neurons is further implicated in cognitive decline [59]. Moreover, 3,4-dihydroxy-phenylglycolaldehyde, the metabolic product of the action of MAO-A on norepinephrine, is increased in locus ceruleus, which is vulnerable during AD, thus further associating a toxic effect for MAO-A and neuronal loss in AD [179]. Estrogen, a neuroprotective hormone, can selectively decrease MAO-A activity and mRNA levels in many brain areas [180, 181], which further supports a contribution by MAO-A to neuronal cell death. In serum withdrawal-induced neuronal apoptosis, MAO-A activity is selectively increased as is the activation of the pro-apoptotic caspase-3 [182, 183]. H₂O₂ generated by MAO induces cell apoptosis in kidney [184], while MAO-A, not MAO-B, can bind with an endogenous neurotoxin, N-methyl(R)salsolinol, to reduce mitochondrial membrane potential ($\Delta\psi_m$), thus suggesting an additional means of inducing cell apoptosis [185]. These neurodegenerative mechanisms may all contribute to AD and PD.

mao-A, but not *mao-B*, gene polymorphisms are tightly associated with the neurological changes in AD [186]. In a recent study, *mao-A* gene polymorphism combined with serotonin transporter gene polymorphism and Apoε4 was clearly linked to late onset AD patients [187], indicating the synergistic potential of various risk factors in AD. Furthermore, administration of olanzapine (an atypical antipsychotic with

neuroprotective potential to AD-related toxicity [188]) significantly increased *mao-A* mRNA levels in rat frontal cortex [189].

MAO-A and MAO-B inhibition are both used as treatment strategies in AD. The MAO-B inhibitor l-deprenyl inhibits the accumulation of fibrillar A β [190]. It is also reported that l-deprenyl can reverse age-related memory impairment [191]. However, these neuroprotective effects may rely on mechanisms independent of MAO-B inhibition, as the concentrations used are lower than those required for MAO-B inhibition, yet they do stimulate nitric oxide production and vasodilatation [192] as well as block apoptosis [127, 131, 193]. MAO-A inhibitors, especially RIMAs, such as moclobemide, are mainly used in the treatment of cognition impairment and depression in AD patients [194].

These combined data support important roles for MAO-A and MAO-B in neuropsychiatric and neurodegenerative disorders. Although the exact mechanisms involved remain unclear, a valid assumption is that part of their effects rely on H₂O₂ production during the enzymatic reaction.

1.2 Intracellular Ca²⁺ signaling

1.2.1 Intracellular Ca²⁺ concentration and adjustment

Calcium is the most abundant mineral and cation in the body, accounting for approximately 1.5% of total body weight. 99% of calcium is stored in bones and teeth, and the other 1% is distributed between extracellular fluids and intracellular space, such as cytosol, mitochondria, endoplasmic reticulum, and nucleus [195]. In the extracellular

fluids, 46-50% of calcium is ionized as Ca^{2+} , which is the only bio-active form; 40% is combined with Ca^{2+} -binding protein such as albumin; less than 10% of Ca^{2+} is bound with citrate or phosphate and sulphate groups to make complexes. In resting cells, intracellular Ca^{2+} is maintained at a low concentration ($\sim 0.1 \mu\text{M}$), which is 10,000 times lower than that found extracellularly [195].

Ca^{2+} plays a crucial role in the anatomy, physiology, and biochemistry of cells and organisms, particularly in cellular signal transduction pathways. Therefore, the concentration of intracellular Ca^{2+} needs to be tightly regulated. When cells are stimulated, extracellular Ca^{2+} enters cells by voltage-dependent Ca^{2+} channels or receptor-operated channels, such as NMDA glutamate receptors, or storage-operated channels when storage in endoplasmic reticulum (ER) is low or depleted. Within the cells, a transient Ca^{2+} elevation can be sequestered by intracellular organelles, such as the endoplasmic reticulum, the mitochondrion, or the nucleus. Ca^{2+} also can be bound with numerous Ca^{2+} -binding proteins, such as calmodulin and calbindin D28K, which is an important buffering protein for Ca^{2+} in the brain [196]. Ca^{2+} extrusion through the plasma-membrane Ca^{2+} -ATPase and Na^+ - Ca^{2+} exchangers is another means of decreasing Ca^{2+} levels back to resting levels [197].

The ER and mitochondria are intracellular organelles that are bi-directional in that they are involved in both uptake and release of free Ca^{2+} , so as to control levels within the cytoplasm. This has been shown during many cellular functions, including gene expression, protein processing, neurotransmitter release, neuronal outgrowth, synapse

formation, and neuronal signal propagation (Fig. 4). The ER is important for the uptake of most of the elevated cytosolic Ca^{2+} (following influx) and it accomplishes this by way of Ca^{2+} pumps, named sarco- and endo-plasmic reticulum Ca^{2+} ATPases. The luminal concentration of free Ca^{2+} in ER can reach 1 mM [198, 199]. The mitochondrion is the second most important organelle associated with uptake of free Ca^{2+} by a specific Ca^{2+} carrier, a uniporter, which can be allosterically activated by Ca^{2+} . Although its molecular nature is still unclear [200], a recent patch clamp study suggests it as a Ca^{2+} -selective ion channel [201]. Its Ca^{2+} -uptake ability is also greater than previously believed as it has recently been shown to accumulate Ca^{2+} up to 800 μM in stimulated intact chromaffin cells [202]. Mitochondrial Ca^{2+} uptake is dependent on $\Delta\psi_m$ [203]. When a large local Ca^{2+} elevation by plasmic ion channels or Ca^{2+} release from the ER occurs, it will drive the mitochondrion to use the full respiratory capacity to accumulate Ca^{2+} [204, 205].

Various stimuli can also induce the release of Ca^{2+} from these organelles back to the cytoplasm to trigger or maintain cellular processes. The release of Ca^{2+} from the ER is initiated by the activation of receptors such as the inositol 1,4,5 triphosphate (IP3) receptor and the ryanodine receptor (RyR) on its membrane, the latter receptor being important for Ca^{2+} -induced Ca^{2+} release [206]. An additional process relies on the high Ca^{2+} concentration gradient between intra- and extra-ER environments that provides the driving force for Ca^{2+} release [207, 208]. Ca^{2+} release from the mitochondrion is operated by the Na^+ - Ca^{2+} exchanger [209, 210], the H^+ - Ca^{2+} exchanger [200, 211] and a transient

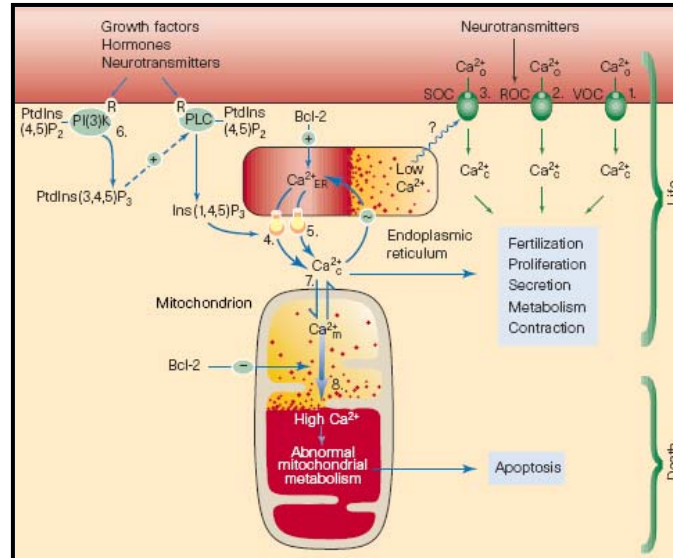


Fig. 4: Ca^{2+} signalling depends on Ca^{2+} from several sources. (in brief) Intracellular cytoplasmic Ca^{2+} (Ca^{2+}_c) levels can increase either from sources outside the cell (Ca^{2+}_o) or from stores within the endoplasmic reticulum (Ca^{2+}_{ER}). Ca^{2+}_o may enter through (1) voltage-operated Ca^{2+} channels (VOCs) in excitable cells such as neurons or muscle cells, or (2) receptor-operated Ca^{2+} channels (ROCs) in response to neurotransmitters. Storage-operated Ca^{2+} channels (SOCs; 3) open when the internal Ca^{2+} stores are depleted; these are mainly found in excitable cells. Ca^{2+}_{ER} is released by two types of channels. Inositol 1,4,5-trisphosphate ($\text{Ins}(1,4,5)\text{P}_3$) is generated by the action of the enzyme phospholipase C (PLC) on phosphatidylinositol 4,5- bisphosphate ($\text{PtdIns}(4,5)\text{P}_2$) at the plasma membrane, in response to the action of growth factors, hormones or neurotransmitters at receptors (R). $\text{Ins}(1,4,5)\text{P}_3$ acts on receptors in the endoplasmic reticulum (4), which cause the release of Ca^{2+}_{ER} from the store. Ryanodine receptors also mediate the release of Ca^{2+}_{ER} (5). Some of the Ca^{2+}_{ER} is rapidly taken up by the mitochondria (Ca^{2+}_m) and is then recycled to the endoplasmic reticulum (7). If the mitochondria become overloaded with Ca^{2+}_m , the result is abnormal mitochondrial metabolism (8), which may activate programmed cell death. (Used with permission: Berridge *et al.* (1998) *Calcium—a life and death signal*. **Nature** 395: p. 645-648)

formation of the mitochondrial permeability transition pore (mPTP) [212, 213], which is known to minimize the effect of toxic Ca^{2+} loads on the mitochondrion [205].

1.2.2 Ca^{2+} homeostasis and neuronal fate

Ca^{2+} homeostasis is the mechanism by which the body maintains proper Ca^{2+} levels by controlling the balance between Ca^{2+} entry from extracellular environment or release from intracellular organelles, and Ca^{2+} buffering, uptake, or extrusion systems. It is well known that many cell functions are sensitive to free intracellular Ca^{2+} concentrations and that Ca^{2+} is one of the most common second messengers modulating signal transduction in response to fluctuations in its availability. The transient rise of free intracellular Ca^{2+} is helpful to cell growth, secretion, metabolism, proliferation, gene expression, *etc.*, whereas sustained elevated levels of Ca^{2+} (improperly buffered or sequestered) will induce cell death by necrosis and apoptosis. Therefore, the modulation of Ca^{2+} signal demands precise regulation.

The first evidence that Ca^{2+} overload could lead to toxicity came from studies based on glutamate/NMDA receptor activation which clearly showed that a large Ca^{2+} influx led to neuronal cell death [214]. In addition, caffeine- and ryanodine-induced Ca^{2+} -release from the ER can also induce cell death [215]. Following the release of Ca^{2+} from the ER, the decrease in Ca^{2+} can activate stress signals that promote the expression of cell death-associated genes. The associated gene products (*i.e.*, proteins) often act to bind with Ca^{2+} in ER, which further decreases Ca^{2+} availability and initiates a detrimental

feed-forward cycle ending with cell death [216]. The release of Ca^{2+} from the ER can also activate the storage-operated Ca^{2+} channel on the plasmic cell membrane [217, 218], which aggravates the cytoplasmic Ca^{2+} level and increases the need for mitochondrial Ca^{2+} uptake. Anti-apoptotic protein Bcl-2 is already shown to maintain Ca^{2+} homeostasis in the ER [219] and mitochondrion [220]. Prolonged elevation of cytoplasmic Ca^{2+} can activate Ca^{2+} -dependent proteases, protein kinases, phospholipases, and endonucleases, which leads to protein and DNA damage and, ultimately, apoptotic cell death [221-223].

Recent evidence shows that toxicity associated with a cellular Ca^{2+} -overload is followed by a significant Ca^{2+} accumulation in mitochondrion that leads to the loss of $\Delta\Psi_m$, ROS production, mitochondrial permeability transition pore formation, and loss of ATP production [205].

Mitochondrial Ca^{2+} -uptake occurs when cytoplasmic Ca^{2+} concentration rise above 300 nM [203]. It first activates many dehydrogenases within the tricarboxylic acid cycle, resulting in the immediate production of ATP [224, 225]. As the accumulation of Ca^{2+} in mitochondria and the production of ATP are both dependent on the $\Delta\Psi_m$, the prolonged Ca^{2+} -uptake will eventually result in a decrease in $\Delta\Psi_m$, with influence on ATP production. Without efficient ATP production, the cell cannot maintain the ionic homeostasis (an ATP-dependent process) and the subsequent swelling ultimately leads to a loss of membrane integrity and necrosis.

An increase in mitochondrial Ca^{2+} enhances oxidative phosphorylation (Fig. 5). The ensuing generation of ROS is clearly a result of mitochondrial Ca^{2+} uptake as a disruption

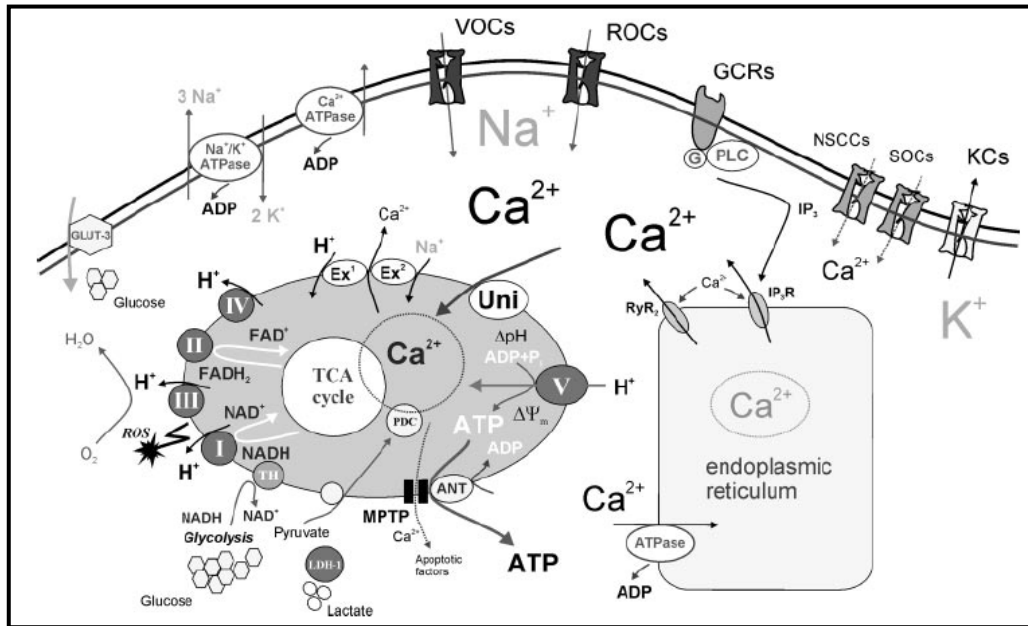


Fig. 5: Mitochondria-mediated generation of reactive oxygen species relies on Ca^{2+} . Highlights within this diagram are: neuronal activity is associated with Ca^{2+} entry via a variety of channels, as well as with Ca^{2+} release from endoplasmic reticulum via receptors for inositol (1,4,5)-trisphosphate (IP₃R) and ryanodine (RyR). Mitochondria that are localized close to Ca^{2+} influx or release sites into the cytoplasm take up Ca^{2+} via the mitochondrial Ca^{2+} uniporter (Uni). NADH and FADH transfer energy from the tricarboxylic acid (TCA) cycle to complex I and complex II of the electron transport chain, which establishes a potential (150–180 mV negative to cytosol, $\Delta\psi_m$) and a proton gradient (ΔpH) across the inner mitochondrial membrane. This prompts protons to actuate complex V (ATP synthase), for Ca^{2+} and for transporters like adenine nucleotide translocase (ANT). The activity of TCA cycle enzymes is stimulated by Ca^{2+} (overlap in circles) and generation of reactive oxygen species (ROS) occurs at complexes I and III, as well as α -ketoglutarate dehydrogenase in the TCA cycle. GLUT-3: glucose transporter-3; TH: nicotinamide nucleotide transhydrogenase; MPTP: mitochondrial permeability transition pore; Ex1: $\text{H}^+/\text{Ca}^{2+}$ exchanger; Ex2: $\text{Na}^+/\text{Ca}^{2+}$ exchanger; KCs: potassium channels. (Used with permission: Kann and Kovac (2007) *Mitochondria and neuronal activity*. *Am J Physiol Cell Physiol* 292: p. C641-657).

of $\Delta\Psi_m$ by toxins that prevent mitochondrial Ca^{2+} -uptake [226] and inhibition of the Ca^{2+} uniporter [227] can prevent ROS generation. ROS are most often produced by complex I and III in the respiration chain in a $\Delta\Psi_m$ -dependent mechanism [228, 229]. However, with prolonged Ca^{2+} -uptake, the $\Delta\Psi_m$ decreases, so $\Delta\Psi_m$ -dependent ROS production is inhibited. As this is contradictory to the observed significant ROS production during Ca^{2+} insults to cells, a $\Delta\Psi_m$ -independent mechanism may exist [230], perhaps reflecting the activation of additional enzymes, such as α -ketoglutarate dehydrogenase [205, 229].

Moreover, Ca^{2+} accumulation in mitochondria can induce the mitochondrial permeability transition pore (mPTP), which is also sensitive to ROS production [231]. The mPTP allows the release of glutathione and cytochrome *c* into the cytoplasm. The loss of glutathione from mitochondria weakens the ability of the mitochondria to detoxify excesses in ROS, while cytoplasmic translocation of cytochrome *c* triggers caspase activation and apoptotic cell death. Furthermore, cytochrome *c* can bind to the IP3 receptor along with IP3, with the additive effect of releasing more Ca^{2+} from the ER to cytosol; this feed-forward cycle enhances Ca^{2+} -induced apoptosis [232].

It is clear that Ca^{2+} as a common second messenger can both benefit and damage cells, depending on the delicate balance between intrusion and extrusion, as well as release and uptake. Ca^{2+} is an important mediator of neuronal activity.

1.2.3 Intracellular Ca^{2+} is elevated in neurodegenerative disorders.

The disruption of Ca^{2+} homeostasis is proposed as an important molecular mechanism underlying neurodegeneration [233]. The loss of homeostasis can result from many factors, including the reduction of Ca^{2+} -binding proteins and disruption of Ca^{2+} -uptake to target organelles, and has been associated with several conditions ranging from aging to neurodegenerative diseases such as Alzheimer's disease and Huntington's disease.

The AD-related $\text{A}\beta$ protein is able to incorporate into the plasma membrane, where, amongst its diverse effects, it can precipitate the formation of Ca^{2+} -permeable pores leading to massive influxes that increase intracellular free Ca^{2+} levels [234]. In familial AD, the presenilin (PS) mutants are reported to induce a higher resting concentration of ER Ca^{2+} [235]. Upon stimulation of the cells, the ER will release a proportionally larger amount of Ca^{2+} to cytoplasm [236]. In contrast, the anti-apoptotic members of the Bcl-2 family of proteins can control the concentration of ER Ca^{2+} [237], apparently by a direct interaction with PS proteins [238].

In Huntington's disease, the mitochondria from patients' lymphoblasts are more sensitive to Ca^{2+} challenge and the $\Delta\Psi\text{m}$ decreases at an earlier time point following a hyperactivity of the NMDA receptor [239].

Ca^{2+} -buffering is compromised during the aging process, as Ca^{2+} -binding proteins can decrease by 75%, an event that is exacerbated during neurodegeneration [240-245]. Ca^{2+} -binding proteins are proteins that contain a motif, the EF-hand, which is present in multiple copies and selectively binds Ca^{2+} with high affinity. Each of these domains

consists of a loop of 12 amino acids of 2 α helices [246]. This motif was first observed between the E and F helices in the classical Ca^{2+} -binding protein parvalbumin [247], hence the name. Ca^{2+} -binding proteins are expressed ubiquitously in the cytoplasm of neuronal processes, thereby making it a neuronal marker. Among these proteins, calbindin-D 28K (CB28K) is the most abundant as it accounts for approximately 1% of the total soluble proteins [248].

The NMR structure of CB28K reveals it consists of 6 distinct EF-hand subdomains, 4 of which bind with Ca^{2+} [249]. CB28K is neuroprotective for neurons, even in cases of extreme toxicity [250-253]; however, it is reduced significantly during aging, and more so in neurodegenerative disorders [245]. The reduction of CB28K in neurons is likely to decrease their capacity to buffer any excess intracellular Ca^{2+} and to leave them vulnerable to any Ca^{2+} overload.

1.3 p38(MAPK) and its signaling pathway

1.3.1 Brief overview of the MAPK signaling pathway

1.3.1.1 Cell signaling

Cells receive stimulation or signals from their environment and must respond to them properly in order to govern basic cellular activities and perform cellular actions. These signals are “transduced” to the inside of the cell where they can act on enzymes or other molecules, such as second messengers, to induce the corresponding cell responses. This process is known as signal transduction.

1.3.1.2 MAPK signalling pathway

Mitogen-activated protein kinase (MAPK) pathway is a highly conserved signal transduction pathway in mammalian cells. It responds to many external stimuli and exerts a variety of cellular responses, including growth, differentiation, inflammation, survival, and apoptosis. The pathway, or “cascade”, involves MAPKK kinase (MAPKKK, MAP3K: activates MEK), MAPK kinase (MAPKK, MEK: activates MAPKs), and MAPKs themselves (Fig. 6). Combinations of extracellular stimuli differentially affect these various “upstream” kinases, and therefore result in seemingly diverse, but very specific cell responses. MAPKKK, MAPKK and MAPK are all serine-threonine selective kinases. In most cases, the MAPKKK is activated by small G proteins such as Ras, Rac, and Rap1. While the mechanisms involved in the activation of MAPKKs and MAPKs are relatively well characterized, the activation of MAPKKKs remains less clear. The phosphorylation of MAPKs (on specific TXY motifs, where T=threonine; X=any amino acid; Y=tyrosine) promotes their enzymatic activity; thereafter, they target and phosphorylate their downstream targets on specific serine or threonine residue(s).

There are three kinds of core MAPKs in this family: (1) extracellular signal-regulated kinases (ERKs) 1 and 2 (ERK1/2); (2) c-Jun NH₂-terminal kinases or stress-activated protein kinases (JNK/SAPK) 1-3 (JNK 1-3); and (3) p38(MAPK) α , β , γ , δ [254]. Sequence comparison reveals that these MAPKs share 40-45% amino acid identity [255]. These three MAPKs contain different TXY motifs: TEY in ERKs, TPY in JNKs, and TGY in p38(MAPK), all of which are located in a loop close to the active site and

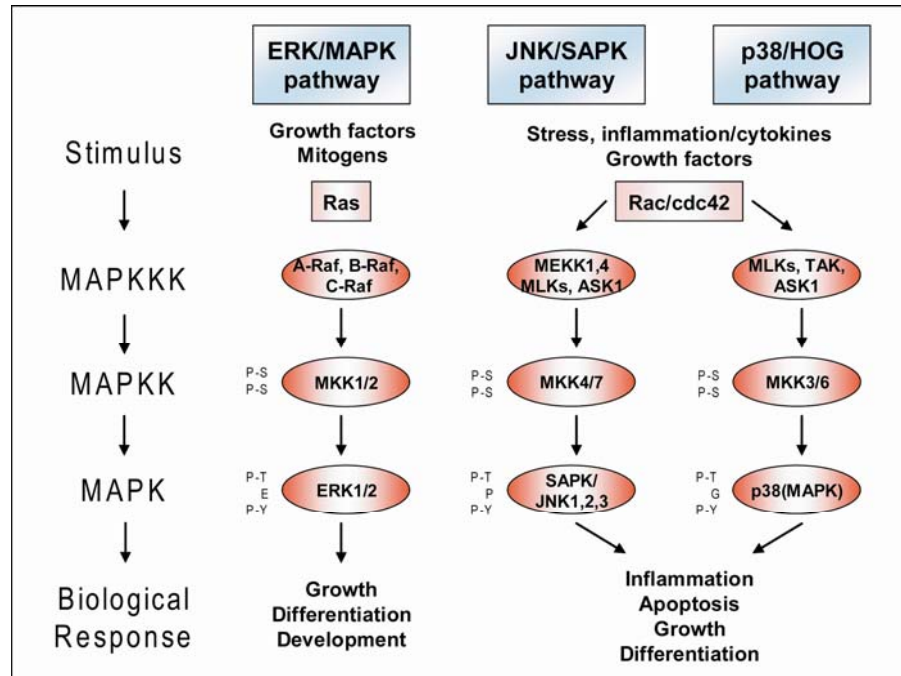


Fig. 6: Schematic of three signaling cascades and the putative motifs targeted by successive kinases in the cascade. The p38(MAPK) pathway is demonstrated on the right. A possible sequence of events could include: a growth factor (*e.g.* TGF- β) binds to its receptor and activates TGF- β -activated kinase (TAK); this kinase would phosphorylate MKK3 or MKK6 on a target serine (P-S, for **p**hospho-**S**erine); once activated, MKK3 or MKK6 can phosphorylate the dual phosphorylation, pTGpY (phospho-threonine, glutamine, phospho-tyrosine) motif in p38(MAPK) and activate it. p38(MAPK) would then target one of many substrates (including MAO-A?) to induce a specific cellular outcome such as inflammation, apoptosis, growth or differentiation. The specific cellular outcome might depend on which growth factor activated the pathway or how many other pathways were affected, all of which contribute to a response.

targeted by specific upstream MAPKKs. Stimulation by specific external factors results in activation by their respective (and specific) upstream kinase; MEK 1, 2 targets/activates ERK, MEK 4, 7 targets/activates JNK, and MEK 3, 6 targets/activates p38(MAPK) [256]. Classically, the ERK pathway is generally involved in the control of cell proliferation and differentiation by mitogens and growth factors, and the JNK and p38(MAPK) pathways are activated by environmental stressors, such as UV radiation, X-rays, heat shock, osmotic shock, and inflammation by cytokines including tumor necrosis factor (TNF) and interleukin-1 (IL-1) [257].

1.3.2 p38(MAPK) as a regulator in neuronal cell fate and cell functions

1.3.2.1 Isoforms and inhibitors of p38(MAPK)

p38(MAPK) is the latest of these three MAPKs to be discovered. It was originally identified as a 38-kDa kinase rapidly phosphorylated in response to endotoxic lipopolysaccharide (LPS) [258]. There are four isoforms of p38(MAPK), α , β , γ , and δ . They share significant amino acid identity; for example, if comparing with the p38(MAPK)- α isoform, 73% amino acid identity to the β isoform, 63% for the γ isoform, and 57% for the δ isoform [259-261]. However, each isoform has its specific expression, activation, and substrate affinity, resulting in their varied functions. p38(MAPK)- α is expressed ubiquitously; p38(MAPK)- β is mainly expressed in the brain and heart; p38(MAPK)- γ is expressed primarily in skeletal muscle; and p38(MAPK)- δ is highly expressed in lung, kidney, gut and salivary gland, as well as endocrinological organs,

such as testis, ovary, adrenal and pituitary gland [261, 262]. Depending on the stimulation and the cells involved, these four isoforms can be activated by different upstream kinases, including the high-affinity MEK3/6 and the low-affinity MEK4 [263, 264]. However, p38(MAPK) isoforms can be inhibited by a type of anti-inflammatory agent, *i.e.* pyridinyl imidazoles, the best known being the commercially available SB203580, which inhibits p38(MAPK) activity by binding to the ATP binding site, but does not inhibit ERK or JNK, or other serine-threonine protein kinases, perhaps due to the different catalytic residues in the regions within or near the ATP binding pocket [265].

1.3.2.2 Intracellular location of p38(MAPK)

p38(MAPK) is expressed in both nucleus and cytoplasm of resting cells, but its cellular localization following cell stimulation is not clear. There is evidence that p38(MAPK) can translocate to nucleus from cytoplasm [266] and that activated p38(MAPK) can be exported from nucleus to cytoplasm to activate its cytosolic substrates [267].

1.3.2.3 Substrates of p38(MAPK)

Activated p38(MAPK) phosphorylates several types of substrates. The first are other protein kinases, termed MAPK-activated protein kinases (MKs). The p38(MAPK)/MK family includes the mitogen- and stress-activated kinases (MSKs), the MAPK-interacting

kinases (MNKs), and MAPK-activated protein kinases 2/3/5 (MK2, MK3, and MK5) [268]. Depending on the signal from the upstream cascade, these substrate kinases of p38(MAPK) can phosphorylate many other proteins, leading to diverse cellular responses. The second group of p38(MAPK) substrates is the main one as it includes many important transcription factors, such as activating transcription factor (ATF)1/2/6, SRF accessory protein (Sap1), growth arrest and DNA damage inducible gene 153 (GADD153), p53, C/EBP β , monocyte enhance factor 2A/2C (MEF2A/2C), MITF1, DDIT3, ELK1, NFAT, Elk-1, NF κ B, Ets-1, and high mobility group-box protein 1 (HBP1) [255, 268, 269]. Additionally, there are other types of substrates for p38(MAPK), such as, cPLA2, Na⁺-H⁺ exchanger isoforms-1 (NHE-1), tau, kerton 8, stathmin and the hyperpolarization-activated cyclic nucleotide-gated channels [270]. Some other proteins can also be activated indirectly by p38(MAPK), such as tyrosine hydroxylase [271], cAMP response element-binding protein (CREB) [272], heat shock protein 27 (HSP27), and tritetraroline (TTP) [255].

1.3.2.4 Cellular functions of neuronal p38(MAPK)

The variety of p38(MAPK) substrates suggests that this pathway has a wide range of functions. Pharmacological inhibition and genetic mutagenesis, as well as knock-out animal models, provide a way to understand the functions of p38(MAPK) in physiological and pathological cellular events.

1.3.2.4.1 p38(MAPK) and neuronal differentiation

The rat pheochromocytoma cell line PC12 is a useful cell culture for the study of neuronal differentiation [273]. When treated with nerve growth factor (NGF), PC12 cells cease to multiply and begin to extend branching processes. The induction of neurite outgrowth by NGF activates two MAPK pathways, ERK [274, 275] and p38(MAPK) [276]. This converging effect can be explained by the fact that the upstream kinase of ERK, *i.e.*, MEK, not only activates ERK, but also p38(MAPK) in some situations, and that CREB, which is a critical transcription factor for NGF-induced cell fate [277], is phosphorylated by both ERK and p38(MAPK) [278]. This “cross-talk” between the MAPKs is an additional means of enhancing the diversity of cellular influences.

Bone morphogenetic protein (BMP)-2, a member of the Transforming Growth Factor- β superfamily, also induces PC12 cell differentiation [279] and activates p38(MAPK), but not ERK [269, 280]. Additionally, in the growth factor-independent PC12 cell differentiation process, p38(MAPK) plays a facilitating role in cAMP-induced neurite outgrowth [281]. The participation of p38(MAPK) in neurite outgrowth is also demonstrated in the MN9D dopaminergic neuronal cell line; the neurite outgrowth in these cells induced by the overexpression of calbindin-D 28K (CB28K) accompanies phosphorylation of p38(MAPK) without the change of JNK or ERK [282].

1.3.2.4.2 p38(MAPK) and neuronal viability

While the JNK pathway is clearly important in neuronal apoptosis [283], the role of the p38(MAPK) pathway in neurons is poorly understood. Even though both can be activated by similar stressors in many situations, p38(MAPK) activation appears complicated. In many models related to apoptosis, p38(MAPK) is activated and phosphorylated [284-287]. However, accumulating evidence suggests that p38(MAPK) signaling has diverse functions, not only in the control of cell death, but also in cell survival. For example, hemoxygenase (HO)-1 is involved in the defense mechanism against oxidative stress-mediated injury that can be induced by nitric oxide (NO) in a p38(MAPK)-dependent mechanism [288]. The transcription mediated by estrogen, which is well known as a neuroprotector, is also regulated by p38(MAPK), which phosphorylates its co-activator GRIP1 [288, 289]. The antidepressant amitriptyline is reported to increase glial cell line-derived neurotrophic factor (GDNF) production and the activity of p38(MAPK), as well as that of JNK and ERK [290]. Moreover, in primary neonatal rat ventricular myocytes, p38(MAPK) activation protects cells from anisomycin-induced apoptosis by activation of NF- κ B [291]. In HeLa cells, the activation of p38(MAPK) prevents apoptosis induced by photodynamic therapy with hypericin [292].

The duration of p38(MAPK) activation appears to be an important determinant of whether prevention or induction of apoptosis occurs. In TNF-induced apoptosis, the kinetics of p38(MAPK) and JNK activation are biphasic. In the early phase treatment,

early activation of p38(MAPK) and JNK supports cell survival, whereas the activation of p38(MAPK) and JNK in the later phase is related to caspase-dependent apoptosis [293]. In contrast, the rapid and transient activation of p38(MAPK) and/or JNK in SKT6 cells exposed to osmotic or heat shock induces cell differentiation rather than apoptosis, although prolonged activation ultimately induces apoptosis [294].

Interestingly, one upstream activator for p38(MAPK), *i.e.*, apoptosis signal-regulating kinase 1 (ASK1), may contribute to the contrasting responses of cell survival and death, mediated by p38(MAPK) in different cell types and/or following different external stimuli [295-297].

These data suggest that p38(MAPK) can determine both cell survival and/or apoptosis, and that the ultimate outcome may rely more on the duration of its activation or on the upstream signal(s) involved.

Recent evidence suggests that activation of the JNK signaling pathway may not be an absolute pro-apoptotic event. In the brain of Alzheimer's disease patients, the c-Jun positive neurons are negative for TUNEL, suggesting that JNK signaling might provide a neuronal protection against the oxidative stress and inflammation insult [298]. Therefore, the observed activation of neuronal p38(MAPK) in early AD [299] cannot be interpreted as only a pro-apoptotic signal.

1.3.2.4.3 p38(MAPK) and other cellular functions

Besides cell differentiation, neurite outgrowth, neural cell survival or death, p38(MAPK) is also reported to be important in neuronal migration, translational control, endocytosis, long-term depression, embryonic development, cancer progression, *etc.* [269, 300].

1.4 Linking Ca^{2+} , MAO-A, and p38(MAPK) in a unique mechanism that contributes to cell fate

1.4.1 Background

1.4.1.1 Ca^{2+} signaling and the increase in MAO-A activity occur coincidentally in many neurological disorders

It is known that NMDA receptor over-activation elevates intracellular Ca^{2+} levels. Interestingly, NMDA receptor function is altered in hepatic encephalopathic brains [301] concomitantly with a selective increase in MAO-A activity [302]. In neurodegenerative disorders, such as AD, Ca^{2+} overload/calbindin reduction [244] and simultaneous changes in MAO activity [176] may contribute to pathological ROS production.

1.4.1.2 Evidence of the direct effect of Ca^{2+} on MAO-A activity

Several research groups have reported that MAO-A activity is selectively elevated by the addition of Ca^{2+} *in vitro* [303, 304]. In addition, neuronal MAO-A and MAO-B are both increased in mice treated with the Ca^{2+} channel agonist (+/-)-Bay K8644 [305].

Moreover, the observed selective increase of MAO-A activity in senescence-accelerated mouse brain is blocked by the Ca²⁺ channel antagonist nimodipine [306]. This combined evidence suggests modulation of MAO-A activity by Ca²⁺ and, as such, the motifs known to bind Ca²⁺, such as DXDXD, DXXD, or DXXXD [307-309], should be evident in the amino acid sequence of the MAO-A protein. This was investigated during the course of the thesis work.

1.4.1.3 p38(MAPK) may regulate *mao-A* transcription, translation, and activity

In the *mao-A* promoter sequence, there is a transcription factor R1 binding sequence that inhibits *mao-A* transcription and activity [63, 310]. Both R1 repressor function and MAO-A activity have been linked to the p38(MAPK) pathway [182]. In PC12 cells, NGF withdrawal induces p38(MAPK) activity and the production of *mao-A* gene which further supports a link between p38(MAPK) and MAO-A [311]. The tricyclic antidepressant amitriptyline increases the synaptic level of monoamines such as 5-HT and noradrenaline (both substrates for MAO-A) and also increases p38(MAPK) activity [290], while p38(MAPK) is reported to also induce tyrosine hydroxylase, which is the important enzyme for catecholamine synthesis [271].

p38(MAPK) function is clearly linked to monoamine systems, yet it is still unclear whether the effect of p38(MAPK) is to activate or inhibit MAO function. p38(MAPK) phosphorylates serine or threonine residues that lie within a specific motif, RXXS/T (where R=Arginine; X=any amino acid; S=serine; T=threonine) [312]. If p38(MAPK) is

capable of directly targeting MAO-A, then the amino acid sequence in the MAO-A protein should contain a putative p38(MAPK) phosphorylation site, RXXS. This was also investigated during the course of the present thesis work.

1.4.2 Hypothesis

Given that Ca^{2+} can enhance MAO-A activity and that p38(MAPK) can affect monoamine systems in some cases by affecting MAO-A function, the hypothesis proposed for this thesis is: p38(MAPK) contributes to Ca^{2+} -sensitive MAO-A function during experimental cell stress.

1.4.3 Objectives of this project

1. Test the effect of Ca^{2+} on MAO *in vitro* (in brain and cell culture extracts).
2. Test the effect of Ca^{2+} on MAO *ex vivo* (by modulating Ca^{2+} levels with the treatment of Ca^{2+} ionophore A23187 or overexpression of CB28K).
3. Determine whether MAO-A contains putative Ca^{2+} binding sites and, if so, mutagenize the sites to test their influence on MAO-A activity.
4. Test the role of p38(MAPK) on MAO-A activity in neuronal cell populations.
5. Determine whether MAO-A contains a putative p38(MAPK) target site(s) and, if so, mutagenize the site(s) to test its (their) influence on MAO-A activity.
6. Test the contribution of p38(MAPK) to Ca^{2+} -regulated MAO-A function in models of cell stress.

7. Whenever possible, include MAO-B as a means of comparing and contrasting its response with that of MAO-A.

2 MATERIALS AND METHODS

2.1 Materials

For lists of chemicals used and supplier addresses, please see Table 1-3.

2.1.1 Plasmids

In the present study, two commercially available mammalian expression vectors were used for cloning; these were pcDNA3.1/Hygro(+) and pCMV/myc/Mito (both from Invitrogen). A third expression vector, pREP-CB28K (CalbindinD-28K, was kindly provided by Dr. A. Pollock (University of California, San Francisco, CA).

The pcDNA3.1/Hygro(+) vector was used for sub-cloning p38(MAPK). The pCMV/myc/Mito vector was used to sub-clone MAO-A or MAO-B. The myc/Mito vector targeted the protein to the mitochondria as a Myc-tagged fusion protein (for ease of detection of the expressed protein). All three vectors contained the ampicillin-resistant gene (amp^R) for selective amplification of recombinant plasmids in bacterial cultures.

Table 1: List of Reagents, Kits and Suppliers

Reagents	Supplier
Absolute Ethanol	BDH
Acrylamide	Bio-Rad
Agarose	Invitrogen
Bovine Serum Albumin	EMD
Bromophenol Blue	EMD
Calcium Chloride	BDH
Chloroform	BDH
Coomassie Brilliant Blue R-250	Sigma
1,2-Diacyl- <i>sn</i> -glycero-3-phospho-L-serine	Sigma
Diethylpyrocarbonate (DEPC)	BDH
Dimethylsuloxide (DMSO)	Sigma
N,N-Dimethylformamide	BDH
3-(4,5-dimethylthiazol-2-yl)-2,5-diphenyl tetrazolium (MTT)	Calbiochem
Ethidium Bromide	Sigma
Ethylene-diamine Tetraacetic Acid Disodium Salt (EDTA)	Sigma
Goat Serum	Sigma
Glacial Acetic Acid	EMD
D-Glucose	BDH
Glycerol	MP Biomedicals
L-Glycine	MP Biomedicals
N-2-Hydroethylpiperazine-N'-2-ethane Sulfide Acid (HEPES)	USB
Hydrochloric Acid (HCl)	EMD
Hoechst 33258 Stain	Sigma
Isobutanol	BDH
Isopropanol	EMD
LiCl	EMD
Magnesium Chloride (MgCl ₂)	EMD
Magnesium Sulfate (MgSO ₄)	EMD
β-Mercaptoethanol	EMD
Methanol	BDH
Non-fat Dry Milk (Carnation)	Nestle
Paraformaldehyde	Sigma
Phenol	Sigma
Phenylmethylsulfonyl Fluoride (PMSF)	Sigma
Polyethylene Glycerol (PEG)	Sigma
Potassium Chloride (KCl)	BDH

Protease Inhibitor Cocktail	Sigma
Sodium Acetate	BDH
Sodium Chloride (NaCl)	VWR
Sodium Dodecyl Sulfate (SDS)	ICN
Sodium Bicarbonate (Na ₂ CO ₃)	EMD
Sodium Fluoride (NaF)	Sigma
Sodium Hydroxide (NaOH)	EMD
Sodium Orthovanadate	Sigma
Sucrose	BDH
N,N'-Methylene-bis-acrylamide	Bio-Rad
N,N,N',N'-Tetramethylethylenediamine (TEMED)	Bio-Rad
Tris-Acetate	EMD
Tris-HCl	ICN
Triton-X100	Sigma
Trizol™	GIBCO-BRL
Trypsin-EDTA	GIBCO-BRL
Tween-20	EMD
Disuccinimidyl suberate (DSS)	PIERCE
2',7'-Dichlorodihydrofluorescein diacetate (H ₂ DCF-DA)	Molecular Probes
Fluo-3AM	Molecular Probes
Cell growth reagents	Supplier
Ampicillin	EMD
Bacto-Agar	BD
Bacto-Tryptone	BD
Bacto-Yeast Extract	BD
Calf Serum	GIBCO-BRL
Collagen Type I (rat tail)	BD
Dulbecco's Modified Eagle's Medium: DEM/Low	Hyclone
Dulbecco's Modified Eagle's Medium: DEM/High	Hyclone
Fetal Bovine Serum	GIBCO-BRL
Opti-MEM Reduced Serum Medium	Invitrogen
Recovery Cell culture Freezing Medium	GIBCO-BRL
Pharmacological Agents	Supplier
A23187	Sigma
SB203580	Cell signalling
LY294002	Cell signalling
PD98059	Cell signalling
Hydrogen Peroxide (H ₂ O ₂)	Sigma
Clorgyline (CLG)	Sigma
L-deprenyl (DEP)	TOCRIS

Transfection Reagents	Supplier
ExGen500	Fermentas
Lipofectamine2000	Invitrogen
Radioactive-substrates	Supplier
¹⁴ C-Serotonin (5-HT)	Perkin-Elmer
¹⁴ C-Phenylalanine (PEA)	Perkin-Elmer
Commercial Kits	Supplier
BCA™ Protein Assay Kit	Pierce
SuperScript™ III First-Strand Synthesis System for RT-PCR	Invitrogen
Qiaex II Gel Extraction Kit 500	Qiagen
Quantum Prep Plasmid Midiprep Kit	Bio-Rad
Quikchange Site-Directed Mutagenesis Kit	Stratagene
JC-1 Mitochondrial Membrane Potential Assay Kit	Invitrogen

Table 2: List of Antibodies and the dilution used for the Western Blotting.

Primary Antibody	Dilution	Supplier
β-Actin	1:3000	Sigma-Aldrich Inc
MAO-A (H-70)	1:1000	Santa Cruz Biotech
MAO-A (T-19)	1:1000	Santa Cruz Biotech
CB28K	1:500	Santa Cruz Biotech
MAO-B	1:1000	Santa Cruz Biotech
C-Myc	1:1000	Santa Cruz Biotech
p38(MAPK)	1:1000	Cell signalling Tech
p-p38(MAPK)	1:500	Cell signalling Tech
p-MK2	1:1000	Sigma-Aldrich Inc
p-Ser	1:1000	Sigma-Aldrich Inc
Secondary Antibody	Dilution	Supplier
Donkey Anti-Goat IgG, HRP-conjugate	1:2000	Santa Cruz Biotech
Goat Anti-Rabbit IgG, HRP-conjugate	1:2000	Cedarlane Laboratories
Goat Anti-Mouse IgG, HRP-conjugate	1:2000	Cedarlane Laboratories

Table 3: Names and Addresses of Suppliers

Supplier	Address
BD (Becton Dickinson)	2771 Bristol Circle, Oakville, ON., Canada
BDH	501-45 th Street West, Saskatoon, SK., Canada
Bio-Rad	5671 McAdam Road, Mississauga, ON., Canada

Cedarlane Laboratories	5516 8 th line, Hornby, ON., Canada
Cell Signaling Tech	159J Cummings Center Beverly, MA 01915, USA
EMD Bioscience Inc	10394 Pacific Center Court, San Diego, CA 92121, USA
Fermentas Life Science	830 Harrington Crt., Burlington, ON., Canada
GIBCO-BRL	Box 9418, Gaithersburg, MD 20898, USA
ICN Biomedicals Inc	15 Morgan, Irvine, CA 932618-2005, USA
Invitrogen	1600 Faraday Avenue, Carlsbad, CA 92008, USA
Molecular Probes	2270 Industrial St., Burlington, ON., Canada
Perkin-Elmer	501 Rowntree Dairy Road, Mississauga, ON., Canada
Santa Cruz Biotech	2161 Delaware Ave., Santa Cruz, CA, USA
Sigma	2149 Winston Park Drive, Oakville, ON., Canada
USB	300 Laurier Blvd., Brockville, ON., Canada
Qiagen	2800 Argentia Road, Unit 7 Mississauga, ON., Canada
Stratagene	11011 N. Torrey Pines Road, La Jolla, CA 92037, USA
Pierce	Box 117, Rockford, IL 61105, USA
VWR	2360 Argentia Road, Mississauga, ON., Canada
TOCRIS	16144 Westwoods Business Park, Ellisville, Missouri 63021, USA
Hyclone	925 West 1800 South, Logan, UT 84321, USA

2.1.2 Competent cells

Competent bacterial cells were processed from DH5 α *E. coli* (American Type Culture Collection (ATCC) # 53868). DH5 α *E. coli* cells were amplified by growing in LB broth overnight and aliquoted as 100 μ l per Eppendorf tube, and stored at -70°C for future use.

The DH5 α competent cells were prepared under sterile conditions according to the following (Molecular Cloning, Sambrook and Russell, 2001):

- a) Pick a single clone of *E. coli* cells from colonies freshly grown at 37°C overnight on an LB-agar plate [2% bacto-agar (Becton Dickinson, Sparks, MD), in LB media for autoclave, 5 ml for each 10 cm plate] and disperse it in 5 ml of LB media in a 15 ml culture tube containing 1% bacto-tryptone, 0.5% bacto-yeast extract [both from Becton Dickinson, Sparks, MD) and 1% NaCl (EMD Chemicals, Gibbstown, NJ); adjusted to pH 7.0 with 5 M NaOH, and autoclaved before use].
- b) Incubate the culture at 37°C overnight, with vigorous shaking.
- c) Transfer 400 μ l of this culture into 40 ml of LB media in a 250 ml flask and incubate the culture at 37°C for approximately one and half hours, with vigorous shaking.
- d) Transfer the culture into a 40 ml centrifuge tube and centrifuge at 3,000xg at 4°C for 3 min. Discard the supernatant and resuspend the pellet in 20 ml of ice-cold autoclaved 0.1 M CaCl₂ (EMD Chemicals, Gibbstown, NJ).
- e) Keep the resuspended solution on ice for 30 min and then centrifuge at 3,000xg, 4°C for 3 min.

- f) Discard the supernatant and resuspend the pellet in 3 ml of ice-cold 0.1 M CaCl₂. Keep the cell solution at 4°C overnight. Add 1.5 ml of 50% glycerol into the cell solution, mix well, and then aliquot 200 µl in each 1.5 ml Eppendorf tube, and store at -70°C for future use.

2.1.3 Cell cultures

Seven cell lines were used during the course of this study. Rat pheochromocytoma (PC12; ATCC# CRL-1721), human neuroblastoma (SH-SY5Y; CRL-2266), mouse neuroblastoma (N2a; CCL-131), human glioblastoma (T98G; CRL-1690), C6 glioma cells (CCL-107) and human embryonic kidney 293A cells (HEK; CRL-1573) were obtained from the American Type Culture Collection, (ATCC); the immortalized mouse hippocampal (HT-22) cells were kindly provided by Dr. P. Maher (The Scripps Research Institute, La Jolla, CA, USA).

The HEK293A cells, N2a cells, T98G cells, HT-22 cells, and C6 cells were incubated at 37°C in a humidified atmosphere, containing 5% CO₂, and grown in low glucose Dulbecco's Modified Eagle's Medium (DMEM), supplemented with 10% heat-inactivated horse serum, 25 units/ml penicillin, and 25 units/ml streptomycin (all from Gibco BRL, Box 9418, Gaithersburg, MD 20898, USA).

The rat pheochromocytoma (PC12) cells were grown in DMEM with 10% heat-inactivated horse serum, 5% fetal bovine serum (Gibco BRL), 25 U/ml penicillin, and 25 U/ml streptomycin. Culture plates and flasks were coated with rat-tail collagen

(BD Biosciences, Bedford, MA, USA). Cell cultures were maintained at 37°C with 5% CO₂.

The human neuroblastoma (SH-SY5Y) cells were incubated at 37°C in a humidified atmosphere (containing 5% CO₂) and grown in high glucose DMEM supplemented with 10% heat-inactivated horse serum, 25 U/ml penicillin, and 25 U/ml streptomycin (all from Gibco BRL).

2.1.4 Rat neuronal cortical culture

Rat cortical cultures were prepared from E20 fetuses of time-pregnant Sprague-Dawley rats (Charles River Canada, Montreal, PQ, Canada) as previously described [313], with some modifications. In brief, the cortical area was dissected in Ca²⁺- and Mg²⁺-free Hank's balanced salt solution (HBSS), supplemented with 15 mM 4-(2-hydroxyethyl)-1-piperazineethanesulfonic acid (HEPES) and antibiotics. Collected tissues were digested at 37°C with 0.25% trypsin- ethylenediamine tetraacetic acid (EDTA) 15 min. The reaction was stopped by the addition of 10% fetal bovine serum (FBS), and tissues were rinsed 3-4 times with HBSS to remove FBS.

Cell suspensions were prepared by repeated aspirations through a Pasteur™ pipette. Following centrifugation at 800xg for 10 min, the medium was removed and the cells resuspended in a chemically defined serum-free NeuroBasal medium, supplemented with 1% N₂, 2% B27, 50 μM L-glutamine, 15 mM HEPES, 10 U/ml penicillin, and 10 μg/ml streptomycin. Neurons were then plated in 6- or 96-well plates (or coverslips) coated

with 25 µg/ml poly-D-lysine and grown at 37°C with a 5% CO₂-humidified atmosphere. Within one day after plating, the medium was replaced with fresh NeuroBasal medium, containing the same components, except for L-glutamine and antibiotics. When the medium was replaced at 4-5 days *in vitro* (DIV), less than 1.0% of the cells showed GFAP positive staining. All treatments were performed at DIV 7.

2.1.5 Animals

All procedures involving animals, including care and maintenance, were executed according to the guidelines set forth by the University of Saskatchewan Animal Care Committee (University of Saskatchewan Protocol #20040094), the Canadian Council on Animal Care, and the National Institutes of Health. The inbred male or female adult Sprague-Dawley rats (350~400 g body weight) and CB57L/6 mice (18-20 g body weight) were housed at a constant temperature (20 ± 1 °C) on a 12-hr light/dark cycle, with free access to food and water.

2.2 Methods

2.2.1 Dissection of rat and mouse brains

In accordance with protocol #20040094, as approved by the University of Saskatchewan Animal Care and Use Committee, both rats and mice were anaesthetized with sodium pentobarbital (65 mg/kg rat body weight or 30 mg/kg mouse body weight) and killed by decapitation. The brains were then quickly removed, and the hippocampus,

striatum, frontal cortex, cerebellum, and neocortex were immediately dissected. All brain samples were stored at -80°C.

2.2.2 Detection of MAO activity in the absence or presence of Ca²⁺

MAO-A and -B activities (nmol/h/mg protein) were estimated radiochemically according to the methods of Holt and Baker [314]:

1. Homogenize the frozen brain tissues or cell pellet in potassium phosphate buffer and on ice with 10 strokes of a Dounce homogenizer.
2. Determine protein concentration and aliquot 100 µg of protein per reaction tube.
3. Gently bubble O₂ through incubation buffer, potassium phosphate (0.2 M, pH 7.8) 30-45 min of O₂ per liter of buffer.
4. Carry out reactions in 1.5 ml centrifuge tubes and include triplicates for each sample.
Place tube racks on ice.
5. When needed, add 1 µl of different concentrations of Ca²⁺ solution, according to the desired final Ca²⁺ concentration. Vortex briefly. Incubate at room temperature for 20 min.
6. To blank tubes, add 10 µl of HCl (3 M).
7. Place tube racks in a water bath at 37°C. To each tube, add 50 µl of appropriate ¹⁴C labeled substrate in a time-dependent order (for MAO-A activity: 250 µM of ¹⁴C-5-HT (NEC-225); for MAO-B activity: 50 µM of ¹⁴C-PEA (NEC-502); incubate for 10 min. (MAO substrates are from PerkinElmer Life Sciences, (Woodbridge, ON)

8. Terminate the reaction by the addition of 10 μl HCl to all samples in the same order as substrate was added, except blank.
9. Add 1 ml of ethyl acetate/toluene (1:1, v/v, water saturated) to each sample and vortex samples briefly.
10. Centrifuge samples in microcentrifuge (setting 4.5) for 30 sec.
11. Carefully pipette 700 μl of the upper organic layer into a small scintillation vial. Do not disturb the aqueous layer; if this happens, re-centrifuge the remaining samples.
12. Add 4 ml of scintillation fluid and count for 3 min for d.p.m.
13. To determine specific activity, add 50 μl of the radiolabeled substrate to scintillation vials to determine the enzyme-specific activity.
14. Do wipe test following every experiment and record substrate usage and wipe test results in the log book.

2.2.3 Kinetic study of MAO activity in the absence or presence of Ca^{2+}

HT-22 cells were harvested and prepared for assay of MAO activity as above: in addition Ca^{2+} (1 mM) was added to a parallel set of tubes. All reaction mixtures were incubated at room temperature for 20 min. The radiolabeled substrate was prepared at different concentrations with oxygenated potassium phosphate buffer (0.2 M, pH 7.8), ranging from 15.625 μM to 5 mM. V_{max} and K_{m} were calculated using Prism 3.0 software.

2.2.4 Plasmid construction and confirmation

2.2.4.1 MAO-A and MAO -B full-length fragment

Human *mao-A* and *mao-B* cDNAs were amplified from yeast expression constructs generously provided by Dr. D.E. Edmondson (Emory University School of Medicine, Atlanta, GA, USA). These were amplified by polymerase chain reaction (PCR) and then subcloned into the pCMV/myc/mito expression vector (Invitrogen Canada Inc.), which allowed for constitutive mitochondrial expression as well as detection using an anti-myc antibody (clone 9E10, Upstate Biotechnologies, Inc.). The PCR primers were flanked by *XhoI* restriction sites as indicated:

Forward: MAOAF (NS) XH (with *XhoI* site (underlined) and no start codon): CGC TCG AGG AGA ATC AAG AGA AG. MAOBF (NS) XH (with *XhoI* site and no start codon): ACC TCG AGA GCA ACA AAT GCG AC.

Reverse: MAOA (R1, with *XhoI* site, but without stop codon) ATA CTC GAG AGA CCG TGG CAG GAG CTT G. MAOB (R1, with *XhoI* site, but without stop codon): CTC TCG AGG ACT CTC ACA AGT AGC CC.

2.2.4.2 p38(MAPK) full-length fragment

The pEBG-p38(MAPK) α expression vector was kindly provided by Dr. B. Zanke (Cross Cancer Institute, Edmonton, AB, Canada). It was amplified by PCR and subcloned into a pcDNA3.1 expression vector (Invitrogen Canada Inc.). The primers of this PCR were flanked with *EcoRV* and *XhoI*, as

Forward: p38HF1V (with *EcoRV* site and start codon): CGA TAT CAT GTC TCA
GGA GAG GCC CAC.

Reverse: p38HR1 (with *XhoI* site): CTC TCG AGT CAG GAC TCC ATC TCT TCT
TG.

2.2.4.3 Subcloning gene fragment into specific vectors

PCR fragments and vectors were digested with appropriate restriction enzymes (all enzymes from MBI Fermentas Life Sciences) for subcloning/ligation, a process by which two DNA fragments, one containing target DNA and the other containing a plasmid vector, are combined by using T4 DNA ligase (MBI Fermentas). For digestion, the reaction was allowed to incubate at 37°C for 2-3 hrs, whereas the reaction mixture for the ligation was incubated at 22°C for 2 hrs or, at 16°C overnight.

2.2.5 Polymerase chain reaction (PCR)

The following general PCR protocol (Sambrook, 1989: total reaction volume 50 µl) served for all PCR experiments performed in this study. Optimal reaction conditions (*i.e.* total volumes of reaction mixtures, primers, concentrations of DNA polymerase, incubation temperatures and times, template DNA, as well as MgCl₂) were optimized for each DNA fragment.

1. To a sterile thin wall PCR tube on ice, add and mix the following components:
 - 5 µl 10× PCR buffer (includes MgCl₂)

- 5 μ l dNTP mixture (Invitrogen, 2 mM)
 - 1.5 μ l Sense primer (20 μ M)
 - 1.5 μ l Anti-Sense primer (20 μ M)
 - 1 ng Template plasmid
 - 0.5 μ l *pfu* DNA polymerase (MBI Fermentas)
 - Autoclaved distilled water, up to 50 μ l per reaction
2. Cap the tube and centrifuge briefly to collect the contents on the tube bottom. Put the sample in the PCR thermal cycler and incubate at 95°C for 0.5 min to completely denature the template.
 3. Perform 25-30 cycles of PCR amplification as follows:
 - Denature at 94°C for 30 sec
 - Anneal at 52-55°C for 30 sec
 - Extend at 72°C for 1 min
 4. Incubate the sample at 72°C for an additional 5 min and maintain the reaction at 4°C.
The sample can then be stored at -20°C until use.
 5. Visualize the amplification products by Agarose (Invitrogen) gel electrophoresis with ethidium bromide and DNA molecular weight standards (MBI Fermentas).
 6. Purification of the amplified DNA products from the Agarose gel was performed by QIAEX II Gel Extraction Kit (Qiagen), according to the manufacturer's protocol.

2.2.6 Transformation

Bacterial transformation is a process used to introduce a foreign plasmid into bacterial cells and to use the bacteria for amplification of this plasmid. The procedure for bacterial transformation (Sambrook, 1989) includes the following steps:

1. Take out competent *E. coli* cells from -80°C freezer.
2. Turn on water bath to 42°C.
3. Put 50 µl competent cells into a 1.5 ml tube (Eppendorf).
4. Keep tubes on ice.
5. Add 1 µl of cDNA into *E. coli* competent cells and incubate on ice for 30 min.
6. Put tube(s) with DNA and *E. coli* into 42°C water bath for 45 sec.
7. Put tubes back on ice for 2 min to reduce damage to the *E. coli* cells.
8. Add 500 µl of SOC medium and incubate tubes at 37°C for 0.5 hr.
9. Spread the resulting culture on DYT plates (with Ampicillin added). Grow overnight.
10. Pick colonies about 12-16 hrs later.

2.2.7 Plasmid DNA preparation

Plasmid DNA preparation was performed according to the DNA Maxiprep Protocol (Sambrook et al, 1989), as follows:

1. Pick a single colony and inoculate into 5 ml of TB (Bacto-tryptone, 12 g, Bacto-Yeast Extract, 24 g, and Glycerol, 4 ml in 1000 ml, autoclaved) containing 100 mg/l ampicillin. Shake at 250 RPM, overnight.

2. Disperse the bacterial culture to 500 ml TB containing 100 mg/l ampicillin. Shake at 250 RPM, overnight.
3. Centrifuge cells in a rotor (Allegra™ 25R, Beckman Coulter Inc.) in the 250 ml bottle at 5000xg for 15 min.
4. Resuspend cell pellet in 100 ml of STE buffer (500 mM NaCl, 10 mM Tris-Cl, 1 mM EDTA, pH 8.0) by vortexing and pipetting up and down. Centrifuge cells at 5000xg for 15 min.
5. Remove supernatant and add 20 ml of Sol I (50 mM Glucose, 10 mM EDTA, pH 8.0, 25 mM Tris-Base, pH 8.0) to the pellet and resuspend cells completely. A good suspension is consistent without clumps of cell pellet.
6. Add 40 ml of Sol II (0.2 N NaOH/1% SDS lysis solution). Mix gently by inverting tube 5 times. Store at room temperature for 5-10 min, until the solution becomes clear, yellow.
7. Add 20 ml of Sol III (5 M potassium acetate solution, pH 4.8). This solution neutralizes NaOH in the previous lysis step, while precipitating the genomic DNA and SDS in an insoluble white, rubbery precipitate. Shake bottle thoroughly. Incubate on ice for 5 min. Centrifuge at 5000xg for 20 min.
8. Filter the supernatant through 4 layers of cheesecloth into a clean 250 ml bottle. The cheesecloth catches any fragments of SDS/genomic DNA aggregate.
9. Precipitate the nucleic acids by adding 48 ml of isopropanol and let stand for 10 min at room temperature. Centrifuge at 5000xg for 15 min.

10. Aspirate off all the isopropanol supernatant. Rinse the pellet and walls of bottle with 85% ethanol at room temperature. Let ethanol evaporate for a few minutes at room temperature.
11. Dissolve the pellet in 3 ml of TE buffer (10 mM Tris-Cl, 1 mM EDTA, pH 7.5). Transfer nucleic acid suspension to a 50 ml tube. Add 4.8 ml of 5 M cold LiCl solution to precipitate RNA. Leave on ice for 10 min and centrifuge at 9000xg for 10 min.
12. Pour off the supernatant containing plasmid DNA into a clean 50 ml tube. Add an equal volume of isopropanol and precipitate the nucleic acids on ice for 10 min. Centrifuge at 9000xg for 10 min.
13. Aspirate off all the isopropanol supernatant. Rinse the pellet and walls of bottle with 85% ethanol at room temperature. Let ethanol evaporate for a few minutes at room temperature.
14. Dissolve the pellet in 0.5 ml of TE buffer. Transfer TE solution into a 1.5 ml Eppendorf tube. Add 5 μ l of RNase A solution (10 mg/ml stock, stored at -20°C), vortex and incubate at 37°C for 20 to 30 min to digest remaining RNA.
15. Precipitate the plasmid DNA with PEG solution (13% w/v 1.6 M NaCl/PEG 8000) by adding 0.4 ml and incubating 1 hr overnight on ice. This step discriminates very large plasmid DNA from small nucleic acid fragments as only the larger plasmid DNA precipitate.

16. Spin the PEG solution in the centrifuge at 12000xg for 2 min. Aspirate off the supernatant PEG buffer and dissolve the PEG pellet in 0.5 ml of TE buffer.
17. Extract proteins from the plasmid DNA adding about 0.3 ml PCIA (phenol/chloroform/isoamyl alcohol). Vortex vigorously for 30 sec. and centrifuge at full speed for 5 min at room temperature. Note organic PCIA layer will be at the bottom of the tube.
18. Remove upper aqueous layer containing the plasmid DNA, carefully avoiding the white precipitated protein layer above the PCIA layer, and transfer to a clean 1.5 ml Eppendorf tube. Repeat 3 times.
19. Add NaCl solution to a final concentration of 125 mM and mix well. Add 1 ml of absolute ethanol to precipitate the plasmid DNA, usually on ice for 10 min, and centrifuge at full speed for 5 min at room temperature.
20. Aspirate off ethanol solution and resuspend or dissolve DNA pellet in 0.3 to 0.5 ml of TE buffer or H₂O. This is the final stock of plasmid DNA, which is suitable for DNA sequencing and long-term storage.
21. Measure the concentration of the plasmid DNA by diluting stock into water at 1:300. The absorbance at 260 nm, multiplied by the dilution factor and 50 is the DNA concentration in units of mg/ml for a 1 cm path length cuvette (*i.e.* 50 mg/ml/OD₂₆₀).

2.2.8 Plasmid Transfection

Transfection is the process used to introduce plasmid DNA into eukaryotic cells. This typically involves opening transient pores or 'holes' in the cell plasma membrane to allow uptake of plasmid DNA. Transfection is frequently carried out by mixing a cationic lipid with the material to produce liposomes, which, after application, fuse with the cell plasma membrane and deposit their cargo inside.

In this study, ExGen 500 was applied as a transfection reagent. ExGen500 is a sterile solution of linear polyethylenimine (PEI) molecules (22 kDa) in water at a concentration of 5.47 mM in terms of nitrogen residues. PEI has a high cationic-charge density potential, making it an excellent DNA condensing and gene-delivering agent. A sterile solution of 150 mM NaCl is required to dilute ExGen 500 and plasmid DNA.

2.2.8.1 Homemade preparation of ExGen 500

The ExGen 500 used in this study was either supplied by MBI Fermentas or homemade, according the following protocol:

- Start with 8 ml of nanopure H₂O.
- Adjust pH to 2.0, with concentrated HCl.
- Weigh 10 mg of PEI.
- Dissolve PEI completely in 8 ml acidified nanopure H₂O (pH 2.0), check pH of solution after dissolving completely and adjust to pH 2.0 if necessary.
- Once PEI is completely dissolved, change pH to 7.0.

- Adjust to a final volume of 10 ml.
- Sterilize by using a 0.2 mm filter syringe.
- Aliquot 1 ml to an Eppendorf tube and store at -20°C for future use. Do not use PEI solutions that are older than 2 months.

2.2.8.2 Transfection using ExGen 500

Transfection was carried out according the following procedure, as recommended by MBI Fermentas:

1. Prepare the following immediately prior to transfection. Use 1 µg of DNA per 3.3 µl (6 equivalents) of ExGen 500 per well of a 24-well plate. Subsequent optimization may further increase the transfection efficiency in a particular application, depending on the cell line and the gene expressed.
2. Dilute 1µg of DNA in 100 µl of 150 mM NaCl. Vortex gently and spin down briefly.
3. Add 3.3 µl of ExGen 500 (not the reverse order) and immediately vortex-mix the solution for 10 sec.
4. Incubate at room temperature for 10 min.
5. Add 100 µl of the ExGen 500/DNA mixture to each well. Generally, the volume of the ExGen 500/DNA mixture represents 1/10 of the total volume of the culture medium.
6. Gently rock the plate back and forth, and from side-to-side to achieve even distribution of the complexes.

7. Incubate for 4 hrs. Replace with fresh complete growth media.
8. Incubate at 37°C for 24 to 48 hrs. The transfected gene expression can be monitored 24 to 48 hrs (transient expression).

2.2.9 Protein concentration determination

The presence of protein in a sample can be determined by measuring the light absorbance at 280 nm. Bovine serum albumin (BSA, BCATM protein assay kit, Pierce) is the most commonly used standard for protein assays. A standard curve of known BSA concentrations is constructed first, and then the concentration of the unknown sample is determined by comparison to this curve.

2.2.10 Immunoblot and immunoprecipitation

2.2.10.1 Western blot or immunoblot (IB)

Immunoblot is a method used to detect the protein expression level in a given sample of tissue homogenate or cell extract. It uses gel electrophoresis to separate denatured proteins by mass. The proteins are then transferred out of the gel and onto a membrane (typically nitrocellulose or PVDF), where they are "probed" using antibodies specific to the protein. As a result, the size, processing, or amount of protein in a given sample can be examined and also compared with several groups. Immunoblot was performed according to the following detailed procedures (Sambrook et al, 1989).

1. Prepare SDS-PAGE gel consisting of 4% Stacking gel and 10% Resolving gel (volumes listed below for two gels, each 1 mm thick).

10% Resolving gel (10 ml)

- ddH₂O, 4.01 ml
- Buffer A, 2.5 ml
- 30% Acrylamide, 3.33 ml
- 10% APS, 50 µl
- 10% SDS, 100 µl
- TEMED, 10 µl

4% Stacking gel (5 ml)

- ddH₂O, 3 ml
- Buffer C, 1.25 ml
- 30% Acrylamide, 0.67 ml
- 10% APS, 50 µl
- 10% SDS, 50 µl
- TEMED, 5 µl

Buffer A: 1.5 M Tris-HCL, pH 8.8, 0.5% SDS

Buffer C: 0.5 M Tris-HCL, pH 6.8, 0.5% SDS

Except for ddH₂O (double-distilled H₂O) and 10% SDS, the following other solutions were stored at 4°C: 30% Acrylamide (Bio-Rad); APS, SDS, and TEMED (Sigma-Aldrich).

2. Load prepared protein samples up to 30 µl per well with protein ladder (Bio-Rad) onto 1 mm thick gels and run gel in 1× Running buffer (25 mM Tris-HCl, 0.1% SDS and 250 mM Glycine) at 110 V until bromophenol blue dye reaches bottom of gel.
3. Transfer the proteins from the gel to an Immuno-Blot PVDF membrane (Bio-Rad) in 1×Transfer buffer (25 mM Tris-HCl, 250 mM Glycine, 0.00375% SDS, and 20% Methanol) at 0.23 A for 30-60 min on ice.

4. Briefly wash the membrane for 30 sec in 1×TBST buffer (25 mM Tris-HCl, pH 7.4, 150 mM NaCl, and 0.1% Tween-20, Sigma-Aldrich) and soak the membrane in 10-15 ml “blocking solution” (5% instant skim milk in 1×TBS buffer) for 60 min with gentle shaking at room temperature.
5. Incubate the membrane in a primary antibody diluted with 1×TBST for 2 hrs at room temperature or overnight at 4°C with gentle shaking, and then rinse the membrane in 1×TBST buffer for 10 min, 3 times at room temperature on a rocker.
6. Incubate the membrane with the HRP-conjugated secondary antibody (1:2000~5000, diluted with 1×TBST); gently shake at room temperature for 1 hr, and then rinse the membrane in 1×TBST buffer for 10 min, 3 times at room temperature on a rocker.
7. Incubate the membrane for 1 min in ECLTM Western Blotting Detection Reagent (GE Healthcare) and expose to X-Ray film (KODAK) and develop to visualize proteins.
8. If required, re-expose the membrane. Strip the membrane with 1×stripping buffer (65 mM Tris-HCl, pH 6.8, 2% SDS and 100 mM β-mercaptoethanol, Sigma-Aldrich) for 30 min at 50°C. Wash the stripped membrane for 3×10 min in a large volume of 1×TBST buffer at room temperature on a rocker, prior to blocking in 5% milk 1×TBS solution.

2.2.10.2 Immunoprecipitation (IP)

Immunoprecipitation is the technique used for isolating an antigen out of solution using an antibody specific to that antigen, and is a standard method used to assess

protein-protein interaction. The protein of interest is isolated with a specific antibody and proteins sticking to this protein are subsequently identified by western blot. Immunoprecipitation was carried out according to the following steps (Sambrook et al, 1989):

- Harvest cells following the appropriate treatment (drug, transfection *etc.*) and wash with PBS, twice.
- Completely remove the supernatant and resuspend the cell pellet in 1 ml of cold lysis buffer, containing 1x protease inhibitor cocktail.
- Lyse the cells by placing the tube on ice for 30 min.
- Spin cell lysate at 10,000xg at 4°C for 15 min.
- Collect supernatant, without disturbing the pellet, and transfer to a clean tube.
- Determine protein concentration.
- Aliquot 300-500 µg (1 µg/µl) per tube for IP.
- Add 3-5 µg of antibody (1 µg:100 µg, antibody: protein).
- Rock at 4°C, overnight.
- Add 30 µl sepharose or agarose (mix completely well immediately before addition). Use sepharose A for primary rabbit antibody and sepharose G for primary mouse antibody.
- Rock at 4°C, for 1 hr.
- Spin at 10,000 g for 5 min and leave the pellet undisturbed.

- Rinse with 500 μ l lysis buffer, spin at 10,000xg for 5 min, twice. Get rid of the supernatant as much as possible, still leaving the pellet undisturbed.
- Add 25 μ l 1x loading buffer, gently mix with finger.
- Denature protein at 95~100°C for 5 min.
- Spin down the beads at 10,000xg for 5 min.
- Separate supernatant from sepharose or agarose pellet, and load onto the gel.
- Follow manufacturer's instruction for SDS-PAGE.

2.2.11 Reverse transcriptase polymerase chain reaction (RT-PCR)

Reverse transcriptase polymerase chain reaction (RT-PCR) is a laboratory technique for amplifying a defined piece of a RNA molecule. The RNA strand is first reverse-transcribed into its complementary DNA, followed by amplification of the resulting DNA using polymerase chain reaction. According to the protocol of Invitrogen's SuperscriptTM III First-Strand Synthesis System for RT-PCR, the steps were described below.

2.2.11.1 RNA extraction

1. Extract RNA from naïve or treated cells.
2. Mix 0.75 ml of TRI REAGENT LS (Invitrogen Canada Inc.) with the cell pellet by passing the suspension several times through a pipette. Let sit at room temperature for 5 min to permit the complete dissociation of nucleoprotein complexes.

3. Add 0.1 ml of BCP (Invitrogen Canada Inc.) to cover the samples tightly, shake vigorously for 15 sec, and incubate 2 to 15 min at room temperature. Centrifuge the sample at 12,000xg for 15 minutes at 4°C.
4. Carefully transfer the colorless, upper aqueous phase (approximately 0.6 ml) containing the RNA into a clean micro-centrifuge tube, avoiding removal of the material collected at the interface (containing DNA) and the organic phase (containing protein).
5. Add 0.5 ml of isopropanol (Sigma-Aldrich) into the aqueous phase and gently mix the solution. Allow the RNA to precipitate at room temperature for 10 min, then centrifuge at 12,000xg for 10 min at 4°C.
6. Remove the supernatant and wash the RNA pellet once with 1.0 ml of 75% ethanol (in water treated with DEPC, denatures RNases). Vortex the sample and centrifuge at 7500xg for 5 min at 4°C, or, if the RNA pellet accumulates on the side of the tube and has a tendency to float, spin at 12,000xg for 5 min to ensure sedimentation of the pellet before the ethanol is totally removed.
7. Remove the ethanol wash and briefly air-dry the RNA pellet for 3~5 min at room temperature, then dissolve the pellet with 20 µl of DEPC-treated water by passing the solution through a pipette tip a few times and incubating at 55°C for 10-15 min.
8. RNA concentration is determined by spectrophotometry (Du640 spectrophotometer, Beckman Coulter Inc. An OD ratio 260/280 between 1.6-1.9 is considered free of DNA and protein.

9. Store the total RNA at -70°C .

2.2.11.2 First-strand cDNA synthesis

To obtain the first-strand cDNA for PCR, reverse transcription using the total RNA isolated from the cell pellet was performed according to the following procedures. The total volume of reactive solution was 50 μl (Invitrogen).

1. Add and mix the components as listed, to a 0.5 ml thin-wall PCR tube:
 - 1-5 ng Total RNA
 - 1 μl Oligo(dT)₂₀ Primer (Invitrogen, 50 μM)
 - 1 μl dNTP mix (Invitrogen, 10 mM)
 - DEPC-treated water, up to 10 μl .
2. Incubate the mixture at 65°C for 5 min and then put on ice for at least 1 min.
3. Prepare the following cDNA Synthesis Mix, adding each component to each tube in the following order:
 - 2 μl 10 \times RT buffer (Invitrogen)
 - 4 μl 25 mM MgCl_2
 - 2 μl 0.1 M DTT (dithiothreitol)
 - 1 μl RNaseOUT (40 units/ μl)
 - 1 μl SuperScript III Reverse Transcriptase (200 units/ μl)
4. Add 10 μl of cDNA synthesis mix to each RNA/primer mixture, mix gently, and collect by brief centrifugation. Incubate at 50°C for 50 min.

5. Terminate the reaction at 85°C for 5 min and chill on ice.
6. Collect the reactions by brief centrifugation. Add 1 µl of RNase H to each tube and incubate for 20 min at 37°C to remove the RNA template from the cDNA:RNA hybrid molecule.
7. Store the cDNA at -20°C or use immediately for PCR.

2.2.12 Subcellular fractionation

The subcellular fractionation method was used to separate the different intracellular organelles and cell compartments. Cells are lysed and subcellular components are separated by a series of centrifugations at increasing speeds. Following each centrifugation, the organelles that sediment to the bottom of the tube are recovered in the pellet. The supernatant is then recentrifuged at a higher speed to sediment the next-largest organelles. The aim in this study was to get obtain a mitochondrion-enriched fraction. All steps were performed on ice, according to the following procedure [315].

1. Harvest cells as usual, wash the cell pellet with 1X PBS twice.
2. Resuspend the cell pellet with 1 ml 1X PBS, save 100 µl for total cell lysate (TCL) and lyse as usual; lyse the other 900 µl for subcellular fractionation.
3. Spin cell suspension at 2500xg for 5 min, add 320 µl suspension buffer to pellet (containing 20 mM HEPES-KOH (pH 7.5), 320 mM sucrose, 10 mM KCl, 1.5 mM MgCl, 1 mM EGTA, 1 mM dithiothreitol, 1 mM orthovanadate, and a protease inhibitor cocktail).

4. Homogenize using 15-20 strokes, on ice.
5. Spin homogenates as follows: 900xg, 10 min at 4°C to get the P1 pellet containing cell debris, cell membrane and nuclei.
6. Transfer the supernatant to a fresh tube, spin at 18,000xg, 50 min at 4°C to get the P2 mitochondria-enriched pellet. Save the supernatant as cytosol.
7. Rinse all the pellets with buffer containing protease inhibitor cocktail, suspend pellets in lysis buffer (volume depends on pellet size). Determine protein concentration.
8. Determine protein expression by immunoblot.

2.2.13 Site-directed mutagenesis

In vitro site-directed mutagenesis is a technique used for carrying out vector modification and studying protein structure-function relationships. In this study, we used the QuikChange site-directed mutagenesis kit (Stratagene) to make point mutations, *e.g.* targeted mutations of specific nucleotides in the plasmid DNA, resulting in substitutions of amino acids in the translated protein). The plasmid DNA is replicated using *PfuTurbo*® DNA polymerase as it replicates both plasmid strands with high fidelity and without displacing the mutant oligonucleotide primers. The basic procedures in the protocol the manufacturer provided utilize a super-coiled double-stranded DNA (dsDNA) vector, with an insert of interest and two synthetic oligonucleotide primers containing the desired mutation.

The primers must be individually designed, according to the desired mutation. The following considerations, according to Stratgene, should be made for designing mutagenic primers:

1. Both of the mutagenic primers must contain the desired mutation and anneal to the same sequence on opposite strands of the plasmid.
2. Primers should be between 25 and 45 bases in length, with a melting temperature (T_m) of $\geq 78^\circ\text{C}$.
3. The desired mutation (deletion or insertion) should be in the middle of the primer with ~ 10 to 15 bases of correct sequence on both sides.
4. Optimally, the primers should have a minimum GC content of 40% and should terminate in one or more C or G bases.
5. Mutagenesis includes the following steps:
 - Synthesize two complementary oligonucleotides containing the desired mutation, flanked by unmodified nucleotide sequence.
 - Prepare the sample reaction(s) as indicated below:
 - 5 μl of 10 \times reaction buffer
 - X μl (5-50 ng) of dsDNA template
 - X μl (125 ng) of oligonucleotide primer #1
 - X μl (125 ng) of oligonucleotide primer #2
 - 1 μl of dNTP mix
 - ddH₂O to a final volume of 50 μl

1 μ l of *PfuTurbo*[®] DNA polymerase (2.5 U/ μ l)

6. Denature the template at 95°C for 30 sec. Run PCR with various cycle numbers according to the type of the mutant: Point mutations, 12 cycles; Single amino acid changes, 16 cycles; Multiple amino acid deletions or insertions, 18 cycles. Each cycle includes the following steps:
 - Denature at 95°C for 30 sec
 - Anneal at 55°C for 1 min
 - Extension at 68°C for 1 min/kbp plasmid length
7. Following temperature cycling, place the reaction on ice for 2 min to cool the reaction to $\leq 37^\circ\text{C}$.
8. Add 1 μ l of the *Dpn* I restriction enzyme (10 U/ μ l) directly to each amplification reaction. Gently and thoroughly mix each reaction mixture by pipetting the solution up and down several times. Spin down the reaction mixtures in a microcentrifuge for 1 min and immediately incubate each reaction at 37°C for 1 hr to digest the parental (*i.e.*, the non-mutated) supercoiled dsDNA.
9. Transform the mutated plasmid to XL1-blue competent cells provided by the kit and express it.

In the present study, the primers for MAO-A or MAO-B and p38 mutants include:

MAO-A(D61A): forward: CTA TAA GGA ATG GAC ATG TTG CTT ACG TAG

ATG TTG GTG GAG C; reverse: GCT CCA CCA ACA TCT ACG TAA GCA

ACA TGC TCA TTC CTT ATA G.

MAO-A(D248A): forward: CCT GTC ACT CAC GTT GCC CAG TCA AGT GAC

AAC; reverse: GTT GTC ACT TGA CTG GGC AAC GTG AGT GAC AGG.

MAO-A(D328G): forward: GCT GCA TGA TCA TTG AAG GTG AAG ATG CTC

CAA TTT C; reverse: GAA ATT GGA GCA TCT TCA CCT TCA ATG ATC

ATG CAG C.

p38(T/E): forward: CAC ACT GAT GAT GAG ATG GAA GGC TAC GTG GCT

ACC AGG; reverse: CCT GGT AGC CAC GTA GCC TTC CAT CTC ATC

ATC AGT GTG

p38 (T/E Y/D, activated form): forward: GAT GAT GAG ATG GAA GGC GAC

GTG GCT ACC AGG TGG TAC; reverse: GTA CCA CCT GGT AGC CAC

GTC GCC TTC CAT CTC ATC ATC.

p38(T/A): forward: CAC TGA TGA TGA GAT GGC AGG CTA CGT GGC TAC;

reverse: GTA GCC ACG TAG CCT GCC ATC TCA TCA TCA GTG.

p38(T/A Y/F, dominant negative form): forward: GAG ATG GCA GGC TTC GTG

GCT ACC AGG; reverse: CCT GGT AGC CAC GAA GCC TGC CAT CTC.

MAO-A(S/A): forward: GGC ACC ACT CGG ATA TTC GCT GTC ACC AAT

GGT GGC CAG; reverse: CTG GCC ACC ATT GGT GAC AGC GAA TAT

CCG AGT GGT GCC.

MAO-A(S/E): forward: GGC ACC ACT CGG ATA TTC GAG GTC ACC AAT

GGT GGC CAG; reverse: CTG GCC ACC ATT GGT GAC CTC GAA TAT

CCG AGT GGT GCC.

MAO-B(S/A): forward: CAC AAC AAG AAT CAT CGC GAC AAC AAA TGG
AGG AC; reverse: GTC CTC CAT TTG TTG TCG CGA TGA TTC TTG TTG
TG.

MAO-B(S/E): forward: CAC AAC AAG AAT CAT CGA GAC AAC AAA TGG
AGG AC; reverse: GTC CTC CAT TTG TTG TCT CGA TGA TTC TTG TTG
TG.

MAO-A(Y/F): forward: TGC TGC CAA ACT CTT GAC TGA ATT TGG CGT
TAG TGT TTT GGT TTT AG; reverse: CTA AAA CCA AAA CAC TAA CGC
CAA ATT CAG TCA AGA GTT TGG CAG CA.

MAO-A(Y/D): forward: TGC TGC CAA ACT CTT GAC TGA AGA TGG CGT
TAG TGT TTT GGT TTT AG; reverse: CTA AAA CCA AAA CAC TAA CGC
CAT CTT CAG TCA AGA GTT TGG CAG CA.

To confirm the desired mutations and the absence of extraneous mutations, all the mutants were sequenced at the Plant Biotechnology Institute (University of Saskatchewan) through the start codon using a primer specific to the CMV promoter in pCMV: CGC AAA TGG GCG GTA GGC GTG; or a primer specific to the promoter T₇₋₂₀ in pcDNA3.1: TAA TAC GAC TCA CTA TAG GG.

2.2.14 DSS cross-linking reaction

Disuccinimidyl suberate (DSS) (Pierce Chemical Co.) is a homo-bifunctional, non-cleavable, and membrane permeable cross-linker. It contains an amine-reactive

N-hydroxysuccinimide (NHS) ester at each end of an 8-carbon spacer arm. NHS esters react with primary amines at pH 7-9 to form stable amide bonds, along with release of the *N*-hydroxysuccinimide leaving group. Proteins, including antibodies, generally have several primary amines in the side chain of lysine (K) residues and the *N*-terminus of each polypeptide that are available as targets for NHS-ester cross-linking reagents.

DSS application is helpful to determine the intracellular protein interaction prior to cell lysis, allowing for the detection of weak or transient protein interactions. The procedure includes several steps according to the protocol the manufacturer provided, as described below.

Cells were plated in 100 mm² dishes. Before harvesting for immunoblotting, the cells were incubated with the chemical cross-linker disuccinimidyl suberate (DSS; concentration at 0.1 mM) for 0.5 hr at room temperature. The DSS stock solution was prepared in DMSO; the control reaction contained the same amount of DMSO as the cross-linking reaction. Reactions were quenched with 1 M Tris·HCl, pH 7.5, at a final concentration of 50 mM for 15 min at room temperature. Cells were then harvested as usual.

2.2.15 Visualization of intracellular Ca²⁺ levels

Fluo-3-AM (Molecular Probes, Eugene, Oregon, USA) is cell-permeable, visible light-excitable, high affinity Ca²⁺ indicator. It is non-fluorescent in its free ligand form, but when it forms complexes with calcium, its fluorescence increases 60-80 times. It is

widely used to estimate the intracellular free Ca^{2+} concentration. According to the protocol the manufacturer provided, the procedure is listed below.

1. Grow cells in a 12 well-plate with a cover-slip inside each well. Treat the cells.
2. Prepare the loading buffer immediately prior to use. Add 16.5 mg Pluronic F127 to Fluo 3-AM/DMSO solution. Pluronic F127 prevents aggregation of Fluo 3-AM in HBSS and helps uptake with cells. Dilute the Fluo 3-AM solution with HBSS to prepare 4 μM Fluo 3-AM working solution.
3. Remove the cell culture medium, and rinse cells with 1X PBS, twice.
4. Add the Fluo 3-AM working solution to the cells, and incubate at 37°C for 30 min (Kwan et al., 2000) in a time-dependent order.
5. Take the coverslip out and rinse with 1X HBSS, flip over on a bigger glass coverslip.
6. Monitor the fluorescence at 528 nm (excitation: 488-500 nm) on an Olympus FV300 Confocal Laser Scanning Biological Microscope. The intensity of the fluorescence reflects the levels of the intracellular free Ca^{2+} .

2.2.16 Detection of production of reactive oxygen species (ROS)

Formation of reactive oxygen species (ROS) was determined by use of the fluorescent probe 2,7-dichlorofluorescein diacetate (DCFH-DA), as originally described by Keston and Brandt [316]. This fluorescence method is based on the incubation of cells with the probe DCFH-DA, which passively diffuses through cellular membranes, where the

acetates are cleaved by intracellular esterases. Thereafter, the non-fluorescent compound DCFH is oxidized by ROS to the fluorescent compound DCF.

The cells were seeded in a 12-well plate with a coverslip inside one well. After different treatments, the cells were rinsed by PBS twice and then incubated with 5 μ M DCFH-DA (stock solution 5 mM in DMSO) at 37°C in 5% CO₂ atmosphere for 30 min. The extracellular medium was removed and the cells were added to 1.5 ml pre-warmed HEPES-buffered (20 mM) HBSS (pH 7.0), with 5 mM glucose. The thin coverslip was taken out and prepared to check for DCF fluorescence (Ex: 488 nm; Em: 530 nm). The change of DCF fluorescence of living cells allows the quantitation of intracellular ROS.

2.2.17 Nuclear condensation detection by Hoechst staining 33258

The Hoechst stain 33258 fluorescently labels DNA, commonly used to visualize nuclei and mitochondria. The dye is excited by ultraviolet light at around 350 nm, and emits blue/cyan fluorescent light around an emission wavelength at 461 nm, as described previously [317].

Primary cortical cells were cultured in a 12-well plate with a coverslip inside one well. After proper treatments, the medium was removed and the cells rinsed by 1X PBS buffer twice. Cells were fixed by 4% PFA for 20 min at room temperature. Cells were washed with 1X PBS buffer twice. Cells were loaded with Hoechst 33258 stain (10 μ g/ml) for 10 min at room temperature. Morphological evaluation of nuclear condensation and

fragmentation was performed immediately after staining on an Olympus FV300 fluorescence microscope.

2.2.18 JC-1 and the mitochondrial membrane potential

Detection of the mitochondrial permeability transition event provides an early indication of the initiation of cellular apoptosis. The loss of mitochondrial membrane potential ($\Delta\psi_m$) is a hallmark for apoptosis. This process is typically defined as a collapse in the electrochemical gradient across the mitochondrial membrane. Loss of $\Delta\psi_m$ can be detected by a unique fluorescent cationic dye, 5,5',6,6'-tetrachloro-1,1',3,3'-tetraethylbenzamidazolocarboyanin iodide, commonly known as JC-1. In non-apoptotic cells, JC-1 accumulates as aggregates in the mitochondria, resulting in red fluorescence. However, in apoptotic and necrotic cells, JC-1 exists in monomeric form and stains cells green. To measure $\Delta\psi_m$ changes in cells, we used JC-1 Mitochondrial Membrane Potential ($\Delta\psi_m$) Detection Kit (Cat#30001, Cell Signaling Technology Inc., Cummings Center Beverly, MA, USA) with the protocol the manufacturer provided.

For fluorescence microscopy, cells were grown on a glass cover slip in a 12-well plate, and treated as for every experimental design. JC-1 reagent was diluted to 1X immediately prior to use. The cell culture media was removed and loaded with enough diluted 1X JC-1 reagent to cover the cells. The cells were incubated at 37°C in a 5% CO₂ incubator for 15 min. Medium was removed and washed once with 1X assay buffer. One drop of PBS was added and covered with a coverslip. A fluorescence microscope using a

“dual-bandpass” filter was used for immediate observation. The dye will remain in its monomeric form and appear green with an emission at 530 nm. The red aggregates emit at 590 nm.

For fluorescence ratio detection, cells should be cultured to a density not to exceed 1×10^6 cells/ml. Following treatment, 0.5 ml cell suspension is transferred into a sterile centrifuge tube and centrifuged at 400 g for 5 min at room temperature. The supernatant is removed and the cells resuspended in 0.5 ml 1X JC-1 reagent. The cells are then incubated at 37°C in a 5% CO₂ incubator for 15 min, then centrifuged at 400 g for 5 min. The supernatant is removed and the cell pellet resuspended in 2 mL 1X assay buffer, followed by centrifugation twice. The supernatant is then removed and the cell pellet resuspended in 300 µL assay buffer. 100 µL cell suspension is transferred into each of three wells of a black 96-well plate. Red and green fluorescence is measured [red fluorescence (excitation 550 nm, emission 600 nm) and green fluorescence (excitation 485 nm, emission 535 nm)] using a fluorescence plate reader, and the ratio of red fluorescence divided by green fluorescence is then determined. The ratio of red to green fluorescence is decreased in dead cells and in cells undergoing apoptosis compared to healthy cells.

2.3 Statistical analysis

Significance (set at $P < 0.05$) was assessed by unpaired Student's *t*-test (two groups) or by one-way ANOVA (three groups or more) with *post-hoc* analysis relying on

Bonferroni's Multiple Comparison Test. Data are represented as mean \pm standard deviation (S.D.).

3 RESULTS

3.1 Endogenous MAO activity in selected cells and the response of MAO to addition of Ca^{2+} to the reaction solution

3.1.1 MAO gene expression and activity levels differ across cell lines

C6 cells, HT-22 cells, PC12 cells, and N2a cells had higher levels of *mao-A* gene expression than did SH-SY5Y cells and HEK293A cells. T98G cells expressed almost no *mao-A* gene (Fig. 7A). The levels of *mao-B* gene expression were also uneven across the seven cell lines. Two fragments, possible splice variants, were detected in HT-22 cells and N2a cells (Fig. 7A).

The activity levels in corresponding cell lysates did not match the levels of gene expression (for example, N2a cells had high *mao-A* gene expression, but were virtually MAO-A null). Similarly, MAO-B activities also did not match the level of *mao-B* gene expression (Fig. 7B).

The basic conclusion here was that MAO activity did not necessarily concord with gene expression, indicating possible post-transcriptional as well as post-translational regulation of MAO-A function.

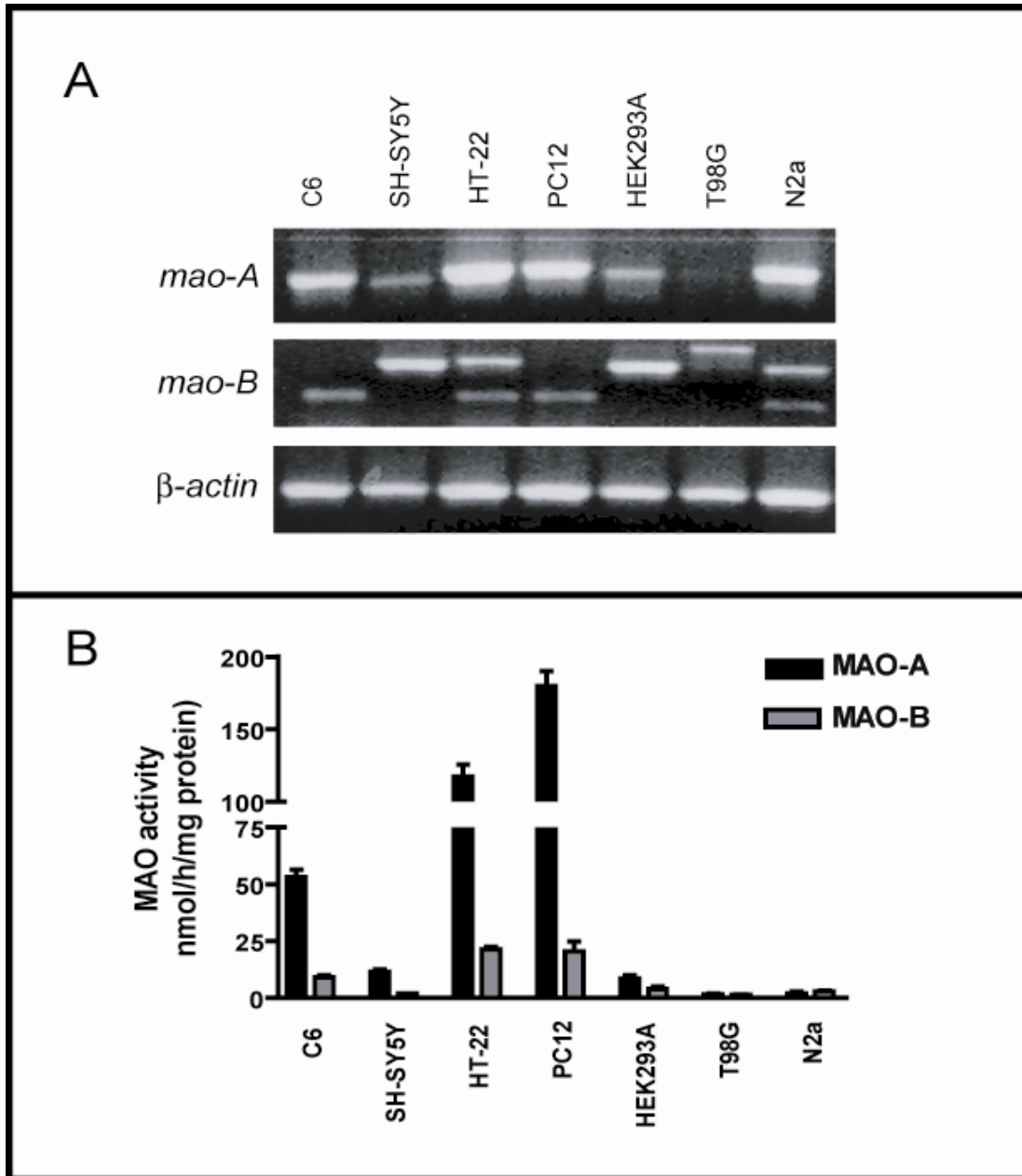


Fig. 7: Gene expression and activity levels of MAO-A and MAO-B in selected cell lines. Cell lines were screened for *mao-A* and *mao-B* gene expression (A, n=3) and MAO activities (B, n \geq 3; except SH-SY5Y and T98G, n=2). The expression of *mao-A* and *mao-B* genes varied across cell lines as did the level of activities in corresponding homogenates, and did not necessarily concord. Data are represented as mean \pm StDev.

3.1.2 MAO activity is dependent on protein concentration

The radioenzymatic assay for MAO activity suggested using 100 µg/100 µL as this lies within the linear range. Using C6 cell lysates, the linear range for this assay was confirmed to lie within the range of 50-200 µg/100 µL (Fig. 8). All subsequent MAO enzyme assays used 100 µg protein/100 µL.

3.1.3 The effect of Ca²⁺ incubation time and Ca²⁺ concentration on MAO-A activity

The optimal incubation of C6 cell lysates of Ca²⁺ was 20 min when MAO-A activity was elevated [$P<0.01$, vs. 0; $F_{(5,23)}=7.971$] (Fig. 9A). Incubating with different concentrations of Ca²⁺ for 20 min, it was shown that the peak effect was at 1mM of Ca²⁺ [$P<0.001$, vs. 0; $F_{(6,20)}=43.98$] (Fig. 9B), confirming previous data [303].

3.1.4 Ca²⁺ selectively enhances MAO-A activity in animal brain tissues

In rat cerebellar homogenates, incubation with Ca²⁺ for 20 min enhanced MAO-A activity (basal levels: 24.07 ± 5.27 nmol/h/mg protein, $P<0.05$, vs. 0; $F_{(6,27)}=4.566$) by approximately 69% (Fig. 10A). In contrast, MAO-B activity (basal levels: 40.66 ± 5.88 nmol/H/mg protein) in rat cerebellar homogenates was not affected by addition of Ca²⁺ (Fig. 10B).

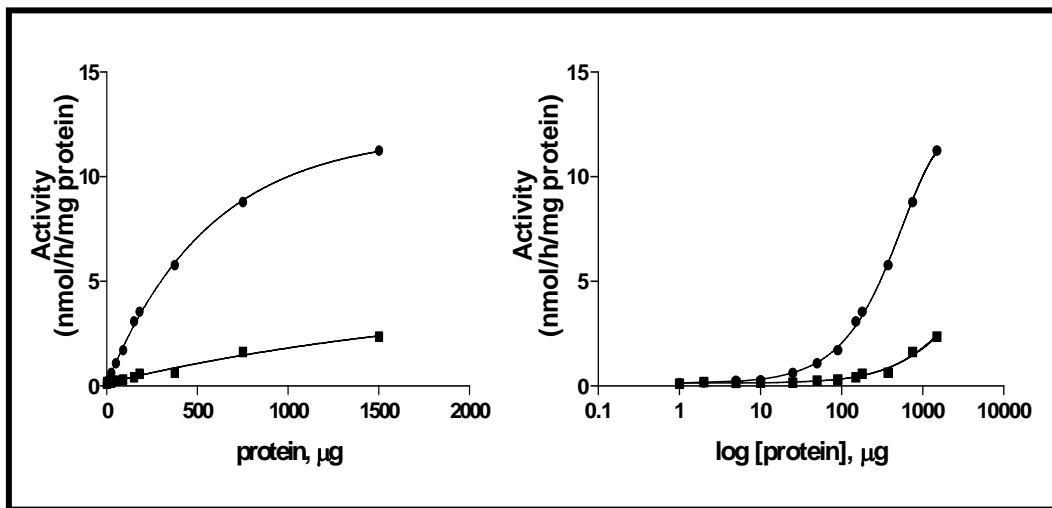


Fig. 8: MAO enzyme activity is dependent on protein concentration. MAO-A (●) and MAO-B (■) activities in C6 glial cell homogenates were assayed using increasing amounts of total protein to determine linear ranges and saturability. Data are represented as mean \pm StDev (n=3). A concentration of 100 $\mu\text{g}/100 \mu\text{L}$ reaction volume was used for the remainder of the MAO radioenzymatic assays.

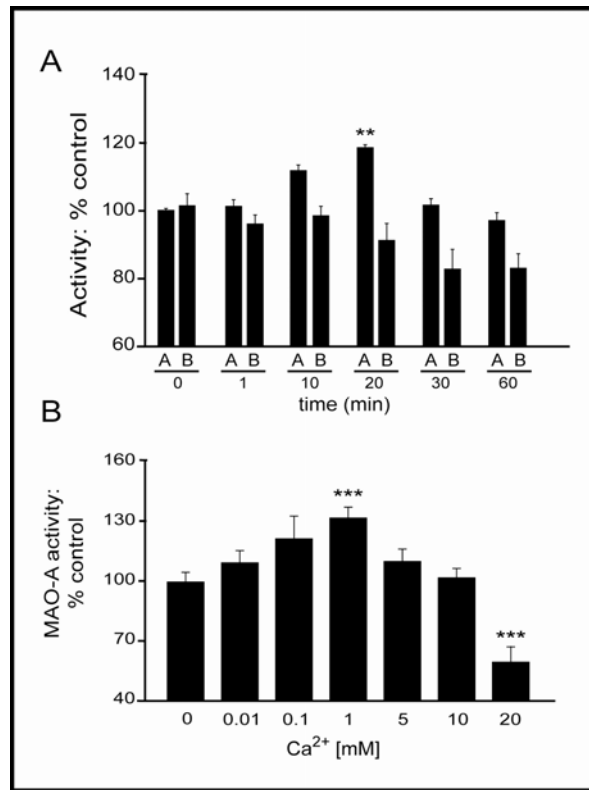


Fig. 9: MAO-A activity in C6 cell homogenates is increased by Ca²⁺ in a time-dependent manner. (A) MAO-A (labelled as “A”) and MAO-B (“B”) activities were determined in C6 cell homogenates incubated with Ca²⁺ (1mM: ref. 303) for different periods of time. A 20-minute incubation with Ca²⁺ appeared to enhance MAO-A activity [$P < 0.01$, vs. 0 mM; $F_{(5,23)} = 7.971$]. (B) MAO-A activity was enhanced by addition of Ca²⁺ to the incubation buffer, and confirmed a peak response at approximately 1mM [$P < 0.001$, vs. 0 mM; $F_{(6,20)} = 43.98$]. Data are represented as mean \pm StDev (n=3).

In mouse hippocampal, cerebellar and cortical homogenates, MAO-A activity was also selectively increased by addition of Ca^{2+} to the incubation buffer ($P < 0.05$, vs. 0; $F_{(6,20)} = 43.98$) (Fig. 10C&D).

3.1.5 The effect of Ca^{2+} on MAO activity in glial C6 cells is sensitive to Mg^{2+}

Incubation of C6 cell homogenate with Ca^{2+} (1 mM) resulted in an increase in MAO-A activity that was blocked with the co-incubation with Mg^{2+} [$F_{(3,12)} = 12.80$, $P = 0.0005$]. MAO-B activity was not affected by incubation with either Ca^{2+} or Mg^{2+} [$F_{(3,12)} = 0.2302$, $P = 0.8376$] (Fig. 11A). Unexpectedly, when further experiments were carried out, the basal level of MAO-A activity decreased and the response of MAO-A to Ca^{2+} was no longer evident (Fig. 11B). At this point it was questionable if cell confluence was a factor.

3.1.6 MAO-A activity in hippocampal HT-22 cells is also selectively enhanced by Ca^{2+} and is sensitive to Mg^{2+}

Because of the observed changes in MAO-A activity in C6 cells, another cell line was needed for characterization studies. MAO-A activity in the hippocampal HT-22 cell line also responded selectively, with a peak response of approximately 20% (with 1 mM Ca^{2+}) [$F_{(7,40)} = 4.481$, $P = 0.0009$] (Fig. 12). MAO-B activity was not influenced by Ca^{2+} [$F_{(6,14)} = 0.8957$, $P = 0.5243$] (Fig. 12). Mg^{2+} , a natural antagonist of Ca^{2+} , blocked the

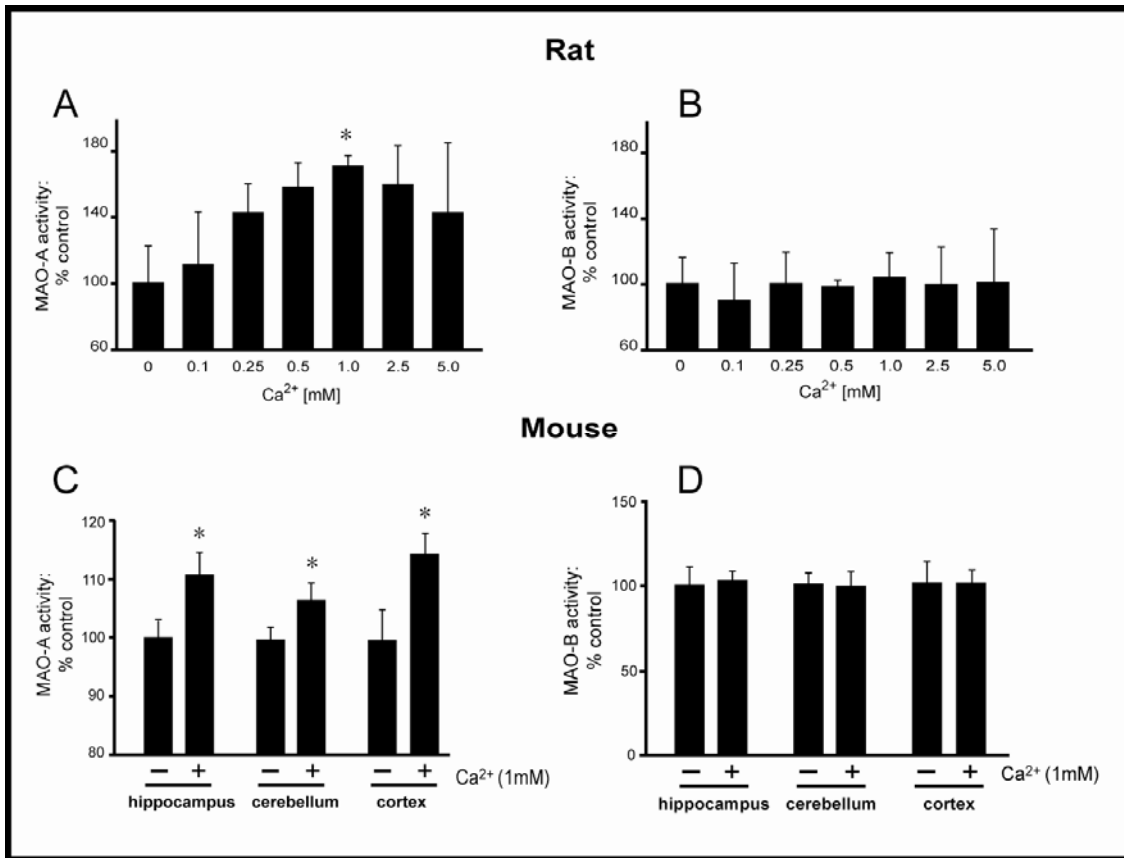


Fig. 10: Ca²⁺ selectively enhances MAO-A activity in regional homogenates from rat and mouse brain. MAO activity was examined in rat cerebellar (A&B) ($P < 0.05$, vs. 0 mM; $F_{(6,27)} = 4.566$) and in mouse hippocampal, cerebellar and cortical (C&D) ($P < 0.05$, vs. 0 mM; $F_{(6,20)} = 43.98$) homogenates. The effect of Ca²⁺ was selective for MAO-A in all samples tested. Data are represented as mean \pm StDev (n=3).

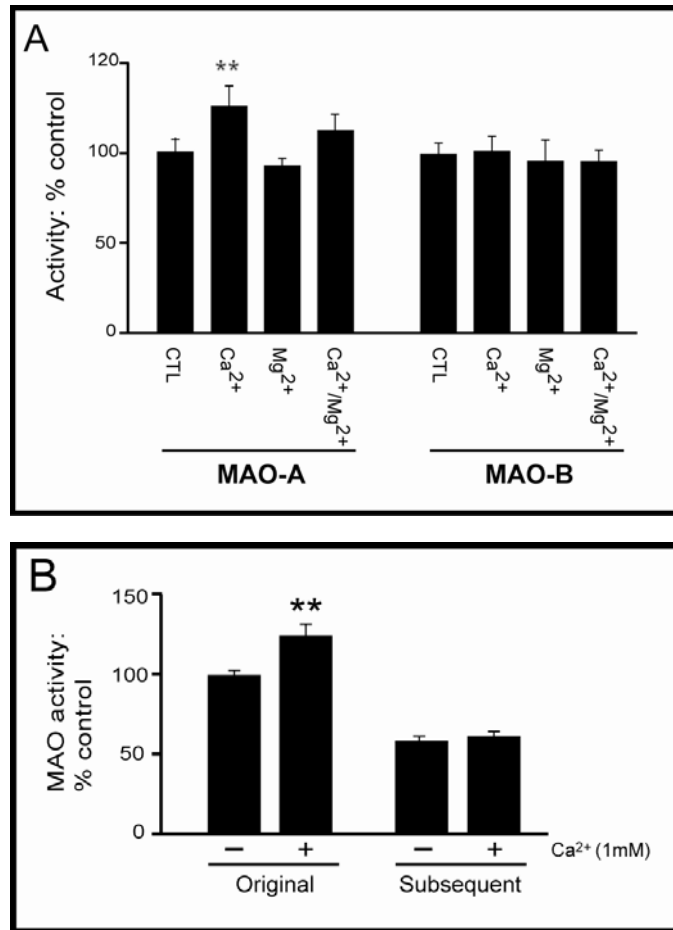


Fig. 11: The effect of Ca²⁺ on MAO-A activity in C6 cell homogenates is not consistent. (A) Incubation of C6 cell homogenate with Ca²⁺ (1 mM) resulted in an increase in MAO-A activity that was sensitive to co-incubation with Mg²⁺ (an antagonist of Ca²⁺) [$F_{(3,12)}=12.80$, $P=0.0005$]. MAO-B activity was not affected by incubation with either Ca²⁺ or Mg²⁺ [$F_{(3,12)}=0.2302$, $P=0.8376$]. (B) It was observed that the basal MAO-A activity as well as its response to Ca²⁺ diminished in subsequent cultures. At this point it was unclear if this was due to the cells having been allowed to grow to confluency. Data are represented as mean \pm StDev (n=3). **: $P<0.01$ versus vehicle control.

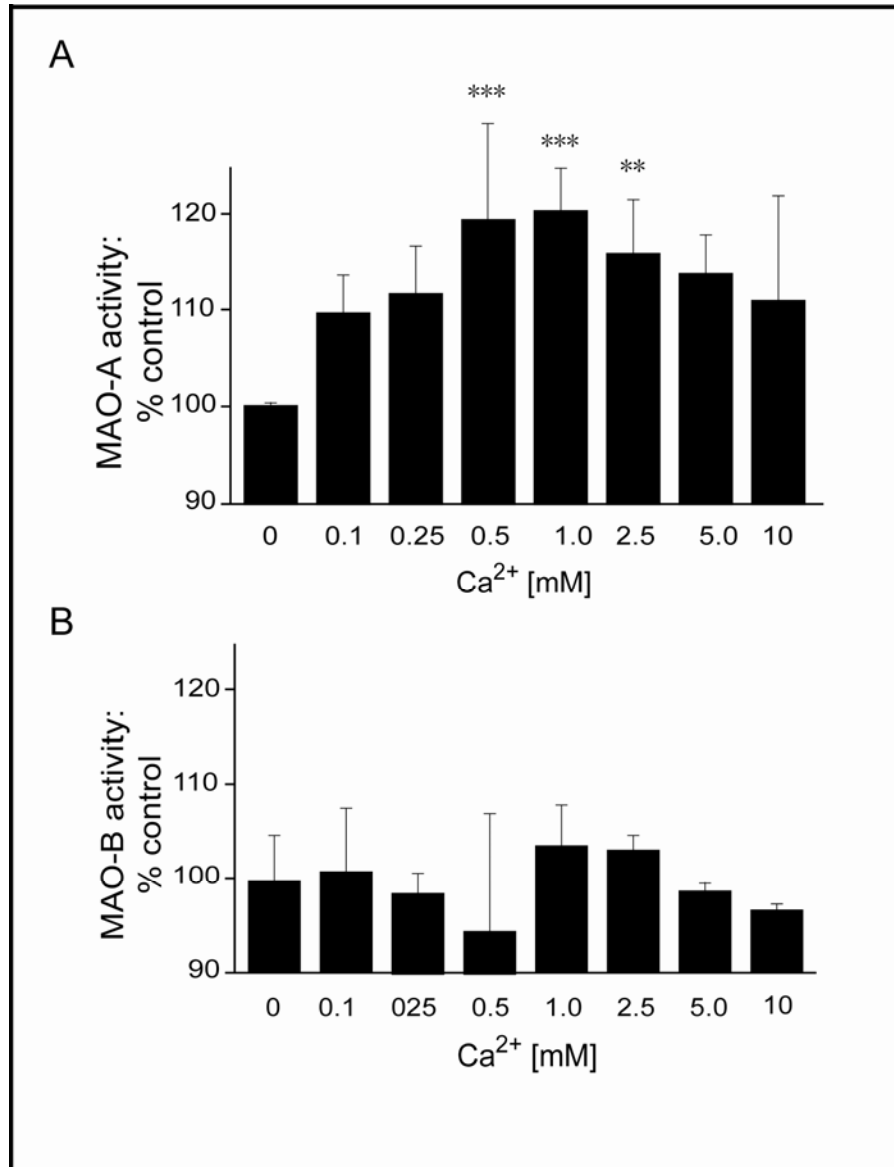


Fig. 12: Ca²⁺ selectively enhances MAO-A activity in HT-22 cell homogenates. (A) MAO-A activity was enhanced by incubation of HT-22 cell homogenates with increasing concentrations of Ca²⁺ [$F_{(7,40)}=4.481$, $P=0.0009$]. (B) Ca²⁺ did not exert any effect on MAO-B activity [$F_{(6,14)}=0.8957$, $P=0.5243$]. Data are represented as mean \pm StDev (n=4). **: $P<0.01$; ***: $P<0.001$, vs. Vehicle control without Ca²⁺.

effect of Ca^{2+} on MAO-A activity, but did not exert any effect on its own [$F_{(6,14)}=9.39$, $P=0.0003$] (Fig. 13), precluding a generalized effect of divalent cations.

3.1.7 Ca^{2+} affects MAO-A kinetics in HT-22 cells

Kinetic analyses of MAO-A activity in HT-22 cells revealed a decrease in K_M (97.97 ± 7.044 with Ca^{2+} , vs. 126.1 ± 21.08 without Ca^{2+} ; $P=0.0244$, $t=2.464$, $df=6$) in the presence of Ca^{2+} (1mM), indicating that Ca^{2+} facilitated the enzymatic reaction. V_{MAX} remained unaltered (713.2 ± 12.32 with Ca^{2+} , vs. 731.1 ± 29.29 without Ca^{2+} ; $P=0.3029$, $t=1.127$, $df=6$) suggesting that Ca^{2+} was potentially acting *via* an allosteric mechanism (Fig. 14).

3.2 Overexpressed MAO-A, but not MAO-B, responds to incubation with Ca^{2+}

mao-A and *mao-B* were amplified by PCR and subcloned into the *XhoI* restriction site of pCMV/myc/Mito expression vector and verified by DNA sequence analysis (Figs. 15-17) which allowed for mitochondrial targeting and a C-terminal myc epitope tag for specific detection of the overexpressed protein (*i.e.* an anti-myc antibody could be used to detect any overexpressed protein).

Plasmid DNA transfection and overexpression (24 and 48 h) of the MAO-A-myc and MAO-B-myc proteins were examined in HEK293A cells (as these cells are virtually functionally MAO-A null, see Fig. 7). Transfection efficiency using the GFP fluorophore was determined to be approximately 60-80% (not shown). Protein expression was

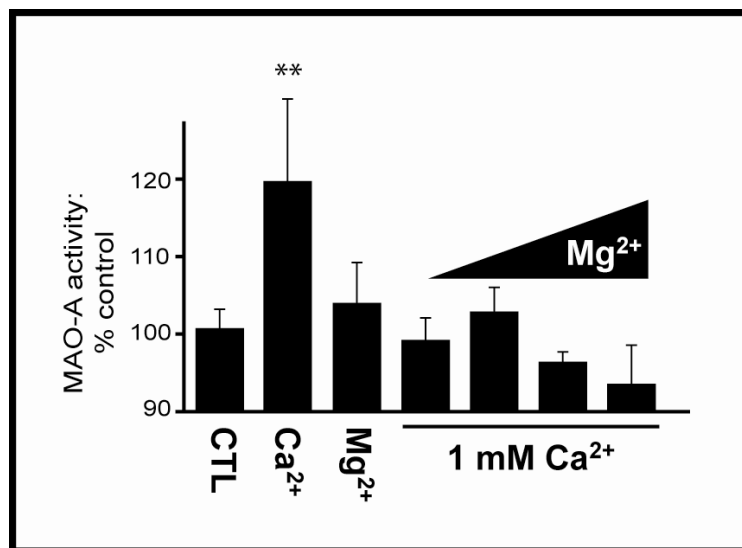


Fig. 13: The response of MAO-A to Ca²⁺ in HT-22 cells is sensitive to Mg²⁺. Inclusion of Ca²⁺ (1 mM) in the incubation buffer increased MAO-A activity in HT-22 cells, but inclusion of Mg²⁺ (an antagonist of Ca²⁺; 1 mM) did not [$F_{(6,14)}=9.39$, $P=0.0003$], indicating the effect of Ca²⁺ on MAO-A activity was specific. The increase in MAO-A activity induced by Ca²⁺ was blocked by the addition of Mg²⁺. Data are represented as mean \pm StDev (n=3). **: $P<0.01$ vs. vehicle control (CTL).

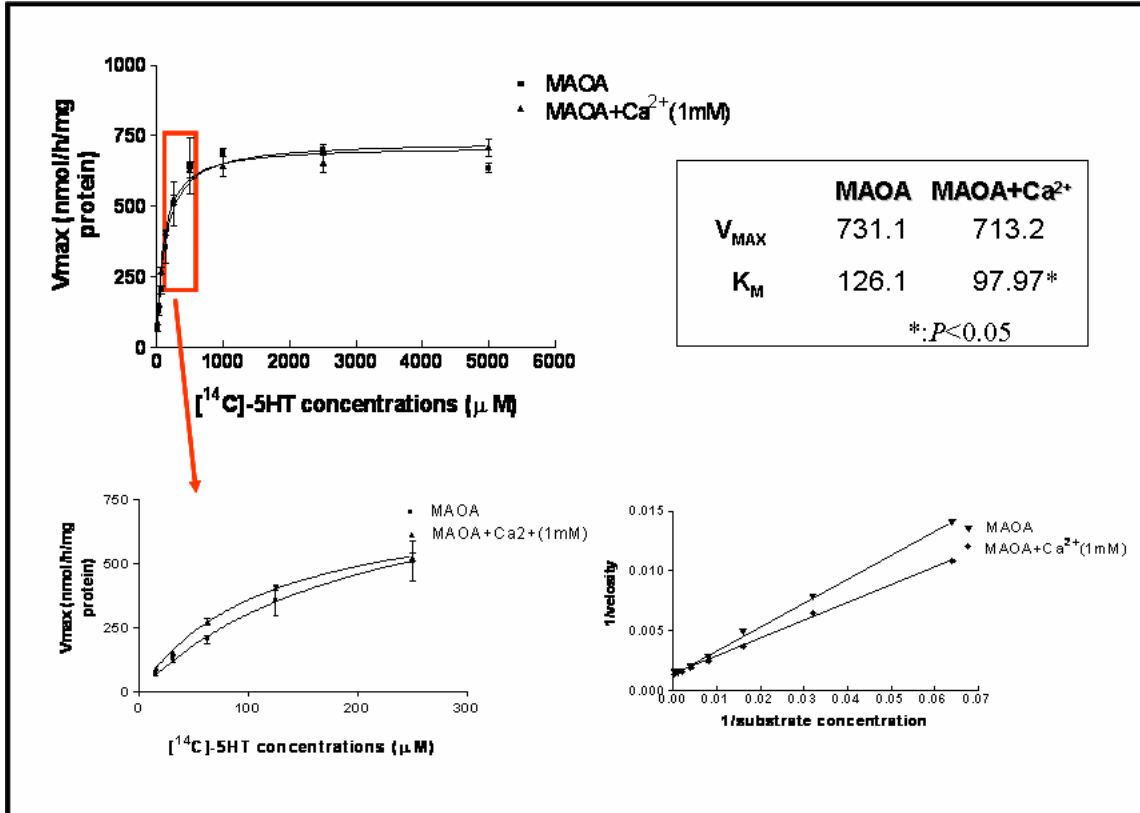


Fig. 14: Ca²⁺ affects MAO-A enzyme kinetics in HT-22 homogenates. Kinetic analysis of HT-22 MAO-A activity in the absence and presence of Ca²⁺ (1mM) revealed that Ca²⁺ decreased the K_M (*:P=0.0244, t=2.464, df=6) and did not affect V_{MAX} (P=0.3029, t=1.127, df=6), suggesting that the enzyme reaction was accelerated. Data are represented as mean ± StDev (n=4).

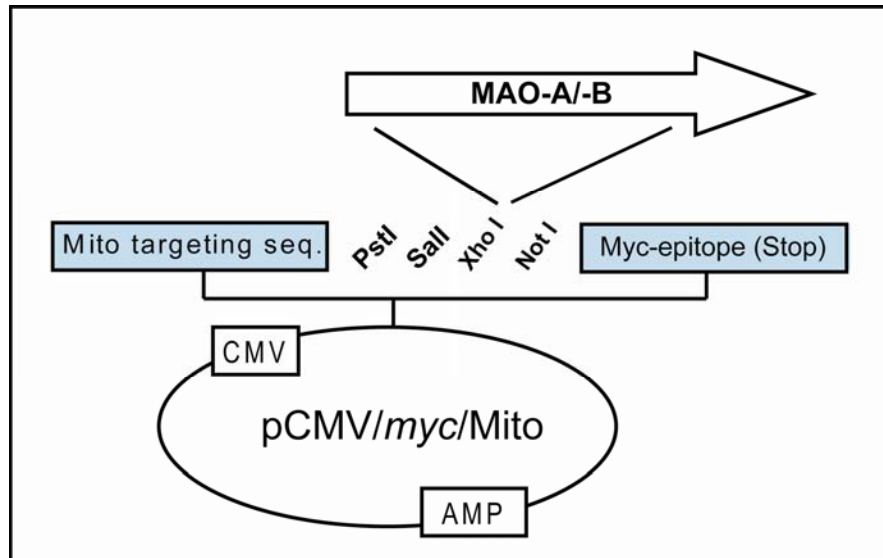


Fig. 15: MAO-A and MAO-B cDNA were fused to a myc-epitope tag to allow monitoring of the overexpressed protein. The diagram shows the multiple cloning site (used for cutting DNA and inserting a gene) flanked by the mitochondrial (Mito) targeting sequence and the C-terminal Myc-epitope tag (before the stop codon) in the the pCMV/myc/Mito expression vector. MAO (-A or -B) cDNA was subcloned in-frame with the Mito targeting sequence and the myc-tag using the *XhoI* and *NotI* restriction sites. CMV: the cytomegalovirus promoter used to facilitate gene expression in mammalian cells. AMP: this gene is included to confer resistance to Ampicillin®, thus allowing for selection of bacterial colonies expressing the plasmid.

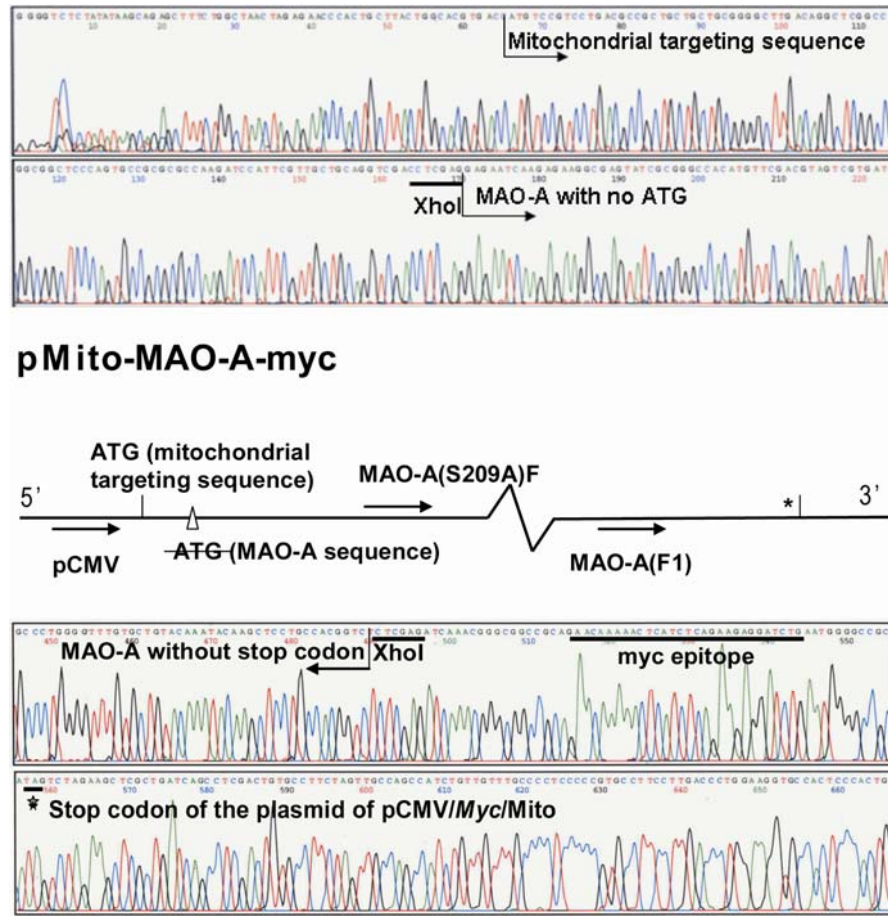


Fig. 16: Representative chromatograms of the cDNA sequence of *mao-A* in the pCMV/Myc/Mito expression vector. The entire open reading frame of the *mao-A* cDNA subcloned into pCMV/Myc/Mito was confirmed by DNA sequencing. The mitochondrial targeting sequence, the *XhoI* restriction site and the *mao-A* gene (with no ATG (start codon) were sequenced using the pCMV primer. The remainder of the sequence, including the end of the *mao-A* cDNA and the myc-epitope tag, was sequenced with the primers MAO-A(S209A)F and the MAO-A(F1) primers (positions are shown in the diagram). ~~ATG~~ indicates where the ATG for the *mao-A* cDNA had been removed (to allow for the fusion protein); “*” indicates the “stop” codon.

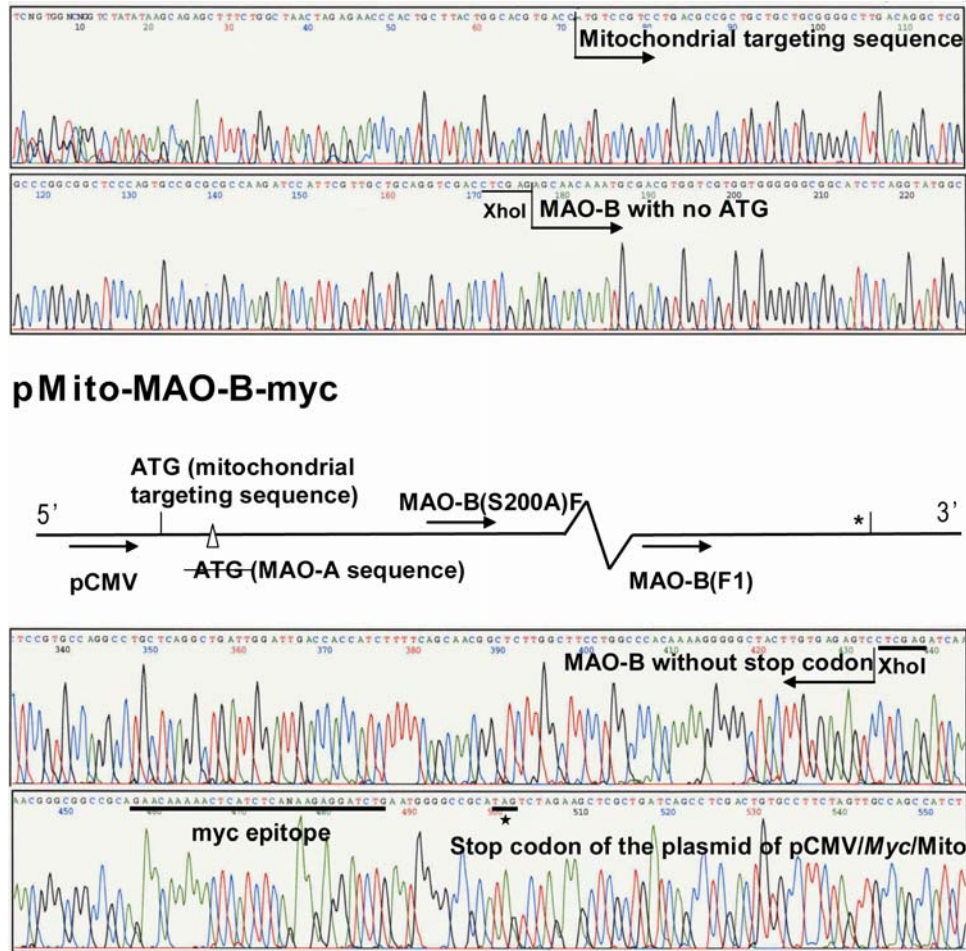


Fig. 17: Representative chromatograms of the cDNA sequence of *mao-B* in the pCMV/Myc/Mito expression vector. The entire open reading frame of the *mao-B* cDNA subcloned into pCMV/Myc/Mito was confirmed by DNA sequencing. The mitochondrial targeting sequence, the *XhoI* restriction site and the *mao-B* gene (with no ATG (start codon) were sequenced using the pCMV primer. The remainder of the sequence, including the end of the *mao-B* cDNA and the myc-epitope tag, was sequenced with the primers MAO-B(S200A)F and the MAO-B(F1) primers (positions are shown in the diagram). ATG indicates where the ATG for the *mao-B* cDNA had been removed (to allow for the fusion protein); “*” indicates the “stop” codon.

dependent on both the amount of DNA used for transfection as well as the time post-transfection (Fig. 18A). In the subsequent experiments, transient transfection was kept at 24 hours and the amount of DNA transfected was kept at 1.0 μg per well of a 24-well plate (or equivalent). Subcellular fractionation revealed that MAO-A-myc expressed was limited, as expected, to the mitochondria-enriched fraction (P_2), as it was not detected in the soluble cytosolic fraction (S) (Fig. 18B).

MAO-A-myc and MAO-B-myc were overexpressed in HEK293A cells for 24 hours to test for their respective enzymatic activities. The overexpressed MAO-A-myc and MAO-B-myc proteins were very active and sensitive to their respective inhibitors, *i.e.* the MAO-A specific inhibitor clorgyline (1 μM , 30 minutes pretreatment) and the MAO-B specific inhibitor l-deprenyl (1 μM , 30 minutes pretreatment) (Fig. 18C).

The mitochondria-enriched P_2 fractions of HEK293A cells overexpressing either MAO-A-myc or MAO-B-myc were incubated with 5 mM Ca^{2+} . The proteins were then resolved by SDS-PAGE and probed with anti-myc antibody. A high molecular weight band was observed in the MAO-A-myc+ Ca^{2+} lane, but not in the MAO-B-myc+ Ca^{2+} lane. Incubation with Mg^{2+} did not result in the appearance of a high molecular weight complex in MAO-A-myc extracts (Fig. 19).

3.3 The effect of mutations of putative Ca^{2+} -binding sites on MAO-A function

The selective effect of Ca^{2+} on MAO-A suggested that putative Ca^{2+} -binding sites might exist in MAO-A, but not in MAO-B. The deduced amino acid sequences of

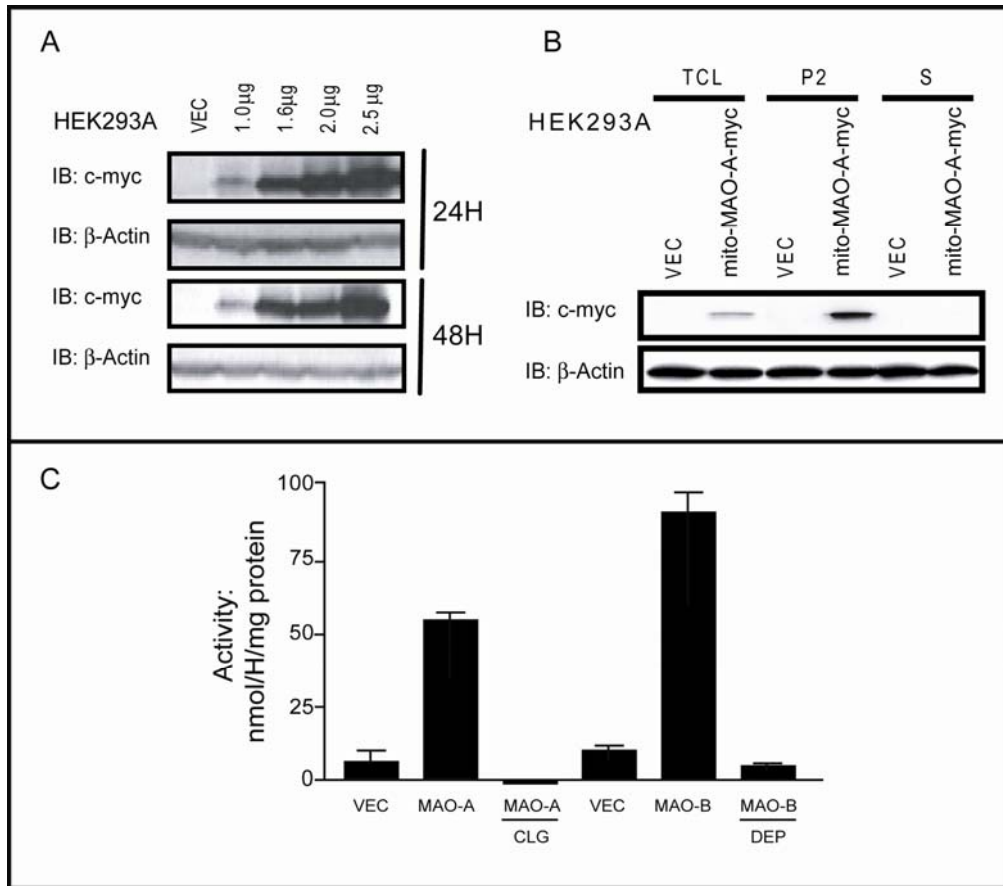


Fig. 18: The expression, subcellular distribution and activity of Myc-epitope tagged MAO-A. HEK293A cells were transfected with increasing quantities of the pMito-MAO-A-Myc plasmid DNA. (A) 24 or 48 hours later cell extracts were probed by immunoblot using the anti-myc antibody and protein expression was confirmed. (B) Subcellular fractionation confirmed that the MAO-A protein was expressed in the P2 mitochondria-enriched fraction and not in the cytosol (S). β -Actin expression was included to demonstrate equal protein loading. (C) The activities of MAO-A or MAO-B (using the pMito-MAO-B-Myc plasmid) in corresponding cell homogenates were inhibited by clorgyline or l-deprenyl ($1\mu\text{M}$, 30 min, preincubation), respectively. Data are represented as mean \pm StDev (six replicates)

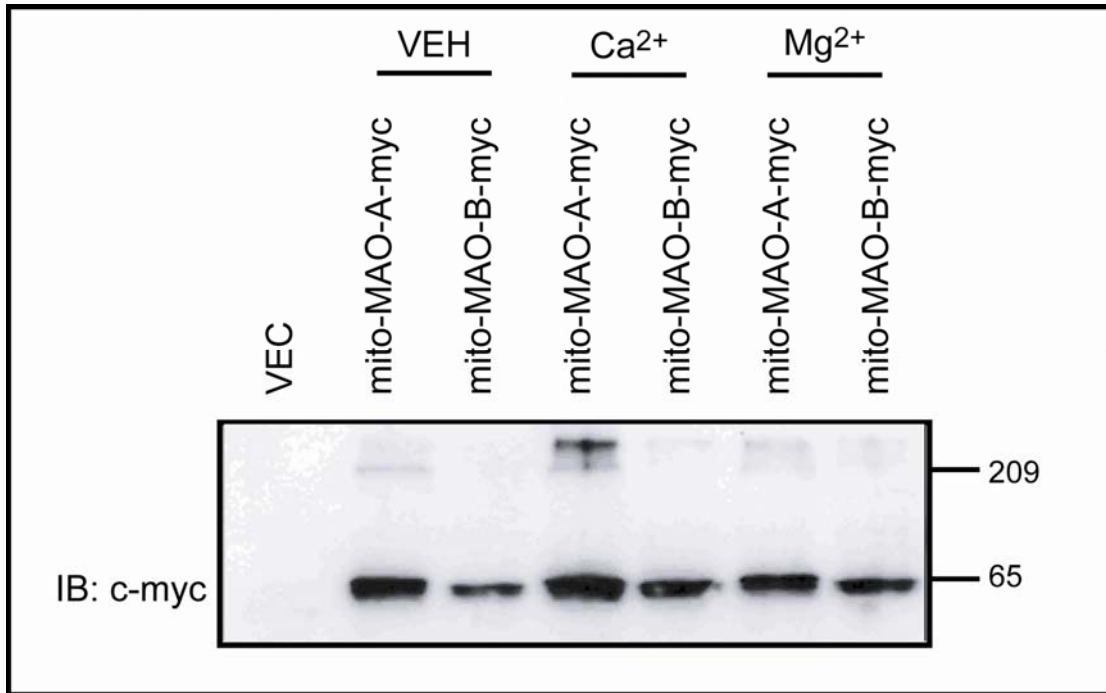


Fig. 19: Ca²⁺ promotes the formation of a high molecular weight complex with overexpressed MAO-A-myc, but not MAO-B-myc. Mitochondrial extracts from HEK293A cells overexpressing either MAO-A-myc or MAO-B-myc were incubated with Ca²⁺ (5 mM, 10 min). A high molecular weight c-myc-specific band was observed in the MAO-A-myc extracts, but not in the MAO-B-myc extracts. Mg²⁺ (5 mM, 10 min) did not exert any effect on either MAO-A-myc or MAO-B-myc.

MAO-A in several mammalian species revealed several putative Ca²⁺-binding sites that follow the general DXD, DXXD and DXXXD motifs [307-309] (Fig. 20). Comparison of the deduced amino acid sequences for MAO-A and MAO-B revealed that some of these motifs were specific for MAO-A; three such putative Ca²⁺-binding motifs specific for MAO-A were targeted for mutagenesis to determine their role in MAO-A function. These motifs were situated at D61, D248, and D328 (Fig. 21, indicated by arrows in boxed motif).

The codons for the aspartate residues (*i.e.* “D”) in the three putative Ca²⁺ binding sites were mutated to substitute the D for an alanine (“A”) for D61 and for D248 or to substitute for glutamine (“G”) for D328 to match the corresponding sequence in MAO-B. The chromatogram confirmed mutagenesis of the respective codons (Fig. 22A). Overexpression of the proteins was confirmed (Fig. 22B), yet activity assays revealed differences in their respective activities [$F_{(4, 20)}=27.1$, $P<0.0001$] (Fig. 22C). MAO-A wild type (WT) and MAO-A(D61A) were both very active, *i.e.* almost 500% over vector-transfected control. MAO-A(D248A) and MAO-A(D328G) were also active (~150-300% over vector-transfected control), but were clearly not as active as MAO-A(WT) (Fig. 22C).

Overexpression of MAO-A(WT) and three Ca²⁺-binding site mutants in HEK293A cells resulted in a pattern of ROS production that paralleled their respective activities (Fig. 23). Transfection itself did not induce ROS production, as demonstrated by the similar levels of ROS in vector-transfected cells and in naïve cells.

Human	Menqekasiaghmfdivviggisglsaakllteygvsvlvleardrv	49
Guinea pig	Massekaspagqifdvviggisglaaakllsehelsvvlvleardrv	
Mouse	Mtdlekpsitghmfdivviggisglaaakllseykinvvlvleardrv	
Rat	Ltdlekpnlaghmfdivgligggisglaaakllseykinvvlvleardrv	
Human	grtytir nehvdyvd vggayvgptqnrilrslskelgietykvnvserlv	98
Guinea pig	grtftvr nehvnwvd vggayvgptqnrilrlakelgletykvnvnerlv	
Mouse	grtytvr nehvkwd vggayvgptqnrilrskdlgietykvnvnerlv	
Rat	grtytvr nehvkwd vggayvgptqnrilrslskelgietykvnvnerlv	
Human	oyvkgktypfrgafppvwnpiayldynnlwrtidnmgkeiptdapweaq	147
Guinea pig	qyvkgktypfrgafppvwnpiayldynnlwrtmddmgkeipndapweap	
Mouse	qyvkgktypfrgafppvwnpiayldynnlwrtmddmgkeipvdapwqar	
Rat	qyvkgktypfrgafppvwnpiayldynnlwrtmdemgkeipvdapwqar	
Human	had kw dkmtmk elid kiwtktarffaylfninvtsephevsalwflw	196
Guinea pig	ha qew dkmtmk dlfd kiwtktakqfatlfninvtsephevsalwflw	
Mouse	ha eed dkmtmk dlid kiwtktarefaylfninvtsephevsalwflw	
Rat	ha qew dkmtmk dlid kiwtktarefaylfninvtsephevsalwflw	
Human	yvkqcggttrifsvtnggqerkfvggsgqvserim dllgd qvklhnpvt	245
Guinea pig	yvkqcggtstrifsvtnggqerkfvggsgqvserim gllgd rvklncpvt	
Mouse	yvrqcggtstrifsvtnggqerkfvggsgqiseqim vllgd kvklsspvt	
Rat	yvrqcggtarifsvtnggqerkfvggsgqvseqim gllgd kvklsspvt	
Human	hvd qssd niiietlnhehyeckyvinaipptltakihfrpelpaernql	294
Guinea pig	yvd qsgg niiietlnhehyeckryvisaipptltakihfrpelpertql	
Mouse	yi dqtdd niiietlnhehyeckyvisaippvltakihfkpelppernql	
Rat	yi dqtdd niiivetlnhehyeckyvisaippiltakihfkpelppernql	
Human	iqrllpmgavikcmmyykeafwkkkdycgcmi ieded apisitlddtkpd	343
Guinea pig	iqrllpmgsvikcmmyyreaafwkkkdycgcmi iedee apisitlddtkpd	
Mouse	iqrllpmgavikcmvykeafwkkkdycgcmi iedee apisitlddtkpd	
Rat	Iqrllpmgavikcmvykeafwkkkdycgcmi iedee apiaitlddtkpd	
Human	gslpaimgfilarkadraklkhkeirkkkicelyakvlgseqalhpvhy	392
Guinea pig	esvpaimgfilarkadraklkhkeirkkkicelyakvlgseqalepvhy	
Mouse	gsmpaimgfilarkaerlaklhkdirkrkicelyakvlgseqalspvhy	
Rat	gslpaimgfilarkadrqaklhkdirkrkicelyakvlgseqalypvhy	
Human	eeknwceeysggcytayfppgimtqygrvirqpvgriffagtetatkw	441
Guinea pig	eeknwceeysggcytayfppgimtqygrvirqpvgriyfagtetatqw	
Mouse	eeknwceeysggcytayfppgimtygrvirqpvgriyfagtetatqw	
Rat	eeknwceeysggcytayfppgimtqygrvirqpvgriyfagtetatqw	
Human	sgymegaveageraarevlnlgkvtekdilwvqepeskdvpaveithtf	490
Guinea pig	sgymegaveageraarevlnalgvakedilwvqepeskdvpaveitrtf	
Mouse	sgymegaveageraarevlnalgvakkdiwvqepeskdvpaveithtf	
Rat	sgymegaveageraarevlnalgvakkdiwveepeskdvpaveithtf	
Human	wernlpsvsgllkiigfstsvtalgvlykykllprs	527
Guinea pig	lernlpsvpgllkiig	506
Mouse	lernlpsvpgllkitgfstsvallcfvlykfkqpqs	526
Rat	lernlpsvpgllkitgvstsvallcfvlykikkllpc	526

Fig. 20: Alignment of the MAO-A deduced amino acid sequences from four mammalian species. There is a high degree of sequence identity across species and several putative Ca²⁺-binding sites, e.g. DXXD, DXXXD and DXD are shown in bold.



Fig. 21: Alignment of the human MAO-A and MAO-B deduced amino acid sequences. Note the high sequence identity (~70%) as well as the lack of identity between putative Ca^{2+} binding motifs, *e.g.* DXXD, DXXXD and DXD, in the two sequences. The D61, D248 and D328 residues (indicated by arrows) are specific to MAO-A and were mutated to Alanine (A) or Glycine (G, in the case of D328, so as to correspond to the MAO-B sequence). Spacing using “...” was included to allow for proper alignment of the two protein sequences.

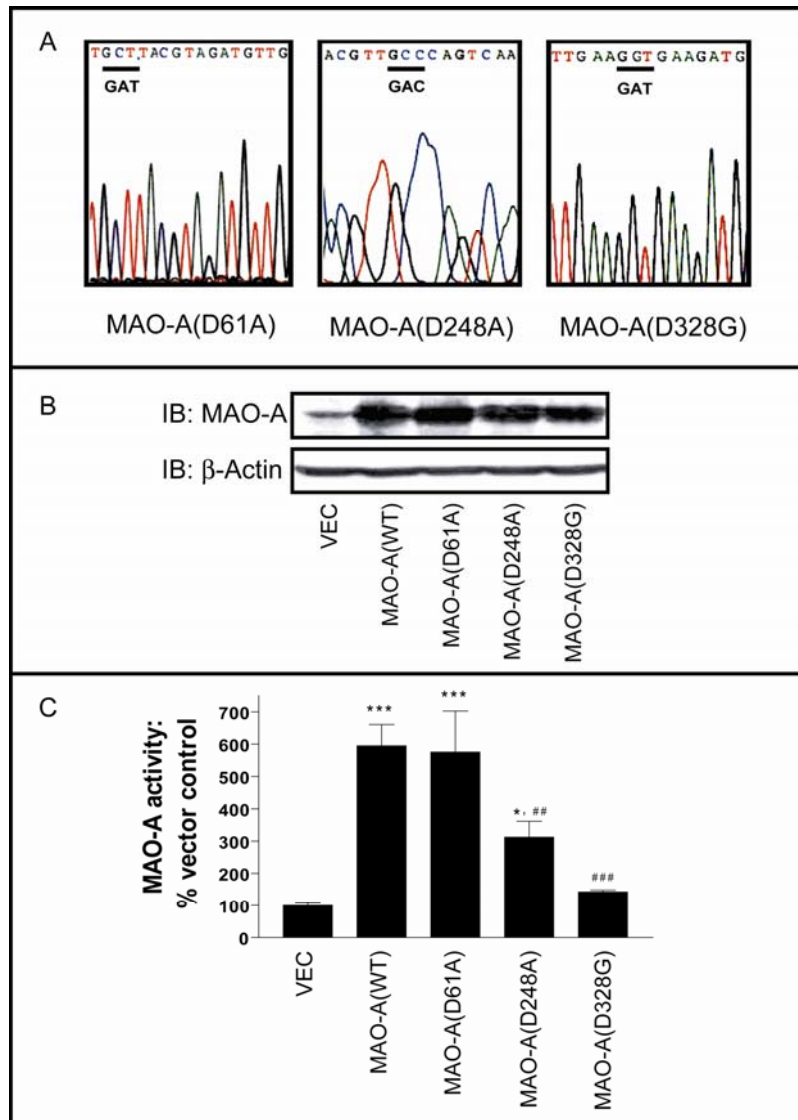


Fig. 22: Ca^{2+} -binding site mutations affect MAO-A activity. (A) Chromatograms of the cDNA sequences that were mutated to allow for targeted amino acid substitutions in the expressed protein. The wild type codon is indicated below the mutated (underlined) codon. (B) The mutated proteins were overexpressed evenly in HEK293A cells (β -Actin expression demonstrates equal protein loading.), yet (C) were not equally as active [$F_{(4, 20)}=27.1$, $P<0.0001$]. Data are represented as mean \pm StDev (n=5). *: $P<0.5$ & ***: $P<0.001$ vs. vector control (VEC); ##: $P<0.01$ & ###: $P<0.001$ vs. MAO-A(WT).

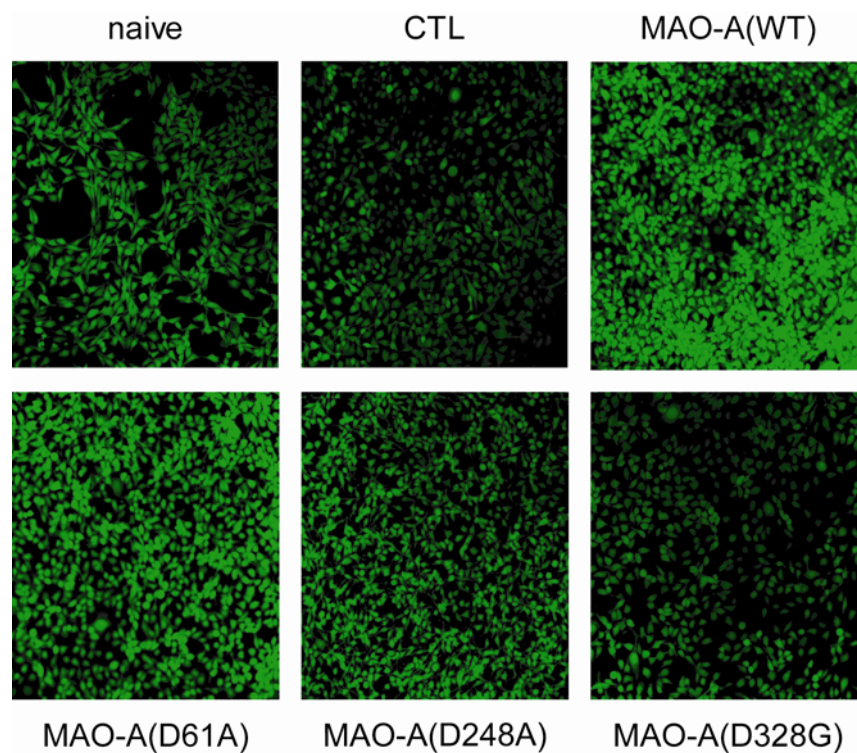


Fig. 23: Ca^{2+} -binding site mutations affect the ability of MAO-A to generate peroxy radicals. The potential of the overexpressed myc-tagged MAO-A(WT) and putative Ca^{2+} -binding mutants on the production of peroxy radicals (a type of reactive oxygen species; ROS) in HEK293A cells was assessed using the H_2O_2 -binding DCF fluorogen. The production of peroxy radicals by the Ca^{2+} -binding mutants diminished in a manner corresponding to their respective activities. Data are representative of three separate experiments.

The toxicity of the overexpressed MAO-A proteins was further demonstrated by the loss of $\Delta\psi_m$ in neuronal N2a cell cultures. This was tested using the JC-1 stain, which was loaded into the cells. The JC-1 stain fluoresces green when it is localized to the cytoplasm as a monomer, and fluoresces red when taken up into the mitochondrion, as a function of the $\Delta\psi_m$, where it exists as a polymer. When the $\Delta\psi_m$ is disrupted, the JC-1 stain is not easily taken up by the mitochondria, resulting in less red fluorescence. Overexpression of the three putative MAO-A Ca^{2+} -binding site mutants as well as the wild type of MAO-A resulted in different ratios of red to green (Fig. 24). MAO-A(WT) and MAO-A(D61A) overexpression resulted in the lowest ratio of red to green fluorescence (reflecting a loss of $\Delta\psi_m$ and indicating apoptotic processes were activated), whereas the other two overexpressed proteins did not affect the JC-1 ratio as significantly. The loss of red fluorescence loosely paralleled their inherent activities, again supporting a toxic role for overexpressed MAO-A and a contribution by Ca^{2+} -binding site(s).

3.4 The three MAO-A Ca^{2+} -binding site mutants associate differently with a high molecular weight complex

A protein's function can be determined by its inclusion in a larger protein complex. To test whether MAO-A exists in such a complex and, if so, does its activity depend on this, HEK293A cells overexpressing either MAO-A(WT) or one of the three putative Ca^{2+} -binding site mutants were treated with DSS, a cell-permeable protein cross-linking reagent. A high molecular weight (HMW, greater than 200 KDa) complex was observed

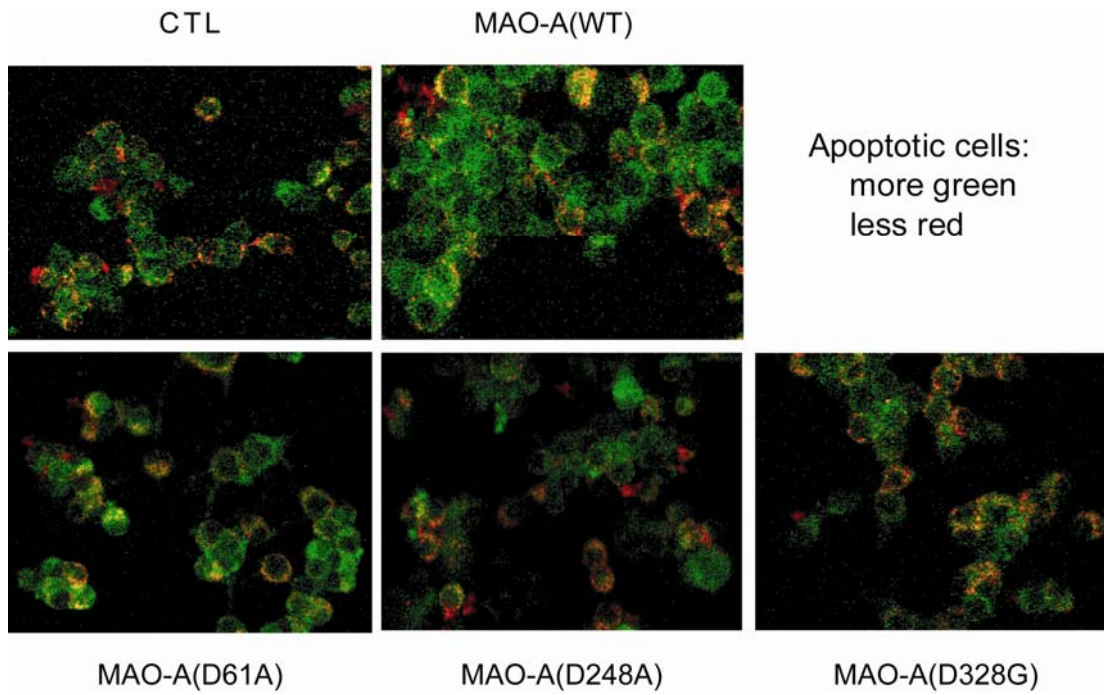


Fig. 24: Ca^{2+} -binding site mutations in MAO-A affect the mitochondrial membrane potential ($\Delta\psi_m$) in N2a cells. The potential of the overexpressed myc-tagged MAO-A(WT) and putative Ca^{2+} -binding mutants to affect $\Delta\psi_m$ in mouse neuroblastoma N2a cells was tested using the JC-1 dye assay. The cultures overexpressing MAO-A(WT) and MAO-A(D61A) were considerably more toxic as determined by the lower ratio of red/green, indicating that the $\Delta\psi_m$ was disrupted. The ratio of green/red in cultures overexpressing MAO-A(D248A) and MAO-A(D328G) was comparable to that in the vector-transfected control group (VEC). Data are representative of two separate experiments.

following treatment with DSS (compared to no DSS treatment) (Fig. 25). Of the four overexpressed MAO-A proteins, MAO-A(D328G) was the least detectable in a HMW complex.

3.5 Overexpressed MAO-A proteins do not respond to Ca^{2+} in HEK293A cells

Neither the activity of overexpressed MAO-A(WT) nor the activities of any of the three MAO-A Ca^{2+} -binding site mutants responded to the addition of Ca^{2+} to the incubation buffer (Fig. 26).

3.6 Overexpressed MAO-A proteins do not respond to Ca^{2+} in N2a cells

MAO-A(WT) and the Ca^{2+} -binding site mutants were overexpressed in N2a cells as these cells were also virtually functionally MAO-A null (see Fig. 7). The activity of the overexpressed protein was evident, but, as with HEK293A cells (see section 3.5, above), there was no response to Ca^{2+} (Fig. 27).

3.7 Cell confluence diminishes MAO-A activity and its response to Ca^{2+} in C6 cells

The lack of response of MAO-A to Ca^{2+} in HEK293A and N2a cells (above) suggested that other factors might be influencing the sensitivity of MAO-A to Ca^{2+} . With this in mind, C6 glial cells, which lost MAO-A activity as well as its sensitivity to Ca^{2+} when confluent (higher passage number?) (*recall* Fig. 11), were re-examined. C6 cells grown to confluence lost MAO-A activity (inhibited to $43.78 \pm 3.3\%$ of MAO-A activity

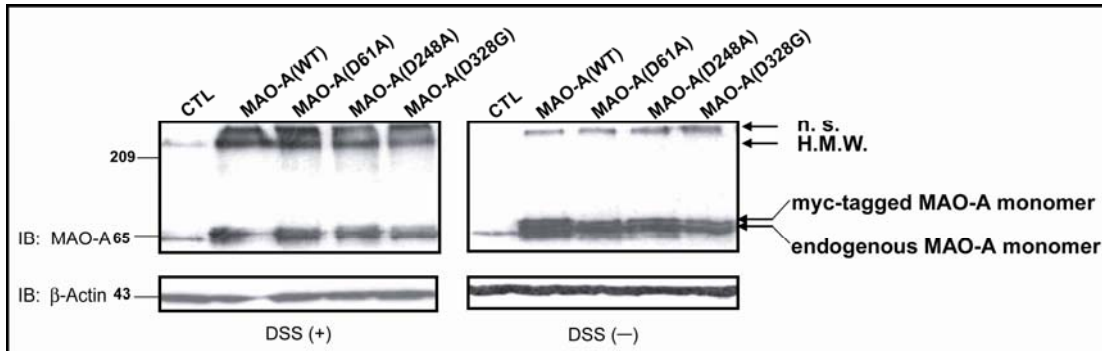


Fig. 25: Mutagenesis of the MAO-A-D328 Ca^{2+} -binding site diminishes its association with a high molecular weight complex. Myc-epitope tagged MAO-A(WT) and the three Ca^{2+} -binding mutants were overexpressed in HEK293A cells. Prior to harvest the cells were treated with the cell permeable cross-linking reagent DSS (1mM, 30 min) or the DMSO vehicle [DSS(-)]. The SDS-PAGE resolved proteins were then probed for MAO-A. A high molecular weight (HMW) complex (>200 kDa) was observed in extracts from the DSS-treated cultures (left). The intensity of the signal of the HMW complex was lowest in MAO-A(D328G) extracts. This HMW complex was not detected in DMSO-treated cultures. β -Actin expression demonstrates equal protein loading. Data represent the results of two separate experiments. n.s.: non-specific band.

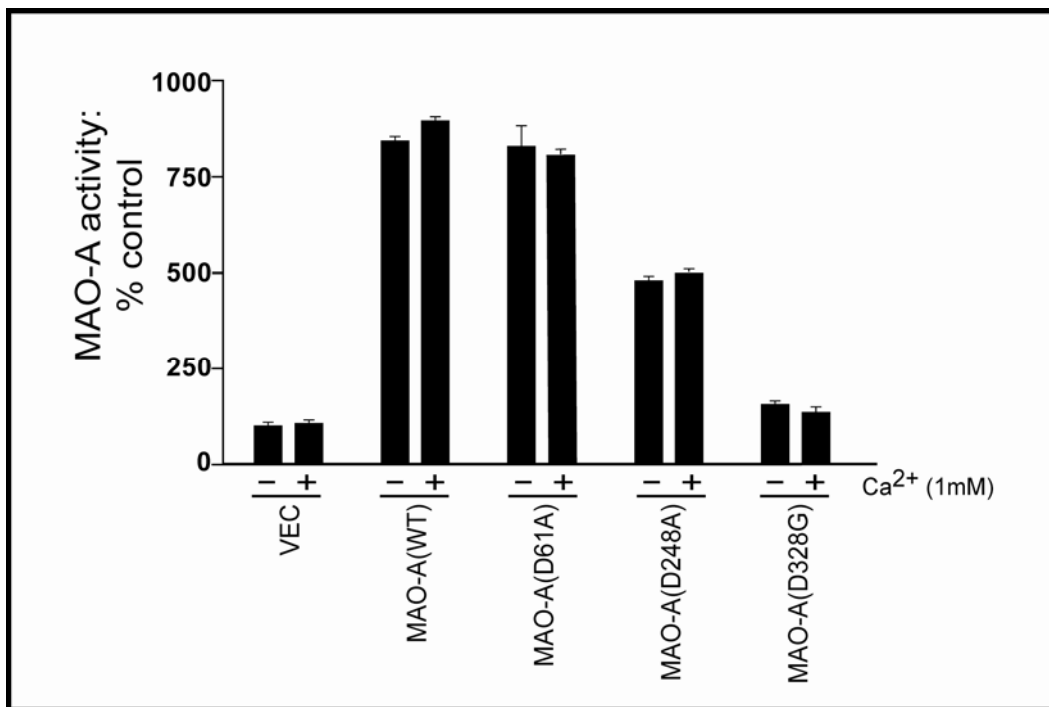


Fig. 26: The activities of overexpressed MAO-A(WT) and Ca²⁺-binding site mutants in HEK293A cell homogenates do not respond to Ca²⁺. None of the overexpressed proteins responded significantly to addition of Ca²⁺ to the reaction buffer. Data are represented as mean \pm StDev (n=5).

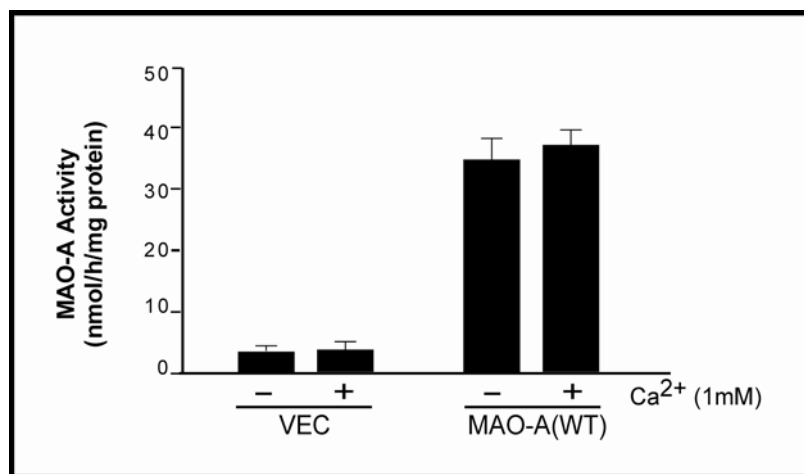


Fig. 27: The activity of overexpressed MAO-A(WT) in N2a cell homogenates does not respond to Ca²⁺. Overexpressed MAO-A did not respond significantly to the addition of Ca²⁺ to the reaction buffer. Data are represented as mean ± StDev (n=3).

in subconfluent cultures, Fig. 28A) ($P=0.0003$, $t=12.25$, $df=4$) as well as their sensitivity to Ca^{2+} (Fig. 28B; same as Fig. 11, included for purposes of comparison) ($P=0.0049$, $t=5.619$, $df=4$). MAO-B activity in confluent cells was not affected (levels were at $93.57 \pm 7.17\%$ of MAO-B activity in subconfluent cell culture, $P=0.8629$, $t=0.1841$, $df=4$) (Fig. 28A). Confluence is already known to affect the phosphorylation of p38(MAPK) in human fibroblasts [318], so p38(MAPK) phosphorylation was also examined in C6 cells grown to confluence. The phosphorylation of p38(MAPK) was clearly increased in confluent C6 cell cultures (Fig. 28C) and suggested an inverse relation between p38(MAPK) phosphorylation and MAO-A activity (and its response to Ca^{2+}).

3.8 p38(MAPK) regulates MAO-A activity and its response to Ca^{2+}

3.8.1 p38(MAPK) phosphorylation was inversely correlated with MAO-A activity level in 4 cell lines.

The levels of p38(MAPK) phosphorylation were examined in the four cell lines used so far (these include C6, HT-22, HEK293A cells & N2a cells). It was observed that MAO-A activity (Fig. 29A) did not correspond with the levels of MAO-A protein (Fig. 29B), but that MAO-A activity was higher in cell lines (*i.e.* C6 & HT-22) that had significantly lower proportions of activated p38(MAPK) [$F_{(3,8)}=99.29$, $P<0.0001$] (Fig. 29C&D). These data supported the hypothesis that p38(MAPK) phosphorylation might be negatively regulating MAO-A activity.

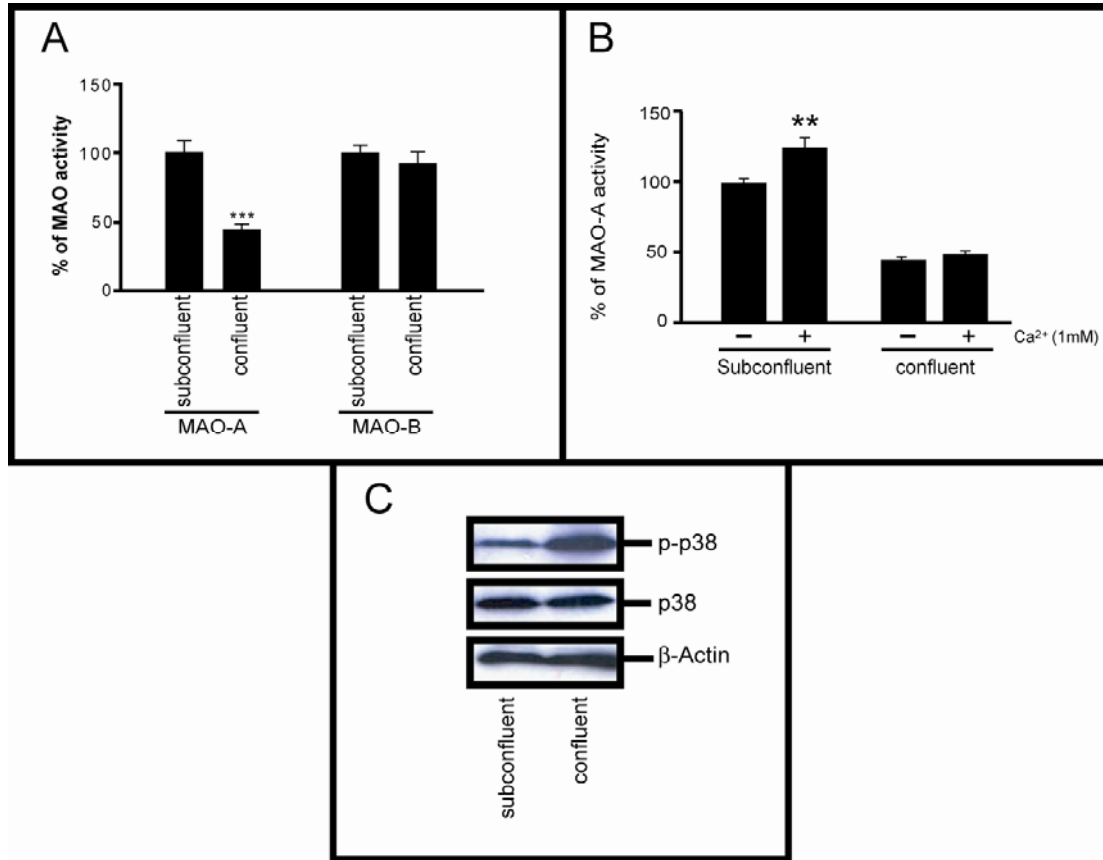


Fig. 28: C6 cell confluence diminishes MAO-A activity and its response to Ca²⁺; correlation with increased phosphorylation of p38(MAPK). (A) Re-examination of MAO-A activity in C6 homogenates revealed that cell confluence influenced basal MAO-A activity (43.78% ± 3.3%, compared to 100% in subconfluent cells; $P=0.0003$, $t=12.25$, $df=4$), but not MAO-B activity ($P=0.8629$, $t=0.1841$, $df=4$). (B) The response of MAO-A to Ca²⁺ demonstrated in subconfluent cells was abolished in confluent cells ($P=0.0049$, $t=5.619$, $df=4$). (C) Confluence is known to activate the p38(MAPK) signaling pathway in human fibroblasts [318]. The confluence of C6 cells clearly affects the phosphorylation (p-p38) of p38(MAPK) in corresponding cell lysates ($n=3$). β-Actin expression demonstrates equal protein loading.

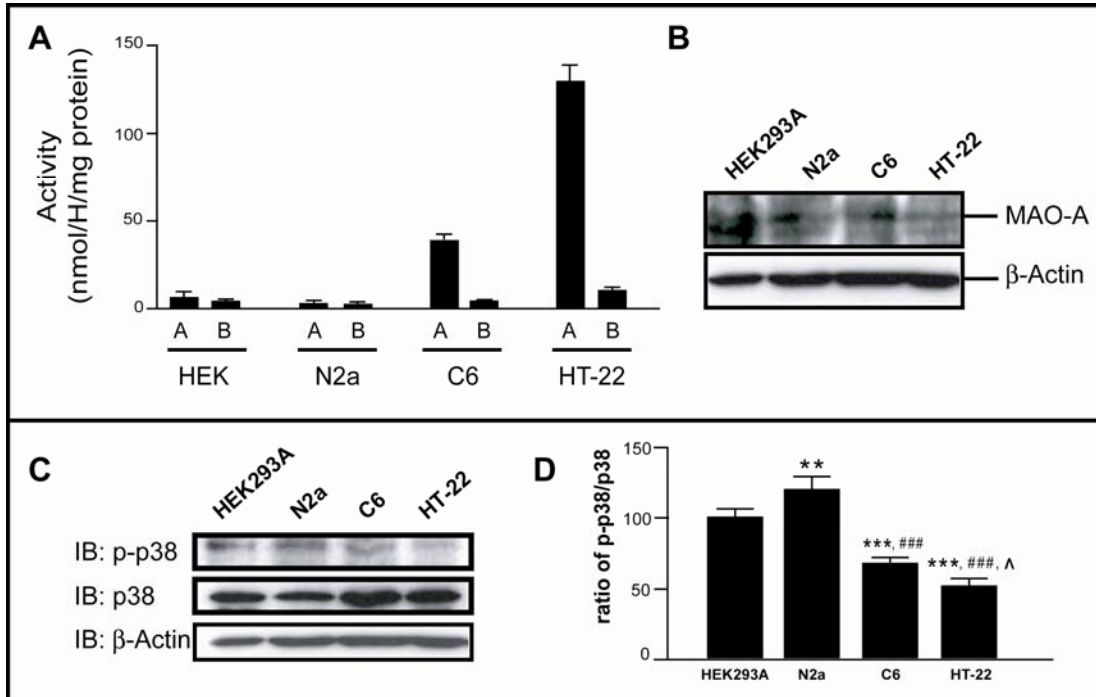


Fig. 29: MAO protein expression and activity, and phosphorylation of p38(MAPK) in four cell lines. (A) The differing levels of MAO-A (labelled as “A”) activities in four cell lines does not (B) correspond with the expression of the MAO-A protein. β -Actin expression was used to demonstrate equal protein loading. (C) MAO-A activity, however, does appear to be inversely related to the level of constitutive p38(MAPK) activation (reflected in the degree of p38(MAPK) phosphorylation, p-p38) as quantified by (D) densitometric analysis of the ratios of phospho-p38 (p-p38) to total p38 in these four cell lines [$F_{(3,8)}=99.29$, $P<0.0001$] (**: $P<0.01$ & ***: $P<0.001$ vs. HEK293A; ###: $P<0.001$ vs. N2a; ^: $P<0.05$ vs. C6).

3.8.2 p38(MAPK) associates with MAO-A protein, but not with MAO-B protein.

Protein-protein interactions are important for many biological functions. The potential association between p38(MAPK) and MAO-A (or MAO-B) was examined in HEK293A cells (low basal MAO-A activity, high p38(MAPK) phosphorylation) and HT-22 cells (high basal MAO-A activity, low p38(MAPK) phosphorylation). Lysates were immunoprecipitated for p38(MAPK) or for MAO-A or MAO-B. MAO-A (but not MAO-B) was detected in p38(MAPK) immunoprecipitates from both HT-22 and HEK293A cells (Fig. 30A), although the association was less in HT-22 cells. These observations were corroborated by the detection of p38(MAPK) in MAO-A, but not in MAO-B, immunoprecipitates (Fig. 30B). This supported the suggestion that p38(MAPK) could regulate MAO-A function.

3.8.3 Chemical p38(MAPK) inhibition increases MAO-A activity and its response to Ca^{2+} .

The influence of p38(MAPK) on MAO-A activity was tested using the specific chemical inhibitor, SB203580, which inhibits the activity, but not the phosphorylation, of p38(MAPK) [319]. A concentration of SB203580 (10 μM) was used based on the published literature [320, 321]. MAPKAP-K2 (MK2) is a downstream target phosphorylated directly by p38(MAPK) [322]. In HT-22 cells, SB203580 decreased MK2 phosphorylation (Fig. 31A) and increased MAO-A activity as well as its response to Ca^{2+} [$F_{(3,12)}=29.67$, $P<0.0001$] (Fig. 31B). MAO-A activity in HEK293A cells

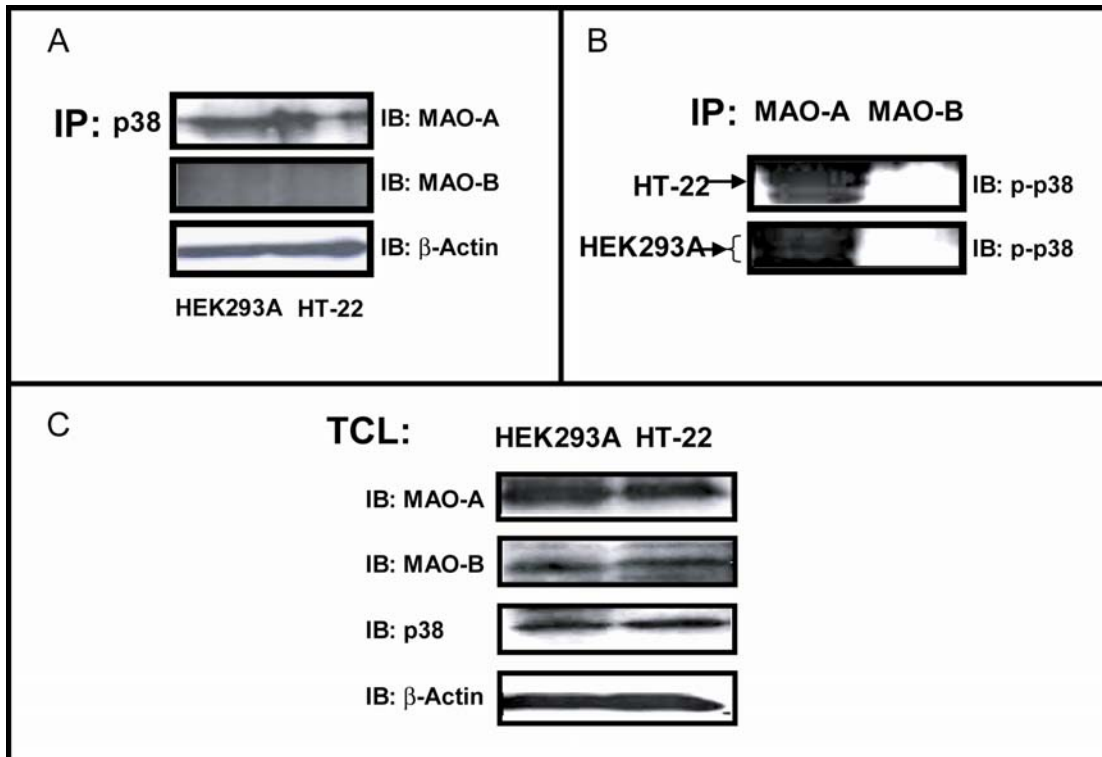


Fig. 30: p38(MAPK) associates selectively with MAO-A protein. (A) Pre-cleared protein extracts from HEK293A and HT-22 cells were immunoprecipitated for p38(MAPK) (p38). The immune complex was resolved by SDS-PAGE and probed for MAO-A or MAO-B using standard immunoblot analysis. MAO-A associated with p38(MAPK), but MAO-B did not. (B) The complementary experiment where either MAO-A or MAO-B was immunoprecipitated confirmed the selective association between MAO-A and p38(MAPK). (C) Total cell lysates (TCL) expressed MAO-A, MAO-B, and p38(MAPK), with β -Actin being used as a loading control.

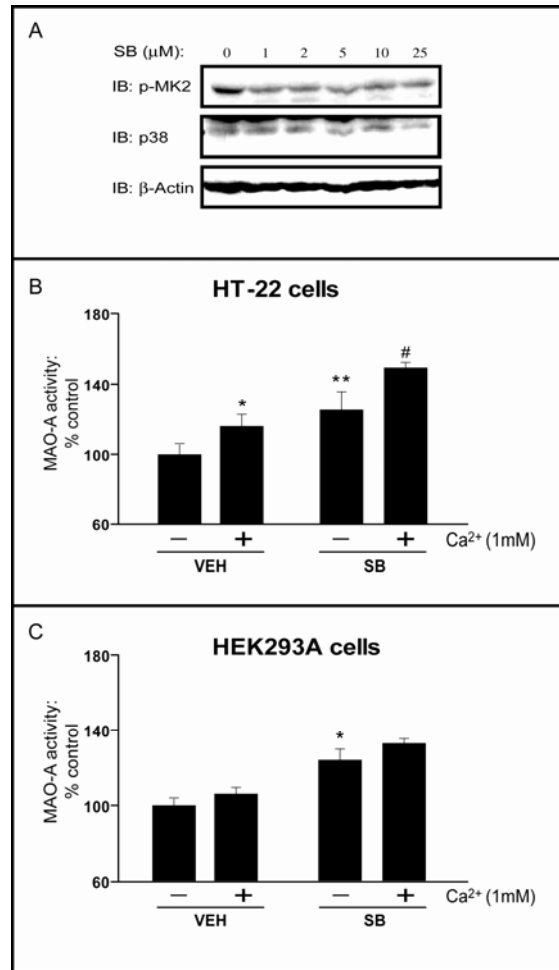


Fig. 31: The specific p38(MAPK) inhibitor SB203580 increases MAO-A activity in HEK293A cells and HT-22 cells. The inhibition of p38(MAPK) in HT-22 cell cultures using SB203580 (SB: 10 μ M, 60 min) (A) decreased the phosphorylation of its downstream target MAPKAPK-2 (MK2), but (B) increased MAO-A activity to $126.4 \pm 10.91\%$ (** vs. VEH, $P < 0.01$). It also enhanced the response of MAO-A to Ca^{2+} (1mM) ($149.5 \pm 0.88\%$, # vs. VEH with Ca^{2+} (1mM), $P < 0.05$) [$F_{(3,12)} = 29.67$, $P < 0.0001$]. (C) In HEK293A cells SB increased basal MAO-A activity (* vs. VEH: $P < 0.05$), but did not significantly increase the response to Ca^{2+} [$F_{(3,12)} = 10.94$, $P = 0.0009$].

treated with SB203580 was also significantly increased [$F_{(3,12)}=10.94$, $P=0.0009$], but the response to Ca^{2+} , although tending to increase, was not significant (Fig. 31C). SB203580 is a pyridinyl imidazole compound and it could be exerting an effect directly on MAO-A as imidazoline is known to bind to, and inhibit, MAO [83, 86, 87]. MAO-A activity in HT-22 cell homogenates was unaffected by addition of SB203580 to the incubation buffer ($P=0.1653$, $t=1.707$, $df=4$) (Fig. 32).

3.8.4 Genetic modulation of p38(MAPK) affects MAO-A activity and its response to Ca^{2+} .

The pEBG-p38(MAPK) α expression vector, obtained from Dr. Brent Zanke (Cross Cancer Institute, Edmonton, AB), was used for PCR-amplification of p38(MAPK). The resulting p38(MAPK) cDNA was subcloned into the *EcoRV* and *XhoI* restriction sites of pcDNA3.1. Using *EcoRI* (note, *EcoRI* restriction sites flank the multiple cloning site and there is one additional *EcoRI* restriction site within the p38(MAPK) cDNA; Fig. 33) Restrictive digestion of p38/pcDNA3.1 with *EcoRI* gave the expected band pattern, thus confirming the presence of p38(MAPK) cDNA within the expression vector. This was further confirmed by the band pattern obtained using *Sall* restriction analysis (Fig. 33) as well as by DNA sequencing using the T₇₋₂₀ primer. The TGY motif necessary for full activation of p38(MAPK) by its upstream kinases MEK3 or MEK6 is evident (Fig. 34) and DNA sequencing of the entire open reading frame indicated that no mutations had been introduced to the cDNA during the PCR amplification process.

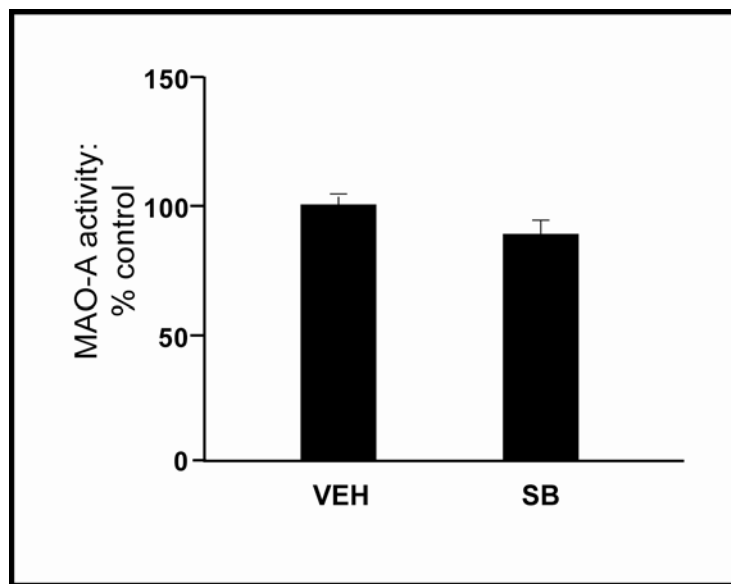


Fig. 32: SB203580 added directly to HT-22 homogenates does not affect MAO-A activity. SB203580 (SB, 10 μ M, 60 min) was added directly to HT-22 homogenates to test whether its effects were occurring as a consequence of direct interaction with the MAO-A protein. No significant effect was observed ($P=0.1653$, $t=1.707$, $df=4$).

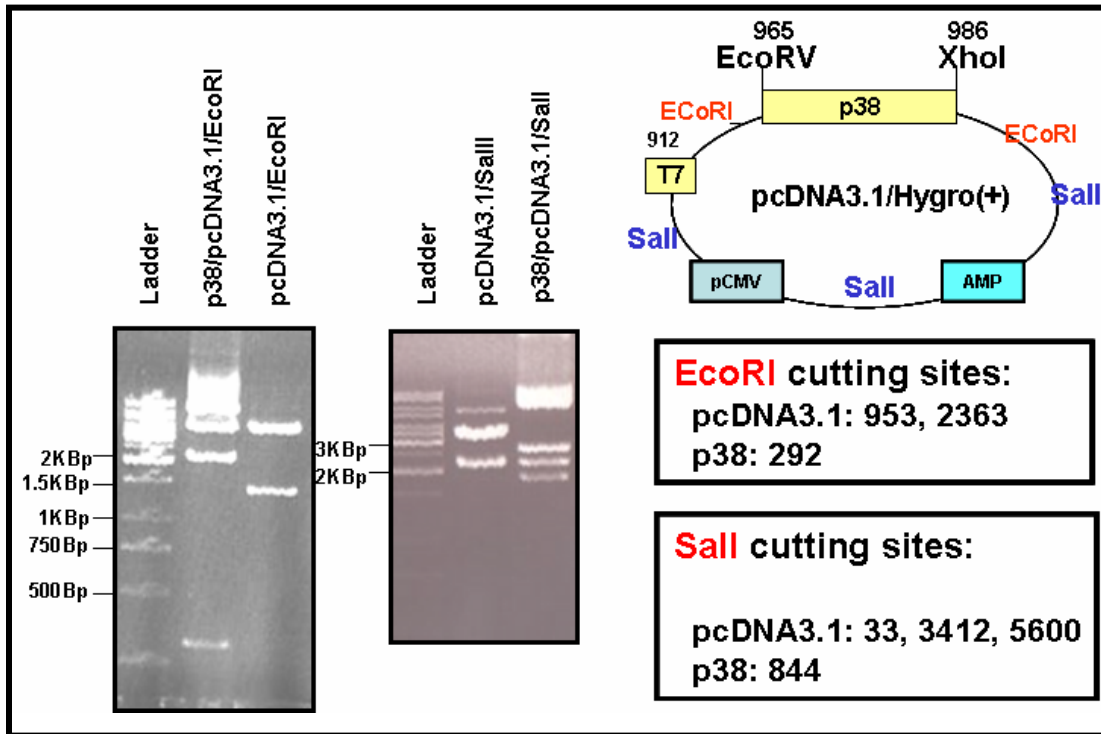


Fig. 33: p38(MAPK) cDNA was subcloned into the pcDNA3.1/Hygro(+) expression vector. p38(MAPK) cDNA was subcloned into the *EcoRV* and *XhoI* restrictions sites in the pcDNA3.1/Hygro(+) expression vector (top, right). Band size (in base pair: Bp) following restriction analysis using *EcoRI* or *Sall* (bottom, left) confirmed the presence of the inserted gene as well as its orientation. The positions of the *EcoRI* and *Sall* restriction sites in the pcDNA3.1-p38(MAPK) plasmid DNA used to calculate the sizes of the expected bands are shown in the boxes on the lower right.

pcDNA3.1-p38

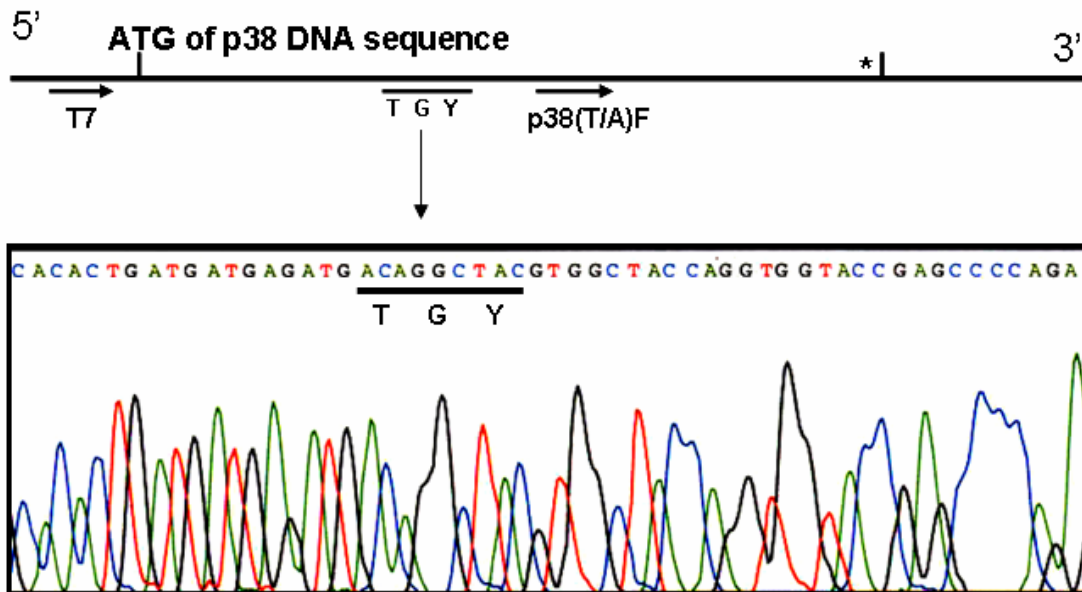


Fig. 34: The sequence of p38(MAPK) cDNA in the pcDNA3.1/Hygro(+) vector was confirmed by sequence analysis. The plasmid-specific T7 primer was used to sequence across the ATG (start codon) for p38(MAPK) and the 3' end of the sequence was obtained using the p38(T/A)F primer (corresponding chromatogram not shown). The cDNA sequence shown in the chromatogram (bottom) shows the position of the codons corresponding to the TGY motif, a dual phosphorylation site linked to p38(MAPK) activation and targeted in subsequent experiments (see Figure 35) for generating activated and dominant negative forms of the enzyme.

Mutagenesis of the “TGY” dual phosphorylation activation motif to “EGD” or “AGF” resulted in an activated form of p38(MAPK) and a dominant negative form of p38(MAPK), respectively (Fig. 35). This is based on the notion that mutating a “T” to an “E” or a “Y” to a “D” mimics phosphorylation of the “T” and “Y”, respectively, whereas mutating the “T” to an “A” or a “Y” to an “F” precludes phosphorylation on these sites (and, hence, inactivates the kinase). This was accomplished using the Quikchange mutagenesis kit.

3.8.4.1 Overexpression of p38(MAPK) mutants affects MAO-A activity, but not gene expression, in HT-22 cells.

Overexpression of the constitutively active form of p38(MAPK)-AF induced the phosphorylation of the p38(MAPK) substrate MK2 in HT-22 cells, whereas overexpression of the dominant negative form of p38(MAPK)-DN did not (Fig. 36). Neither mutant exerted any effect on the expression of *mao-A* or *mao-B* genes in these same cells (Fig. 36).

Overexpression of p38(MAPK)-DN resulted in an increase in MAO-A activity and also enhanced the response of MAO-A to Ca^{2+} . In contrast, overexpression of p38(MAPK)-AF diminished MAO-A activity to $25.64 \pm 2.83\%$ of basal MAO-A activity and also blocked the response of MAO-A to Ca^{2+} [$F_{(5,24)}=78.48$, $P<0.0001$] (Fig. 37).

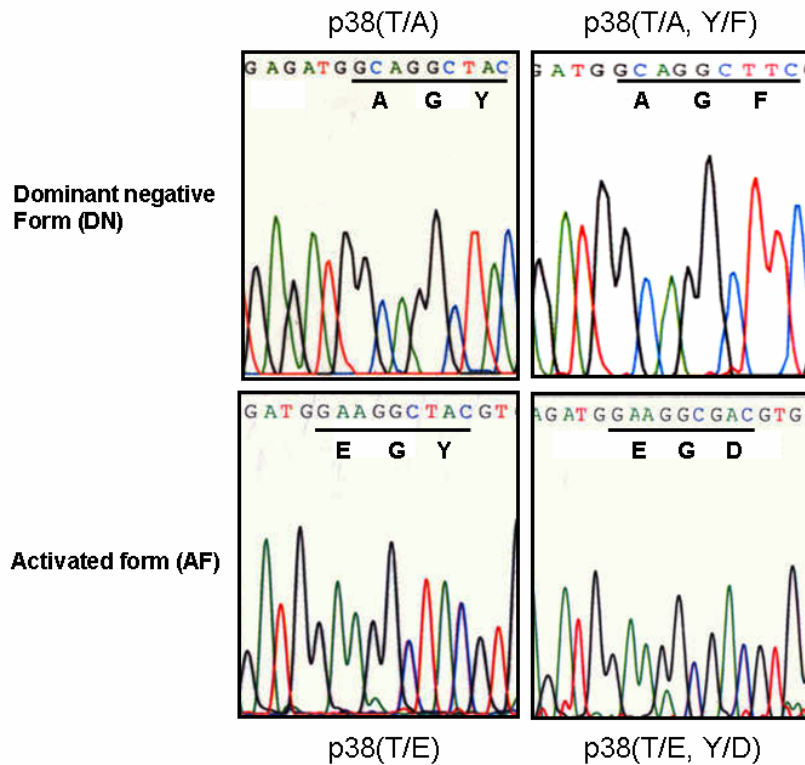


Fig. 35: Mutagenesis of the “TGY” motif in p38(MAPK). cDNA sequences confirm the codons (underlined) that were mutated to allow for targeted amino acid substitutions in the expressed protein. The corresponding amino acid is indicated below the mutated codon. Generation of the dominant negative (DN: upper panels) first required mutagenesis of the “T” to an “A” (left), then mutagenesis of the “Y” to an “F”. Similarly, the activated form (AF: bottom panels) necessitated sequential mutagenesis, *i.e.* first the codon for “T” was mutated to a codon for “E”, then the codon for “Y” was mutated to a codon for “D”.

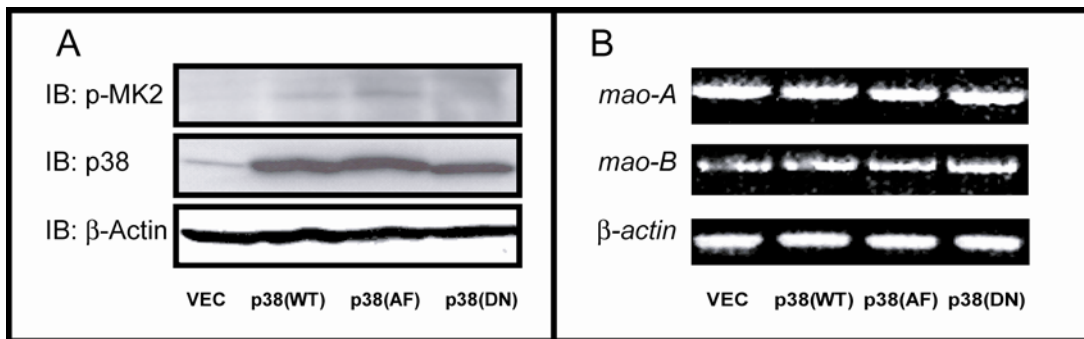


Fig. 36: Activated and dominant negative forms of p38(MAPK) do not affect *mao-A* or *mao-B* gene expression in HT-22 cells. (A) Overexpression of p38(MAPK) wild type [p38(WT)], the activated form [p38(AF)] and the dominant negative [p38(DN)] form were confirmed by immunoblot. The constitutive activation of p38(MAPK) was confirmed by the phosphorylation of its downstream substrate, MAPKAPK-2 (MK2). β -Actin expression was used to demonstrate equal protein loading. (B) None of the overexpressed proteins affected *mao-A* or *mao-B* gene expression in these cells.

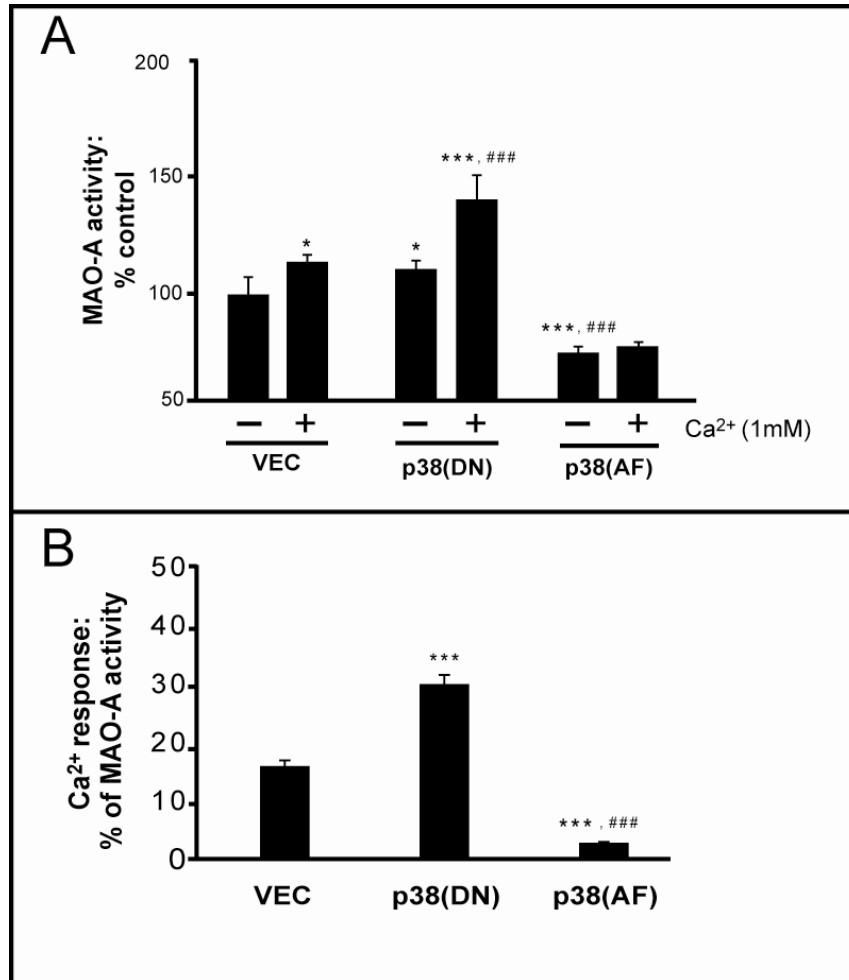


Fig. 37: The overexpression of p38(MAPK) mutant proteins affects MAO-A activity and its response to Ca²⁺ in HT-22 cells. (A) Overexpression of dominant negative p38(MAPK)-DN [p38(DN)] increased endogenous MAO-A activity (122.84 ± 4.28% of control) and its response to 1mM Ca²⁺ (146.34 ± 12.68%, shown again in (B) for ease of interpretation). Overexpression of constitutively active p38(MAPK)-AF [p38(AF)] greatly diminished endogenous (A) MAO-A activity (74.36 ± 2.83% of control) and (B) blocked any response to Ca²⁺ (76.76 ± 4.05%) [F_(5,24)=78.48, P<0.0001]. *: P<0.05 &***: P<0.001 vs CTL; ###: P<0.001 vs p38DN.

3.8.4.2 The effect of activated p38(MAPK) is cell line-dependent.

It was reported that *mao-A* gene expression might be downstream target of the p38(MAPK) pathway in PC12 cells [311]. This was confirmed by overexpression of the p38(MAPK)-AF ($P=0.0001$, $t=15.33$, $df=4$) (Fig. 38A&B), yet, surprisingly, there was no change in MAO-A activity ($P=0.6582$, $t=0.4771$, $df=4$) (Fig. 38C). The efficiency of p38(MAPK)-AF was confirmed by the change in phosphorylation of its substrate MK2 in these cells (Fig. 38D).

The effect of overexpressing p38(MAPK) wild type either alone or in combination with its upstream activating kinase, MEK3, was examined in SH-SY5Y cells treated with cytotoxic agent hydrogen peroxide (H_2O_2 , 100 μ M, 2 hours before harvest). H_2O_2 induced the phosphorylation of [endogenous] p38(MAPK) and this was potentiated in cells overexpressing p38(MAPK) wild type or co-expressing p38(MAPK) and MEK3 (Fig. 39A). Changes in *mao-A* gene expression were only evident in cultures overexpressing p38(MAPK) [$F_{(4,10)}=39.04$, $P<0.0001$] (Fig. 39B). This did not necessarily concord with MAO-A activity levels, which were highest in cultures overexpressing the MEK3 construct alone (note, MAO-A activity in cultures overexpressing p38(MAPK) were high, but not as high as those in cultures overexpressing MEK3) [$F_{(4,15)}=31.51$, $P<0.0001$] (Fig. 39C).

These combined data clearly indicate that p38(MAPK) is exerting cell line-dependent effects on *mao-A* gene and activity. The effect of MEK3 also reveals the

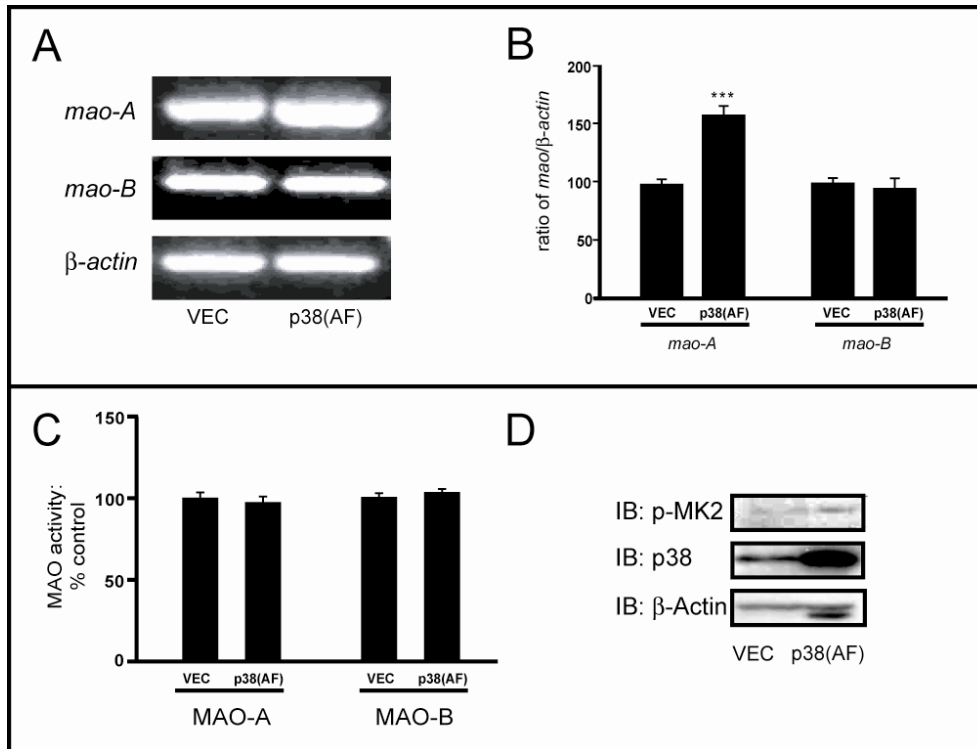


Fig. 38: The overexpression of p38(MAPK) mutant proteins affects *mao-A* gene expression, but not MAO-A activity, in PC12 cells. (A) p38(MAPK)-AF [p38(AF)] increased *mao-A* ($P=0.0001$, $t=15.33$, $df=4$), but not *mao-B*, gene expression as confirmed by (B) densitometric analysis (expressed relative to β -actin gene expression). (C) Overexpression of p38(AF) did not affect MAO-A activity ($P=0.1577$, $t=1.735$, $df=4$) or MAO-B activity ($P=0.2031$, $t=1.52$, $df=4$) in these same cells. (D) The overexpression and constitutive activity of p38(AF) was confirmed by the change in phosphorylation of its substrate MK2.

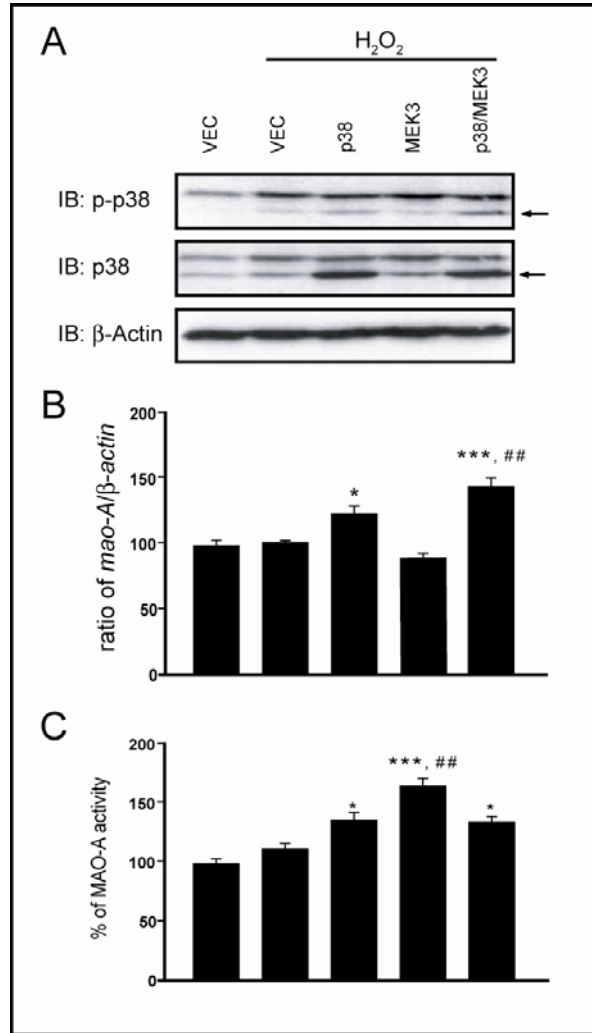


Fig. 39: The effects of overexpression of p38(MAPK) and its upstream kinase MEK3 on *mao-A* gene expression and MAO-A activity in SH-SY5Y cells. (A) Hydrogen peroxide (H₂O₂, 100 μM, 2 hours) induced the phosphorylation of p38(MAPK) (p-p38) in SH-SY5Y cells overexpressing p38MAPK (p38) ± MEK3. (B) This corresponded with an increase in *mao-A* gene expression [F_(4,10)=39.04, P<0.0001] (*: P<0.05; ***: P<0.001, vs. VEC with H₂O₂). (C) MEK3 induced MAO-A activity independent of any change in *mao-A* gene expression in these cells. [F_(4,15)=31.51, P<0.0001] (*: P<0.05; ***: P<0.001, vs. VEC with H₂O₂; ##: P<0.01, vs. p38 with H₂O₂).

potential for additional post-translational modification of MAO-A by components of the p38(MAPK) signalling pathway.

3.8.5 The mutation of a putative p38(MAPK) phosphorylation site in MAO-A influences its activity and sensitivity to Ca²⁺.

As p38(MAPK) could associate with MAO-A (Fig. 30) and p38(MAPK) clearly affected MAO-A activity (Fig. 37), the possibility existed that p38(MAPK) was exerting its effects directly on MAO-A. Examination of the deduced amino acid sequence of MAO-A (Fig. 40) revealed a putative RXXS p38(MAPK) phosphorylation motif [312]. In this motif serine would be the amino acid that would be phosphorylated. Interestingly, MAO-B also contained such a motif (Fig. 40).

The RXXS²⁰⁹ motif in MAO-A4 was mutated so that the serine, *i.e.* "S", was substituted with an alanine (A; precludes phosphorylation) or a glutamic acid (E; mimics phosphorylation). Both mutations were confirmed by DNA sequencing (Fig. 41). The resulting proteins were labeled MAO-A(S/A) and MAO-A(S/E), respectively. Homologous mutations were made in the MAO-B protein (Fig. 41). Mutagenesis of these sites did not affect the expression of the respective MAO-A and MAO-B proteins, although the MAO-A(S/A) protein did migrate at a slightly lower molecular weight (Fig. 42).

The overexpressed MAO-A(WT) and MAO-A(S/A) proteins had similar inherent activities, where overexpression of the MAO-A(S/E) phosphorylation mutant had

A	Menqekasiaghmfdivviggisglsaaakllteygvsvlvleardrvggertytirnehvdyvdvggayvgptqnri	77
BMsnkcdvsvviggisgmaaakllhdsglnvvvleardrvggertytlrnqkvkyvdlggsvvgptqnri	68
A	lrlskelgietykvnvserlvqyvkgktypfrgafppvwnpiayldynnlwrtidnmgkeiptdapweaqhadkwdk	154
B	lrlakelgletykvneverlihvhvkgksypfrgpfppvwnpityldhnnfwrtmddmgreipsdapwkaplaeewdn	145
A	mtmkelidkicwtktarrafaylfvniinvtsephevsalwflwyvkqcggttrifsvtnggqerkfvggsgqvserim	231
B	mtmkellldklcwtesakqlatlfvnlcvtaethevsalwflwyvkqcggttristtnggqerkfvggsgqvserim	222
A	dllgdqvklnhpvthvdqssdniietlnhehyeckyvinaipptltakihfrpelpaernqliqrlpmgavikcmm	308
B	dllgdrvklervviyidqtrenvvetlnhemyeakyvisaipptlgnkihfnpplpmrnqmitrvplgsvikciv	299
A	yykeafwkkkdycgcmiiededapisitlddtkpdgslpaimgfilarkadrlaklhkeirkkkicelyakvlgsqe	385
B	yykepfwrkkdycgcmiidgeeapvaytlddtkpegnyaaimgfilahkarklarltkeerlkklcelyakvlgsle	376
A	alhpvhyeeknwceeqsggcytayfppgimtqygrvirqpvggriffagtetatkwsgymegaveageraarevln	462
B	alepvhyeeknwceeqsggcyttyfppgiltqygrvrlrqpvdriyfadgtetatathws gymegaveageraareilha	453
A	lgkvtekdiwqepeskdvpeithtfwernlpsvsgllkiigf..stsvtalgfvykykllprs	527
B	mgkipedeiwqepesvdvpaqpitttflerhlpsvpgllrliglittifsatalgflahkrllrv	520

Fig. 40: MAO contains a putative p38(MAPK) phosphorylation motif, RXXS. A serine residing in a putative p38(MAPK) phosphorylation motif exists in both MAO-A and MAO-B protein.

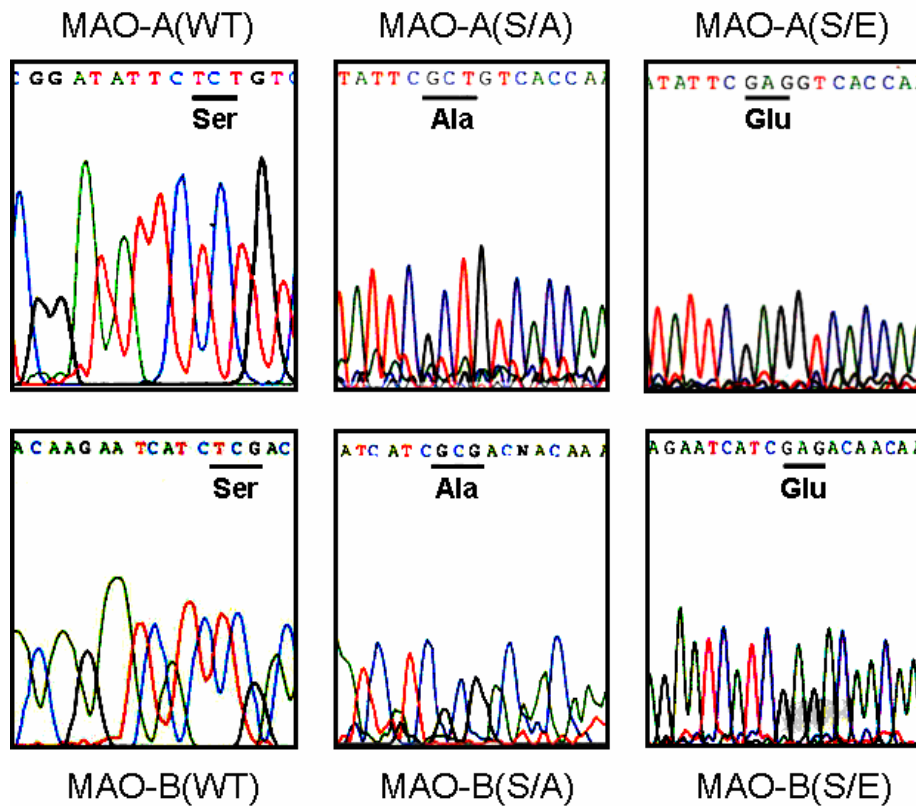


Fig. 41: Confirmation of the mutagenesis of Ser209 in MAO-A cDNA. Chromatograms depict the codon for Serine209 (wild type) in MAO-A cDNA (upper, left), the mutation to an alanine “Ala” codon (upper, middle) and the mutation to a glutamic acid “Glu” codon (upper, right). The corresponding cDNA sequences of the homologous codons in MAO-B (*e.g.* based on Serine200) are depicted in the lower panels.

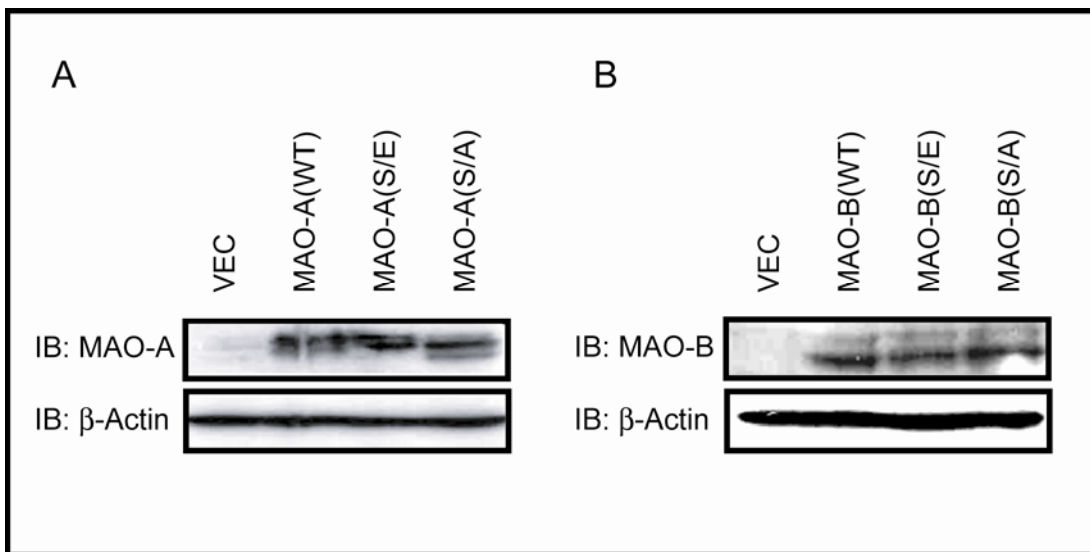


Fig. 42: The overexpression of MAO wild type and Serine substitution mutants in HEK293A cells. (A) MAO-A wild type [MAO-A(WT)] and the Ser209Glu [MAO-A(S/E)] and Ser209Ala [MAO-A(S/A)] proteins were overexpressed in HEK293A cells. (B) The corresponding MAO-B proteins also expressed well in HEK293A cells. β -Actin expression demonstrated equal protein loading in both cases. These data are representative of three separate experiments.

significantly lower activity [$F_{(7,16)}=184.2$, $P<0.0001$] (Fig. 43A). More importantly, the MAO-A(S/A) [dephosphorylated] mutant had significantly greater sensitivity to Ca^{2+} , whereas the MAO-A(S/E) mutant actually was inhibited by Ca^{2+} [$F_{(3,8)}=555.8$, $P<0.0001$] (Fig. 43B). The homologous mutations in MAO-B did not significantly affect MAO-B activity [$F_{(3,8)}=130.8$, $P<0.0001$] (Fig. 44A). The corresponding serine substitution mutants in MAO-A did not change MAO-B activity ($P>0.05$) (Fig. 44B).

Cross-linking experiments revealed that the activities of the MAO-A(S/A) and MAO-A(S/E) mutants appeared to coincide with their detection in a high molecular weight complex (Fig. 45), in a manner similar to that already observed for the MAO-A Ca^{2+} -binding mutants (see Fig. 45).

3.8.6 p38(MAPK) associates with, and phosphorylates, MAO-A.

The myc-tagged MAO-A(WT) was overexpressed in HEK293A either alone or in combination with p38(MAPK)-AF or p38(MAPK)-DN. In addition, MAO-A(S/A) was co-expressed with p38(MAPK)-AF (Fig. 46). Co-immunoprecipitation experiments revealed that MAO-A(WT) associated with both p38(MAPK)-AF and p38(MAPK)-DN, and was seryl phosphorylated only by p38(MAPK)-AF (Fig. 46). In contrast, MAO-A(S/A) neither associated with p38(MAPK)-AF, nor was it seryl phosphorylated (Fig. 46). Overexpression of MAO-A(S/E) and MAO-A(S/A) in N2a cells revealed a similar pattern of MAO-A activities [$F_{(3,8)}=51.55$, $P<0.0001$] (Fig. 47A) as seen previously in the HEK293A cells (Fig. 43). The significantly higher level of MAO-A

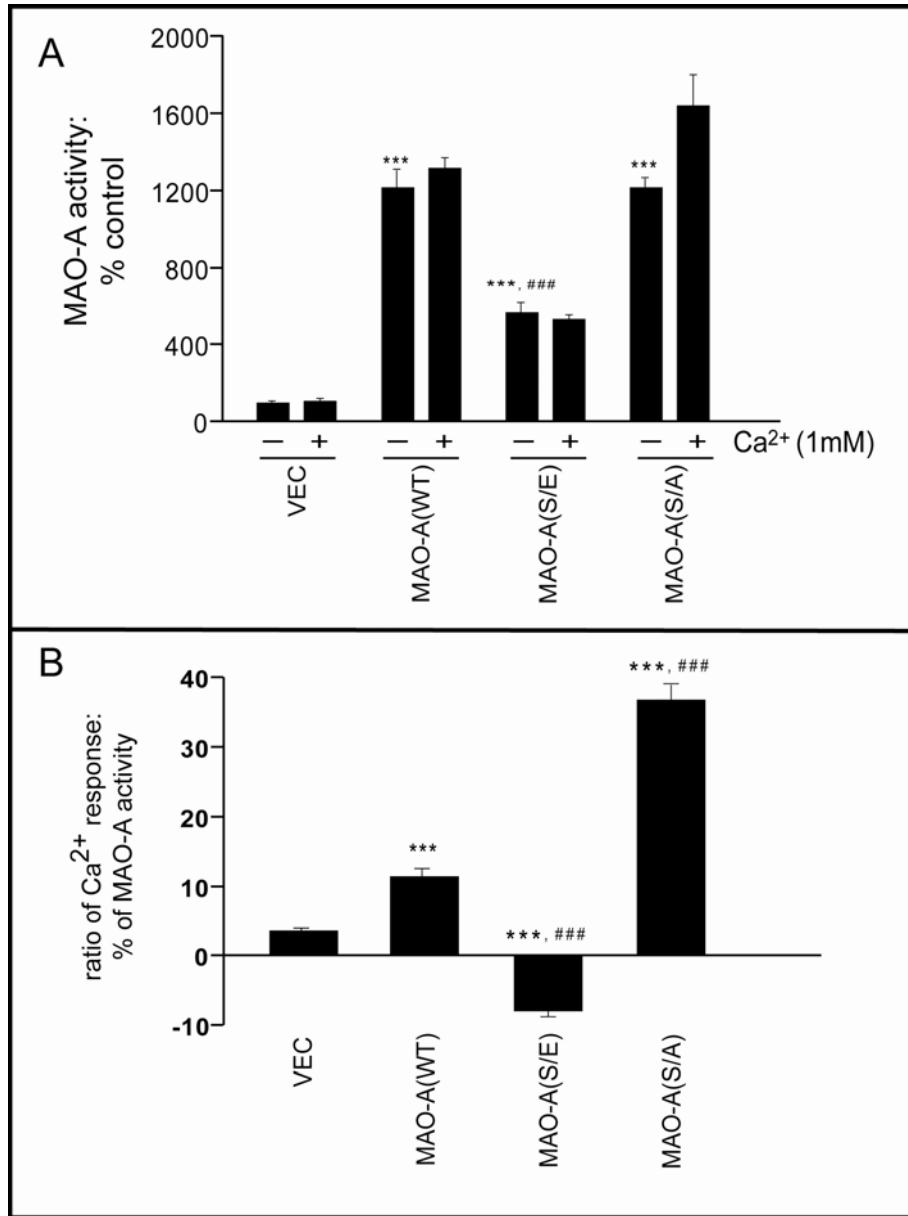


Fig. 43: The MAO-A Serine209 substitution mutants have different activities and sensitivities to Ca²⁺ in HEK293A cells. The MAO-A(S/E) phosphorylation mimic (A) has significantly lower inherent activity than do the MAO-A(WT) and MAO-A(S/A) proteins [$F_{(7,16)}=184.2$, $P<0.0001$], and (B) does not respond to Ca²⁺, whereas the MAO-A(S/A) protein is very sensitive to Ca²⁺ [$F_{(3,8)}=555.8$, $P<0.0001$]. The data represent mean \pm StDev (n=3). ***: $P<0.001$ vs. VEC; ###: $P<0.001$ vs. MAO-A(WT).

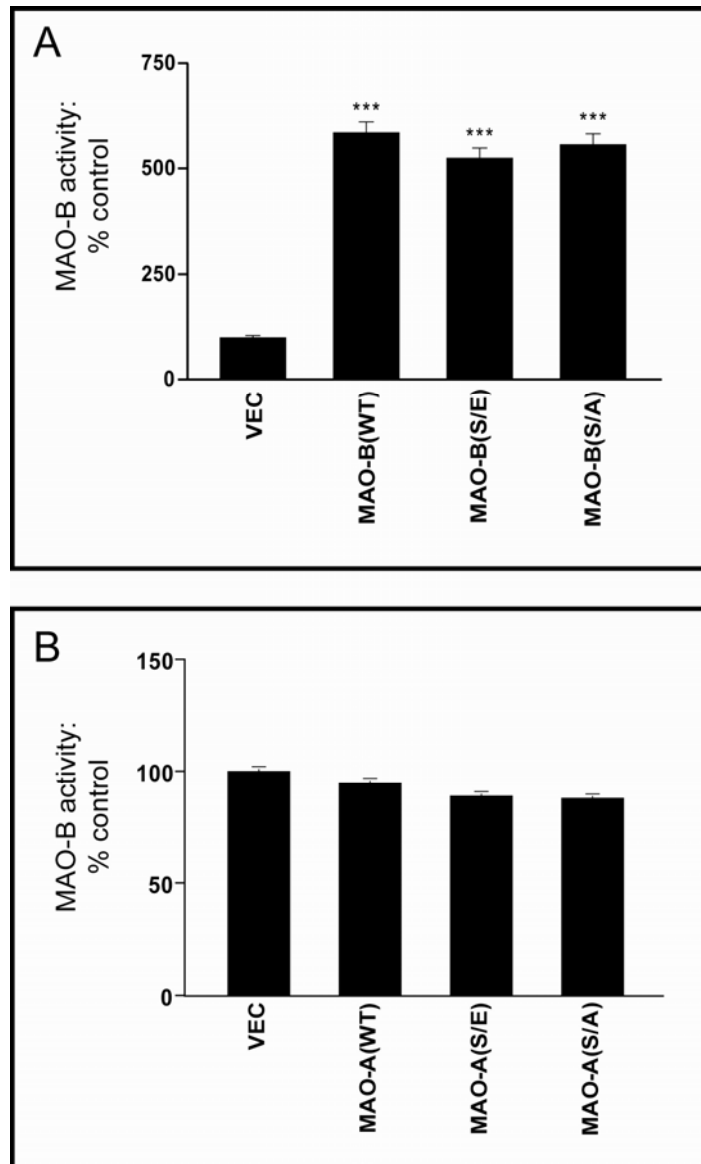


Fig. 44: The MAO-B Serine200 substitution mutants do not affect the activity of the overexpressed protein in HEK293A. (A) MAO-B wild type [MAO-B(WT)], the Ser200 phosphorylation mimic [MAO-B(S/E)] and the dephosphorylation mutant [MAO-B(S/A)] were overexpressed in HEK293A cells (see Fig. 43) and were equally active [$F_{(3,8)}=130.8$, $P<0.0001$] (***) vs. VEC, $P<0.001$). (B) The corresponding Serine substitution mutants in MAO-A did not change MAO-B activity ($P>0.05$).

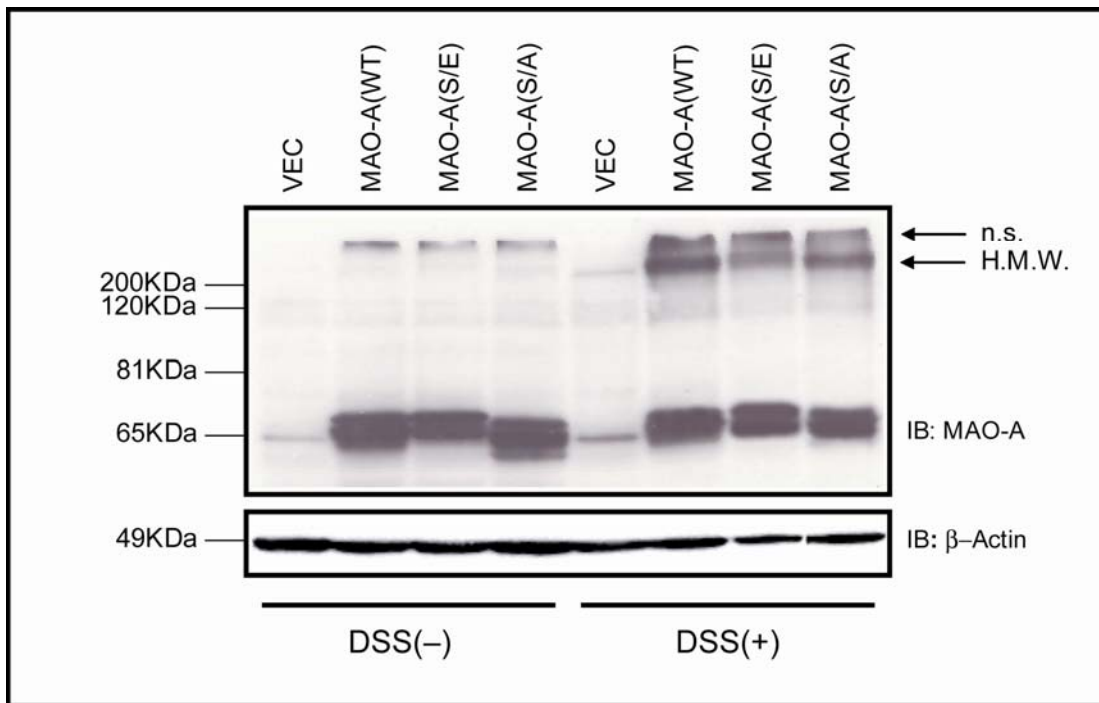


Fig. 45: The MAO-A(S/E) protein is less associated with a high molecular complex.

Myc-epitope tagged MAO-A(WT) and the two serine substitution mutants were overexpressed in HEK293A cells. Prior to harvest, the cells were treated with the cross-linking reagent DSS (1mM, 30 min) or the DMSO vehicle [DSS(-)]. The SDS-PAGE resolved proteins were then probed for the myc-epitope. A high molecular weight (HMW) complex (>200 kDa) was observed in all extracts, although the intensity of the signal of the HMW complex was lowest in MAO-A(S/E) extracts. This HMW complex was not detected in DMSO-treated cultures. β -Actin expression demonstrates equal protein loading. Data represent the results of three separate experiments. n.s.: non-specific band.

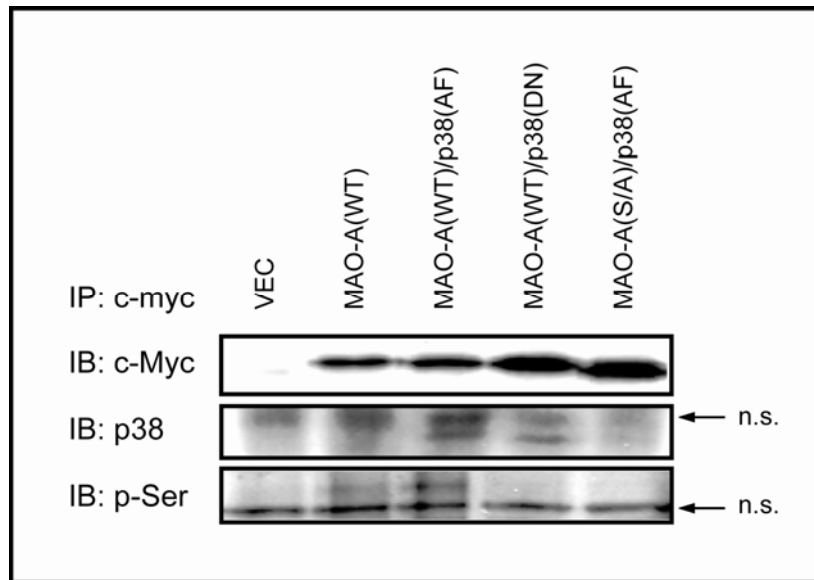


Fig. 46: p38(MAPK) associates with, and phosphorylates, MAO-A. Lysates from HEK293A cells co-expressing MAO-A(WT) and either p38(MAPK)-AF [p38(AF)] or p38(MAPK)-DN [p38(DN)] were immunoprecipitated with anti-c-myc antibody. The SDS-PAGE-resolved proteins were probed for p38(MAPK) or for phospho-serine (p-Ser). While MAO-A-myc associated with both p38(AF) and p38(DN), a p-Ser signal was evident only in the p38(AF) lane. Overexpressed MAO-A(S/A) (far right lane) neither associated with p38(AF), nor was it serine-phosphorylated. These data are representative of three experiments.

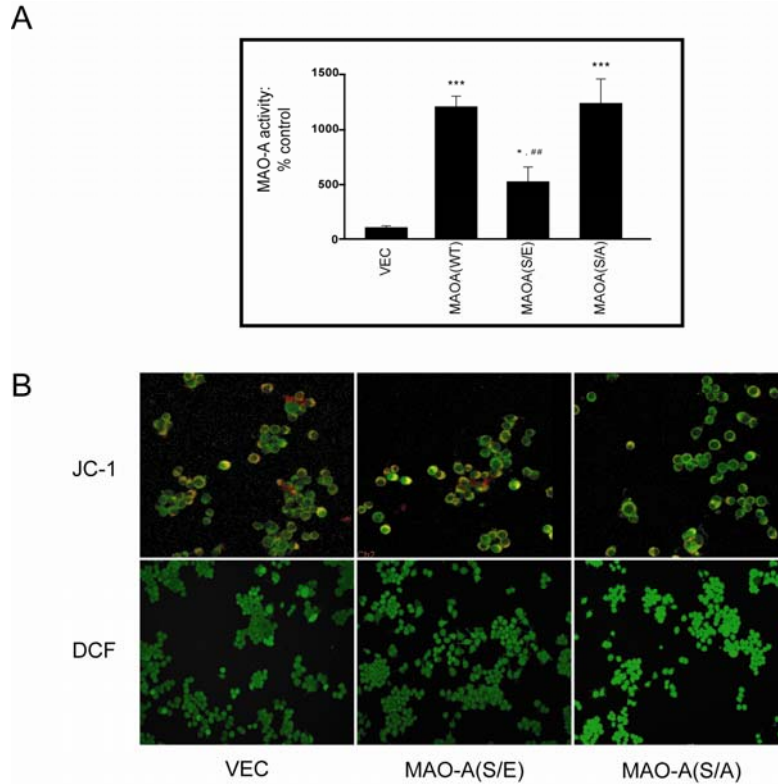


Fig. 47: The MAO-A Serine209 substitution mutants exert different effects on mitochondrial membrane potential ($\Delta\psi_m$) and reactive oxygen species (ROS) production in N2a cells. (A) The overexpressed MAO-A(WT), MAO-A(S/A), and MAO-A(S/E) proteins have a similar pattern of activities in N2a cells to that determined previously in HEK293A cells [$F_{(3,8)}=51.55$, $P<0.0001$] (see Figure 43) . *: $P<0.05$ & ***: $P<0.001$ vs. VEC; ##: $P<0.01$ vs. MAO-A(WT). (B) The activities of the Serine209 substituted MAO-A proteins correspond with their ability to disrupt $\Delta\psi_m$ (as determined using JC-1 fluorescence imaging: JC-1). Recall, a lower red/green ratio indicates disruption of the $\Delta\psi_m$ (a sign of apoptosis). Their activities also correspond with their ability to generate ROS (as determined using H_2O_2 -sensitive DCF fluorescence imaging: DCF). The data are representative of three experiments.

activity in N2a cells overexpressing MAO-A(S/A) parallels a significantly greater level of toxicity, as demonstrated by the greater loss of $\Delta\psi_m$ (visualized using JC-1 staining) and the concurrent increase in H₂O₂-sensitive DCF fluorescence (Fig. 47B). These combined data support a protective role for phosphorylated MAO-A-Serine209 and implicates p38(MAPK) in the process.

3.8.7 Chemical inhibition of p38(MAPK) results in ROS production that is mediated, in part, by MAO-A.

HT-22 cells treated with the p38(MAPK) inhibitor SB203580 displayed a significant increase in peroxy radical production (determined using the H₂O₂-sensitive DCF fluorogen). This was partially attenuated by pretreatment with the specific MAO-A inhibitor clorgyline (CLG, 1 μ M) for 60 min (Fig. 48).

3.8.8 Chemical inhibition of p38(MAPK) increases MTT conversion.

MTT conversion, normally used as a means of determining cell viability, was increased in HT-22 cells treated with the p38(MAPK) inhibitor SB203580. This was not affected by pretreatment with the specific MAO-A inhibitor clorgyline (CLG, 1 μ M) for 60 min [$F_{(3,20)}=10.21$, $P=0.0003$] (Fig. 49).

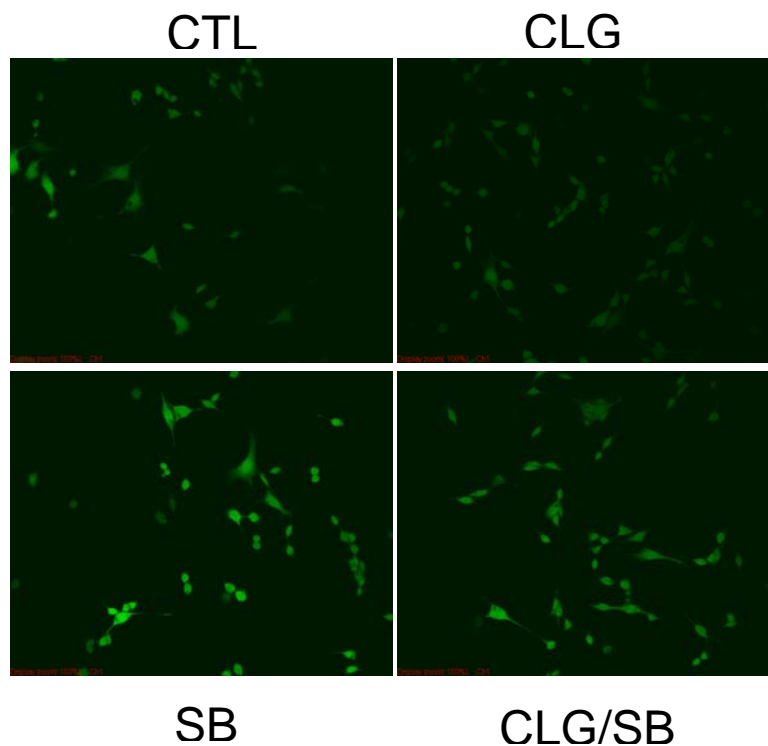


Fig. 48: The p38(MAPK) inhibitor SB203580 induces reactive oxygen species production *via* a MAO-A sensitive mechanism in HT-22 cells. Treatment of HT-22 cells with SB203580 (SB: 10 μ M, 60 min) resulted in an increase in DCF-sensitive peroxy radical production that was partially reversed by specific inhibition of MAO-A with clorgyline (CLG: 1 μ M, 60 min). These results are representative of two-three experiments.

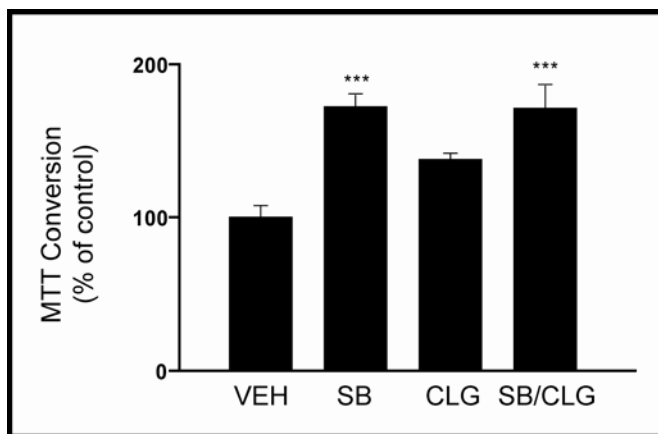


Fig. 49: The p38(MAPK) inhibitor SB203580 increases MTT conversion in HT-22 cells. HT-22 cells were treated with SB203580 (SB, 10 μ M, 60 min) and “viability” was tested using the 3-(4,5-dimethylthiazol-2-yl)-2,5-diphenyl tetrazolium bromide (MTT) conversion assay (used routinely to determine cell “viability”). SB induced an increase in MTT conversion as did the specific MAO-A inhibitor clorgyline (CLG: 1 μ M, 60 min) [$F_{(3,20)}=10.21$, $P=0.0003$]. ***: $P<0.001$ vs. VEH. Data are presented as mean \pm StDev (n=3).

3.8.9 Chemical inhibition of p38(MAPK) diminishes mitochondrial membrane potential in an MAO-A-sensitive manner.

Treatment of HT-22 cells with SB203580 decreased the ratio of red to green fluorescence, indicating a loss of $\Delta\psi_m$. This decrease was reversed by the pretreatment of specific MAO-A inhibitor CLG (1 μ M, 60 min) [$F_{(3,8)}=17.03$, $P=0.0008$] (Fig. 50).

3.8.10 The sensitivity of MAO-A to Ca^{2+} is revealed by chemical inhibition of p38(MAPK).

The activities of overexpressed MAO-A proteins (including the Ca^{2+} -binding mutants) were previously shown not to respond to the addition of Ca^{2+} to the incubation buffer (see Fig. 26). Treatment of similarly transfected cells with SB203580 revealed their sensitivity to Ca^{2+} , except for the MAO-A(D61A) protein, which still did not respond [$F_{(5,12)}=82.33$, $P<0.0001$] (Fig. 51).

3.9 Manipulation of Ca^{2+} levels in cultures affects MAO-A activity.

3.9.1 The Ca^{2+} ionophore A23187 increases MAO-A activity independent of a change in *mao-A* expression.

The Ca^{2+} ionophore A23187 is commonly used to increase the levels of free intracellular Ca^{2+} . Treatment of HT-22 cells with A23187 (10 μ M, 30 min) induced a large increase in free Ca^{2+} , as shown by the increase in the Ca^{2+} -sensitive Fluo-3 AM fluorescence that paralleled a significant increase in ROS production (Fig. 52A).

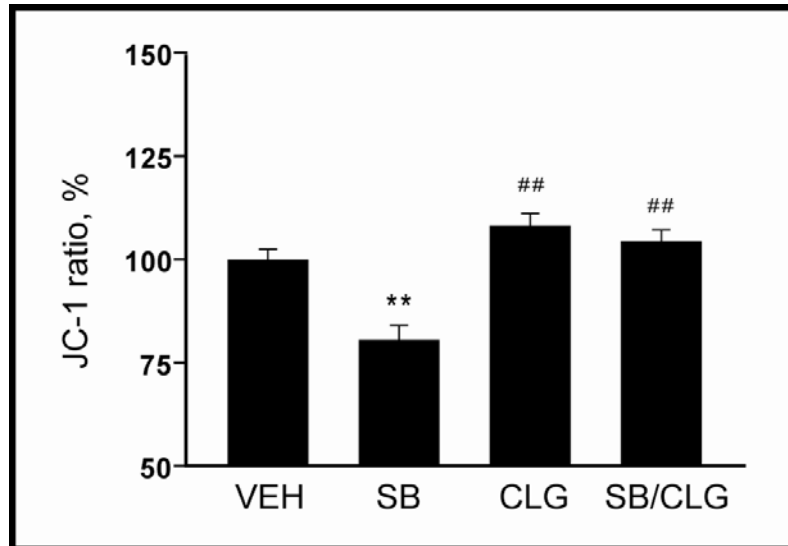


Fig. 50: The p38(MAPK) inhibitor SB203580 decreases mitochondrial membrane potential ($\Delta\psi_m$) via a MAO-A sensitive mechanism in HT-22 cells. Treatment of HT-22 cells with SB203580 (SB: 10 μ M, 60 min) resulted in a significant loss of $\Delta\psi_m$, as determined by the lower red/green JC-1 ratio (indicating apoptosis) which was reversed by treatment with the specific MAO-A inhibitor clorgyline (CLG: 1 μ M, 60 min) [$F_{(3,8)}=17.03$, $P=0.0008$]. **: $P<0.01$ vs. vehicle control (VEH); #: $P<0.01$ vs. SB. Data are presented as mean \pm StDev (n=3).

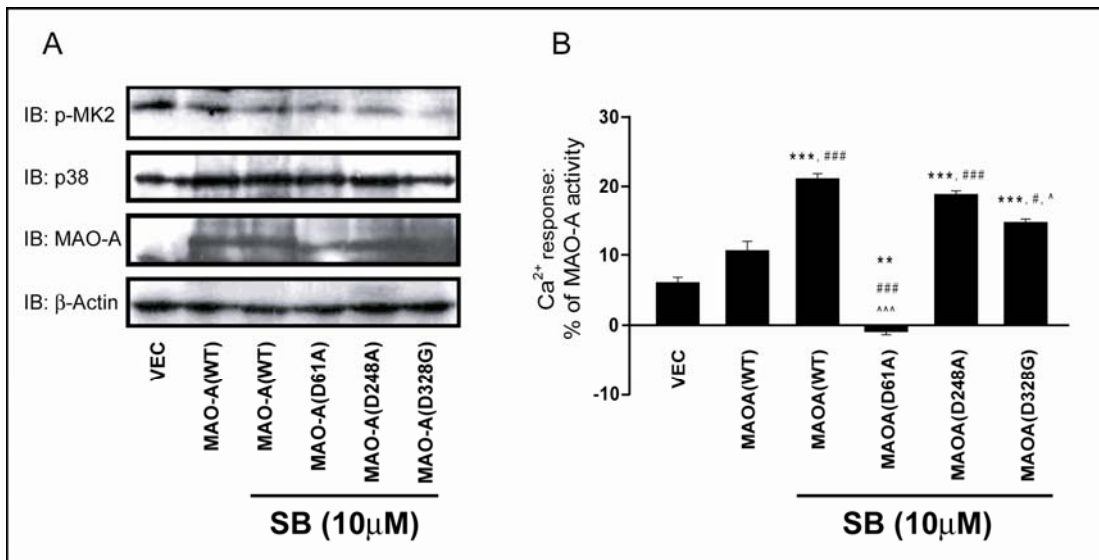


Fig. 51: MAO-A Ca²⁺-binding site mutants respond in distinct manners to Ca²⁺, as revealed by inhibition of p38(MAPK) with SB203580 in HEK293A cells. (A) Cells overexpressing MAO-A wild type (WT) and the Ca²⁺-binding site mutants (see Fig. 22-26) were treated with SB203580 (SB: 10 μ M, 60 min). The effect of SB was confirmed by the loss of phosphorylation of the p38(MAPK) substrate, MK2). β -Actin expression was used to demonstrate equal protein loading. **(B)** The effect of Ca²⁺ (1 mM) on MAO-A activity in corresponding homogenates revealed that SB increased Ca²⁺-sensitive MAO-A activity in all homogenates except the one from cultures overexpressing MAO-A(D61A) [$F_{(5,12)}=82.33$, $P<0.0001$]. **: $P<0.01$ & ***: $P<0.001$ vs. vector control (VEC); #: $P<0.05$; ###: $P<0.001$ vs. MAO-A(WT); ^: $P<0.05$ & ^^: $P<0.001$ vs. MAO-A(WT)/SB.

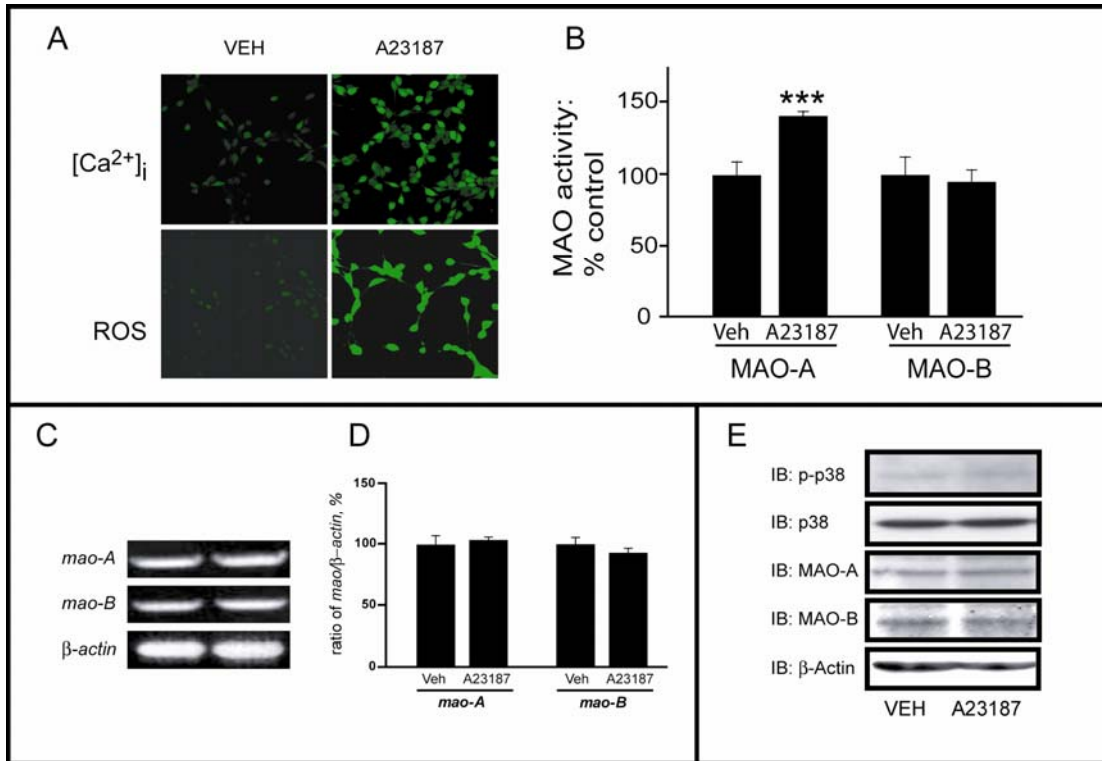


Fig. 52: The Ca^{2+} ionophore A23187 increases MAO-A activity and function in HT-22 cells. (A) Treatment of HT-22 cells with A23187 (10 μ M, 30 min) resulted in increased levels of free intracellular Ca^{2+} , $[Ca^{2+}]_i$ (determined using the Ca^{2+} -binding Fluo-3 AM fluorescent dye) as well as increased production of reactive oxygen species (ROS), as assessed using the H_2O_2 -sensitive DCF fluorogen. (B) This corresponded with a selective increase in MAO-A activity (***: $P=0.0002$, $t=6.824$, $df=6$ vs. control levels). Treatment with A23187 did not affect (C) *mao-A* or *mao-B* gene expression (D, results of densitometric analysis of *mao* gene expression relative to β -actin gene expression) or (E) MAO-A or MAO-B protein expression. β -Actin expression demonstrates equal protein loading.

Examination of MAO-A and MAO-B activities revealed that only MAO-A activity was increased by treatment with A23187 ($P=0.0002$, $t=6.824$, $df=6$) (Fig. 52B). A23187 did not affect either *mao-A* (or *mao-B*) gene expression (Fig. 52C&D) or MAO-A (or MAO-B) protein expression (Fig. 52E). The levels of phosphorylated p38(MAPK) were not detectably affected by treatment with A23187 (Fig. 52E). The production of ROS induced by A23187 was attenuated by pretreatment with the MAO-A specific inhibitor clorgyline (CLG: 1 μ M, 60 min) (Fig. 53).

3.9.2 Overexpression of the Ca²⁺-binding protein CB28K decreases MAO-A activity independent of a change in *mao-A* expression.

Overexpression of calbindinD-28K (CB28K) (Fig. 54A) was used to decrease the levels of intracellular free Ca²⁺ (Fig. 54B). Overexpression of CB28K did not affect MAO-A protein expression (Fig. 54A), nor did it affect *mao-A* gene expression (Fig. 54C&D), but it did result in a selective decrease in MAO-A activity ($P=0.0007$, $t=5.561$, $df=6$) (Fig. 54E). In addition, it caused a rightward shift in the response curve of MAO-A to Ca²⁺ (Fig. 54F). These effects coincided with a decrease in ROS production (Fig. 55) as well as an increase in the phosphorylation of p38(MAPK) (Fig. 56).

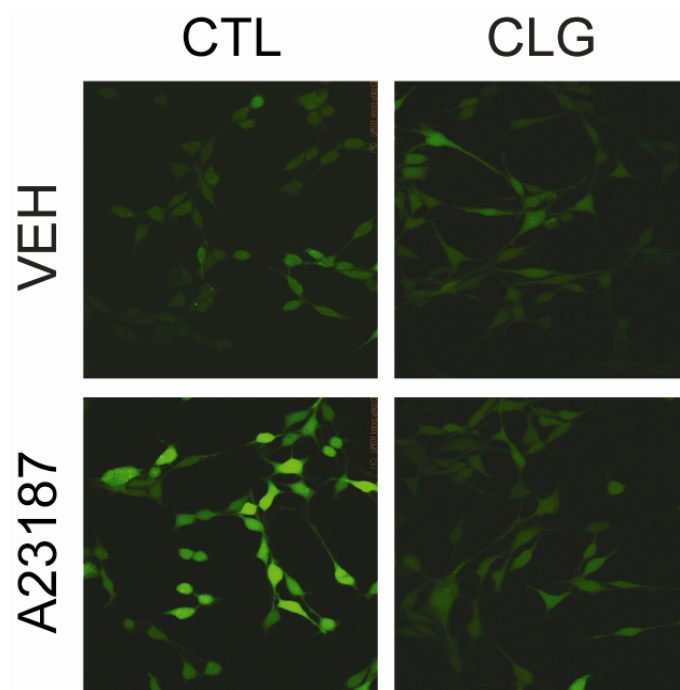


Fig. 53: The Ca^{2+} ionophore A23187 induces reactive oxygen species production via a MAO-A sensitive mechanism in HT-22 cells. Treatment of HT-22 cells with the A23187 (5 μM , 30 min) resulted in increased production of reactive oxygen species as assessed using the H_2O_2 -sensitive DCF fluorogen which was blocked by specific MAO-A inhibition with CLG (1 μM , 60 min). Results represent two-three separate experiments.

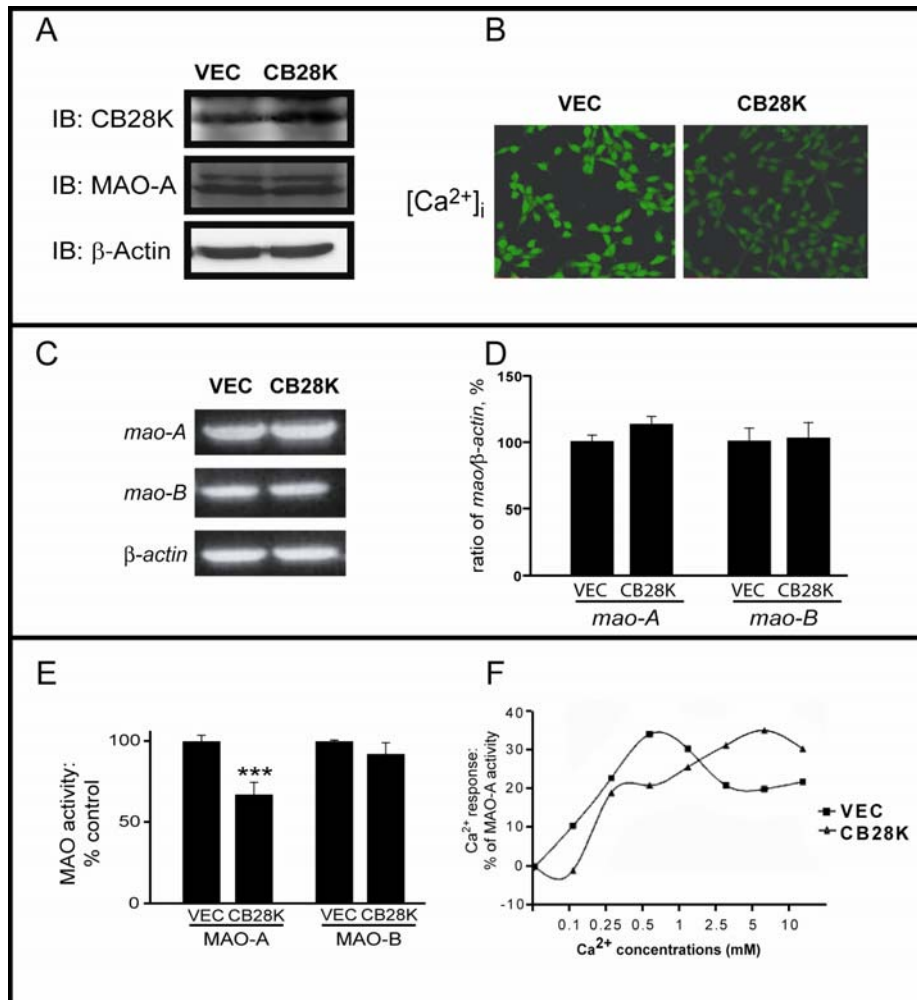


Fig. 54: Overexpression of the Ca²⁺-binding protein calbindinD-28K (CB28K) decreases MAO-A activity as well as its sensitivity to Ca²⁺ in HT-22 cells. (A) Overexpression of CB28K (B) diminishes the levels of intracellular free Ca²⁺ ([Ca²⁺]_i) in HT-22 cells. While (A) MAO-A protein expression and (C, D) *mao-A* gene expression are not affected, (E) overexpression of CB28K does result in a selective decrease in MAO-A activity (*) *P*=0.0007, *t*=5.561, *df*=6, vs. vector control (VEC)). (F) Overexpression of CB28K also affects the sensitivity of MAO-A to Ca²⁺ as shown by right-shift in the peak response of MAO-A to Ca²⁺.**

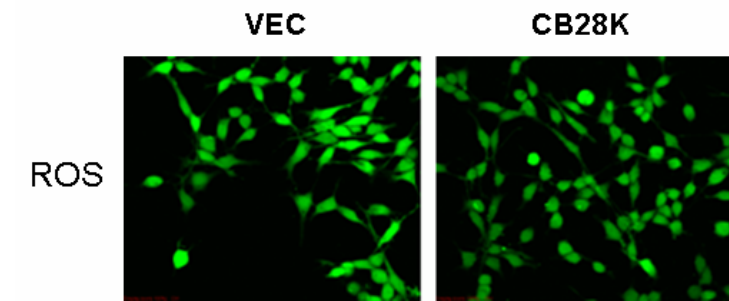


Fig. 55: Overexpression of the Ca^{2+} -binding protein calbindinD-28K (CB28K) diminishes reactive species production in HT-22 cells. Overexpression of CB28K resulted in a decrease in the levels of reactive oxygen species, as assessed using the H_2O_2 -sensitive DCF fluorogen.

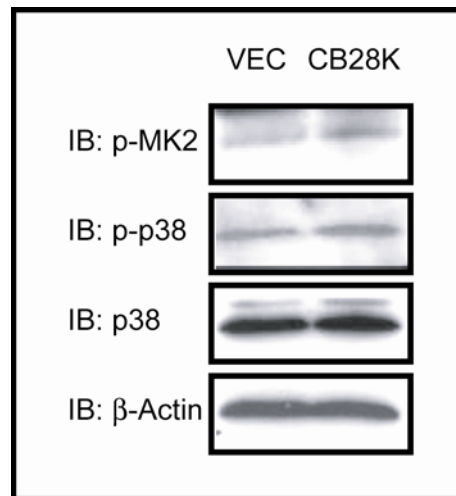


Fig. 56: Overexpression of the Ca^{2+} -binding protein calbindinD-28K (CB28K) results in the activation of p38(MAPK) in HT-22 cells. Overexpression of CB28K resulted in increased phosphorylation of p38(MAPK) (p-p38) as well as a corresponding increase in the phosphorylation of MAPKAPK-2 (p-MK2), a downstream target of p38(MAPK). β -Actin expression was used to demonstrate equal protein loading.

3.10 The AD-related peptide β -amyloid ($A\beta$) induces chromatin condensation in primary neuronal cultures; potentiation by inhibition of p38(MAPK) and protection by inhibition of MAO-A.

Primary cortical cultures treated with the p38(MAPK) inhibitor SB203580 showed significant increases in chromatin (nuclear) condensation, as determined by Hoechst 33258 staining [$F_{(7,34)}=380.2$, $P<0.0001$] (Fig. 57). This was reversed by inhibition of MAO-A with clorgyline. Treatment of cortical cultures with the AD-related peptide $A\beta(1-42)$ induced chromatin condensation in an even greater number of cells. This was also reversed by inhibition of MAO-A (Fig. 57). Treatment with SB203580 did not impact the effect of $A\beta(1-42)$, but it did diminish the protection afforded by MAO-A inhibition (Fig. 57).

The link between $A\beta$ toxicity and MAO-A was corroborated by the demonstration that MAO-A inhibition with clorgyline was able to reverse the generation of ROS (and cellular swelling) in HT-22 cells treated with $A\beta$ (Fig. 58).

3.12 Additional means of post-translational modification of MAO-A activity

Preliminary investigations revealed that inhibition of the PI3K/Akt signalling pathway (with LY294002) as well as inhibition of the ERK1/2 signalling pathway (with PD98059) could both increase MAO-A activity [$F_{(5,13)}=6.997$, $P=0.0028$], but not the response to Ca^{2+} [$F_{(2,6)}=219.3$, $P<0.0001$] (Fig. 59). Examination of the MAO-A deduced amino acid sequence revealed several TXY motifs (possible phosphorylation

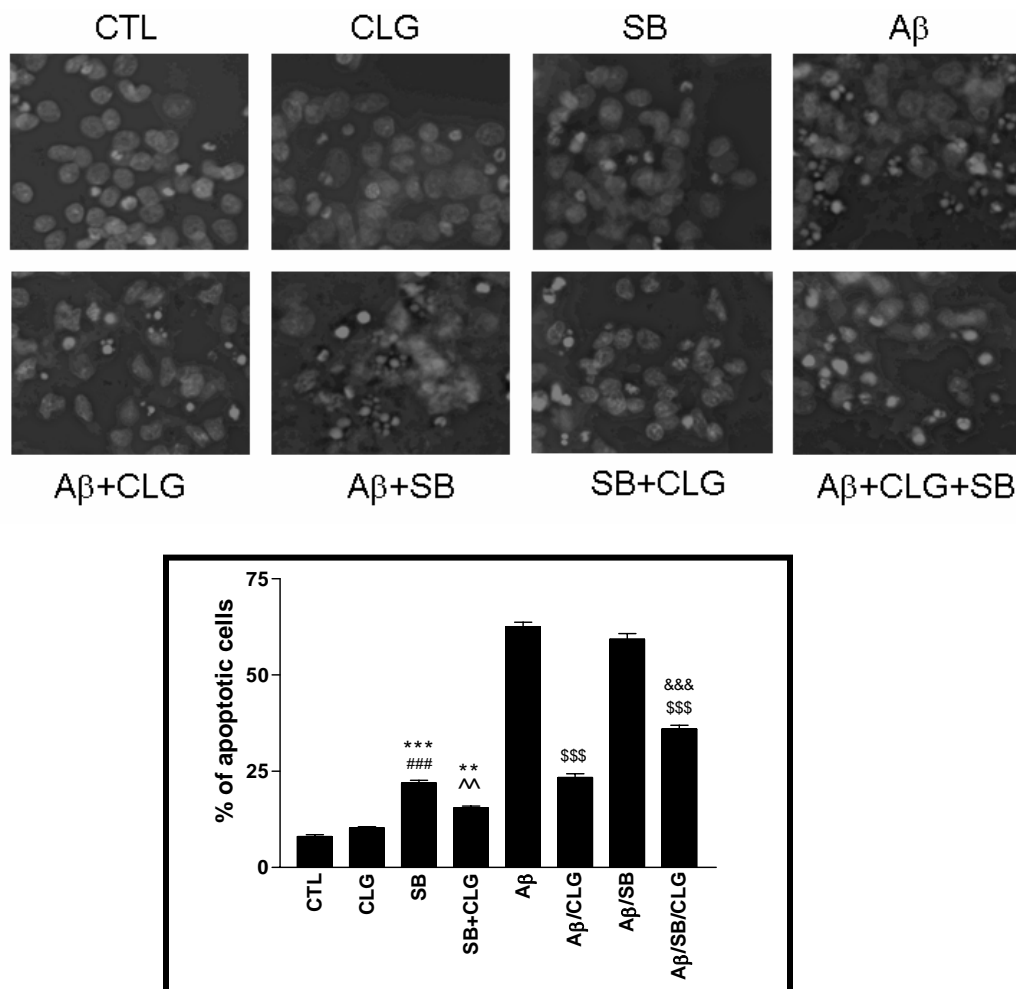


Fig. 57: Specific p38(MAPK) inhibition is toxic to primary cortical cultures via MAO-A sensitive mechanism: contribution to the toxicity of the AD-related peptide, β -amyloid (A β). p38(MAPK) inhibition with SB203580 (SB) induces nuclear condensation in primary cortical neurons that is sensitive to specific MAO-A inhibition with clorgyline (CLG) (assessed by Hoechst 33258 stain, top panels). SB did not affect A β (1-42)-induced toxicity, but did attenuate the protection afforded by CLG in A β (1-42)-treated cultures [$F_{(7,34)}=380.2$, $P<0.0001$]. **: $P<0.01$; ***: $P<0.001$ vs. CTL, ###: $P<0.001$ vs. CLG, ^^: $P<0.01$ vs. SB, \$\$\$: $P<0.001$ vs. A β , &&&: $P<0.001$ vs. A β /CLG.

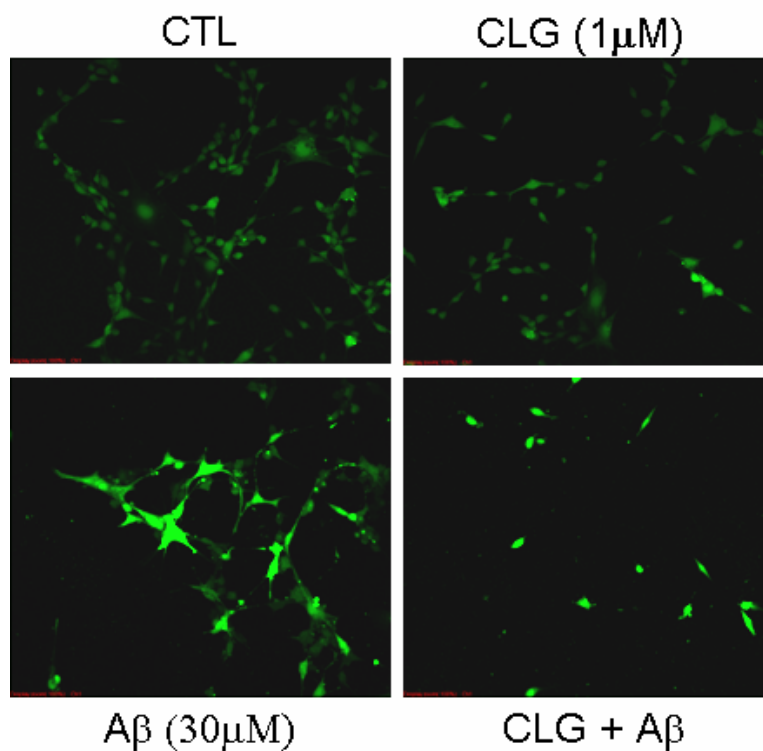


Fig. 58: The ROS production induced by AD-related peptide A β was attenuated by specific MAO-A inhibition in HT-22 cells. Treatment of HT-22 cells with A β (1-40) (30 μ M, 24 h) resulted in an increase in the generation of reactive oxygen species production, as assessed using the H₂O₂-sensitive DCF fluorogen. Furthermore, the cells appeared swollen. These effects were partially attenuated by specific MAO-A inhibition with clorgyline (CLG: 1 μ M, 60 min).

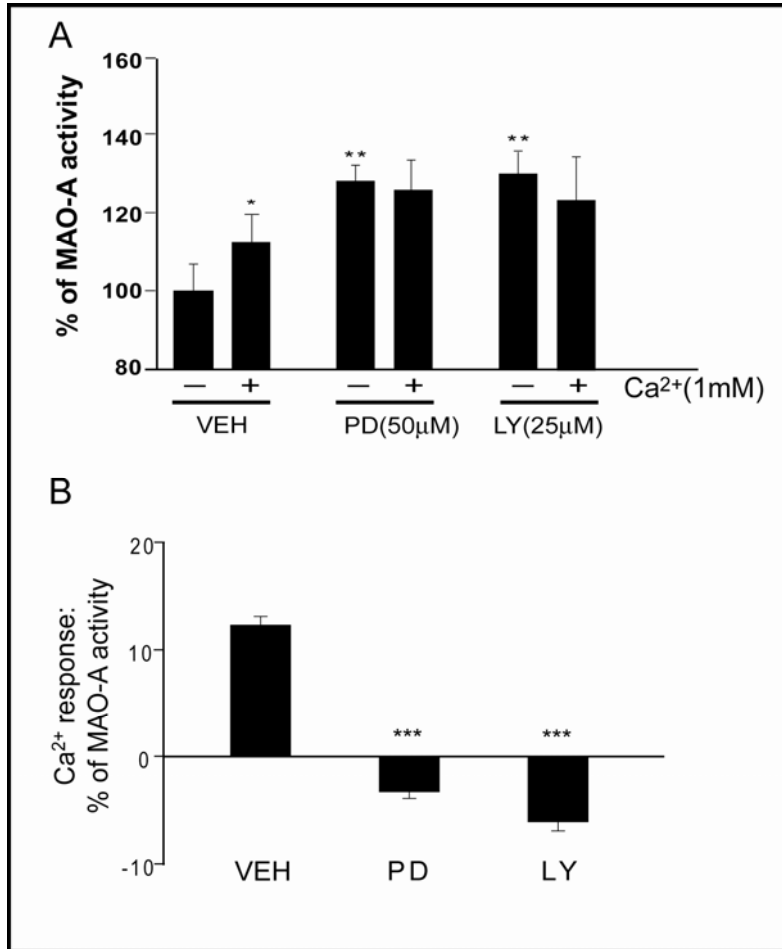


Fig. 59: Inhibition of the ERK and PI3K pathways also enhance MAO-A activity, but not the response to Ca²⁺. (A) Preliminary investigations revealed that MAO-A activity was sensitive to inhibition of two other signalling cascades, namely the ERK and PI3K cascades in HT-22 cells [$F_{(5,13)}=6.997$, $P=0.0028$]. The inhibition of both cascades also inhibited the response of MAO-A to Ca²⁺ (re-depicted in (B) for ease of interpretation). ERK was inhibited specifically with PD98059 (PD: 50 μM, 30 min), whereas PI3K was specifically inhibited with LY294002 (LY: 25 μM, 30 min). Data are represented as mean ± STDev (n=3) (** vs. VEH: $P<0.01$).

sites for MKKs and ERK) (Fig. 60). Notably, the first TXY motif, *e.g.* T³³EY³⁵, was specific to MAO-A. The Y³⁵ (tyrosine35) was substituted with either an F (Y/F) or a D (Y/D) (Fig. 61A). The corresponding MAO-A(Y/F) protein was moderately less active than MAO-A wild type, whereas the MAO-A(Y/D) protein was basically inactive [$F_{(3,15)}=128.5$, $P<0.0001$] (Fig. 61B). Their respective activities did not concord with their protein overexpression levels (Fig. 61C).

A	Menqekasiaghmfdvsvvgggisglsaaakl	lteygs	svlvleardrvggtrtytirnehvdyvdvggayvgptqnri	77																									
BMsnkcdvsvvgggisgmaaaakl	hdsgl	svlvleardrvggtrtytlrnqkvkyvdlggsvvgptqnri	68																									
A	lrlskelgietykvnvserlvqyvkgtypfrgafppvwnpiayldynnlwrtidnmgkeiptdapweaqhadkwdk			154																									
B	lrlakelgletykneverlihhvkgksypfrgpfppvwnpityldhnnfwrtmddmgreipsdapwkaplaeedn			145																									
A	mtmkelidkicwtktarrrfaylfvniinvntsephevsalwflwyvkqcggttrifsvtnggqerkfvggsgqvserim			231																									
B	mtmkelldklcwtesakqlatlfnlcvtaethevsalwflwyvkqcggttriiSttnggqerkfvggsgqvserim			222																									
A	dllgdqvklnhpvthvdqssdniietlnhehyeckyvinaipptltakihfrpelpaernqliqrlpmgavikcmm			308																									
B	dllgdrvklervpiyidqtrenvlvetlnhemyeakyvisaipptlgmkihfnpplpmmrnqmitrvplgsvikciv			299																									
A	yykeafwkkkdydcgcmiiededapisitlddtkpdgslpaimgfilarkadrlaklhkeirkkkicelyakvlgsqe			385																									
B	yykepfwrkkdydcgtmiidgeeapvaytlddtkpegnyaaimgfilahkarklarltkeerlkklcelyakvlgsle			376																									
A	alhpvhyeeknwceeqysgg	tyayf	pgim	tqygr	vlrqpvg	riffag	tetat	kws	gym	egave	agera	arev	lng	462															
B	alepvhyeeknwceeqysgg	tytyf	pgilt	tqygr	vlrqp	vdiy	fag	tetat	hws	gym	egave	agera	areil	ha	453														
A	lgkvtetekdiwqepeskdv	paveit	htf	wern	lpsv	gllki	igf	..	stsv	tal	gf	vly	kyk	llprs	527														
B	mgkipedeiwqepesvd	paqp	ittt	f	ler	hlp	sv	gllrl	ig	l	t	t	i	f	s	a	t	al	g	f	l	ah	k	r	g	ll	lv	rv	520

Fig. 60: Comparison of MAO-A and MAO-B amino acid sequences reveals a TXY motif that is specific to MAO-A. Alignment of the human MAO-A and MAO-B deduced amino acid sequences revealed several TXY motifs, which are potential target sites for ERK and/or MEKs (boxed) motifs. The motif at T³³EY³⁵ is exclusive to MAO-A and, consequently, was mutagenized (see next figure) to determine the role of this motif in regulation of MAO-A activity.

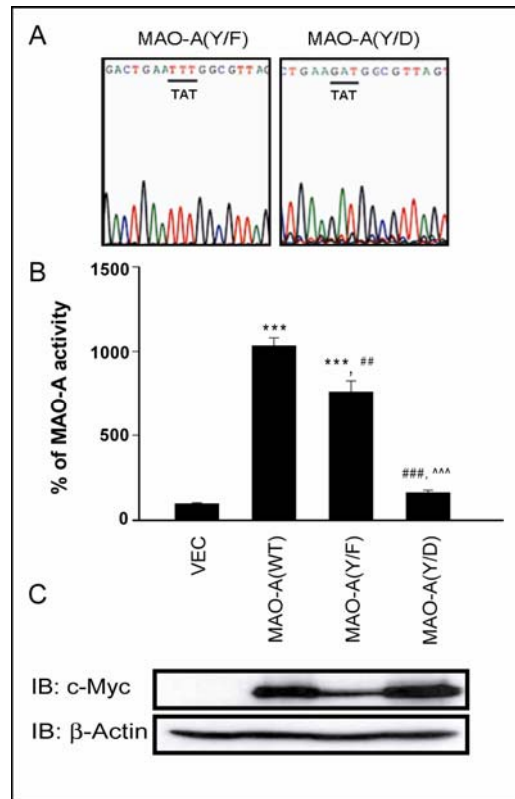


Fig. 61: Mutagenesis of tyrosine(Y35) in MAO-A affects MAO-A activity. (A) cDNA sequences indicating the codons (underlined) that were mutated to allow for targeted amino acid substitutions within the T³³EY³⁵ motif in MAO-A. The cDNA sequence shows the wild type codon “TAT” that was mutagenized to either “TTT” (top left, allowing for a Y-to-F (phenylalanine) substitution in the expressed protein) or to “GAT” (top right, allowing for a Y-to-D (aspartate) substitution in the expressed protein). (B) The activity of the overexpressed MAO-A(Y/F) protein was partly reduced compared to that of MAO-A(WT), whereas the MAO-A(Y/D) protein had basically no activity [$F_{(3,15)}=128.5$, $P<0.0001$]. (C) Activities did not correspond with the expression levels of the respective proteins. Data are presented as mean \pm STDev (n=5). ***: $P<0.001$ vs. vector control (VEC). ##: $P<0.01$ vs. MAO-A(WT). ###: $P<0.001$ vs. MAO-A(WT).

4 DISCUSSION

MAO function is implicated in neuropsychiatry due to its ability to regulate the levels of biogenic neurotransmitters. It can also contribute to neurodegeneration given that H_2O_2 , an important precursor to free radicals implicated in oxidative stress, is produced as a by-product of deamination. Although the regulation of MAO is crucial, endogenous mechanisms involved in its regulation are not clearly defined.

The current thesis provides evidence for a unique mechanism based on the availability of Ca^{2+} as well as on the activation of a kinase, p38(MAPK), that is often associated with cell stress (Fig. 62-63). This mechanism might contribute to several MAO-related pathologies, but given that the current thesis work indicates a selective effect on MAO-A, the contribution of this mechanism to pathologies linked to dysfunction of MAO-B, such as Parkinson's disease, might not be as clear.

The effect of Ca^{2+} on brain homogenates and cultured cell homogenates is selective for MAO-A and is maximal at approximately 1 mM. This is a significantly higher concentration than the [physiological] nanomolar concentrations of Ca^{2+} normally found within the cells and suggests pathological relevance. The response of MAO-A to Ca^{2+} occurs in different regions of rat and mouse brain, such as the hippocampus, cortex, and cerebellum, and thus supports a generalized effect of Ca^{2+} on regional MAO-A function.

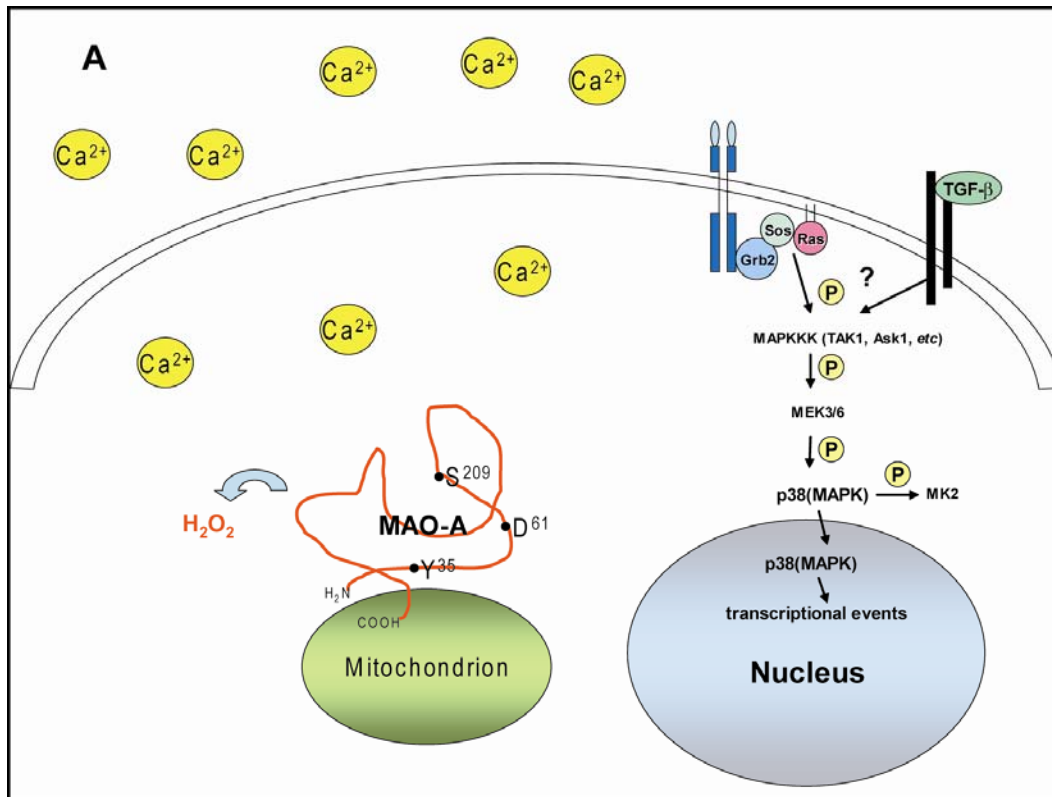


Fig. 62: Schematic depicting how p38(MAPK) might protect the cell during a transient stress that involves an increase in Ca^{2+} and a corresponding increase in MAO-A activity. (note, this figure includes panels B & C on the following page). (A) Under normal circumstances a modest amount of Ca^{2+} enters the cell, MAO-A function is normal and p38(MAPK) might have modest constitutive activity (depicted by the yellow “P” circles). The effect of p38(MAPK) on nuclear events is minor. (B) During a minor or transient stressful event (indicated by the orange “lightning” bolt), more Ca^{2+} enters the cell and this activates MAO-A; consequently, more H_2O_2 is generated and some of this H_2O_2 will activate p38(MAPK) (depicted by the orange “P” circles), which will, in turn, phosphorylate MAO-A on Serine209; this will limit the effect of Ca^{2+} on MAO-A activity as well as on basal MAO-A activity; H_2O_2 production and any associated damage is thereby minimized. The effect of p38(MAPK) on nuclear events is still minor. (C) The stressor is very potent (three “lightning” bolts) and allows a massive influx of Ca^{2+} into the cell and also fully activates p38(MAPK) (depicted by the red “P” circles); the effect of Ca^{2+} goes beyond simply activating MAO-A and causes damage on its own, whereas the activation of the p38(MAPK) pathway now activates other toxic downstream effectors, some of which exert substantial toxic nuclear effects. The beneficial effect of p38(MAPK)-mediated phosphorylation on MAO-A activity is lost in the generalized disruptive cellular response.

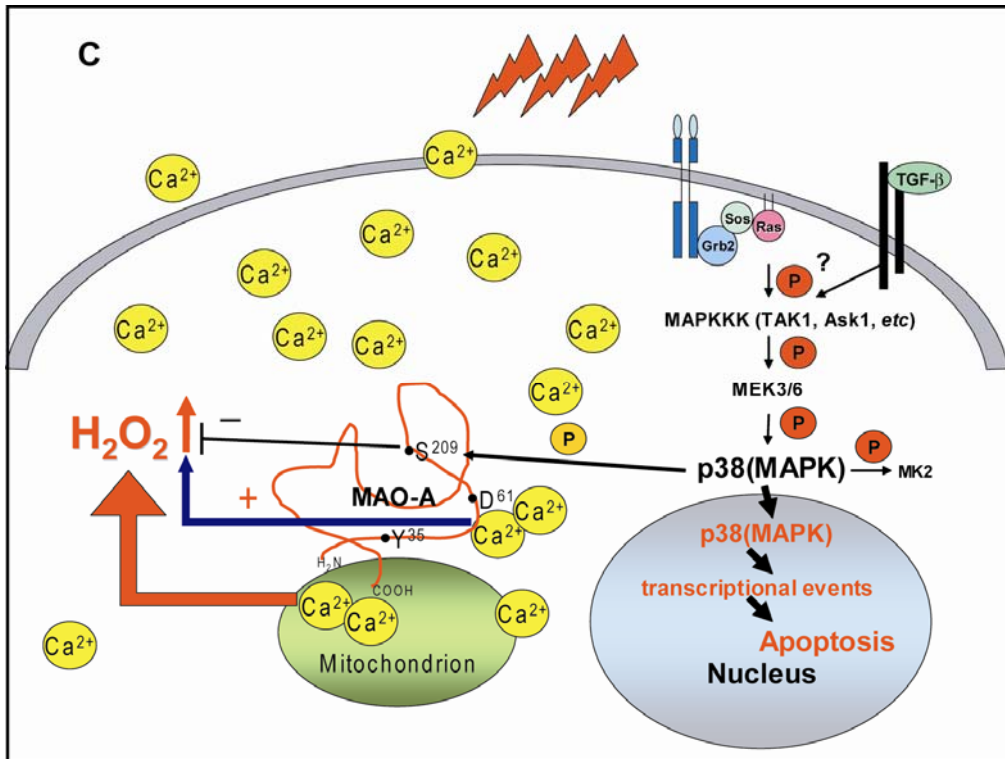
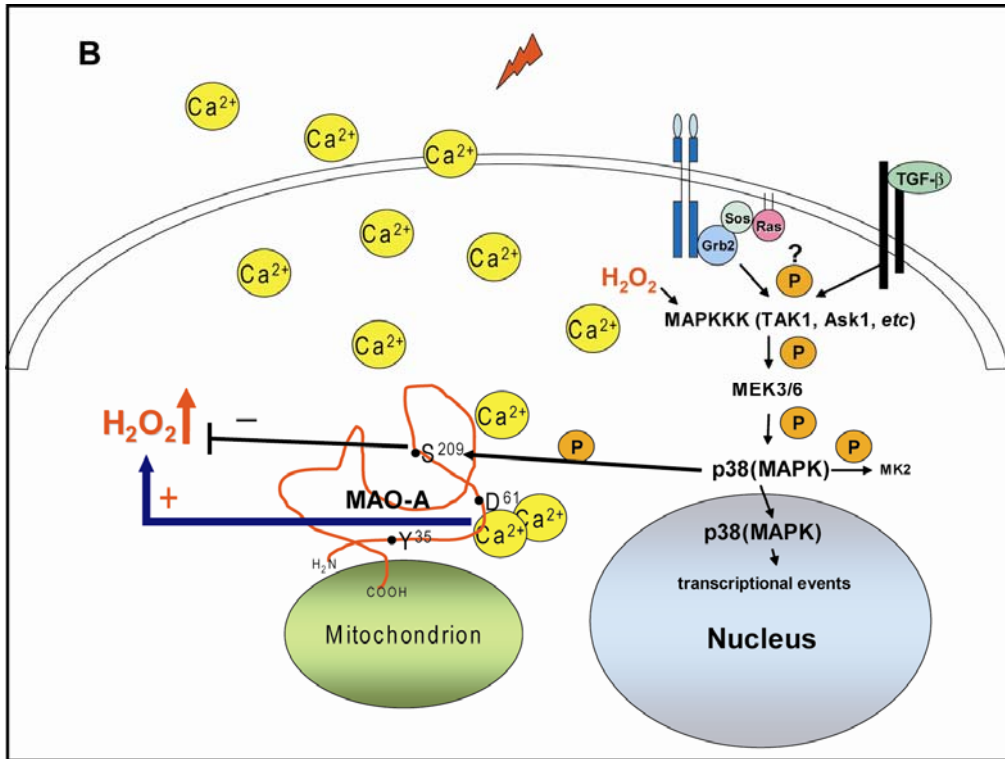


Fig. 63: Continued from Fig. 62.

Interestingly, the mitochondria can modulate cytoplasmic Ca^{2+} homeostasis by accumulating Ca^{2+} into the very high micromolar range [202]. Furthermore, elevated Ca^{2+} concentrations localized to microdomains may also represent unique means of modulating localized mitochondrial membrane and/or matrix function [323], including the activation of dehydrogenases [324]. In neurons and chromaffin cells, mitochondria rapidly and reversibly buffer Ca^{2+} during cell stimulation to help clear large Ca^{2+} loads [325-327]. The ensuing overloading of mitochondria with Ca^{2+} may be involved in several pathological conditions, including ischemia-reperfusion lesions, neurotoxicity and neurodegenerative diseases, where ATP depletion, overproduction of ROS and release of apoptotic factors lead to cell damage [328].

In the present study, Ca^{2+} increases MAO-A activity by ~20% (addition of Ca^{2+} to the reaction buffer) and ~35% (treatment with the Ca^{2+} ionophore A23187). This seems modest (and might have been more obvious if the activity assay was carried out in mitochondria-enriched fractions). However, [^{11}C]-harmine binding to MAO-A is only 34% greater in untreated depressed patients compared to normal controls [329], indicating that even a modest change in MAO-A function can significantly impact brain function. The decrease in K_M , without any alteration to V_{MAX} , of the substrate oxidation suggests that Ca^{2+} accelerates MAO-A activity, but not by a direct effect on the substrate binding site.

Regulation of MAO function by ions is not limited to Ca^{2+} [303-305]. Indeed, the transition metal Al^{3+} increases both MAO-A [330] and MAO-B [331] activity *in vitro*,

whereas Zn^{2+} selectively inhibits MAO-A activity [304], the latter effect being competable by Ca^{2+} . Interestingly, the toxicity of Al^{3+} , which has been linked to AD, is reported to depend on an increase in free intracellular Ca^{2+} [332, 333]. The observation that Mg^{2+} can block the effect of Ca^{2+} on MAO-A activity is not surprising given that it is an antagonist for Ca^{2+} [334]. However, it is interesting that Mg^{2+} is effective in treating major depression [335], a pathology classically associated with MAO-A/monoaminergic [dys]function. It is also interesting that the antidepressant fluoxetine (as well as its metabolite norfluoxetine) is an effective blocker of both T-type and N-type Ca^{2+} channels [336, 337] and that blockade of the N-type Ca^{2+} with nimodipine blocks the selective increase in MAO-A activity observed in senescence-accelerated mouse brain [306]. MAO inhibition by the anti-tuberculosis drug isoniazid could rely on its ability to block vitamin D synthesis (presumably leading to less Ca^{2+} absorption) [338, 339].

In neuronal cells, Ca^{2+} -binding proteins are ubiquitously expressed. Of these, calbindinD-28K (CB28K) is the most abundant, comprising about 1% of all soluble proteins. CB28K is reduced in aging and, even more so, in neurodegenerative diseases [340]. The reduction of CB28K disrupts Ca^{2+} buffering, exacerbates Ca^{2+} -mediated stress signals, and leaves neurons more vulnerable to toxic insults, whereas the overexpression of CB28K attenuates apoptosis [250, 252, 253]. In the present study, mouse hippocampal HT-22 cells overexpressing CB28K have lower levels of free intracellular Ca^{2+} and have significantly lower basal MAO-A activity (MAO-B activity remains unaffected). Furthermore, the MAO-A in these cells is not as responsive to Ca^{2+} . The immediate

conclusion to be drawn from these data is that the ability of CB28K to reduce MAO-A-mediated events, apparently because of a concurrent reduction in available Ca^{2+} , could be contributing to the protection afforded by CB28K [252]. Yet CB28K can also exert Ca^{2+} -independent effects such as binding directly to, and inhibiting, caspase-3 [341], and promoting neuronal MND9 cell differentiation *via* activation of p38(MAPK) [282]. In keeping with the latter observation, the overexpression of CB28K in HT-22 cells also activates p38(MAPK) and as the reduction in MAO-A activity in these cells is not accompanied by any reduction in MAO-A protein or in *mao-A* gene, this suggests a possible post-translational regulation of MAO-A and implicates p38(MAPK) in the process.

A role for post-translational modification of MAO-A as a contributing factor to its activity is further suggested by the observation that *mao-A* gene expression across cell lines does not match MAO-A protein expression, which itself does not necessarily match MAO-A activity. Comparison across the cell lines further revealed that cell lines with lower MAO-A activities often have higher constitutive levels of phosphorylated p38(MAPK). This is even more marked for C6 cells grown to confluence, which not only selectively lose their inherent MAO-A activity, but MAO-A is no longer as responsive to Ca^{2+} . Cell confluence was already known to result in the hyperactivation of p38(MAPK) [318]. This would support a regulatory role for p38(MAPK) in MAO-A function that would benefit the cell.

Support for a pro-survival role for p38(MAPK) is demonstrated by the increase in MAO-A activity and the induction of apoptosis (inferred by the loss of $\Delta\psi_m$ and the increase in ROS production) in cells treated with the specific p38(MAPK) inhibitor, SB203580. A link between MAO-A and apoptosis in SB203580-treated cells is supported by the protection afforded by specific MAO-A inhibition. The observation that SB203580 treatment actually increases MTT conversion is counterintuitive as an increase in MTT conversion is commonly used to demonstrate an increase in “viability”. However, if SB203580 treatment is affecting the activity of MAO-A, a mitochondrial enzyme, then it is quite possible that SB203580 can also affect other mitochondrial enzymes, including succinate dehydrogenase, the enzyme responsible for MTT conversion. This would mean that the MTT assay is an unreliable means for demonstrating that “inhibition” of p38(MAPK) can “enhance” viability; any conclusions in the p38(MAPK) literature that are based on this assay would be highly questionable.

It has recently been shown that staurosporine can induce MAO-A-sensitive apoptosis, independently of any transcriptional event, *via* a p38(MAPK)-dependent mechanism [183]. However, other lines of evidence have linked p38(MAPK) to induction of *mao-A* gene expression during nerve growth factor withdrawal-induced apoptosis in PC12 cells [311] and serum-withdrawal-induced apoptosis in SK-N-BE(2)-C cells [182]. These observations suggest that any effect of p38(MAPK) on *mao-A* gene or protein might be cell line-dependent. Yet these results may be misleading as these models of cell

stress activate the entire p38(MAPK) pathway and would not allow for determination of the specific role for p38(MAPK).

To better determine the role of p38(MAPK) in the regulation of MAO-A function, a constitutively active form of p38(MAPK), p38(MAPK)-AF (bearing T180E/Y182D substitutions), and a dominant negative mutant, p38(MAPK)-DN (bearing T180A/Y182F substitutions), were generated. Overexpression of p38(MAPK)-AF induces *mao-A* gene expression in PC12 cells, confirming the observations made by De Zutter and colleagues using these same cells [311]. Surprisingly, there is not a corresponding increase in endogenous MAO-A activity. In contrast, overexpression of p38(MAPK)-AF does not alter *mao-A* gene expression, but does significantly reduce MAO-A activity in the HT-22 cells, thus further supporting the potential for post-translational modification of MAO-A. p38(MAPK)-mediated regulation of MAO-A activity is confirmed by the increase in activity observed in HT-22 cells overexpressing the p38(MAPK)-DN protein or treated with the specific p38(MAPK) inhibitor, SB203580. The observation that SB203580 induces endogenous MAO-A activity in both HEK293A and HT-22 cells is not surprising given that p38(MAPK) associates with MAO-A, but not with MAO-B, in these same cell lines. What is intriguing, however, is that SB203580 alters the sensitivity of MAO-A to Ca^{2+} only in the HT-22 cell line. This could be indicating that p38(MAPK) may be exerting several effects with respect to regulation of MAO-A function; one effect would regulate the inherent activity of the enzyme, whereas the other effect would regulate the enzyme's sensitivity to Ca^{2+} . SB203580, a pyridinyl imidazole compound, can

theoretically bind to, and allosterically modulate, MAO-A [86], apparently by binding in close proximity to the flavin in the active site [342]. Imidazoline compounds also bind to other deaminating enzymes such as semicarbazide sensitive amine oxidase [343]. This is not an issue herein as SB203580, at concentrations used during the course of cell culture studies, does not affect MAO-A activity when added directly to the reaction buffer (although some inhibition of MAO-A activity is observed at higher concentrations).

The above-mentioned effect of chemical p38(MAPK) inhibition (with SB203580) on MAO-A activity is corroborated by substitution of Serine209 (which resides in a putative RXXS p38(MAPK) phosphorylation motif [312]), with either an alanine (A), which precludes phosphorylation on this residue, or with a glutamic acid (E), which is routinely used to mimic the phosphorylated state of proteins. Indeed, the “dephosphorylated” MAO-A(S/A) is fully active and is very responsive to Ca^{2+} , the latter effect being significantly greater than that observed with MAO-A(WT) [much the same as what is observed with chemical inhibition of p38(MAPK)]. In contrast, the MAO-A(S/E) phosphorylation mimic was less active and did not respond to Ca^{2+} . These combined effects confirm that p38(MAPK) could be eliciting several effects with regard to MAO-A; one effect would determine MAO-A activity itself while the other effect would determine its response to Ca^{2+} .

The differences in activities of the MAO-A(S/A) and MAO-A(S/E) mutants correspond to their different abilities to induce toxicity, as demonstrated by the greater

potential for the MAO-A(S/A) dephosphorylation mimic to generate ROS and to induce a greater loss of $\Delta \psi_m$.

A negative feedback mechanism is suggested by these data. The ability of H₂O₂ (the by-product of MAO-A-mediated catabolism) to activate p38(MAPK) (demonstrated herein in SH-SY5Y cells) is not new. Indeed, H₂O₂ can activate several signalling cascades, including the ERK and p38(MAPK) pathways [344], apparently *via* a Ca²⁺-dependent mechanism [345]. But if this is considered in the present hypothesis, then the generation of H₂O₂ (by MAO's?) could activate p38(MAPK), which, in turn, could phosphorylate MAO-A and reduce its potential for generating more H₂O₂. This would diminish the toxic effect of H₂O₂, thus acting as a pro-survival [compensatory, feedback] mechanism during periods of modest and/or transient cell stress. This novel mechanism might also contribute to the mode of action for drugs with relevance to neuropsychiatry. For example, the selective serotonin reuptake inhibitor, fluoxetine (Prozac), is routinely used to treat depression as well as obsessive-compulsive disorder. While its efficacy is attributed predominantly to its ability to increase synaptic concentrations of serotonin (5-HT), fluoxetine has been shown to also inhibit MAO-A function [314, 346] and, more recently, to block Ca²⁺ uptake [336, 337] and activate p38(MAPK) [347]. These effects do not appear to be a consequence of increased 5-HT availability [348]. The influence of this mechanism might also reach beyond neuropsychiatry. For example, glucocorticoid-mediated stress can induce *mao-A* gene and protein expression in skeletal muscle [349], whereas MAO-A-mediated oxidative stress is important during

postischemic myocardial damage [350]. Interestingly, preischemic treatment of myocytes with low doses of H₂O₂ (*i.e.* preconditioning) not only activates p38(MAPK) [351, 352], but also mitigates subsequent damage induced by a Ca²⁺ overload [352].

While the previous discussion is based on suggestion and correlational evidence, the fact that MAO-A(WT) associated with both p38(MAPK)-AF and p38(MAPK)-DN, and was serine-phosphorylated by p38(MAPK)-AF, surely provides strong evidence of a direct effect of p38(MAPK) on MAO-A. Additional evidence of this is provided by the fact that MAO-A(S/A) can not be serine-phosphorylated. This, in addition to the fact that neuroblastoma N2a cells overexpressing MAO-A(S/A) are less viable than those overexpressing MAO-A(S/E), clearly provides for a protective role for the phosphorylation of MAO-A Serine209 and supports the notion that MAO-A is a novel substrate for p38(MAPK) *in vivo*. While it is unclear how the phosphorylation of MAO-A on Serine209 can affect its function, it is interesting to note that Serine209 resides in the cavity shaping loop that contributes to the structure of the catalytic site of human MAO-A [78] and could clearly limit access of any substrate. It is important to note that substitution of Serine209 for an “A” or an “E” does not shift the substrate specificity of the overexpressed MAO-A protein to that of MAO-B. While substitution of the phenylalanine at position -1, *i.e.* phenylalanine208 immediately upstream of Serine209, does not induce a shift in human MAO-A [69], it does in rat MAO-A [68]. Furthermore, the homologous residue in human MAO-B, *i.e.* isoleucine199, clearly dictates inhibitor specificity [353]. The species-dependence for the differential contribution of these sites to

MAO function is unclear; it could be indicating subtle differences in species' MAO conformations, or perhaps species differences in other residues that could potentially be differentially post-translationally modified. It should be noted that substitutions in MAO-B on Serine200 (homologous to the MAO-A Serine209 substitutions) do not exert any effect on the activity of overexpressed proteins. This suggests that p38(MAPK) is probably selective for MAO-A function *in vivo*. The reason for this selectivity is also unclear. While both MAO-A and MAO-B are very similar in the amino acid sequences flanking the RXXS motif, any effect of p38(MAPK) could rely on different conformations of the two proteins, thus limiting access to this site by p38(MAPK), and/or the influence of another post-translational modification that could supercede the effect of Serine200 phosphorylation in MAO-B. This discrepancy warrants further investigation.

The fact that MAO-A activity is selectively enhanced by addition of Ca^{2+} to the reaction buffer also suggests the presence of Ca^{2+} -binding sites that are specific to this isoform. Based on the reported sequence of putative Ca^{2+} -binding motifs [307-309], three such motifs are found to be specific for MAO-A. These were D^{61}XXD , DXXXD^{248} , and DXD^{328} . Following their expression in human embryonic kidney (HEK) 293A cells (used because of their low endogenous MAO-A activity and their transfectability), it is observed that the mutageneses of these sites affect the inherent activities of the expressed proteins differently, which are reflected in differences in their respective toxicity profiles. The lower inherent activity of the MAO-A(D248A) mutant can result from the fact that this residue is found within one of the FAD-binding domains [77] and can therefore

interfere with association of this co-factor. The lack of inherent activity of the MAO-A(D328G) mutant has been observed before and has been attributed to possible effects on the active site [66]. Interestingly, the activities of the respective MAO-A Ca^{2+} -binding mutants appear to correlate with their presence in a high molecular weight complex. Normally, MAO-A is purified as a monomer [77]; however, it is quite possible for a bioactive protein to associate with a multimeric protein complex, one that perhaps includes various modulators. Although the actual reason for the inclusion of MAO-A in this larger complex remains unclear, it is interesting to speculate (i) that its inclusion is an obligate requirement for full activity, or (ii) that the complex might simply be a trafficking mechanism allowing for the proper packaging and re-localization of MAO-A from the Golgi/ER to the mitochondria. Support for a role for this complex in activity, however, is provided by the observation that the MAO-A(S/E) phosphorylation mimic, which is also nearly devoid of any inherent activity, is also barely detectable in the high molecular weight complex. p38(MAPK) was not detectable in the high molecular weight complex, which is perhaps not surprising, as a kinase would be expected to have a rapid association and dissociation from its substrate(s).

Unexpectedly, the MAO-A wild type and the three putative Ca^{2+} -binding site mutants do not respond to Ca^{2+} when overexpressed in HEK293A cells. It has already been determined that HEK293A cells have a significant level of constitutively active p38(MAPK) and that p38(MAPK) affects both basal MAO-A activity as well as its response to Ca^{2+} . In light of this, the response to Ca^{2+} of the three MAO-A Ca^{2+} -binding

site mutants was tested in HEK293A cells treated with the chemical p38(MAPK) inhibitor SB203580. Not surprisingly, and in keeping of a role for p38(MAPK) in the response of MAO-A to Ca^{2+} , inhibition of p38(MAPK) allows the overexpressed proteins, with the exception of the D61A mutant, to respond to Ca^{2+} . This implies that the D61 residue in MAO-A is very important for mediating the response to Ca^{2+} , particularly in a phosphorylated p38(MAPK)-rich environment. Interestingly, D61 is particular to human MAO-A, whereas D248 and D328 are found in many species (see Fig. 20). As D61 is not itself a target for phosphorylation, then p38(MAPK), *via* the phosphorylation of Serine209, must be influencing protein topography and, by extension, binding site geometries and/or conformational integrity. Examination of the effect of Serine209 phosphorylation on the conformation of MAO-A can give great insight into its function and can help with the design of newer and/or better tolerated drugs.

Reactive oxygen species (ROS) are a group of molecules comprised of, but not limited to, H_2O_2 , superoxide anion, singlet oxygen, and hydroxyl radicals. Among these, H_2O_2 plays a key role in oxidative stress because it is generated metabolically, appears in nearly all oxidative stress conditions, and is able to diffuse freely across the cell membrane. At low levels, H_2O_2 is also recognized as a second messenger that can dictate Ca^{2+} release [354] and stimulate proliferation or enhance survival [355]. At higher concentrations, it is well known to lead to cell death.

Excessive ROS is the source of oxidative stress and is a well-accepted etiopathology for neurodegenerative disorders such as Alzheimer's disease (AD). It is known that the

AD-related A β peptide is toxic, and that part of its mechanism of action is the perturbation of cellular Ca²⁺ homeostasis [356, 357] as a direct consequence of the formation of A β ion channels that are permeable to Ca²⁺ [358, 359]. In HT-22 cells, A β elevates Ca²⁺, as expected, and also increases the production of ROS in an MAO-A-sensitive manner. In primary cortical cells, A β -induced apoptosis occurs *via* an MAO-A-sensitive mechanism that is influenced by p38(MAPK). Obviously MAO-A and p38(MAPK) participate jointly in the toxicity profile of A β .

In keeping with this, the overexpression of CB28K is also known to be neuroprotective in models of AD, apparently as a result of its Ca²⁺-binding properties. Yet the observation that overexpression of CB28K induces the phosphorylation of p38(MAPK) could be revealing another mechanism underlying the neuroprotection afforded by CB28K. The fact that overexpression of CB28K and the phosphorylation of p38(MAPK) coincide with a reduction in MAO-A activity (without any concurrent loss in gene or protein expression) and a diminished response of MAO-A to Ca²⁺ supports a toxic contribution by both MAO-A and Ca²⁺ in these models, and implicates p38(MAPK) in the process. The substantial loss of CB28K expression, considered critical to the pathogenesis of AD, and any inferred loss of p38(MAPK) activity, therefore could explain the heightened vulnerability of cells immunoreactive for both CB28K and MAO-A in AD brain [59].

A link between Ca²⁺, MAO and AD is further implied by the ability of CB28K to protect against apoptosis, including that induced by A β [250, 360-362] and by the fact

Ca²⁺ signalling can be altered early in AD, well before any detectable A β deposition [363]. A link between Ca²⁺ and MAO-A is further suggested by the observation that dihydropyridine Ca²⁺ channel blockers, which are known to block the aging-related, selective increase in MAO-A [306], may improve learning and behavioural deficits in animals [364] and may improve age- and AD-related memory impairment in the human population [365, 366]. As cells co-immunoreactive for CB28K and MAO-A are often reduced during AD [59, 367], any loss of CB28K can, theoretically, facilitate MAO-A-mediated H₂O₂ production in an increasingly toxic A β environment, leading to localized cell death. A β can increase Ca²⁺ availability [368], possibly through its effect on ryanodine receptors [369]. A pathological contribution by MAO-A in AD is also suggested by the accumulation of toxic metabolites of MAO-mediated deamination in AD patients [370] as well as by the MAO-A-sensitive ROS production associated with treatment of HT-22 cells and primary neuronal cultures with A β [371]. A closer *in vivo* examination of the effect of Ca²⁺ on MAO-A as well as a closer examination of the relation between Ca²⁺/CB28K and MAO-A in AD tissues is certainly warranted.

As only the C-terminal tail of MAO is membrane-bound, most of the protein remains exposed for possible cytoplasmic post-translational modification. It is surprising, therefore, that very little is known regarding the potential for post-translational modification of MAO-A. Ca²⁺ as well as p38(MAPK) clearly, and selectively, enhance MAO-A activity (present study), whereas ubiquitination may be necessary for insertion of MAO-A and MAO-B into the mitochondrial membrane [372, 373]. Preliminary

investigations reveal that mutagenesis of tyrosine35, which resides in a motif recognized by ERK (another MAPK), influences MAO-A function significantly. A role for ERK (and even a role for the PI3K/Akt pathway) is corroborated by the fact that inhibition of the ERK (and PI3K) pathway result in enhanced MAO-A activity. Of particular interest, however, is the fact that inhibition of ERK or PI3K only affects the basal activity of MAO-A, but not its sensitivity to Ca^{2+} , which remains specific for p38(MAPK) inhibition. Also of interest is the fact that H_2O_2 can activate the p38(MAPK) pathway as well as the ERK and PI3K/Akt pathways [345], suggesting that the generation of H_2O_2 can, in principle, activate all three pathways that in turn can, *via* feedback inhibition, help diminish the contribution of MAO-A to stress and potentially to cell toxicity. This effect may not be limited to H_2O_2 . Indeed, another highly diffusible molecule, H_2S , also exerts protection that is sensitive to inhibition of the ERK and JNK pathways, but not to inhibition of the p38(MAPK) pathway [374]. Perhaps an ERK-mediated regulation of MAO-A, specifically *via* tyrosine35 in MAO-A, plays a role here?

Certain amino acid residues appear to mediate co-factor binding or access to the catalytic site, whereas other residues may be targets for post-translational modification (because of their potential for phosphorylation, *e.g.* Tyrosines, Serines, Threonines). Histidine382 might be acting as a nucleophile during MAO-B-mediated catalysis [87]. Cysteine374 and 406 in MAO-A and Cysteine156, 365 and 397 in MAO-B contribute to catalytic activity [75, 375]. These authors suggest that the contribution of Cysteine406 to MAO-A activity and Cysteine397 to MAO-B activity may rely on their role in binding of

FAD. Yet the binding of FAD may not necessarily determine catalytic activation of MAO-A as much as it might determine the structural core for the active conformation of the enzyme [376]. The role of cysteine residues and their ability to influence FAD binding, binding site geometries and/or conformational integrity in both MAO-A and MAO-B is relatively clear [75, 375]. While the contribution of tyrosines, serines and threonines to MAO function is undeniable, their contribution has never been discussed in terms of their potential for being phosphorylated. Tyrosine44 (as well as Glutamate34) is necessary for the initial binding of FAD by MAO-B [74]. Tyrosine326 determines substrate specificity and inhibitor binding in MAO-B and substitution of the homologous residue in MAO-A, *i.e.* Isoleucine335, to a Tyrosine switches its substrate specificity to that of MAO-B [66]. Mutagenesis of Tyrosine435 in MAO-B does not significantly alter active site structure or activity, yet mutagenesis of the homologous site in MAO-A (*i.e.* Tyrosine444) renders it completely unstable upon extraction from membrane preparations [377] and results in a complete loss of ability to oxidize serotonin (but not phenylalanine!) [378]. Threonine428 ([379] and Threonine158 (but not serine394) [87] in MAO-B appear to be critical for enzymatic activity. Interestingly, the residue shown to exert significant effect on MAO-A function in the current project, *i.e.* Serine209, lies within "cavity shaping loop" which contributes to the structure of the catalytic site of human MAO-A [78].

These combined observations provide for a unique mechanism for the selective regulation of MAO-A. The effect of p38(MAPK) on MAO-A appears to be cell-line

specific as it induces *mao-A* gene expression, but does not induce MAO-A activity in PC12 cells ([311], present study), it induces *mao-A* gene expression and MAO-A activity in H₂O₂-treated SH-SY5Y cells (present study), but induces MAO-A activity independent of any change in *mao-A* gene expression in staurosporine-treated SH-SY5Y cells [183]. In the cells used herein (*e.g.* HEK293A, HT-22, N2a, and C6) p38(MAPK) has a clear inhibitory effect on MAO-A activity and determines the sensitivity of MAO-A to Ca²⁺. This would, theoretically diminish the toxicity of MAO-A during stressful events, particularly those associated with an increase in Ca²⁺ availability. These combined observations are important as many of these are CNS-derived cell lines and as such could be giving insight into the function of the brain. One immediate conclusion is that patient-to-patient variability in terms of response to antidepressant drugs could potentially include a p38(MAPK)/MAO-A-sensitive component. Similarly, variability in MAO phosphorylation between patients could also explain why inhibition of this enzyme appears to be useful in improving the cognitive dysfunction in certain patients with AD, while having no effect in other patients.

5 FUTURE DIRECTIONS

The present study has revealed many new properties of MAO-A function and regulation. Some observations warrant further examination. These include, but are not limited to: examination of the role of the high molecular weight complex in MAO-A function; determination of the role of Tyr³⁵ phosphorylation in MAO-A function and protein stability; determination of how p38(MAPK)-mediated phosphorylation of MAO-A affects, *via* Serine209, MAO-A function and its sensitivity to Ca²⁺ (is this due to a conformational change of the activation loop?). Why does the phosphorylation of Serine209 in MAO-A exert such a potent effect, while phosphorylation of the homologous residues in MAO-B, *e.g.* Serine200, does not appear to have any effect on this isoform? Do the MAO-A and MAO-B proteins exist in different phosphorylation states in extracts from AD patients' brains? In Parkinson's disease patients' brains? In [untreated] depressed patients' brains? Do antidepressants alter the phosphorylation states of the MAO proteins? Do phosphorylation states of MAO proteins contribute to non-neuropsychiatric conditions such as cardiomyopathies? Obviously, the mechanism described in this thesis could have an impact on any pathology where MAO is implicated and should be considered when interpreting the relevant published data that would suggest a role for MAO's, but which can not demonstrate a change in the actual expression of the protein or in the *ex vivo* activity of the MAO protein [*e.g.* following a long post-mortem interval].

References

1. Greenawalt, J.W. and C. Schnaitman, *An appraisal of the use of monoamine oxidase as an enzyme marker for the outer membrane of rat liver mitochondria*. J Cell Biol, 1970. **46**(1): p. 173-9.
2. Hare, M.L., *Tyramine oxidase: A new enzyme system in liver*. Biochem J, 1928. **22**(4): p. 968-79.
3. Blaschko, H., D. Richter, and H. Schlossmann, *The oxidation of adrenaline and other amines*. Biochem J, 1937. **31**(12): p. 2187-96.
4. Johnston, J.P., *Some observations upon a new inhibitor of monoamine oxidase in brain tissue*. Biochem Pharmacol, 1968. **17**(7): p. 1285-97.
5. Grimsby, J., K. Chen, L.J. Wang, et al., *Human monoamine oxidase A and B genes exhibit identical exon-intron organization*. Proc Natl Acad Sci U S A, 1991. **88**(9): p. 3637-41.
6. Bach, A.W., N.C. Lan, D.L. Johnson, et al., *cDNA cloning of human liver monoamine oxidase A and B: molecular basis of differences in enzymatic properties*. Proc Natl Acad Sci U S A, 1988. **85**(13): p. 4934-8.
7. Derry, J.M., N.C. Lan, J.C. Shih, et al., *Localization of monoamine oxidase A and B genes on the mouse X chromosome*. Nucleic Acids Res, 1989. **17**(20): p. 8403.
8. Lan, N.C., C. Heinzmann, A. Gal, et al., *Human monoamine oxidase A and B genes map to Xp 11.23 and are deleted in a patient with Norrie disease*. Genomics, 1989. **4**(4): p. 552-9.
9. Toninello, A., P. Pietrangeli, U. De Marchi, et al., *Amine oxidases in apoptosis and cancer*. Biochim Biophys Acta, 2006. **1765**(1): p. 1-13.
10. Buffoni, F. and H. Blaschko, *Benzylamine oxidase and histaminase: Purification and crystallization of an enzyme from pig plasma*. Proc R Soc Lond B Biol Sci, 1964. **161**: p. 153-67.
11. Sourkes, T.L., *Copper, biogenic amines, and amine oxidases*. Ciba Found Symp, 1980. **79**: p. 143-56.
12. Ochiai, Y., K. Itoh, E. Sakurai, et al., *Substrate selectivity of monoamine oxidase A, monoamine oxidase B, diamine oxidase, and semicarbazide-sensitive amine oxidase in COS-1 expression systems*. Biol Pharm Bull, 2006. **29**(12): p. 2362-6.
13. Finberg, J.P. and M.B. Youdim, *Selective MAO A and B inhibitors: their mechanism of action and pharmacology*. Neuropharmacology, 1983. **22**(3 Spec No): p. 441-6.
14. Knoll, J. and K. Magyar, *Some puzzling pharmacological effects of monoamine oxidase inhibitors*. Adv Biochem Psychopharmacol, 1972. **5**: p. 393-408.
15. White, H.L. and A.T. Glassman, *Multiple binding sites of human brain and liver monoamine oxidase: substrate specificities, selective inhibitions, and attempts to separate enzyme forms*. J Neurochem, 1977. **29**(6): p. 987-97.
16. Fowler, C.J. and B.A. Callingham, *Substrate-selective activation of rat liver mitochondrial monoamine oxidase by oxygen*. Biochem Pharmacol, 1978. **27**(16): p. 1995-2000.
17. Grimsby, J., N.C. Lan, R. Neve, et al., *Tissue distribution of human monoamine oxidase A and B mRNA*. J Neurochem, 1990. **55**(4): p. 1166-9.
18. Jahng, J.W., T.A. Houpt, T.C. Wessel, et al., *Localization of monoamine oxidase A and B mRNA in the rat brain by in situ hybridization*. Synapse, 1997. **25**(1): p. 30-6.

19. Kitahama, K., T. Maeda, R.M. Denney, et al., *Monoamine oxidase: distribution in the cat brain studied by enzyme- and immunohistochemistry: recent progress*. Prog Neurobiol, 1994. **42**(1): p. 53-78.
20. Thorpe, L.W., K.N. Westlund, L.M. Kochersperger, et al., *Immunocytochemical localization of monoamine oxidases A and B in human peripheral tissues and brain*. J Histochem Cytochem, 1987. **35**(1): p. 23-32.
21. Egashira, T. and Y. Yamanaka, *Further studies on the synthesis of A-form monoamine oxidase*. Jpn J Pharmacol, 1981. **31**(5): p. 763-70.
22. Glover, V., M. Sandler, F. Owen, et al., *Dopamine is a monoamine oxidase B substrate in man*. Nature, 1977. **265**(5589): p. 80-1.
23. O'Carroll, A.M., C.J. Fowler, J.P. Phillips, et al., *The deamination of dopamine by human brain monoamine oxidase. Specificity for the two enzyme forms in seven brain regions*. Naunyn Schmiedeberg's Arch Pharmacol, 1983. **322**(3): p. 198-202.
24. Waldmeier, P.C., A. Delini-Stula, and L. Maitre, *Preferential deamination of dopamine by an A type monoamine oxidase in rat brain*. Naunyn Schmiedeberg's Arch Pharmacol, 1976. **292**(1): p. 9-14.
25. Egashira, T., T. Yamamoto, and Y. Yamanaka, *Some interrelated properties of A and B form monoamine oxidase in monkey brain mitochondria*. Jpn J Pharmacol, 1984. **34**(3): p. 327-34.
26. Garrick, N.A. and D.L. Murphy, *Species differences in the deamination of dopamine and other substrates for monoamine oxidase in brain*. Psychopharmacology (Berl), 1980. **72**(1): p. 27-33.
27. Langston, J.W., I. Irwin, E.B. Langston, et al., *Pargyline prevents MPTP-induced parkinsonism in primates*. Science, 1984. **225**(4669): p. 1480-2.
28. Fuller, R.W. and S.K. Hemrick-Luecke, *Mechanisms of MPTP (1-methyl-4-phenyl-1,2,3,6-tetrahydropyridine) neurotoxicity to striatal dopamine neurons in mice*. Prog Neuropsychopharmacol Biol Psychiatry, 1985. **9**(5-6): p. 687-90.
29. Chiba, K., A. Trevor, and N. Castagnoli, Jr., *Metabolism of the neurotoxic tertiary amine, MPTP, by brain monoamine oxidase*. Biochem Biophys Res Commun, 1984. **120**(2): p. 574-8.
30. Westlund, K.N., R.M. Denney, R.M. Rose, et al., *Localization of distinct monoamine oxidase A and monoamine oxidase B cell populations in human brainstem*. Neuroscience, 1988. **25**(2): p. 439-56.
31. Rodriguez, M.J., J. Saura, C.C. Finch, et al., *Localization of monoamine oxidase A and B in human pancreas, thyroid, and adrenal glands*. J Histochem Cytochem, 2000. **48**(1): p. 147-51.
32. Saura, J., E. Nadal, B. van den Berg, et al., *Localization of monoamine oxidases in human peripheral tissues*. Life Sci, 1996. **59**(16): p. 1341-9.
33. Saura, J., R. Kettler, M. Da Prada, et al., *Quantitative enzyme radioautography with 3H-Ro 41-1049 and 3H-Ro 19-6327 in vitro: localization and abundance of MAO-A and MAO-B in rat CNS, peripheral organs, and human brain*. J Neurosci, 1992. **12**(5): p. 1977-99.
34. Mahy, N., N. Andres, C. Andrade, et al., *Age-related changes of MAO-A and -B distribution in human and mouse brain*. Neurobiology (Bp), 2000. **8**(1): p. 47-54.
35. Rodriguez, M.J., J. Saura, E. Billett, et al., *MAO-A and MAO-B localisation in human lung and spleen*. Neurobiology (Bp), 2000. **8**(3-4): p. 243-8.

36. Rodriguez, M.J., J. Saura, E.E. Billett, et al., *Cellular localization of monoamine oxidase A and B in human tissues outside of the central nervous system*. Cell Tissue Res, 2001. **304**(2): p. 215-20.
37. Konradi, C., K. Jellinger, P. Riederer, et al., *Histochemistry of MAO-A and MAO-B in the locus coeruleus of the Mongolian gerbil*. J Neural Transm, 1987. **70**(3-4): p. 369-76.
38. Owen, F., A.J. Cross, R. Lofthouse, et al., *Distribution and inhibition characteristics of human brain monoamine oxidase*. Biochem Pharmacol, 1979. **28**(7): p. 1077-80.
39. Westlund, K.N., T.J. Krakower, S.W. Kwan, et al., *Intracellular distribution of monoamine oxidase A in selected regions of rat and monkey brain and spinal cord*. Brain Res, 1993. **612**(1-2): p. 221-30.
40. Egashira, T., T. Yamamoto, and Y. Yamanaka, *Isoelectric focusing of isoenzymes of monkey brain monoamine oxidase*. Life Sci, 1984. **34**(10): p. 915-21.
41. Obata, T., T. Egashira, and Y. Yamanaka, *Evidence for existence of A and B form monoamine oxidase in mitochondria from dog platelets*. Jpn J Pharmacol, 1987. **44**(2): p. 105-11.
42. Solatunturi, E. and M.K. Paasonen, *Intracellular distribution of monoamine oxidase, 5-hydroxytryptamine and histamine in blood platelets of rabbit*. Ann Med Exp Biol Fenn, 1966. **44**(3): p. 427-30.
43. Saura, J., Z. Bleuel, J. Ulrich, et al., *Molecular neuroanatomy of human monoamine oxidases A and B revealed by quantitative enzyme radioautography and in situ hybridization histochemistry*. Neuroscience, 1996. **70**(3): p. 755-74.
44. Riederer, P., C. Konradi, V. Schay, et al., *Localization of MAO-A and MAO-B in human brain: a step in understanding the therapeutic action of L-deprenyl*. Adv Neurol, 1987. **45**: p. 111-8.
45. Konradi, C., J. Kornhuber, L. Froelich, et al., *Demonstration of monoamine oxidase-A and -B in the human brainstem by a histochemical technique*. Neuroscience, 1989. **33**(2): p. 383-400.
46. Saura, J., J.G. Richards, and N. Mahy, *Differential age-related changes of MAO-A and MAO-B in mouse brain and peripheral organs*. Neurobiol Aging, 1994. **15**(4): p. 399-408.
47. Sivasubramaniam, S.D., C.C. Finch, M.J. Rodriguez, et al., *A comparative study of the expression of monoamine oxidase-A and -B mRNA and protein in non-CNS human tissues*. Cell Tissue Res, 2003. **313**(3): p. 291-300.
48. Bond, P.A. and R.L. Cundall, *Properties of monoamine oxidase (MAO) in human blood platelets, plasma, lymphocytes and granulocytes*. Clin Chim Acta, 1977. **80**(2): p. 317-26.
49. Buznikov, G.A., *[Transmitters in early embryogenesis (new data)]*. Ontogenez, 1989. **20**(6): p. 637-46.
50. Buznikov, G.A., Y.B. Shmukler, and J.M. Lauder, *From oocyte to neuron: do neurotransmitters function in the same way throughout development?* Cell Mol Neurobiol, 1996. **16**(5): p. 537-59.
51. Levitt, P., J.A. Harvey, E. Friedman, et al., *New evidence for neurotransmitter influences on brain development*. Trends Neurosci, 1997. **20**(6): p. 269-74.
52. Nicotra, A., L. Falasca, O. Senatori, et al., *Monoamine oxidase A and B activities in embryonic chick hepatocytes: differential regulation by retinoic acid*. Cell Biochem Funct, 2002. **20**(2): p. 87-94.
53. Nicotra, A., F. Pierucci, H. Parvez, et al., *Monoamine oxidase expression during development and aging*. Neurotoxicology, 2004. **25**(1-2): p. 155-65.

54. Lewinsohn, R., V. Glover, and M. Sandler, *Development of benzylamine oxidase and monoamine oxidase A and B in man*. *Biochem Pharmacol*, 1980. **29**(9): p. 1221-30.
55. Shih, J.C. and H. Young, *The alteration of serotonin binding sites in aged human brain*. *Life Sci*, 1978. **23**(14): p. 1441-8.
56. Fowler, C.J., A. Wiberg, L. Oreland, et al., *The effect of age on the activity and molecular properties of human brain monoamine oxidase*. *J Neural Transm*, 1980. **49**(1-2): p. 1-20.
57. Kornhuber, J., C. Konradi, F. Mack-Burkhardt, et al., *Ontogenesis of monoamine oxidase-A and -B in the human brain frontal cortex*. *Brain Res*, 1989. **499**(1): p. 81-6.
58. Shih, J.C., K. Chen, and M.J. Ridd, *Monoamine oxidase: from genes to behavior*. *Annu Rev Neurosci*, 1999. **22**: p. 197-217.
59. Chan-Palay, V., M. Hochli, E. Savaskan, et al., *Calbindin D-28k and monoamine oxidase A immunoreactive neurons in the nucleus basalis of Meynert in senile dementia of the Alzheimer type and Parkinson's disease*. *Dementia*, 1993. **4**(1): p. 1-15.
60. Lan, N.C., C.H. Chen, and J.C. Shih, *Expression of functional human monoamine oxidase A and B cDNAs in mammalian cells*. *J Neurochem*, 1989. **52**(5): p. 1652-4.
61. Chen, K., H.F. Wu, and J.C. Shih, *The deduced amino acid sequences of human platelet and frontal cortex monoamine oxidase B are identical*. *J Neurochem*, 1993. **61**(1): p. 187-90.
62. Zhu, Q.S., J. Grimsby, K. Chen, et al., *Promoter organization and activity of human monoamine oxidase (MAO) A and B genes*. *J Neurosci*, 1992. **12**(11): p. 4437-46.
63. Chen, K., X.M. Ou, G. Chen, et al., *R1, a novel repressor of the human monoamine oxidase A*. *J Biol Chem*, 2005. **280**(12): p. 11552-9.
64. Shih, J.C. and K. Chen, *Regulation of MAO-A and MAO-B gene expression*. *Curr Med Chem*, 2004. **11**(15): p. 1995-2005.
65. Abell, C.W. and S.W. Kwan, *Molecular characterization of monoamine oxidases A and B*. *Prog Nucleic Acid Res Mol Biol*, 2001. **65**: p. 129-56.
66. Geha, R.M., I. Rebrin, K. Chen, et al., *Substrate and inhibitor specificities for human monoamine oxidase A and B are influenced by a single amino acid*. *J Biol Chem*, 2001. **276**(13): p. 9877-82.
67. Grimsby, J., M. Zentner, and J.C. Shih, *Identification of a region important for human monoamine oxidase B substrate and inhibitor selectivity*. *Life Sci*, 1996. **58**(9): p. 777-87.
68. Tsugenno, Y. and A. Ito, *A key amino acid responsible for substrate selectivity of monoamine oxidase A and B*. *J Biol Chem*, 1997. **272**(22): p. 14033-6.
69. Geha, R.M., K. Chen, and J.C. Shih, *Phe(208) and Ile(199) in human monoamine oxidase A and B do not determine substrate and inhibitor specificities as in rat*. *J Neurochem*, 2000. **75**(3): p. 1304-9.
70. Geha, R.M., K. Chen, J. Wouters, et al., *Analysis of conserved active site residues in monoamine oxidase A and B and their three-dimensional molecular modeling*. *J Biol Chem*, 2002. **277**(19): p. 17209-16.
71. Kwan, S.W., J.M. Bergeron, and C.W. Abell, *Molecular properties of monoamine oxidases A and B*. *Psychopharmacology (Berl)*, 1992. **106 Suppl**: p. S1-5.
72. Hsu, Y.P., W. Weyler, S. Chen, et al., *Structural features of human monoamine oxidase A elucidated from cDNA and peptide sequences*. *J Neurochem*, 1988. **51**(4): p. 1321-4.

73. Edmondson, D.E., C. Binda, and A. Mattevi, *The FAD binding sites of human monoamine oxidases A and B*. *Neurotoxicology*, 2004. **25**(1-2): p. 63-72.
74. Zhou, B.P., B. Wu, S.W. Kwan, et al., *Characterization of a highly conserved FAD-binding site in human monoamine oxidase B*. *J Biol Chem*, 1998. **273**(24): p. 14862-8.
75. Wu, H.F., K. Chen, and J.C. Shih, *Site-directed mutagenesis of monoamine oxidase A and B: role of cysteines*. *Mol Pharmacol*, 1993. **43**(6): p. 888-93.
76. Binda, C., F. Hubalek, M. Li, et al., *Structure of the human mitochondrial monoamine oxidase B: new chemical implications for neuroprotectant drug design*. *Neurology*, 2006. **67**(7 Suppl 2): p. S5-7.
77. Edmondson, D.E., L. Decolibus, C. Binda, et al., *New insights into the structures and functions of human monoamine oxidases A and B*. *J Neural Transm*, 2007.
78. De Colibus, L., M. Li, C. Binda, et al., *Three-dimensional structure of human monoamine oxidase A (MAO A): relation to the structures of rat MAO A and human MAO B*. *Proc Natl Acad Sci U S A*, 2005. **102**(36): p. 12684-9.
79. Mitoma, J. and A. Ito, *Mitochondrial targeting signal of rat liver monoamine oxidase B is located at its carboxy terminus*. *J Biochem (Tokyo)*, 1992. **111**(1): p. 20-4.
80. Rebrin, I., R.M. Geha, K. Chen, et al., *Effects of carboxyl-terminal truncations on the activity and solubility of human monoamine oxidase B*. *J Biol Chem*, 2001. **276**(31): p. 29499-506.
81. Edmondson, D.E., A. Mattevi, C. Binda, et al., *Structure and mechanism of monoamine oxidase*. *Curr Med Chem*, 2004. **11**(15): p. 1983-93.
82. Raddatz, R. and S.M. Lanier, *Relationship between imidazoline/guanidinium receptive sites and monoamine oxidase A and B*. *Neurochem Int*, 1997. **30**(1): p. 109-17.
83. Tesson, F., I. Limon-Boulez, P. Urban, et al., *Localization of I2-imidazoline binding sites on monoamine oxidases*. *J Biol Chem*, 1995. **270**(17): p. 9856-61.
84. Raddatz, R., A. Parini, and S.M. Lanier, *Localization of the imidazoline binding domain on monoamine oxidase B*. *Mol Pharmacol*, 1997. **52**(4): p. 549-53.
85. Raddatz, R., A. Parini, and S.M. Lanier, *Imidazoline/guanidinium binding domains on monoamine oxidases. Relationship to subtypes of imidazoline-binding proteins and tissue-specific interaction of imidazoline ligands with monoamine oxidase B*. *J Biol Chem*, 1995. **270**(46): p. 27961-8.
86. Ozaita, A., G. Olmos, M.A. Boronat, et al., *Inhibition of monoamine oxidase A and B activities by imidazol(ine)/guanidine drugs, nature of the interaction and distinction from I2-imidazoline receptors in rat liver*. *Br J Pharmacol*, 1997. **121**(5): p. 901-12.
87. Cesura, A.M., J. Gottowik, H.W. Lahm, et al., *Investigation on the structure of the active site of monoamine oxidase-B by affinity labeling with the selective inhibitor lazabemide and by site-directed mutagenesis*. *Eur J Biochem*, 1996. **236**(3): p. 996-1002.
88. Tsugeno, Y., I. Hirashiki, F. Ogata, et al., *Regions of the molecule responsible for substrate specificity of monoamine oxidase A and B: a chimeric enzyme analysis*. *J Biochem (Tokyo)*, 1995. **118**(5): p. 974-80.
89. Weyler, W., *Functional expression of C-terminally truncated human monoamine oxidase type A in *Saccharomyces cerevisiae**. *J Neural Transm Suppl*, 1994. **41**: p. 3-15.

90. Chen, K., H.F. Wu, and J.C. Shih, *Influence of C terminus on monoamine oxidase A and B catalytic activity*. J Neurochem, 1996. **66**(2): p. 797-803.
91. Shih, J.C. and K. Chen, *MAO-A and -B gene knock-out mice exhibit distinctly different behavior*. Neurobiology (Bp), 1999. **7**(2): p. 235-46.
92. Cases, O., I. Seif, J. Grimsby, et al., *Aggressive behavior and altered amounts of brain serotonin and norepinephrine in mice lacking MAOA*. Science, 1995. **268**(5218): p. 1763-6.
93. Kim, J.J., J.C. Shih, K. Chen, et al., *Selective enhancement of emotional, but not motor, learning in monoamine oxidase A-deficient mice*. Proc Natl Acad Sci U S A, 1997. **94**(11): p. 5929-33.
94. Mejia, J.M., F.R. Ervin, G.B. Baker, et al., *Monoamine oxidase inhibition during brain development induces pathological aggressive behavior in mice*. Biol Psychiatry, 2002. **52**(8): p. 811-21.
95. Brunner, H.G., M. Nelen, X.O. Breakefield, et al., *Abnormal behavior associated with a point mutation in the structural gene for monoamine oxidase A*. Science, 1993. **262**(5133): p. 578-80.
96. Brunner, H.G., M.R. Nelen, P. van Zandvoort, et al., *X-linked borderline mental retardation with prominent behavioral disturbance: phenotype, genetic localization, and evidence for disturbed monoamine metabolism*. Am J Hum Genet, 1993. **52**(6): p. 1032-9.
97. Sims, K.B., A. de la Chapelle, R. Norio, et al., *Monoamine oxidase deficiency in males with an X chromosome deletion*. Neuron, 1989. **2**(1): p. 1069-76.
98. Sims, K.B., L. Ozelius, T. Corey, et al., *Norrie disease gene is distinct from the monoamine oxidase genes*. Am J Hum Genet, 1989. **45**(3): p. 424-34.
99. Chen, K., O. Cases, I. Rebrin, et al., *Forebrain-specific expression of monoamine oxidase A reduces neurotransmitter levels, restores the brain structure, and rescues aggressive behavior in monoamine oxidase A-deficient mice*. J Biol Chem, 2007. **282**(1): p. 115-23.
100. Grimsby, J., M. Toth, K. Chen, et al., *Increased stress response and beta-phenylethylamine in MAOB-deficient mice*. Nat Genet, 1997. **17**(2): p. 206-10.
101. Fowler, J.S., N.D. Volkow, G.J. Wang, et al., *Brain monoamine oxidase A inhibition in cigarette smokers*. Proc Natl Acad Sci U S A, 1996. **93**(24): p. 14065-9.
102. Yu, P.H. and A.A. Boulton, *Irreversible inhibition of monoamine oxidase by some components of cigarette smoke*. Life Sci, 1987. **41**(6): p. 675-82.
103. van Amsterdam, J., R. Talhout, W. Vleeming, et al., *Contribution of monoamine oxidase (MAO) inhibition to tobacco and alcohol addiction*. Life Sci, 2006. **79**(21): p. 1969-73.
104. Jonsson, E.G., N. Norton, K. Forslund, et al., *Association between a promoter variant in the monoamine oxidase A gene and schizophrenia*. Schizophr Res, 2003. **61**(1): p. 31-7.
105. Bland, R.C., *Epidemiology of affective disorders: a review*. Can J Psychiatry, 1997. **42**(4): p. 367-77.
106. Birkmayer, W. and P. Riederer, *Biochemical post-mortem findings in depressed patients*. J Neural Transm, 1975. **37**(2): p. 95-109.
107. Youdim, M.B. and Y.S. Bakhle, *Monoamine oxidase: isoforms and inhibitors in Parkinson's disease and depressive illness*. Br J Pharmacol, 2006. **147 Suppl 1**: p. S287-96.
108. Berton, O. and E.J. Nestler, *New approaches to antidepressant drug discovery: beyond monoamines*. Nat Rev Neurosci, 2006. **7**(2): p. 137-51.

109. Marangell, L.B., M. Martinez, R.A. Jurdi, et al., *Neurostimulation therapies in depression: a review of new modalities*. Acta Psychiatr Scand, 2007. **116**(3): p. 174-81.
110. Holtzheimer, P.E., 3rd and C.B. Nemeroff, *Emerging treatments for depression*. Expert Opin Pharmacother, 2006. **7**(17): p. 2323-39.
111. Holtzheimer, P.E., 3rd and C.B. Nemeroff, *Advances in the treatment of depression*. NeuroRx, 2006. **3**(1): p. 42-56.
112. Nutt, D.J., *The role of dopamine and norepinephrine in depression and antidepressant treatment*. J Clin Psychiatry, 2006. **67 Suppl 6**: p. 3-8.
113. Howland, R.H., *MAOI antidepressant drugs*. J Psychosoc Nurs Ment Health Serv, 2006. **44**(6): p. 9-12.
114. Weinstock, M., E. Gorodetsky, T. Poltyrev, et al., *A novel cholinesterase and brain-selective monoamine oxidase inhibitor for the treatment of dementia comorbid with depression and Parkinson's disease*. Prog Neuropsychopharmacol Biol Psychiatry, 2003. **27**(4): p. 555-61.
115. Bonnet, U., *Moclobemide: therapeutic use and clinical studies*. CNS Drug Rev, 2003. **9**(1): p. 97-140.
116. Arendt, T., *Neurodegeneration and plasticity*. Int J Dev Neurosci, 2004. **22**(7): p. 507-14.
117. Van Den Eeden, S.K., C.M. Tanner, A.L. Bernstein, et al., *Incidence of Parkinson's disease: variation by age, gender, and race/ethnicity*. Am J Epidemiol, 2003. **157**(11): p. 1015-22.
118. Schapira, A.H., *Causes of neuronal death in Parkinson's disease*. Adv Neurol, 2001. **86**: p. 155-62.
119. Poirier, L.J. and T.L. Sourkes, *Influence of the substantia nigra on the catecholamine content of the striatum*. Brain, 1965. **88**: p. 181-92.
120. Savitt, J.M., V.L. Dawson, and T.M. Dawson, *Diagnosis and treatment of Parkinson disease: molecules to medicine*. J Clin Invest, 2006. **116**(7): p. 1744-54.
121. Rascol, O., C. Goetz, W. Koller, et al., *Treatment interventions for Parkinson's disease: an evidence based assessment*. Lancet, 2002. **359**(9317): p. 1589-98.
122. Chen, S. and W. Le, *Neuroprotective therapy in Parkinson disease*. Am J Ther, 2006. **13**(5): p. 445-57.
123. Youdim, M.B., *Monoamine oxidase inhibitors as anti-depressant drugs and as adjunct to L-dopa therapy of Parkinson's disease*. J Neural Transm Suppl, 1980(16): p. 157-61.
124. Riederer, P. and M.B. Youdim, *Monoamine oxidase activity and monoamine metabolism in brains of parkinsonian patients treated with l-deprenyl*. J Neurochem, 1986. **46**(5): p. 1359-65.
125. Birkmayer, W., J. Knoll, P. Riederer, et al., *Increased life expectancy resulting from addition of L-deprenyl to Madopar treatment in Parkinson's disease: a longterm study*. J Neural Transm, 1985. **64**(2): p. 113-27.
126. Birkmayer, W., J. Knoll, P. Riederer, et al., *(-)-Deprenyl leads to prolongation of L-dopa efficacy in Parkinson's disease*. Mod Probl Pharmacopsychiatry, 1983. **19**: p. 170-6.
127. Magyar, K. and B. Szende, *(-)-Deprenyl, a selective MAO-B inhibitor, with apoptotic and anti-apoptotic properties*. Neurotoxicology, 2004. **25**(1-2): p. 233-42.

128. Tatton, W., R. Chalmers-Redman, and N. Tatton, *Neuroprotection by deprenyl and other propargylamines: glyceraldehyde-3-phosphate dehydrogenase rather than monoamine oxidase B*. J Neural Transm, 2003. **110**(5): p. 509-15.
129. Jenner, P., *Preclinical evidence for neuroprotection with monoamine oxidase-B inhibitors in Parkinson's disease*. Neurology, 2004. **63**(7 Suppl 2): p. S13-22.
130. Tatton, W.G. and R.M. Chalmers-Redman, *Modulation of gene expression rather than monoamine oxidase inhibition: (-)-deprenyl-related compounds in controlling neurodegeneration*. Neurology, 1996. **47**(6 Suppl 3): p. S171-83.
131. Tatton, W.G., J.S. Wadia, W.Y. Ju, et al., *(-)-Deprenyl reduces neuronal apoptosis and facilitates neuronal outgrowth by altering protein synthesis without inhibiting monoamine oxidase*. J Neural Transm Suppl, 1996. **48**: p. 45-59.
132. Youdim, M.B. and P.F. Riederer, *A review of the mechanisms and role of monoamine oxidase inhibitors in Parkinson's disease*. Neurology, 2004. **63**(7 Suppl 2): p. S32-5.
133. Youdim, M.B., D. Edmondson, and K.F. Tipton, *The therapeutic potential of monoamine oxidase inhibitors*. Nat Rev Neurosci, 2006. **7**(4): p. 295-309.
134. Youdim, M.B., T. Amit, M. Falach-Yogev, et al., *The essentiality of Bcl-2, PKC and proteasome-ubiquitin complex activations in the neuroprotective-antiapoptotic action of the anti-Parkinson drug, rasagiline*. Biochem Pharmacol, 2003. **66**(8): p. 1635-41.
135. Magyar, K. and D. Haberle, *Neuroprotective and neuronal rescue effects of selegiline: review*. Neurobiology (Bp), 1999. **7**(2): p. 175-90.
136. Haefely, W., W.P. Burkard, A.M. Cesura, et al., *Biochemistry and pharmacology of moclobemide, a prototype RIMA*. Psychopharmacology (Berl), 1992. **106 Suppl**: p. S6-14.
137. Reynolds, G.P. and P. Riederer, *Assessment of MAO inhibitors using postmortem human brain tissue: biochemical and therapeutic implications*. Mod Probl Pharmacopsychiatry, 1983. **19**: p. 255-9.
138. Youdim, M.B., G.G. Collins, M. Sandler, et al., *Human brain monoamine oxidase: multiple forms and selective inhibitors*. Nature, 1972. **236**(5344): p. 225-8.
139. Youdim, M.B. and M. Weinstock, *Therapeutic applications of selective and non-selective inhibitors of monoamine oxidase A and B that do not cause significant tyramine potentiation*. Neurotoxicology, 2004. **25**(1-2): p. 243-50.
140. Colzi, A., F. D'Agostini, A.M. Cesura, et al., *Monoamine oxidase-A inhibitors and dopamine metabolism in rat caudatus: evidence that an increased cytosolic level of dopamine displaces reversible monoamine oxidase-A inhibitors in vivo*. J Pharmacol Exp Ther, 1993. **265**(1): p. 103-11.
141. Davidson, J.R., *Pharmacotherapy of social phobia*. Acta Psychiatr Scand Suppl, 2003(417): p. 65-71.
142. Bottlaender, M., F. Dolle, I. Guenther, et al., *Mapping the cerebral monoamine oxidase type A: positron emission tomography characterization of the reversible selective inhibitor [¹¹C]befloxatone*. J Pharmacol Exp Ther, 2003. **305**(2): p. 467-73.
143. Yamamoto, M., *Depression in Parkinson's disease: its prevalence, diagnosis, and neurochemical background*. J Neurol, 2001. **248 Suppl 3**: p. III5-11.

144. Ferri, C.P., M. Prince, C. Brayne, et al., *Global prevalence of dementia: a Delphi consensus study*. Lancet, 2005. **366**(9503): p. 2112-7.
145. Blennow, K., M.J. de Leon, and H. Zetterberg, *Alzheimer's disease*. Lancet, 2006. **368**(9533): p. 387-403.
146. Selkoe, D.J. and M.B. Podlisny, *Deciphering the genetic basis of Alzheimer's disease*. Annu Rev Genomics Hum Genet, 2002. **3**: p. 67-99.
147. Gatz, M., C.A. Reynolds, L. Fratiglioni, et al., *Role of genes and environments for explaining Alzheimer disease*. Arch Gen Psychiatry, 2006. **63**(2): p. 168-74.
148. Gerlach, M., P. Riederer, and M.B. Youdim, *Molecular mechanisms for neurodegeneration. Synergism between reactive oxygen species, calcium, and excitotoxic amino acids*. Adv Neurol, 1996. **69**: p. 177-94.
149. Christen, Y., *Oxidative stress and Alzheimer disease*. Am J Clin Nutr, 2000. **71**(2): p. 621S-629S.
150. Yu, P.H., *Involvement of cerebrovascular semicarbazide-sensitive amine oxidase in the pathogenesis of Alzheimer's disease and vascular dementia*. Med Hypotheses, 2001. **57**(2): p. 175-9.
151. Gabrylewicz, T., M. Barcikowska, and D.L. Jarczewska, *[Alzheimer's disease therapy--theory and practice]*. Wiad Lek, 2005. **58**(9-10): p. 528-35.
152. Farlow, M.R., *NMDA receptor antagonists. A new therapeutic approach for Alzheimer's disease*. Geriatrics, 2004. **59**(6): p. 22-7.
153. Citron, M., *Beta-secretase inhibition for the treatment of Alzheimer's disease--promise and challenge*. Trends Pharmacol Sci, 2004. **25**(2): p. 92-7.
154. Harrison, T., I. Churcher, and D. Beher, *gamma-Secretase as a target for drug intervention in Alzheimer's disease*. Curr Opin Drug Discov Devel, 2004. **7**(5): p. 709-19.
155. Hooper, N.M. and A.J. Turner, *The search for alpha-secretase and its potential as a therapeutic approach to Alzheimer's disease*. Curr Med Chem, 2002. **9**(11): p. 1107-19.
156. Dejaegere, T. and B. de Strooper, *[Secretases as therapeutic targets for the treatment of Alzheimer's disease]*. Verh K Acad Geneesk Belg, 2004. **66**(1): p. 29-58; discussion 58-9.
157. van Horsen, J., P. Wesseling, L.P. van den Heuvel, et al., *Heparan sulphate proteoglycans in Alzheimer's disease and amyloid-related disorders*. Lancet Neurol, 2003. **2**(8): p. 482-92.
158. House, E., J. Collingwood, A. Khan, et al., *Aluminium, iron, zinc and copper influence the in vitro formation of amyloid fibrils of Abeta42 in a manner which may have consequences for metal chelation therapy in Alzheimer's disease*. J Alzheimers Dis, 2004. **6**(3): p. 291-301.
159. Liu, Q., H.G. Lee, K. Honda, et al., *Tau modifiers as therapeutic targets for Alzheimer's disease*. Biochim Biophys Acta, 2005. **1739**(2-3): p. 211-5.
160. Nakashima, H., T. Ishihara, P. Suguimoto, et al., *Chronic lithium treatment decreases tau lesions by promoting ubiquitination in a mouse model of tauopathies*. Acta Neuropathol (Berl), 2005. **110**(6): p. 547-56.
161. Morinaga, A., M. Hirohata, K. Ono, et al., *Estrogen has anti-amyloidogenic effects on Alzheimer's beta-amyloid fibrils in vitro*. Biochem Biophys Res Commun, 2007. **359**(3): p. 697-702.
162. Schipper, H.M., *Oxysterols, cholesterol homeostasis, and Alzheimer disease*. J Neurochem, 2007. **102**(6): p. 1727-37.

163. Heneka, M.T. and M.K. O'Banion, *Inflammatory processes in Alzheimer's disease*. J Neuroimmunol, 2007. **184**(1-2): p. 69-91.
164. Solomon, B., *Clinical immunologic approaches for the treatment of Alzheimer's disease*. Expert Opin Investig Drugs, 2007. **16**(6): p. 819-28.
165. Starkstein, S.E. and R. Mizrahi, *Depression in Alzheimer's disease*. Expert Rev Neurother, 2006. **6**(6): p. 887-95.
166. Ebadi, M., H. Brown-Borg, J. Ren, et al., *Therapeutic efficacy of selegiline in neurodegenerative disorders and neurological diseases*. Curr Drug Targets, 2006. **7**(11): p. 1513-29.
167. Opazo, C., X. Huang, R.A. Cherny, et al., *Metalloenzyme-like activity of Alzheimer's disease beta-amyloid. Cu-dependent catalytic conversion of dopamine, cholesterol, and biological reducing agents to neurotoxic H(2)O(2)*. J Biol Chem, 2002. **277**(43): p. 40302-8.
168. Smith, M.A., K. Hirai, K. Hsiao, et al., *Amyloid-beta deposition in Alzheimer transgenic mice is associated with oxidative stress*. J Neurochem, 1998. **70**(5): p. 2212-5.
169. Butterfield, D.A., A. Castegna, C.M. Lauderback, et al., *Evidence that amyloid beta-peptide-induced lipid peroxidation and its sequelae in Alzheimer's disease brain contribute to neuronal death*. Neurobiol Aging, 2002. **23**(5): p. 655-64.
170. Adolfsson, R., C.G. Gottfries, L. Oreland, et al., *Increased activity of brain and platelet monoamine oxidase in dementia of Alzheimer type*. Life Sci, 1980. **27**(12): p. 1029-34.
171. Parnetti, L., G.P. Reboldi, C. Santucci, et al., *Platelet MAO-B activity as a marker of behavioural characteristics in dementia disorders*. Aging (Milano), 1994. **6**(3): p. 201-7.
172. Reinikainen, K.J., L. Paljarvi, T. Halonen, et al., *Dopaminergic system and monoamine oxidase-B activity in Alzheimer's disease*. Neurobiol Aging, 1988. **9**(3): p. 245-52.
173. Emilsson, L., P. Saetre, J. Balciuniene, et al., *Increased monoamine oxidase messenger RNA expression levels in frontal cortex of Alzheimer's disease patients*. Neurosci Lett, 2002. **326**(1): p. 56-60.
174. Nakamura, S., T. Kawamata, I. Akiguchi, et al., *Expression of monoamine oxidase B activity in astrocytes of senile plaques*. Acta Neuropathol (Berl), 1990. **80**(4): p. 419-25.
175. Saura, J., J.M. Luque, A.M. Cesura, et al., *Increased monoamine oxidase B activity in plaque-associated astrocytes of Alzheimer brains revealed by quantitative enzyme radioautography*. Neuroscience, 1994. **62**(1): p. 15-30.
176. Kennedy, B.P., M.G. Ziegler, M. Alford, et al., *Early and persistent alterations in prefrontal cortex MAO A and B in Alzheimer's disease*. J Neural Transm, 2003. **110**(7): p. 789-801.
177. Sparks, D.L., V.M. Woeltz, and W.R. Markesbery, *Alterations in brain monoamine oxidase activity in aging, Alzheimer's disease, and Pick's disease*. Arch Neurol, 1991. **48**(7): p. 718-21.
178. Sherif, F., C.G. Gottfries, I. Alafuzoff, et al., *Brain gamma-aminobutyrate aminotransferase (GABA-T) and monoamine oxidase (MAO) in patients with Alzheimer's disease*. J Neural Transm Park Dis Dement Sect, 1992. **4**(3): p. 227-40.
179. Burke, W.J., S.W. Li, C.A. Schmitt, et al., *Accumulation of 3,4-dihydroxyphenylglycolaldehyde, the neurotoxic monoamine oxidase A metabolite of norepinephrine, in locus ceruleus cell bodies in Alzheimer's disease: mechanism of neuron death*. Brain Res, 1999. **816**(2): p. 633-7.

180. Gundlach, C., N.Z. Lu, and C.L. Bethea, *Ovarian steroid regulation of monoamine oxidase-A and -B mRNAs in the macaque dorsal raphe and hypothalamic nuclei*. Psychopharmacology (Berl), 2002. **160**(3): p. 271-82.
181. Holschneider, D.P., T. Kumazawa, K. Chen, et al., *Tissue-specific effects of estrogen on monoamine oxidase A and B in the rat*. Life Sci, 1998. **63**(3): p. 155-60.
182. Ou, X.M., K. Chen, and J.C. Shih, *Monoamine oxidase A and repressor R1 are involved in apoptotic signaling pathway*. Proc Natl Acad Sci U S A, 2006. **103**(29): p. 10923-8.
183. Fitzgerald, J.C., C. Ufer, and E.E. Billett, *A link between monoamine oxidase-A and apoptosis in serum deprived human SH-SY5Y neuroblastoma cells*. J Neural Transm, 2007. **114**(6): p. 807-10.
184. Bianchi, P., M.H. Seguelas, A. Parini, et al., *Activation of pro-apoptotic cascade by dopamine in renal epithelial cells is fully dependent on hydrogen peroxide generation by monoamine oxidases*. J Am Soc Nephrol, 2003. **14**(4): p. 855-62.
185. Yi, H., Y. Akao, W. Maruyama, et al., *Type A monoamine oxidase is the target of an endogenous dopaminergic neurotoxin, N-methyl(R)salsolinol, leading to apoptosis in SH-SY5Y cells*. J Neurochem, 2006. **96**(2): p. 541-9.
186. Takehashi, M., S. Tanaka, E. Masliah, et al., *Association of monoamine oxidase A gene polymorphism with Alzheimer's disease and Lewy body variant*. Neurosci Lett, 2002. **327**(2): p. 79-82.
187. Nishimura, A.L., C. Guindalini, J.R. Oliveira, et al., *Monoamine oxidase a polymorphism in Brazilian patients: risk factor for late-onset Alzheimer's disease?* J Mol Neurosci, 2005. **27**(2): p. 213-7.
188. Wei, Z., D.D. Mousseau, J.S. Richardson, et al., *Atypical antipsychotics attenuate neurotoxicity of beta-amyloid(25-35) by modulating Bax and Bcl-X(l/s) expression and localization*. J Neurosci Res, 2003. **74**(6): p. 942-7.
189. Chen, M.L. and C.H. Chen, *Chronic antipsychotics treatment regulates MAOA, MAOB and COMT gene expression in rat frontal cortex*. J Psychiatr Res, 2007. **41**(1-2): p. 57-62.
190. Ono, K., K. Hasegawa, H. Naiki, et al., *Anti-Parkinsonian agents have anti-amyloidogenic activity for Alzheimer's beta-amyloid fibrils in vitro*. Neurochem Int, 2006. **48**(4): p. 275-85.
191. de Lima, M.N., D.C. Laranja, F. Caldana, et al., *Reversal of age-related deficits in object recognition memory in rats with l-deprenyl*. Exp Gerontol, 2005. **40**(6): p. 506-11.
192. Thomas, T., *Monoamine oxidase-B inhibitors in the treatment of Alzheimer's disease*. Neurobiol Aging, 2000. **21**(2): p. 343-8.
193. Youdim, M.B., O. Bar Am, M. Yogev-Falach, et al., *Rasagiline: neurodegeneration, neuroprotection, and mitochondrial permeability transition*. J Neurosci Res, 2005. **79**(1-2): p. 172-9.
194. Gareri, P., G. Stilo, I. Bevacqua, et al., *Antidepressant drugs in the elderly*. Gen Pharmacol, 1998. **30**(4): p. 465-75.
195. Brini, M., *Ca(2+) signalling in mitochondria: mechanism and role in physiology and pathology*. Cell Calcium, 2003. **34**(4-5): p. 399-405.
196. Mattson, M.P., R.E. Rydel, I. Lieberburg, et al., *Altered calcium signaling and neuronal injury: stroke and Alzheimer's disease as examples*. Ann N Y Acad Sci, 1993. **679**: p. 1-21.

197. Gibbons, S.J., J.R. Brorson, D. Bleakman, et al., *Calcium influx and neurodegeneration*. Ann N Y Acad Sci, 1993. **679**: p. 22-33.
198. Solovyova, N. and A. Verkhratsky, *Monitoring of free calcium in the neuronal endoplasmic reticulum: an overview of modern approaches*. J Neurosci Methods, 2002. **122**(1): p. 1-12.
199. Meldolesi, J., *Rapidly exchanging Ca^{2+} stores in neurons: molecular, structural and functional properties*. Prog Neurobiol, 2001. **65**(3): p. 309-38.
200. Bernardi, P., *Mitochondrial transport of cations: channels, exchangers, and permeability transition*. Physiol Rev, 1999. **79**(4): p. 1127-55.
201. Kirichok, Y., G. Krapivinsky, and D.E. Clapham, *The mitochondrial calcium uniporter is a highly selective ion channel*. Nature, 2004. **427**(6972): p. 360-4.
202. Montero, M., M.T. Alonso, E. Carnicero, et al., *Chromaffin-cell stimulation triggers fast millimolar mitochondrial Ca^{2+} transients that modulate secretion*. Nat Cell Biol, 2000. **2**(2): p. 57-61.
203. Gunter, T.E., D.I. Yule, K.K. Gunter, et al., *Calcium and mitochondria*. FEBS Lett, 2004. **567**(1): p. 96-102.
204. Gunter, T.E. and D.R. Pfeiffer, *Mechanisms by which mitochondria transport calcium*. Am J Physiol, 1990. **258**(5 Pt 1): p. C755-86.
205. Kann, O. and R. Kovacs, *Mitochondria and neuronal activity*. Am J Physiol Cell Physiol, 2007. **292**(2): p. C641-57.
206. Albrecht, M.A., S.L. Colegrove, J. Hongpaisan, et al., *Multiple modes of calcium-induced calcium release in sympathetic neurons I: attenuation of endoplasmic reticulum Ca^{2+} accumulation at low $[Ca^{2+}]_i$ during weak depolarization*. J Gen Physiol, 2001. **118**(1): p. 83-100.
207. Petersen, O.H., A. Tepikin, and M.K. Park, *The endoplasmic reticulum: one continuous or several separate $Ca(2+)$ stores?* Trends Neurosci, 2001. **24**(5): p. 271-6.
208. Verkhratsky, A., *Endoplasmic reticulum calcium signaling in nerve cells*. Biol Res, 2004. **37**(4): p. 693-9.
209. Baysal, K., D.W. Jung, K.K. Gunter, et al., *Na^{+} -dependent Ca^{2+} efflux mechanism of heart mitochondria is not a passive $Ca^{2+}/2Na^{+}$ exchanger*. Am J Physiol, 1994. **266**(3 Pt 1): p. C800-8.
210. Jung, D.W., K. Baysal, and G.P. Brierley, *The sodium-calcium antiport of heart mitochondria is not electroneutral*. J Biol Chem, 1995. **270**(2): p. 672-8.
211. Gunter, K.K., M.J. Zuscik, and T.E. Gunter, *The Na^{+} -independent Ca^{2+} efflux mechanism of liver mitochondria is not a passive $Ca^{2+}/2H^{+}$ exchanger*. J Biol Chem, 1991. **266**(32): p. 21640-8.
212. Ichas, F., L.S. Jouaville, and J.P. Mazat, *Mitochondria are excitable organelles capable of generating and conveying electrical and calcium signals*. Cell, 1997. **89**(7): p. 1145-53.
213. Zoratti, M. and I. Szabo, *The mitochondrial permeability transition*. Biochim Biophys Acta, 1995. **1241**(2): p. 139-76.
214. Reynolds, I.J. and T.G. Hastings, *Glutamate induces the production of reactive oxygen species in cultured forebrain neurons following NMDA receptor activation*. J Neurosci, 1995. **15**(5 Pt 1): p. 3318-27.

215. Pan, Z., D. Damron, A.L. Nieminen, et al., *Depletion of intracellular Ca²⁺ by caffeine and ryanodine induces apoptosis of chinese hamster ovary cells transfected with ryanodine receptor*. J Biol Chem, 2000. **275**(26): p. 19978-84.
216. Berridge, M.J., M.D. Bootman, and P. Lipp, *Calcium--a life and death signal*. Nature, 1998. **395**(6703): p. 645-8.
217. Parekh, A.B. and J.W. Putney, Jr., *Store-operated calcium channels*. Physiol Rev, 2005. **85**(2): p. 757-810.
218. Petersen, O.H. and N.V. Fedirko, *Calcium signalling: store-operated channel found at last*. Curr Biol, 2001. **11**(13): p. R520-3.
219. He, H., M. Lam, T.S. McCormick, et al., *Maintenance of calcium homeostasis in the endoplasmic reticulum by Bcl-2*. J Cell Biol, 1997. **138**(6): p. 1219-28.
220. Murphy, A.N., D.E. Bredesen, G. Cortopassi, et al., *Bcl-2 potentiates the maximal calcium uptake capacity of neural cell mitochondria*. Proc Natl Acad Sci U S A, 1996. **93**(18): p. 9893-8.
221. Wang, H.G., N. Pathan, I.M. Ethell, et al., *Ca²⁺-induced apoptosis through calcineurin dephosphorylation of BAD*. Science, 1999. **284**(5412): p. 339-43.
222. Carragher, N.O., *Calpain inhibition: a therapeutic strategy targeting multiple disease states*. Curr Pharm Des, 2006. **12**(5): p. 615-38.
223. Wang, K.K., R. Posmantur, R. Nadimpalli, et al., *Caspase-mediated fragmentation of calpain inhibitor protein calpastatin during apoptosis*. Arch Biochem Biophys, 1998. **356**(2): p. 187-96.
224. Balaban, R.S., *Cardiac energy metabolism homeostasis: role of cytosolic calcium*. J Mol Cell Cardiol, 2002. **34**(10): p. 1259-71.
225. McCormack, J.G. and R.M. Denton, *Intracellular calcium ions and intramitochondrial Ca²⁺ in the regulation of energy metabolism in mammalian tissues*. Proc Nutr Soc, 1990. **49**(1): p. 57-75.
226. Kowaltowski, A.J., E.S. Naia-da-Silva, R.F. Castilho, et al., *Ca²⁺-stimulated mitochondrial reactive oxygen species generation and permeability transition are inhibited by dibucaine or Mg²⁺*. Arch Biochem Biophys, 1998. **359**(1): p. 77-81.
227. Li, Y., D.F. Boehning, T. Qian, et al., *Hepatitis C virus core protein increases mitochondrial ROS production by stimulation of Ca²⁺ uniporter activity*. Faseb J, 2007.
228. Votyakova, T.V. and I.J. Reynolds, *DeltaPsi(m)-Dependent and -independent production of reactive oxygen species by rat brain mitochondria*. J Neurochem, 2001. **79**(2): p. 266-77.
229. Starkov, A.A., G. Fiskum, C. Chinopoulos, et al., *Mitochondrial alpha-ketoglutarate dehydrogenase complex generates reactive oxygen species*. J Neurosci, 2004. **24**(36): p. 7779-88.
230. Kudin, A.P., N.Y. Bimpong-Buta, S. Vielhaber, et al., *Characterization of superoxide-producing sites in isolated brain mitochondria*. J Biol Chem, 2004. **279**(6): p. 4127-35.
231. Kowaltowski, A.J., L.E. Netto, and A.E. Vercesi, *The thiol-specific antioxidant enzyme prevents mitochondrial permeability transition. Evidence for the participation of reactive oxygen species in this mechanism*. J Biol Chem, 1998. **273**(21): p. 12766-9.
232. Boehning, D., R.L. Patterson, L. Sedaghat, et al., *Cytochrome c binds to inositol (1,4,5) trisphosphate receptors, amplifying calcium-dependent apoptosis*. Nat Cell Biol, 2003. **5**(12): p. 1051-61.

233. Mattson, M.P., *Neuronal life-and-death signaling, apoptosis, and neurodegenerative disorders*. Antioxid Redox Signal, 2006. **8**(11-12): p. 1997-2006.
234. Kawahara, M. and Y. Kuroda, *Molecular mechanism of neurodegeneration induced by Alzheimer's beta-amyloid protein: channel formation and disruption of calcium homeostasis*. Brain Res Bull, 2000. **53**(4): p. 389-97.
235. Leissring, M.A., Y. Akbari, C.M. Fanger, et al., *Capacitative calcium entry deficits and elevated luminal calcium content in mutant presenilin-1 knockin mice*. J Cell Biol, 2000. **149**(4): p. 793-8.
236. Yoo, A.S., I. Cheng, S. Chung, et al., *Presenilin-mediated modulation of capacitative calcium entry*. Neuron, 2000. **27**(3): p. 561-72.
237. Pinton, P., D. Ferrari, P. Magalhaes, et al., *Reduced loading of intracellular Ca^{2+} stores and downregulation of capacitative Ca^{2+} influx in Bcl-2-overexpressing cells*. J Cell Biol, 2000. **148**(5): p. 857-62.
238. Passer, B.J., L. Pellegrini, P. Vito, et al., *Interaction of Alzheimer's presenilin-1 and presenilin-2 with Bcl-X(L). A potential role in modulating the threshold of cell death*. J Biol Chem, 1999. **274**(34): p. 24007-13.
239. Bezprozvanny, I. and M.R. Hayden, *Deranged neuronal calcium signaling and Huntington disease*. Biochem Biophys Res Commun, 2004. **322**(4): p. 1310-7.
240. Bu, J., V. Sathyendra, N. Nagykerly, et al., *Age-related changes in calbindin-D28k, calretinin, and parvalbumin-immunoreactive neurons in the human cerebral cortex*. Exp Neurol, 2003. **182**(1): p. 220-31.
241. de Jong, G.I., P.A. Naber, E.A. Van der Zee, et al., *Age-related loss of calcium binding proteins in rabbit hippocampus*. Neurobiol Aging, 1996. **17**(3): p. 459-65.
242. Potier, B., P. Krzykowski, Y. Lamour, et al., *Loss of calbindin-immunoreactivity in CA1 hippocampal stratum radiatum and stratum lacunosum-moleculare interneurons in the aged rat*. Brain Res, 1994. **661**(1-2): p. 181-8.
243. Yamada, T., P.L. McGeer, K.G. Baimbridge, et al., *Relative sparing in Parkinson's disease of substantia nigra dopamine neurons containing calbindin-D28K*. Brain Res, 1990. **526**(2): p. 303-7.
244. Geula, C., N. Nagykerly, C.K. Wu, et al., *Loss of calbindin-D28K from aging human cholinergic basal forebrain: relation to plaques and tangles*. J Neuropathol Exp Neurol, 2003. **62**(6): p. 605-16.
245. Iritani, S., K. Niizato, and P.C. Emson, *Relationship of calbindin D28K-immunoreactive cells and neuropathological changes in the hippocampal formation of Alzheimer's disease*. Neuropathology, 2001. **21**(3): p. 162-7.
246. Heizmann, C.W. and K. Braun, *Changes in Ca^{2+} -binding proteins in human neurodegenerative disorders*. Trends Neurosci, 1992. **15**(7): p. 259-64.
247. Permyakov, E.A., V.N. Medvedkin, Y.V. Mitin, et al., *Noncovalent complex between domain AB and domains CD*EF of parvalbumin*. Biochim Biophys Acta, 1991. **1076**(1): p. 67-70.
248. Oberholtzer, J.C., C. Buettger, M.C. Summers, et al., *The 28-kDa calbindin-D is a major calcium-binding protein in the basilar papilla of the chick*. Proc Natl Acad Sci U S A, 1988. **85**(10): p. 3387-90.

249. Kojetin, D.J., R.A. Venters, D.R. Kordys, et al., *Structure, binding interface and hydrophobic transitions of Ca²⁺-loaded calbindin-D(28K)*. Nat Struct Mol Biol, 2006. **13**(7): p. 641-7.
250. Yenari, M.A., M. Minami, G.H. Sun, et al., *Calbindin d28k overexpression protects striatal neurons from transient focal cerebral ischemia*. Stroke, 2001. **32**(4): p. 1028-35.
251. Ichimiya, Y., P.C. Emson, C.Q. Mountjoy, et al., *Calbindin-immunoreactive cholinergic neurones in the nucleus basalis of Meynert in Alzheimer-type dementia*. Brain Res, 1989. **499**(2): p. 402-6.
252. Guo, Q., S. Christakos, N. Robinson, et al., *Calbindin D28k blocks the proapoptotic actions of mutant presenilin 1: reduced oxidative stress and preserved mitochondrial function*. Proc Natl Acad Sci U S A, 1998. **95**(6): p. 3227-32.
253. McMahan, A., B.S. Wong, A.M. Iacopino, et al., *Calbindin-D28k buffers intracellular calcium and promotes resistance to degeneration in PC12 cells*. Brain Res Mol Brain Res, 1998. **54**(1): p. 56-63.
254. Kumar, S., P.C. McDonnell, R.J. Gum, et al., *Novel homologues of CSBP/p38 MAP kinase: activation, substrate specificity and sensitivity to inhibition by pyridinyl imidazoles*. Biochem Biophys Res Commun, 1997. **235**(3): p. 533-8.
255. Zarubin, T. and J. Han, *Activation and signaling of the p38 MAP kinase pathway*. Cell Res, 2005. **15**(1): p. 11-8.
256. Derijard, B., J. Raingeaud, T. Barrett, et al., *Independent human MAP-kinase signal transduction pathways defined by MEK and MKK isoforms*. Science, 1995. **267**(5198): p. 682-5.
257. Tibbles, L.A. and J.R. Woodgett, *The stress-activated protein kinase pathways*. Cell Mol Life Sci, 1999. **55**(10): p. 1230-54.
258. Han, J., J.D. Lee, L. Bibbs, et al., *A MAP kinase targeted by endotoxin and hyperosmolarity in mammalian cells*. Science, 1994. **265**(5173): p. 808-11.
259. Jiang, Y., C. Chen, Z. Li, et al., *Characterization of the structure and function of a new mitogen-activated protein kinase (p38beta)*. J Biol Chem, 1996. **271**(30): p. 17920-6.
260. Li, Z., Y. Jiang, R.J. Ulevitch, et al., *The primary structure of p38 gamma: a new member of p38 group of MAP kinases*. Biochem Biophys Res Commun, 1996. **228**(2): p. 334-40.
261. Wang, X.S., K. Diener, C.L. Manthey, et al., *Molecular cloning and characterization of a novel p38 mitogen-activated protein kinase*. J Biol Chem, 1997. **272**(38): p. 23668-74.
262. Jiang, Y., H. Gram, M. Zhao, et al., *Characterization of the structure and function of the fourth member of p38 group mitogen-activated protein kinases, p38delta*. J Biol Chem, 1997. **272**(48): p. 30122-8.
263. Meier, R., J. Rouse, A. Cuenda, et al., *Cellular stresses and cytokines activate multiple mitogen-activated-protein kinase kinase homologues in PC12 and KB cells*. Eur J Biochem, 1996. **236**(3): p. 796-805.
264. Enslin, H., D.M. Brancho, and R.J. Davis, *Molecular determinants that mediate selective activation of p38 MAP kinase isoforms*. Embo J, 2000. **19**(6): p. 1301-11.
265. Young, P.R., M.M. McLaughlin, S. Kumar, et al., *Pyridinyl imidazole inhibitors of p38 mitogen-activated protein kinase bind in the ATP site*. J Biol Chem, 1997. **272**(18): p. 12116-21.

266. Raugeaud, J., S. Gupta, J.S. Rogers, et al., *Pro-inflammatory cytokines and environmental stress cause p38 mitogen-activated protein kinase activation by dual phosphorylation on tyrosine and threonine*. J Biol Chem, 1995. **270**(13): p. 7420-6.
267. Ben-Levy, R., S. Hooper, R. Wilson, et al., *Nuclear export of the stress-activated protein kinase p38 mediated by its substrate MAPKAP kinase-2*. Curr Biol, 1998. **8**(19): p. 1049-57.
268. Roux, P.P. and J. Blenis, *ERK and p38 MAPK-activated protein kinases: a family of protein kinases with diverse biological functions*. Microbiol Mol Biol Rev, 2004. **68**(2): p. 320-44.
269. Takeda, K. and H. Ichijo, *Neuronal p38 MAPK signalling: an emerging regulator of cell fate and function in the nervous system*. Genes Cells, 2002. **7**(11): p. 1099-111.
270. Wynne, P., *p38 mitogen-activated protein kinase: a novel modulator of hyperpolarization-activated cyclic nucleotide-gated channels and neuronal excitability*. J Neurosci, 2006. **26**(44): p. 11253-4.
271. Thomas, G., J. Haavik, and P. Cohen, *Participation of a stress-activated protein kinase cascade in the activation of tyrosine hydroxylase in chromaffin cells*. Eur J Biochem, 1997. **247**(3): p. 1180-9.
272. Tan, Y., J. Rouse, A. Zhang, et al., *FGF and stress regulate CREB and ATF-1 via a pathway involving p38 MAP kinase and MAPKAP kinase-2*. Embo J, 1996. **15**(17): p. 4629-42.
273. Greene, L.A. and A.S. Tischler, *Establishment of a noradrenergic clonal line of rat adrenal pheochromocytoma cells which respond to nerve growth factor*. Proc Natl Acad Sci U S A, 1976. **73**(7): p. 2424-8.
274. Pang, L., T. Sawada, S.J. Decker, et al., *Inhibition of MAP kinase kinase blocks the differentiation of PC-12 cells induced by nerve growth factor*. J Biol Chem, 1995. **270**(23): p. 13585-8.
275. Fukuda, M., Y. Gotoh, T. Tachibana, et al., *Induction of neurite outgrowth by MAP kinase in PC12 cells*. Oncogene, 1995. **11**(2): p. 239-44.
276. Morooka, T. and E. Nishida, *Requirement of p38 mitogen-activated protein kinase for neuronal differentiation in PC12 cells*. J Biol Chem, 1998. **273**(38): p. 24285-8.
277. Mayr, B. and M. Montminy, *Transcriptional regulation by the phosphorylation-dependent factor CREB*. Nat Rev Mol Cell Biol, 2001. **2**(8): p. 599-609.
278. Xing, J., J.M. Kornhauser, Z. Xia, et al., *Nerve growth factor activates extracellular signal-regulated kinase and p38 mitogen-activated protein kinase pathways to stimulate CREB serine 133 phosphorylation*. Mol Cell Biol, 1998. **18**(4): p. 1946-55.
279. Paralkar, V.M., B.S. Weeks, Y.M. Yu, et al., *Recombinant human bone morphogenetic protein 2B stimulates PC12 cell differentiation: potentiation and binding to type IV collagen*. J Cell Biol, 1992. **119**(6): p. 1721-8.
280. Iwasaki, S., A. Hattori, M. Sato, et al., *Characterization of the bone morphogenetic protein-2 as a neurotrophic factor. Induction of neuronal differentiation of PC12 cells in the absence of mitogen-activated protein kinase activation*. J Biol Chem, 1996. **271**(29): p. 17360-5.
281. Hansen, T.O., J.F. Rehfeld, and F.C. Nielsen, *Cyclic AMP-induced neuronal differentiation via activation of p38 mitogen-activated protein kinase*. J Neurochem, 2000. **75**(5): p. 1870-7.
282. Choi, W.S., S.Y. Chun, G.J. Markelonis, et al., *Overexpression of calbindin-D28K induces neurite outgrowth in dopaminergic neuronal cells via activation of p38 MAPK*. Biochem Biophys Res Commun, 2001. **287**(3): p. 656-61.

283. Xia, Z., M. Dickens, J. Raingeaud, et al., *Opposing effects of ERK and JNK-p38 MAP kinases on apoptosis*. Science, 1995. **270**(5240): p. 1326-31.
284. Assefa, Z., A. Vantieghem, M. Garmyn, et al., *p38 mitogen-activated protein kinase regulates a novel, caspase-independent pathway for the mitochondrial cytochrome c release in ultraviolet B radiation-induced apoptosis*. J Biol Chem, 2000. **275**(28): p. 21416-21.
285. Gomez-Lazaro, M., M.F. Galindo, R.M. Melero-Fernandez de Mera, et al., *Reactive oxygen species and p38 mitogen-activated protein kinase activate Bax to induce mitochondrial cytochrome c release and apoptosis in response to malonate*. Mol Pharmacol, 2007. **71**(3): p. 736-43.
286. Xu, Z., B.R. Wang, X. Wang, et al., *ERK1/2 and p38 mitogen-activated protein kinase mediate iNOS-induced spinal neuron degeneration after acute traumatic spinal cord injury*. Life Sci, 2006. **79**(20): p. 1895-905.
287. Segura Torres, J.E., V. Chaparro-Huerta, M.C. Rivera Cervantres, et al., *Neuronal cell death due to glutamate excitotoxicity is mediated by p38 activation in the rat cerebral cortex*. Neurosci Lett, 2006. **403**(3): p. 233-8.
288. Chen, K. and M.D. Maines, *Nitric oxide induces heme oxygenase-1 via mitogen-activated protein kinases ERK and p38*. Cell Mol Biol, 2000. **46**(3): p. 609-17.
289. Frigo, D.E., A. Basu, E.N. Nierth-Simpson, et al., *p38 mitogen-activated protein kinase stimulates estrogen-mediated transcription and proliferation through the phosphorylation and potentiation of the p160 coactivator glucocorticoid receptor-interacting protein 1*. Mol Endocrinol, 2006. **20**(5): p. 971-83.
290. Hisaoka, K., M. Takebayashi, M. Tsuchioka, et al., *Antidepressants increase glial cell line-derived neurotrophic factor production through monoamine-independent activation of protein tyrosine kinase and extracellular signal-regulated kinase in glial cells*. J Pharmacol Exp Ther, 2007. **321**(1): p. 148-57.
291. Zechner, D., R. Craig, D.S. Hanford, et al., *MKK6 activates myocardial cell NF-kappaB and inhibits apoptosis in a p38 mitogen-activated protein kinase-dependent manner*. J Biol Chem, 1998. **273**(14): p. 8232-9.
292. Assefa, Z., A. Vantieghem, W. Declercq, et al., *The activation of the c-Jun N-terminal kinase and p38 mitogen-activated protein kinase signaling pathways protects HeLa cells from apoptosis following photodynamic therapy with hypericin*. J Biol Chem, 1999. **274**(13): p. 8788-96.
293. Roulston, A., C. Reinhard, P. Amiri, et al., *Early activation of c-Jun N-terminal kinase and p38 kinase regulate cell survival in response to tumor necrosis factor alpha*. J Biol Chem, 1998. **273**(17): p. 10232-9.
294. Nagata, Y. and K. Todokoro, *Requirement of activation of JNK and p38 for environmental stress-induced erythroid differentiation and apoptosis and of inhibition of ERK for apoptosis*. Blood, 1999. **94**(3): p. 853-63.
295. Matsuzawa, A. and H. Ichijo, *Molecular mechanisms of the decision between life and death: regulation of apoptosis by apoptosis signal-regulating kinase 1*. J Biochem (Tokyo), 2001. **130**(1): p. 1-8.

296. Takeda, K., T. Hatai, T.S. Hamazaki, et al., *Apoptosis signal-regulating kinase 1 (ASK1) induces neuronal differentiation and survival of PC12 cells*. J Biol Chem, 2000. **275**(13): p. 9805-13.
297. Tobiume, K., A. Matsuzawa, T. Takahashi, et al., *ASK1 is required for sustained activations of JNK/p38 MAP kinases and apoptosis*. EMBO Rep, 2001. **2**(3): p. 222-8.
298. Thakur, A., X. Wang, S.L. Siedlak, et al., *c-Jun phosphorylation in Alzheimer disease*. J Neurosci Res, 2007. **85**(8): p. 1668-73.
299. Sun, A., M. Liu, X.V. Nguyen, et al., *P38 MAP kinase is activated at early stages in Alzheimer's disease brain*. Exp Neurol, 2003. **183**(2): p. 394-405.
300. Bradham, C. and D.R. McClay, *p38 MAPK in development and cancer*. Cell Cycle, 2006. **5**(8): p. 824-8.
301. Rao, V.L., *Nitric oxide in hepatic encephalopathy and hyperammonemia*. Neurochem Int, 2002. **41**(2-3): p. 161-70.
302. Mousseau, D.D., G.B. Baker, and R.F. Butterworth, *Increased density of catalytic sites and expression of brain monoamine oxidase A in humans with hepatic encephalopathy*. J Neurochem, 1997. **68**(3): p. 1200-8.
303. Kosenko, E.A., N.I. Venediktova, and G. Kaminskii Iu, *[Calcium and ammonia stimulate monoamine oxidase A activity in brain mitochondria]*. Izv Akad Nauk Ser Biol, 2003(5): p. 542-6.
304. Egashira, T., K. Sakai, M. Sakurai, et al., *Calcium disodium edetate enhances type A monoamine oxidase activity in monkey brain*. Biol Trace Elem Res, 2003. **94**(3): p. 203-11.
305. Samantaray, S., G. Chandra, and K.P. Mohanakumar, *Calcium channel agonist, (+/-)-Bay K8644, causes a transient increase in striatal monoamine oxidase activity in Balb/c mice*. Neurosci Lett, 2003. **342**(1-2): p. 73-6.
306. Kabuto, H., I. Yokoi, A. Mori, et al., *Neurochemical changes related to ageing in the senescence-accelerated mouse brain and the effect of chronic administration of nimodipine*. Mech Ageing Dev, 1995. **80**(1): p. 1-9.
307. Handschuh, G., B. Lubber, P. Hutzler, et al., *Single amino acid substitutions in conserved extracellular domains of E-cadherin differ in their functional consequences*. J Mol Biol, 2001. **314**(3): p. 445-54.
308. Ozawa, M., J. Engel, and R. Kemler, *Single amino acid substitutions in one Ca²⁺ binding site of uvomorulin abolish the adhesive function*. Cell, 1990. **63**(5): p. 1033-8.
309. Reid, R.E., *A synthetic 33-residue analogue of bovine brain calmodulin calcium binding site III: synthesis, purification, and calcium binding*. Biochemistry, 1987. **26**(19): p. 6070-3.
310. Ou, X.M., K. Chen, and J.C. Shih, *Glucocorticoid and androgen activation of monoamine oxidase A is regulated differently by R1 and Sp1*. J Biol Chem, 2006. **281**(30): p. 21512-25.
311. De Zutter, G.S. and R.J. Davis, *Pro-apoptotic gene expression mediated by the p38 mitogen-activated protein kinase signal transduction pathway*. Proc Natl Acad Sci U S A, 2001. **98**(11): p. 6168-73.
312. Bulavin, D.V., Y. Higashimoto, I.J. Popoff, et al., *Initiation of a G2/M checkpoint after ultraviolet radiation requires p38 kinase*. Nature, 2001. **411**(6833): p. 102-7.
313. Thakran, P., M.P. Leuschen, and M. Ebadi, *Metallothionein induction in rat hippocampal neurons in primary culture*. In Vivo, 1989. **3**(3): p. 191-7.

314. Holt, A. and G.B. Baker, *Inhibition of rat brain monoamine oxidase enzymes by fluoxetine and norfluoxetine*. Naunyn Schmiedeberg's Arch Pharmacol, 1996. **354**(1): p. 17-24.
315. Cole, L.J., M.C. Fishler, and V.P. Bond, *Subcellular fractionation of mouse spleen radiation protection activity*. Proc Natl Acad Sci U S A, 1953. **39**(8): p. 759-72.
316. Keston, A.S. and R. Brandt, *The fluorometric analysis of ultramicro quantities of hydrogen peroxide*. Anal Biochem, 1965. **11**: p. 1-5.
317. Qing, H., H. Xu, Z. Wei, et al., *The ability of atypical antipsychotic drugs vs. haloperidol to protect PC12 cells against MPP⁺-induced apoptosis*. Eur J Neurosci, 2003. **17**(8): p. 1563-70.
318. Faust, D., I. Dolado, A. Cuadrado, et al., *p38alpha MAPK is required for contact inhibition*. Oncogene, 2005. **24**(53): p. 7941-5.
319. Kumar, S., M.S. Jiang, J.L. Adams, et al., *Pyridinylimidazole compound SB 203580 inhibits the activity but not the activation of p38 mitogen-activated protein kinase*. Biochem Biophys Res Commun, 1999. **263**(3): p. 825-31.
320. Hall-Jackson, C.A., M. Goedert, P. Hedge, et al., *Effect of SB 203580 on the activity of c-Raf in vitro and in vivo*. Oncogene, 1999. **18**(12): p. 2047-54.
321. Park, J.S., S.H. Jung, H. Seo, et al., *SB203580 enhances interleukin-1 receptor antagonist gene expression in IFN-gamma-stimulated BV2 microglial cells through a composite nuclear factor-kappaB/PU.1 binding site*. Neurosci Lett, 2007. **416**(2): p. 169-74.
322. ter Haar, E., P. Prabhakar, X. Liu, et al., *Crystal structure of the p38 alpha-MAPKAP kinase 2 heterodimer*. J Biol Chem, 2007. **282**(13): p. 9733-9.
323. Rizzuto, R. and T. Pozzan, *Microdomains of intracellular Ca²⁺: molecular determinants and functional consequences*. Physiol Rev, 2006. **86**(1): p. 369-408.
324. Robb-Gaspers, L.D., G.A. Rutter, P. Burnett, et al., *Coupling between cytosolic and mitochondrial calcium oscillations: role in the regulation of hepatic metabolism*. Biochim Biophys Acta, 1998. **1366**(1-2): p. 17-32.
325. White, R.J. and I.J. Reynolds, *Mitochondria accumulate Ca²⁺ following intense glutamate stimulation of cultured rat forebrain neurones*. J Physiol, 1997. **498** (Pt 1): p. 31-47.
326. Herrington, J., Y.B. Park, D.F. Babcock, et al., *Dominant role of mitochondria in clearance of large Ca²⁺ loads from rat adrenal chromaffin cells*. Neuron, 1996. **16**(1): p. 219-28.
327. Xu, T., M. Naraghi, H. Kang, et al., *Kinetic studies of Ca²⁺ binding and Ca²⁺ clearance in the cytosol of adrenal chromaffin cells*. Biophys J, 1997. **73**(1): p. 532-45.
328. Duchen, M.R., *Contributions of mitochondria to animal physiology: from homeostatic sensor to calcium signalling and cell death*. J Physiol, 1999. **516** (Pt 1): p. 1-17.
329. Meyer, J.H., N. Ginovart, A. Boovariwala, et al., *Elevated monoamine oxidase a levels in the brain: an explanation for the monoamine imbalance of major depression*. Arch Gen Psychiatry, 2006. **63**(11): p. 1209-16.
330. Zatta, P., V. Nicosia, and P. Zambenedetti, *Evaluation of MAO activities on murine neuroblastoma cells upon acute or chronic treatment with aluminium (III) or tacrine*. Neurochem Int, 1998. **32**(3): p. 273-9.
331. Zatta, P., P. Zambenedetti, and M. Milanese, *Activation of monoamine oxidase type-B by aluminum in rat brain homogenate*. Neuroreport, 1999. **10**(17): p. 3645-8.

332. Gandolfi, L., M.P. Stella, P. Zambenedetti, et al., *Aluminum alters intracellular calcium homeostasis in vitro*. *Biochim Biophys Acta*, 1998. **1406**(3): p. 315-20.
333. Garruto, R.M., C. Swyt, C.E. Fiori, et al., *Intraneuronal deposition of calcium and aluminium in amyotrophic lateral sclerosis of Guam*. *Lancet*, 1985. **2**(8468): p. 1353.
334. Fleckenstein-Grun, G., S. Matyas, and L. Dumont, *Voltage dependence of the pharmacological Mg²⁺ block of the Ca²⁺ entry into vascular smooth muscle cells*. *Magnes Res*, 1997. **10**(2): p. 101-6.
335. Eby, G.A. and K.L. Eby, *Rapid recovery from major depression using magnesium treatment*. *Med Hypotheses*, 2006. **67**(2): p. 362-70.
336. Traboulsie, A., J. Chemin, E. Kupfer, et al., *T-type calcium channels are inhibited by fluoxetine and its metabolite norfluoxetine*. *Mol Pharmacol*, 2006. **69**(6): p. 1963-8.
337. Deak, F., B. Lasztocki, P. Pacher, et al., *Inhibition of voltage-gated calcium channels by fluoxetine in rat hippocampal pyramidal cells*. *Neuropharmacology*, 2000. **39**(6): p. 1029-36.
338. Obradovic, D., H. Gronemeyer, B. Lutz, et al., *Cross-talk of vitamin D and glucocorticoids in hippocampal cells*. *J Neurochem*, 2006. **96**(2): p. 500-9.
339. Baciewicz, A.M. and T.H. Self, *Isoniazid interactions*. *South Med J*, 1985. **78**(6): p. 714-8.
340. Iacopino, A.M. and S. Christakos, *Specific reduction of calcium-binding protein (28-kilodalton calbindin-D) gene expression in aging and neurodegenerative diseases*. *Proc Natl Acad Sci U S A*, 1990. **87**(11): p. 4078-82.
341. Bellido, T., M. Huening, M. Raval-Pandya, et al., *Calbindin-D28k is expressed in osteoblastic cells and suppresses their apoptosis by inhibiting caspase-3 activity*. *J Biol Chem*, 2000. **275**(34): p. 26328-32.
342. Jones, T.Z., L. Giurato, S. Guccione, et al., *Interactions of imidazoline ligands with the active site of purified monoamine oxidase A*. *Febs J*, 2007. **274**(6): p. 1567-75.
343. Holt, A., B. Wieland, and G.B. Baker, *Allosteric modulation of semicarbazide-sensitive amine oxidase activities in vitro by imidazoline receptor ligands*. *Br J Pharmacol*, 2004. **143**(4): p. 495-507.
344. Blanc, A., N.R. Pandey, and A.K. Srivastava, *Synchronous activation of ERK 1/2, p38mapk and PKB/Akt signaling by H2O2 in vascular smooth muscle cells: potential involvement in vascular disease (review)*. *Int J Mol Med*, 2003. **11**(2): p. 229-34.
345. Blanc, A., N.R. Pandey, and A.K. Srivastava, *Distinct roles of Ca²⁺, calmodulin, and protein kinase C in H2O2-induced activation of ERK1/2, p38 MAPK, and protein kinase B signaling in vascular smooth muscle cells*. *Antioxid Redox Signal*, 2004. **6**(2): p. 353-66.
346. Mukherjee, J. and Z.Y. Yang, *Monoamine oxidase A inhibition by fluoxetine: an in vitro and in vivo study*. *Synapse*, 1999. **31**(4): p. 285-9.
347. Ha, E., K.H. Jung, B.K. Choe, et al., *Fluoxetine increases the nitric oxide production via nuclear factor kappa B-mediated pathway in BV2 murine microglial cells*. *Neurosci Lett*, 2006. **397**(3): p. 185-9.
348. Cloez-Tayarani, I., U.S. Kayyali, B.L. Fanburg, et al., *5-HT activates ERK MAP kinase in cultured-human peripheral blood mononuclear cells via 5-HT1A receptors*. *Life Sci*, 2004. **76**(4): p. 429-43.

349. Manoli, I., H. Le, S. Alesci, et al., *Monoamine oxidase-A is a major target gene for glucocorticoids in human skeletal muscle cells*. *Faseb J*, 2005. **19**(10): p. 1359-61.
350. Bianchi, P., O. Kunduzova, E. Masini, et al., *Oxidative stress by monoamine oxidase mediates receptor-independent cardiomyocyte apoptosis by serotonin and postischemic myocardial injury*. *Circulation*, 2005. **112**(21): p. 3297-305.
351. Wu, X.J., Y.J. Zheng, Y.Y. Cui, et al., *Propofol attenuates oxidative stress-induced PC12 cell injury via p38 MAP kinase dependent pathway*. *Acta Pharmacol Sin*, 2007. **28**(8): p. 1123-8.
352. Blunt, B.C., A.T. Creek, D.C. Henderson, et al., *H₂O₂ activation of HSP25/27 protects desmin from calpain proteolysis in rat ventricular myocytes*. *Am J Physiol Heart Circ Physiol*, 2007. **293**(3): p. H1518-25.
353. Hubalek, F., C. Binda, A. Khalil, et al., *Demonstration of isoleucine 199 as a structural determinant for the selective inhibition of human monoamine oxidase B by specific reversible inhibitors*. *J Biol Chem*, 2005. **280**(16): p. 15761-6.
354. Zheng, Y. and X. Shen, *H₂O₂ directly activates inositol 1,4,5-trisphosphate receptors in endothelial cells*. *Redox Rep*, 2005. **10**(1): p. 29-36.
355. Stone, J.R. and T. Collins, *The role of hydrogen peroxide in endothelial proliferative responses*. *Endothelium*, 2002. **9**(4): p. 231-8.
356. Resende, R., C. Pereira, P. Agostinho, et al., *Susceptibility of hippocampal neurons to Abeta peptide toxicity is associated with perturbation of Ca²⁺ homeostasis*. *Brain Res*, 2007. **1143**: p. 11-21.
357. Rui, Y., R. Li, Y. Liu, et al., *Acute effect of beta amyloid on synchronized spontaneous Ca²⁺ oscillations in cultured hippocampal networks*. *Cell Biol Int*, 2006. **30**(9): p. 733-40.
358. Simakova, O. and N.J. Arispe, *Early and late cytotoxic effects of external application of the Alzheimer's Abeta result from the initial formation and function of Abeta ion channels*. *Biochemistry*, 2006. **45**(18): p. 5907-15.
359. Stefani, M. and C.M. Dobson, *Protein aggregation and aggregate toxicity: new insights into protein folding, misfolding diseases and biological evolution*. *J Mol Med*, 2003. **81**(11): p. 678-99.
360. Wernyj, R.P., M.P. Mattson, and S. Christakos, *Expression of calbindin-D28k in C6 glial cells stabilizes intracellular calcium levels and protects against apoptosis induced by calcium ionophore and amyloid beta-peptide*. *Brain Res Mol Brain Res*, 1999. **64**(1): p. 69-79.
361. Mattson, M.P., B. Rychlik, C. Chu, et al., *Evidence for calcium-reducing and excito-protective roles for the calcium-binding protein calbindin-D28k in cultured hippocampal neurons*. *Neuron*, 1991. **6**(1): p. 41-51.
362. Phillips, R.G., T.J. Meier, L.C. Giuli, et al., *Calbindin D28K gene transfer via herpes simplex virus amplicon vector decreases hippocampal damage in vivo following neurotoxic insults*. *J Neurochem*, 1999. **73**(3): p. 1200-5.
363. Brorson, J.R., V.P. Bindokas, T. Iwama, et al., *The Ca²⁺ influx induced by beta-amyloid peptide 25-35 in cultured hippocampal neurons results from network excitation*. *J Neurobiol*, 1995. **26**(3): p. 325-38.

364. Quevedo, J., M. Vianna, D. Daroit, et al., *L-type voltage-dependent calcium channel blocker nifedipine enhances memory retention when infused into the hippocampus*. *Neurobiol Learn Mem*, 1998. **69**(3): p. 320-5.
365. Heidrich, A., M. Rosler, and P. Riederer, [*Pharmacotherapy of Alzheimer dementia: therapy of cognitive symptoms--new results of clinical studies*]. *Fortschr Neurol Psychiatr*, 1997. **65**(3): p. 108-21.
366. Yamada, M., Y. Itoh, N. Suematsu, et al., *Apolipoprotein E genotype in elderly nondemented subjects without senile changes in the brain*. *Ann Neurol*, 1996. **40**(2): p. 243-5.
367. Yew, D.T. and W.Y. Chan, *Early appearance of acetylcholinergic, serotonergic, and peptidergic neurons and fibers in the developing human central nervous system*. *Microsc Res Tech*, 1999. **45**(6): p. 389-400.
368. Smith, I.F., K.N. Green, and F.M. LaFerla, *Calcium dysregulation in Alzheimer's disease: recent advances gained from genetically modified animals*. *Cell Calcium*, 2005. **38**(3-4): p. 427-37.
369. Supnet, C., J. Grant, H. Kong, et al., *Amyloid-beta-(1-42) increases ryanodine receptor-3 expression and function in neurons of TgCRND8 mice*. *J Biol Chem*, 2006. **281**(50): p. 38440-7.
370. Burke, W.J., S.W. Li, H.D. Chung, et al., *Neurotoxicity of MAO metabolites of catecholamine neurotransmitters: role in neurodegenerative diseases*. *Neurotoxicology*, 2004. **25**(1-2): p. 101-15.
371. Liu, Y. and D. Piasecki, *A cell-based method for the detection of nanomolar concentrations of bioactive amyloid*. *Anal Biochem*, 2001. **289**(2): p. 130-6.
372. Zhuang, Z.P., B. Marks, and R.B. McCauley, *The insertion of monoamine oxidase A into the outer membrane of rat liver mitochondria*. *J Biol Chem*, 1992. **267**(1): p. 591-6.
373. Zhuang, Z., M. Hogan, and R. McCauley, *The in vitro insertion of monoamine oxidase B into mitochondrial outer membranes*. *FEBS Lett*, 1988. **238**(1): p. 185-90.
374. Yonezawa, D., F. Sekiguchi, M. Miyamoto, et al., *A protective role of hydrogen sulfide against oxidative stress in rat gastric mucosal epithelium*. *Toxicology*, 2007. **241**(1-2): p. 11-8.
375. Vintem, A.P., N.T. Price, R.B. Silverman, et al., *Mutation of surface cysteine 374 to alanine in monoamine oxidase A alters substrate turnover and inactivation by cyclopropylamines*. *Bioorg Med Chem*, 2005. **13**(10): p. 3487-95.
376. Hiro, I., Y. Tsugeno, I. Hirashiki, et al., *Characterization of rat monoamine oxidase A with noncovalently-bound FAD expressed in yeast cells*. *J Biochem (Tokyo)*, 1996. **120**(4): p. 759-65.
377. Li, M., C. Binda, A. Mattevi, et al., *Functional role of the "aromatic cage" in human monoamine oxidase B: structures and catalytic properties of Tyr435 mutant proteins*. *Biochemistry*, 2006. **45**(15): p. 4775-84.
378. Nandigama, R.K., J.R. Miller, and D.E. Edmondson, *Loss of serotonin oxidation as a component of the altered substrate specificity in the Y444F mutant of recombinant human liver MAO A*. *Biochemistry*, 2001. **40**(49): p. 14839-46.
379. Lewis, D.A., K.N. Dalby, and C.W. Abell, *Conserved elements of the cytochrome P-450 superfamily found in monoamine oxidase B*. *Neurotoxicology*, 2004. **25**(1-2): p. 73-8.

Appendix I: Permission to reproduce published figures

The American Physiological Society
9650 Rockville Pike, Bethesda, MD 20814-3991, USA
Phone: (301) 634-7070
Fax: (301) 634-7243

November 12, 2007

Ms. Susan Xia Cao
University of Saskatchewan
Neuropsychiatry Research Unit
103 Wiggins Road
Saskatoon, SK, Canada
S7N 5E4

Dear Ms. Cao

The American Physiological Society grants you permission to use figure one from the following Cell Physiology article for your dissertation: Oliver Kann and Richard Kovács

Mitochondria and neuronal activity

Am J Physiol Cell Physiol 292: C641-C657, 2007. First published November 8, 2006;
doi:10.1152/ajpcell.00222.2006

The University of Saskatchewan is granted permission to make a copy of the dissertation electronically available on its web site.

The American Physiological Society publication must be credited as the source with the words “used with permission” added.

Sincerely,

Ms. Margaret Reich
Director of Publications
The American Physiological Society

**NATURE PUBLISHING GROUP LICENSE
TERMS AND CONDITIONS**

Nov 20, 2007

This is a License Agreement between Xia Cao ("You") and Nature Publishing Group ("Nature Publishing Group"). The license consists of your order details, the terms and conditions provided by Nature Publishing Group, and the payment terms and conditions.

License Number	1833181311344
License date	Nov 20, 2007
Licensed content publisher	Nature Publishing Group
Licensed content publication	Nature
Licensed content title	Calcium - a life and death signal
Licensed content author	Michael J. Berridge, Martin D. Bootman, Peter Lipp
Volume number	395
Issue number	6703
Pages	645-648
Year of publication	1998
Portion used	Figures / tables
Requestor type	Student
Type of Use	Thesis / Dissertation
PO Number	
Total	\$0.00
Terms and Conditions	

Terms and Conditions for Permissions

Nature Publishing Group hereby grants you a non-exclusive license to reproduce this material for this purpose, and for no other use, subject to the conditions

below:

1. NPG warrants that it has, to the best of its knowledge, the rights to license reuse of this material. However, you should ensure that the material you are requesting is original to Nature Publishing Group and does not carry the copyright of another entity (as credited in the published version). If the credit line on any part of the material you have requested indicates that it was reprinted or adapted by NPG with permission from another source, then you should also seek permission from that source to reuse the material.
2. Permission granted free of charge for material in print is also usually granted for any electronic version of that work, provided that the material is incidental to the work as a whole and that the electronic version is essentially equivalent to, or substitutes for, the print version. Where print permission has been granted for a fee, separate permission must be obtained for any additional, electronic re-use (unless, as in the case of a full paper, this has already been accounted for during your initial request in the calculation of a print run). NB: In all cases, web-based use of full-text articles must be authorized separately through the 'Use on a Web Site' option when requesting permission.
3. Permission granted for a first edition does not apply to second and subsequent editions and for editions in other languages (except for signatories to the STM Permissions Guidelines, or where the first edition permission was granted for free).
4. Nature Publishing Group's permission must be acknowledged next to the figure, table or abstract in print. In electronic form, this acknowledgement must be visible at the same time as the figure/table/abstract, and must be hyperlinked to the journal's homepage.
5. The credit line should read:

Reprinted by permission from Macmillan Publishers Ltd: [JOURNAL NAME]
(reference citation), copyright (year of publication)

For AOP papers, the credit line should read:

Reprinted by permission from Macmillan Publishers Ltd: [JOURNAL NAME],

advance online publication, day month year (doi: 10.1038/sj. [JOURNAL ACRONYM]. XXXXX)

6. Adaptations of single figures do not require NPG approval. However, the adaptation should be credited as follows:

Adapted by permission from Macmillan Publishers Ltd: [JOURNAL NAME] (reference citation), copyright (year of publication)

7. Translations of 401 words up to a whole article require NPG approval. Please visit <http://www.macmillanmedicalcommunications.com> for more information. Translations of up to a 400 words do not require NPG approval. The translation should be credited as follows:

Translated by permission from Macmillan Publishers Ltd: [JOURNAL NAME] (reference citation), copyright (year of publication).

We are certain that all parties will benefit from this agreement and wish you the best in the use of this material. Thank you.

v1.1

APPENDIX II: ETHICS APPROVAL

Memorandum

TO: Dr. Mousseau, Psychiatry - Neuropsychiatric Research Unit

FROM: UCACS Protocol Review Committee, Animal Resources Centre

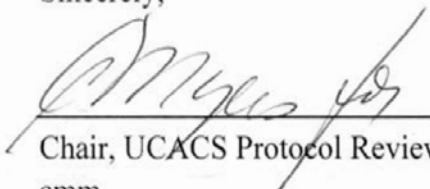
DATE: 16-Nov-06

RE: Animal Care Committee Review of Your Protocol - Examination of species differences in monoamine oxidase mRNA expression and enzymatic activity

PROTOCOL ID: 20040094

The Protocol Review Committee of the University Committee on Animal Care and Supply recently reviewed and approved the above-noted protocol for the next twelve months.

Thank you.
Sincerely,



Chair, UCACS Protocol Review Committee
cmm